An Investigation on the Efficiency of Sophorolipids in Removing Arsenic from Mine Tailings

Fereshteh Arab

A Thesis
In the Department
of
Building, Civil and Environmental Engineering

Presented in Partial Fulfillment of the Requirements
For the Degree of
Doctor of Philosophy (Civil Engineering) at
Concordia University
Montreal, Quebec, Canada

October 2017

CONCORDIA UNIVERSITY

SCHOOL OF GRADUATE STUDIES

This is to certify that the thesis prepared

By: **Fereshteh Arab**

Entitled: **An investigation on the efficiency of sophorolipids in removing arsenic from mine tailings**

and submitted in partial fulfillment of the requirements for the degree of

Doctor of Philosophy (Civil Engineering)

complies with the regulations of the University and meets the accepted standards with respect to originality and quality.

Signed by the final examining committee:

	Chair
Dr. A. Awasthi	
	External Examiner
Dr. Guy Mercier	
	External to Program
Dr. A. De Visscher	
	Examiner
Dr. S. Li	
	Examiner
Dr. F. Haghighat	
	Thesis Supervisor
Dr. Catherine N. Mulligan	

Approved by

Dr. Fariborz Haghighat, Graduate Program Director

November 24, 2017

Date of Defence

Dr. Amir Asif, Dean of Faculty Engineering and Computer Science

ABSTRACT

An investigation on the efficiency of sophorolipids in removing arsenic from mine tailings

Fereshteh Arab, Ph.D.
Concordia University, 2017

In many places around the world, arsenic is considered a primary pollutant in water due to its high toxicity. Various methods have been developed for the treatment of arsenic contaminated soil and water. In this study, the efficiency of high lactonic sophorolipids (SL18), in removing arsenic and heavy metals from mine tailings through the process of soil washing, was evaluated. Sophorolipids are capable of increasing the solubility of organic compounds and binding metalloids and heavy metals and are biocompatible, rapidly biodegradable, and non-toxic.

To investigate the efficiency of sophorolipids in heavy metal/metalloid removal, a series of batch and column tests, using different concentrations of sophorolipids (0.1, 0.5, 1, 2, 3, 4 and 5%), at different pH levels (2, 4, 6, 8, 10 and 12), and at three different temperatures (15ºC, 23ºC and 35ºC) was performed. Furthermore, the effect of sophorolipids on the speciation of arsenic, and the effectiveness of sophorolipids on different fractions of the mine tailings were examined. The results of this investigation show that using a 1% sophorolipid solution in a column test resulted in the removal of 83% of the arsenic. To identify the mechanism of removal of arsenic from mine tailings, the effect of sophorolipids on mine tailing sample through a sequential extraction procedure combined with Scanning Electron Microscopy (SEM), X-ray powder diffraction (XRD) scans was investigated. Also, the spectrum of sophorolipids was studied using Fourier-transform infrared spectroscopy (FTIR) and the effect of the presence of arsenic and iron on its functional groups was determined. Dynamic light scattering (DLS) measurements were used to find the effect of pH and mine tailing constituents on the size of micelles.

Investigations on the mechanism of sophorolipid assisted arsenic removal confirmed that the formation of arsenic complexes with sophorolipid functional groups, reducing the interfacial tension and solubilization, changing the net charge of surfaces and ion exchange are the main mechanisms. The impact of each mechanism is chiefly governed by the pH. The results from this

study shed light on the mechanism of arsenic removal by biosurfactants and can aid in the development of a sustainable and environmentally friendly solution for mine tailing remediation.

ACKNOWLEDGMENTS

I would like to express my deepest gratitude to my advisor Professor Dr. Catherine Mulligan. You have been a tremendous mentor for me. I would like to thank you for believing in me and encouraging my research and for allowing me to grow as a researcher. Your help and advice on my research have been priceless.

I would like to express sincere appreciation to Prof. Dr. Haghighat, Prof. Dr. Li, Prof. Dr. Mercier and Dr. De Visscher for serving as my committee members and their time and comments.

Special thanks to my children. Words cannot express how grateful I am to my daughters, who have always been there for me through the thick and thin.

I would like to thank Ecover Co. for providing sophorolipids for my research, and Mr. Benny Nordahn, Mine Systems Officer at Giant Mine, for collecting and sending me the mine tailing samples, which I used in my research.

TABLE OF CONTENTS

LIST OF TABLES

LIST OF FIGURES

LIST OF ABBREVIATIONS

AANDC	Aboriginal Affairs and Northern Development Canada
AAS	Atomic absorption spectrophotometry
ASTM	American Society for Testing Materials
ANOVA	Analysis of variance
CCME	Canadian Council of Ministers of the Environment
CEC	Cation Exchange Capacity
DMAA	Dimethyl acrylamide
DI	Deionized water
EGME	Ethylene Glycol Monomethyl Ether
EPA	Environmental Protection Agency
ESP	Electrostatic Precipitator
FTIR	Fourier transform infrared spectroscopy
ICDD	International Centre for Diffraction Data
ITRC	Interstate Technology & Regulatory Council
ICP-MS	Inductively coupled plasma mass spectrometry
LC-ICP-MS	Liquid chromatography-inductively coupled plasma mass spectrometry
MMAA	Monomethyl arsenic acid
MT	Mine tailing
Rha	Rhamnolipids
RT	Room temperature
SEM	Scanning Electron Microscopy
SEM-EDS	Scanning Electron Microscopy-Energy Dispersive Spectroscopy
SF	Soil flushing
SG	Specific Gravity
SL	Sophorolipids
SSA	Specific Surface Area, m^2/g
SSE	Selective Sequential Extraction

SW	Soil washing
TCA	Trichloroacetic acid
UF	Ultrafiltration

LIST OF SYMBOLS

D_h	Particle size
k_B	Boltzmann's constant
T	Thermodynamic temperature
$D_{t:}$	The translational diffusion coefficient
Eh	Redox Potential
K	Hydraulic conductivity
pI	Isoelectric point
Γ	Surface tension
μ, η	dynamic viscosity
N	kinematic viscosity
P	Density
Ψ	Water potential
υ_s	symmetric stretching
υ_{as}	asymmetric stretching
C	Speed of light (cm/s)
N	Frequency in Hertz (sec^{-1})
$\tilde{v}$	Wavenumber (cm^{-1})
Λ	Wavelength (cm)
N	Refractive index
z_j	Zeta potential

CHAPTER ONE: INTRODUCTION

1.1 General background

Environmental pollution is a major concern, and if not prevented, will have dire implications for the future of our environment. The ecology of our planet has developed into what it is today through millions of years of selection, and often the best solutions for these environmental problems can be found in the natural world.

Arsenic contamination affects millions around the world (Smith et al., 2000). It can have a variety of implications for a population, given the extent of exposure within the population. Some common adverse health effects associated with long-term exposure to arsenic include: skin lesions, skin cancer, internal cancers such as bladder, kidney, and lung cancer, neurological effects, hypertension, cardiovascular disease, pulmonary disease, peripheral vascular disease, and diabetes mellitus (Morales & Chen, 2000; Smith et al., 2000).

1.2 Problem statement

Arsenic is found in gold mineral deposits in the form of arsenopyrite. Mine tailings are considered major environmental contamination sources around the globe (Dushenko et al., 1995). For example, it has been estimated that mine tailings from past mining activities at Giant Mine, Yellowknife contain a quarter-million tons of arsenic, which are deposited near the shores of The Great Slave Lake. There have been many reports on heavy metals and arsenic from these mine tailings being transported to the local ground or surface water. There have been reports about the accidental release of mine tailings due to malfunctioning chambers, or seeping contaminated water from storage areas (Constantine & Price, 1983, Clark & Raven, 2004, Walker et al., 2005, Andrade et al., 2010, Keeling & Sandlos, 2012). This highlights the importance of cleaning up and treating these mine tailings and the fact that storing these hazardous by-products is not an ideal solution.

At the first step, it is crucial to determine the extent of the threat of the mine tailing which are stored in tailing ponds. This can be done by determining the composition, size, and structure of the particles in these tailings. The second problem involves choosing an efficient and environmentally method for remediation of these tailing.

During recent decades, numerous methods have been developed for the treatment of soil and water contaminated with heavy metals. Some methods being developed are phytomining, rhyzostabilization, soil amendments, soil capping, excavation, landfills, thermal treatment, stabilization, solidification and chemical extraction (Slizovskiy & Hatzinger, 2011; Wang & Mulligan, 2009 a; Guemiza et al., 2017). Although many of these methods were successful in removing heavy metals from the soil, most of them are not environmentally friendly. For example, stabilization is an effective method for the treatment of contaminated soil and sediments, but it is not an environmentally friendly method (Czaplicki et al., 2016).

Thermal treatments is another method which has been shown to be an effective method for the removal of organic contaminants, but not only the expense of the operation of this method is concerning, also the need for the remediation of the toxic fumes from this method and the cost of further remediation of heavy metals makes the thermal treatment an unsuitable choice especially for the soil contaminated with several types of contaminants (Guemiza et al., 2017). Bioremediation has been known as an effective and environmentally friendly method for the removal of contaminants, although, the process of bioremediation is time-consuming. According to Guemiza et al. (2017), the efficiency of the bioremediation in removal of contaminants depends on the parameters such as type of contamination and the initial concentration of the contaminant, temperature, and moisture. Moreover, in the process of in situ bioremediation, there is a risk of the release of contaminants to the groundwater and surface water and being carried outside of the site before completion of the remediation.

One of the environmentally friendly approaches for removing heavy metals from soil is by using an effective, biocompatible, biodegradable surfactant during the process of soil washing and flushing (Arab and Mulligan, 2016). In recent years, the use of biosurfactants for the removal of heavy metals from contaminated soil has been receiving more attention from researchers around

the world. Recent research has shown that biosurfactants can successfully remove heavy metals from contaminated soil and mine tailings (Mulligan, 2009b).

In the current study, the efficiency of sophorolipids (SL), in removing arsenic from mine tailings were evaluated and compared. There was an investigation on the interaction of biosurfactants with arsenic and other heavy metals present in mine tailings, and how the presence of other heavy metals in the medium, or modification of biosurfactants enhances the process of arsenic removal. The result of these investigations will be used to develop an efficient and environmentally friendly system for the treatment of mine tailings.

1.3 Research objectives

The focus of this study was to:

- Determine the physiochemical properties of the mine tailing sample from Giant mine, Yellowknife, NWT, Canada
- Determine the efficiency of sophorolipids in removing metal/ metalloids from mine tailings during the process of soil washing
- Determine the mechanism of removal of arsenic from mine tailings

1.4 Scope and limitations of this study

- This research was conducted to investigate
- The effect of sophorolipids on different fractions of the mine tailings.
- The mechanism of mobilizing arsenic by biosurfactants.
- The main purpose of this research is to develop an effective remediation method for the treatment of mine tailings containing heavy metals and metalloids, such as arsenic, using biosurfactants.
- Batch experiments were conducted to determine the effect of reaction time, pH, temperature and biosurfactant concentration on the rate of arsenic mobilization.

- Based on the results of the batch tests, column tests were also conducted to illustrate the efficiency of these biosurfactants on the removal of arsenic from mine tailings.
- More specifically, this research was conducted in two phases:
- An investigation on the efficiency of sophorolipids in arsenic removal
- An investigation of the process of sophorolipid assisted arsenic removal.
- And these steps were accomplished by:
- How and in what conditions these biosurfactants enhance the process of the removal.
- The role of other heavy metals present in the medium, which affect the removal of arsenic
- Analysis of the interaction of biosurfactants with arsenic and other heavy metals present in mine tailings and their speciation.
- Investigation of the arsenic content, associated with different fractions of the mine tailing sample before the process of treatment and after treatment by these biosurfactants.
- Experimental studies in this research were limited to the mine tailing sample from Giant Mine, Yellowknife, NWT, Canada.

1.5 Organization of this thesis

In summary, this study first focused on finding an environmentally friendly method to remove heavy metals and metalloids from contaminated soil and sediment. The next step consisted of selecting an environmentally friendly and economically feasible agent to use in the process of remediation. Evaluating the efficiency of the selected agent in the removal of heavy metals and metalloids was the next step, which was followed by an investigation on the removal mechanism by the selected agent. This thesis is organized into two sections. The first section of the thesis consists of two parts. The first part includes the abstract, table of contents and acknowledgments. The second section encompasses the results and discussion, which includes two subsections focusing on the sophorolipid assisted removal of elements from mine-tailings and an investigation on the mechanism of removal by sophorolipids. Chapter five encompasses conclusions and recommendations.

CHAPTER TWO: LITERATURE REVIEW

2.1 Arsenic

Arsenic is a metalloid, having both metallic and non-metallic properties. It is the 20th most abundant element in the earth's crust (Mandal and Suzuki, 2002). Arsenic exists in four common oxidation states: a) As (0), metalloid arsenic; b) As (+3), arsenite; c) As (+5), arsenate and d) As (-3), arsine. Arsenate and arsenite are the two most common forms of arsenic existing in the earth's crust. This metalloid has received more attention during the past decades due to its widespread distribution within soil and water, and the increase of its concentration due to anthropogenic activities, which puts the lives of millions of people at risk.

Arsenite and arsenate are two prevalent oxidation states for inorganic arsenic. Arsenite, which is the trivalent form of arsenic, is more mobile than the pentavalent form of arsenic (arsenate). Although arsenite is expected to be found in reducing environment and arsenate, in oxidizing condition, because of the slow redox kinetics, arsenate and arsenite can be found together. On the other hand, the presence of elements such as iron and sulfur interferes with the redox potential (Welch et al., 1988; Masscheleyn et al., 1991, Yu et al., 2016). Furthermore, activity of some microorganisms and algae can induce the redox transformation between arsenate and arsenite, both in anaerobic and aerobic condition (Guemiza et al., 2017). The pH level of the environment also determines the speciation of arsenate and arsenite. Figure 2.1 shows the speciation of arsenite and arsenate at different pH levels.

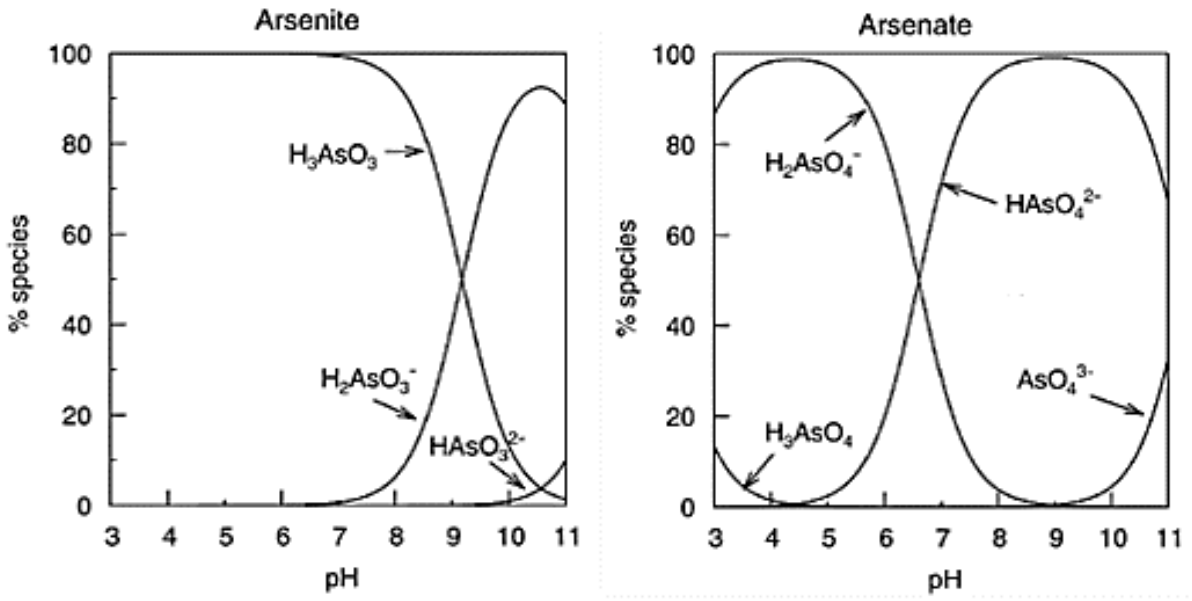

Figure 2.1. Speciation of As (III)) and As (V) as a function of pH (Smedley and Kinniburgh, 2002)

As it can be seen in Figure 2.1, protonate/deprotonate of arsenate and arsenite depend on the pH of the solution. For example, the dominant forms of arsenate at pH 3 to 11 are the negatively charged $H_2AsO_4^-$ and $HAsO_4^{2-}$. At the same time, H_3AsO_3 is the dominant form of arsenite at pH levels lower than pH 9. Disassociation constants of arsenate (2.20) are much lower than pKa for arsenite (9.22) (Wagman et al., 1982). Table 2.1 shows the dissociation constants of arsenic species (Based on Wagman et al., 1982).

Table 2.1. Dissociation constants of arsenic species (adapted from Wagman et al., 1982).

Arsenic species	pK_{al}	pK_{a2}	pK_{a3}
$HAsSO_4$	2.20	6.97	11.53
H_3AsO_3	9.22	12.13	13.4

Although arsenic is soluble over a wide range of pH, in both reducing and oxidizing conditions (Bowell et al., 2014), arsenic solubility in different species of arsenic is different even for the same species, and solubility is different. As the protonation/ dissociation of arsenic species are affected by pH. Dissociation constants of arsenate (2.20) are much lower than pKa for arsenite (9.22) (Wagman et al., 1982). At the depth of tailings which there is no oxygen, anaerobic bacteria

could reduce arsenate to the more mobile form, arsenite. Experiments of Wu et al., (2012) showed that in an eight-day incubation of a soil sample spiked with arsenate in an anaerobic condition, microbial activities could transform 70% of arsenate to arsenite after 8 days, and eventually all the arsenate reduced to arsenite and was released into the soil solution. Simultaneously, iron in the soil reduced from ferric form to ferrous iron and was released into the soil solution. On the surface of tailings, oxidation of arsenic slows down the release of this component. Although, weathering and oxidation of pyrite and arsenopyrite, generation of acid mine drainage (AMD), as well as, the runoff from these tailing could accelerate the process of release of these components. Experiments, conducted by Bowell (1994), on the effect of organic acid on the solubility of different arsenic species (As (V), DMAA, MMAA and As(III)) showed that at pH levels lower than 7, arsenate is the most mobile form of arsenic and arsenite is the lease mobile speciation of arsenic. In contrast, when pH is higher than 7, arsenite became the second most mobile speciation of arsenic after arsenate.

2.2 Maximum recommended concentration of arsenic in soil and water

The maximum concentration of inorganic arsenic recommended for the dry components of soil is 32 mg/kg in residential areas, and 640 mg/kg in commercial areas (Environment Agency, 2009d). The maximum concentration of arsenic in drinking water, as recommended by the World Health Organization (WHO, 1993), is 10-35 µg/L. Yet, in many places, the levels are drastically higher (WHO, 1993).

The range of arsenic present in groundwater can vary considerably from region to region, depending on the geology and the climate of the area. It can range from 0.5 µg/L to 5000 µg/L (Smedley & Kinniburgh, 2002). In many regions, freshwater, including groundwater, has an arsenic concentration less than 10 µg/L, and typically less than 1.0 µg/L (Smedley & Kinniburgh, 2002). However, in other regions, even the groundwater exceeds the maximum threshold for human consumption. For instance, Rahman et al., (2006)'s investigations showed that in certain rural districts in southern Bangladesh, the arsenic concentration in 70% of the functioning tube wells

exceeded the recommended limits for drinking water. The arsenic concentration in drinking water from some of these wells was as high as 3644 µg/L.

2.3 Arsenic toxicity and significance of arsenic speciation on its toxicity and exposure routes

Contamination can have a variety of implications for a population, given the degree of exposure. Exposure to high levels of arsenic, or long-term exposure to lower levels of this element, is linked to a range of short term and long term health problems. Arsenic is a potent poison and is considered to be a primary pollutant in water due to its high toxicity (Smith & Rahman, 2000). Inorganic forms of arsenic are usually more toxic than organic forms of arsenic (Jain & Ali, 2000), although, some organic arsenic compounds, such as monomethyl arsonic acid (MMA) and dimethyl arsenic acid (DMA), have been shown to be highly toxic (Brown et al., 1997).

Exposure to a high level of this metalloid, or even long-term exposure to lower levels of arsenic, is linked to many short terms and long-term health problems, and some forms of congenital disabilities. A high concentration of arsenic is classified as a Class A carcinogenic (EPA, 1998), it increases the risk of cancer. In Canada, inorganic compounds of arsenic are classified as Group 1 carcinogens (carcinogenic to humans) (CEPA, 1996). Likewise, the International Agency for Research on Cancer (IARC, 2012) classified arsenic and inorganic arsenic compounds as carcinogenic to humans (Group 1).

Some common adverse health effects associated with long-term exposure to arsenic include: skin lesions, skin cancer, internal cancers such as bladder, kidney, and lung cancer, neurological effects, hypertension, cardiovascular disease, pulmonary disease, peripheral vascular disease, diabetes mellitus, mental retardation, and developmental disabilities (Brinkle et al., 2009; Rahman, 2006; Morales & Chen, 2000; Smith et al., 2000). Exposure to arsenic during the period of embryonic growth and fetal development causes permanent adverse effects, such as birth defects (Milton et al., 2005; Shalat et al., 1996). Numerous studies have shown the negative correlation

between the amount of arsenic intake from contaminated food and water, and the IQ of children (Brinkle et al., 2009, Nahar et al., 2014 a and b).

Arsenic V is known to have properties that interfere with cellular metabolism. Arsenic III can interfere with enzyme and protein function, thus impairing the process of DNA repair. This leads to an increase in the frequency of genetic mutations, thus increasing the chance that a mutation that causes cancer will occur (Mazumder et al., 1998).

This hazardous element, even at high concentrations, has no color, smell, or taste, and can only be detected through laboratory testing. Several routes of exposure are: a) via consumption of arsenic contaminated water, or by eating fruits and grains that have been grown in arsenic-contaminated soils or irrigated with arsenic contaminated water, b) exposure via skin and c) exposure via inhalation. The most common source of arsenic exposure is via consumption of contaminated food and water.

Arsenic is not only a threat to humans. It also threatens the life of animals and plants that live in contaminated areas. According to Canadian Soil Quality Guidelines for the Protection of Environmental and Human Health (1997), there are only a few types of plants that can grow in soil with high concentrations of inorganic arsenic. However, the majority of plants are unable to grow in arsenic-contaminated soils, and cannot survive in highly contaminated soil.

2.4 Arsenic sources

The release of arsenic into the environment has two main types of sources: a) anthropogenic and b) natural. Although each of these two categories has a significant impact in releasing arsenic into the water, and are usually independent of each other, anthropogenic activities could have a noticeable impact on natural activities. For example, the weathering of the crust causes the mobilization of the arsenic found within it. However, the environmental conditions that result in the release of this element from rocks to water or air are not always natural. As the release of arsenic is strongly controlled by geochemical parameters, such as pH and redox of the environments (Warner, 2001; Holm and Wilson, 2006), many anthropogenic activities that affect

the geochemical condition of their surroundings, speed up the process of weathering and release of this element.

2.5 Natural sources

The natural release of arsenic into the environment could be the result of biogenic activities, such as the biologically mediated release of the element from rocks. It can also be because of geogenic activities, such as the eruption of volcanoes, and the weathering of rocks containing arsenic. The weathering and erosion of rocks is a natural process that releases fragments of rock, exposes them to air and oxidation, breaks them down, and mobilizes some of their minerals and fragments. However, during the past decade, digging wells and excavating into the arsenic-rich layers of the crust caused the release of this element into groundwater, thereby creating a catastrophe in regions where people are consuming these contaminated waters (Chowdhury, 2004, Grantham and Jones, 1977).

In many countries around the globe, for example in Bangladesh, India, Taiwan, China, the United States of America., Argentina, Chile, Mexico and Canada, arsenic is a natural contaminant in groundwater. Arsenic is naturally present in a wide variety of rocks and minerals, including sulfides, oxides, and hydroxides. It contaminates the water by leaching into underground reservoirs, and by migrating via water to affect greater areas. In many rural areas, in which residents depend on water from unmonitored, unregulated private wells, the concentration of this element is much higher than the maximum level of arsenic permitted in water, according to the guidelines. The magnitude of the effect of using these unmonitored wells is much clearer when considering the number of people relying on water from such wells. For example, according to a survey in the United States, 15 million families rely on unmonitored wells as their primary source of water (U.S. Census, 2007); wherein, the concentration of arsenic in 10% of groundwater in the United States exceeds the limit of 10 μg/L (Welch et al., 2000).

The concentration of arsenic in groundwater, which is surrounded by or flows through layers of sediment and rock, is determined by the concentration of arsenic in the formations it passes through, and the geochemical conditions. The type and age of the geological structure are

other important factors. For example, clay is less hydraulically conductive than sand and gravel. Therefore the velocity of water is much lower, and it can affect the arsenic concentration in water. On the other hand, some geological formations contain high amounts of labile arsenic, which contaminates the water that passes these formations. Conversely, anthropogenic activities can change the geochemical factors in the environment, as well as the rate of release of arsenic into groundwater.

2.6 Anthropogenic

Mining, smelting, the combustion of coal, wood treatment, arsenic-based insecticides or herbicides, and industrial pollution all contribute to the presence of high levels of arsenic in the environment (Nordstrom, 2002). Chemicals that are introduced to the surface of the earth migrate to the lower layer of the crust, changing the geochemical environment of aquifers, thus causing changes in the rate of release of trace elements such as arsenic. Introducing substances that contain arsenic to the surface, such as pesticides containing arsenic, results in higher concentrations of this element in surface and groundwater. In the agriculture sector, fertilizers and pesticides used on land not only are potential sources of arsenic contamination, but they can also change the pH and redox of the surrounding soil, and increase or decrease the solubility of arsenic as well as other trace elements in soil. According to Razo et al. (2004), a comparison between water obtained from agricultural wells and from urban regions shows that, regardless of the climate, the concentration of arsenic and other trace elements, as well as dissolved oxygen (DO) and pH values in water from the agricultural region were much higher than in water from urban areas. Arsenic is more soluble in alkaline conditions. Its adsorption has a negative correlation with pH level (Smedley and Kinniburgh, 2002).

The organoarsenic compounds which are added to poultry feed, to control diseases and to improve feed efficiency, are considered another anthropogenic source of arsenic. By consuming 350 g of chicken, between 21.13 to 30.59 μg of inorganic arsenic and 32.50 to 47.07 μg of total arsenic is ingested (Lasky et al., 2004). Landfills could also alter the geochemical conditions of

their surroundings, resulting in a reduction of iron oxide, and a transformation into more soluble forms, therefore mobilizing the arsenic associated with these iron oxides (Delemos et al., 2006).

Mine tailings are considered one of the main environmental contamination sources (Dushenko et al., 1995). In a report by Nriagu and Pacyna (1988), 22% of the arsenic released to the environment could be directly traced back to the mining and metallurgy industries. In gold mines, gold and arsenic are mostly embedded in arsenopyrite (FeAsS), tennantite ($Cu_{12}As_4S_{13}$), and enargite (Cu_3AsS_4) (Razo et al., 2004).

In gold mines, arsenopyrite (FeAsS) (Figure 2.2) has an economic significance because the major portion of the gold is embedded in this mineral (Dos Santos et al., 2017). In arsenopyrite, iron is in the +2 oxidation state (Fe^{+2}) and arsenic and sulfur oxidation states are -1 (As- and S^-) (Jones and Nesbitt, 2002). Arsenopyrite is not stable in an oxidizing environment and is oxidized in the presence of oxygen. Oxidation of arsenopyrite results in the releasing As (V) and As (III). It was shown that oxidation rate of arsenopyrite depends on the presence of other minerals and elements. Arsenopyrite in ores is accompanied with other sulfide minerals such as pyrite, for instance, according to Dos Santos et al. (2017), the rate of oxidation of arsenopyrite in the presence of pyrite increases. It was shown that interaction of pyrite and arsenopyrite results in a galvanic reaction, in which, pyrite act as the electron donor (cathode) and arsenopyrite act as an electron receptor (anode) (Beattie and Poling, 1987).

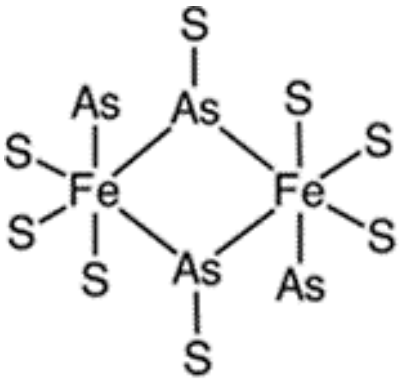

Figure 2.2. Illustration of the structure of arsenopyrite (Dos Santos et al., 2017).

In the process of mining and separating these minerals, some of the arsenic is released into the air and water, and the rest remains in sulfide minerals, discarded as mine tailings. These sulfide minerals are unstable under typical atmospheric conditions (Paktunc, 2013). After some time, oxidation and microbial activities in mine tailings break down the sulfide minerals and produce acid mine drainage (AMD) containing arsenic. Although the presence of neutralizing minerals, such as dolomite, calcite, and siderite, can mask the AMD generation, the released arsenic is stable at different pH levels (Smedley and Kinniburgh, 2002), and can migrate to surface and groundwater after being washed away by precipitation or overflowing rivers. It then proceeds to pollute a greater area and put the health of more inhabitants in danger. Although the release of arsenic has been associated with the generation of acid mine drainage (AMD), there are some reports on the release of arsenic in neutral and alkaline conditions as well (Razo et al., 2004).

2.7 Arsenic speciation

Arsenate [As (V)] and arsenite [As (III)] are the main arsenic compounds in the earth's crust. Reduction or oxidation, as well as methylation reactions, caused by chemical or biological factors, alter these two compounds and change their behavior in the environment. According to Masscheleyn et al. (1991), redox and pH levels affect the speciation state of arsenic. As their experiments have shown, at high redox levels, redox of higher than 200 mV at pH higher than 5.5, arsenate [As (V)] was the dominant species of arsenic in the solution, and then the total solubility of arsenic was at the lowest level at this pH (Figure 2.3). In contrast, at the lower redox levels, for example below 100mV at pH 6.4, arsenite [As (III)] became the dominant species of arsenic. Further decrease in redox potential and solubilization of iron hydroxides, resulted in releasing arsenic to the solution (Masscheleyn et al., 1991). Figure 2.3 demonstrates the effect that pH and redox have on the speciation of arsenic.

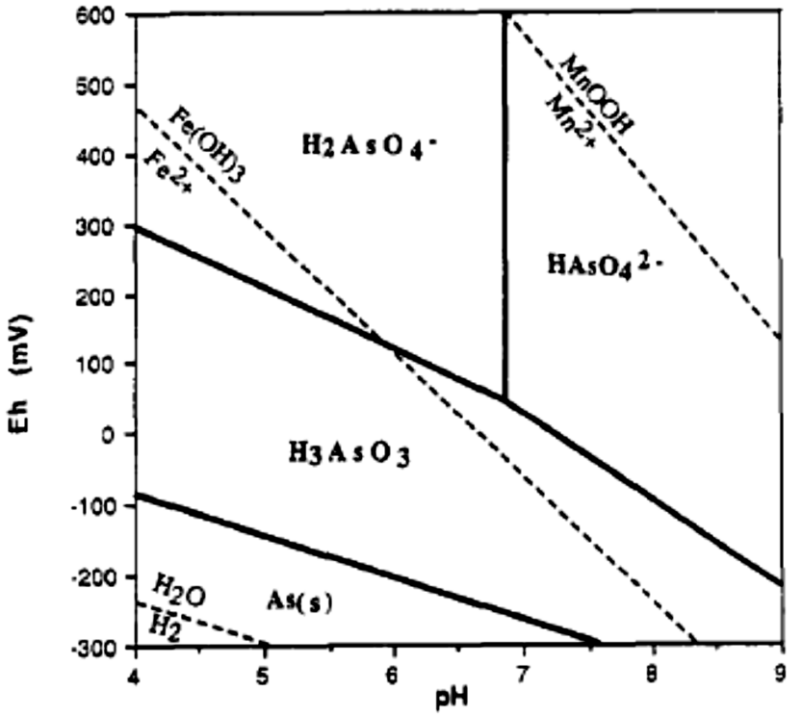

Figure 2.3. Eh-pH diagram for the As- H_2O system (Masscheleyn et al., 1991).

At lower redox levels, not only arsenite is the dominant species, the total solubility of arsenic also increases (Masscheleyn et al., 1991). As the process of oxidation and reduction of arsenic is a slow process, the presence of both oxidation states of arsenic, at all redox levels, is expected (Figure 2.4).

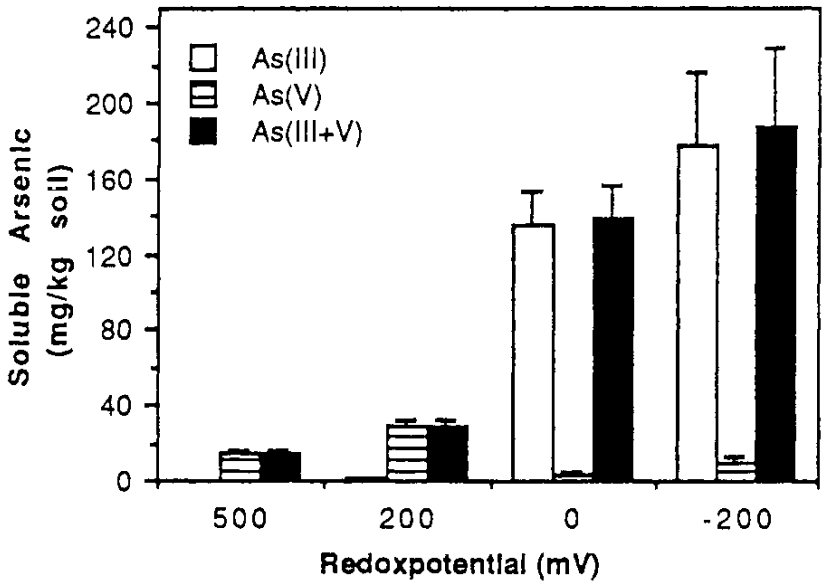

Figure 1.4. Distribution of soluble arsenic species after a 24day at pH 5.2 for 500 mV, 6.7 for 200 mV, 7.0 for 0 mV, and 7.2 for -200 mV (Masscheleyn et al., 1991).

In conclusion, the solubility, mobility, bioavailability, and toxicity of arsenic are highly dependent on its oxidation state. Therefore, investigations on arsenic speciation and factors that affect the speciation, or transform arsenic from one state to another, are necessary for predicting the behavior of arsenic in a certain medium (Masscheleyn et al., 1991).

2.8 Fate and transport of arsenic in the environment

The main factors that control the release and mobility of arsenic compounds are pH, redox conditions, salinity, and the presence of organic compounds (Forstner et al., 1981). Furthermore, the speciation of arsenic has a significant impact on its solubility, as arsenite is more mobile than arsenate. The other significant factor controlling arsenic mobilization is the acid-neutralizing capacity and the acid-producing capability of the soil or sediment.

It has been reported that arsenate mobilization and absorption to soil particles is pH-dependent: According to Dove et al. (1984), in an acidic environment, arsenopyrite oxidation produces arsenate, and combination of iron and arsenate leads to formation scorodite which precipitates;

$FeAsS + 14\ Fe^{3+} + 10H_2O \rightarrow 14Fe^{2+} + SO_4^{2-} + FeAsO_4.2H_2O + 16H^+$ (Dove, 1984).

Furthermore, at lower pH levels, soil particles tend to adsorb arsenate, and at higher pH levels, arsenate tends to be released (Cappuyns et al., 2004). It has been shown that a portion of the arsenic which was released from the weathering of arsenic-bearing minerals in the tailings, bond with newly formed hematite or goethite. Moreover, a fraction of the released arsenic is adsorbed to iron hydroxide minerals in the formations that it passes through, and precipitates, upon which, the rest remains soluble in the groundwater (Kim et al., 2013; Sracek et al., 2014). The percentage of As (III), which is more mobile and more water-soluble form of arsenic, to As (V) increases in deeper groundwaters and a reducing environment (Smedley et al., 1996, Dixit and Hering, 2003).

Corresponding to the fact that arsenate has an affinity to co-precipitate with iron oxyhydroxides, any condition that results in solubilizing iron oxyhydroxides would also lead to arsenate release (Masscheleyn et al., 1991).

$FeAsO_4.2H_2O$ (Scorodite) $+ H_2O \rightarrow H_2AsO_4^- + Fe(OH)_3 + H^+$ (Masscheleyn et al., 1991)

Cappuyns et al. (2004)'s experiments showed that the mobilization and reabsorption behavior of arsenic and phosphorus are similar. Moreover, in a report by Razo et al. (2004), the same similarity between arsenic and molybdenum was shown, as both of these two elements' absorption and desorption is affected by changes in pH and redox condition, and both of them can be found in water as oxyanions. Numerous researchers reported on the correlation between the concentration of arsenic and molybdenum in water from different locations (Warner, 2001; Thomas, 2003).

In mine tailings, the presence of stable minerals such as arsenopyrite and jarosite, and the retention of arsenic on the surface of these iron-bearing minerals, affect the solubility and mobilization of arsenic (Ma et al., 2014; Romero et al., 2014). Arsenopyrite, one of the dominant arsenic minerals, is known to be stable. However, experiments conducted on the effect of hydrogen peroxide on arsenopyrite deduce that hydrogen peroxide (5–50 μM) was able to release arsenic

from this mineral, and increase the mobility of arsenic in the medium (Ma et al., 2014). Then again, as H_2O_2 is a strong oxidizer and oxidation of released arsenic and its transformations to less soluble forms by the production of $FeAsO_4$ precipitates, affect the transportation of arsenic in the environment. The conclusion that the effect of H_2O_2 on arsenic bearing soil and sediments is complex, H_2O_2 enhances the release of arsenic from arsenopyrite, also it could cause the released arsenic to precipitate as arsenate, and the fact that hydrogen peroxide is present in rainwater (up to 200 μM) (Willey et al., 1996; Ma et al., 2014), shows the vulnerability of these minerals to rainfall, and how easily acid rain can cause the weathering of arsenic-bearing minerals in mine tailings and release arsenic to the surface and groundwater. It should be noted that the concentration of H_2O_2 depends on air pollution, as photolysis of ozone (O_3) in the presence of carbon monoxide, and hydrocarbons in the air result in the formation of hydrated hydroperoxy ($H_2O^{\bullet}HO_2$) and hydroperoxyl ($HO_2^{\bullet}$). Interaction of hydroperoxy ($H_2O^{\bullet}HO_2$) and hydroperoxyl ($HO_2^{\bullet}$) results in the production of hydrogen peroxide (H_2O_2) (Gonçalves et al., 2010). In summary, it can be concluded that the presence of arsenic in the environment can be the consequence of the weathering of arsenic-bearing minerals, changes in the organic matter of soil, reductive dissolution of iron oxyhydroxides, and alkaline desorption.

2.9 Geology of Yellowknife

Early investigations in the Yellowknife region found ice lenses containing gold in the permafrost zone, which extended to a depth of 76 m (Boyle, 1951). These deep permafrost regions may have originated in late glacial time (15,500–13,000 ^{14}C yr B.P.) (Bateman, 1949). According to Boyle (1961), in the Yellowknife region, gold can be mainly found in gold-quartz deposits (quartz lenses) which are embedded in the chlorite schist zones. In the Yellowknife area, widespread chlorite schist zones are cutting through greenstone belt, and the quartz lenses were formed alongside the highly folded Precambrian sedimentary rocks.

The Archean greenstone belt is chiefly composed of tholeiitic mafic rocks, similar to the ocean crust. Felsic minerals found in the greenstone belt, originate from felsic dykes which were created, as a result of tectonic and volcanic activities, from sedimentary bedrocks which penetrated

through mafic rocks (*Cousens, 2000)*. Archean greenstone belts contain carbonate rocks with attributes similar to marine sediments. Investigations on these carbonates lead to a determination of the age of belt, which is estimated to be ~2.8 ± 0.2 and ~3.5 ± 0.1 billion years (Veizer et al., 1989).

Boyle (1961) noted that in Yellowknife region, the sedimentary deposits are composed of silica, sulfur, boron, iron, lead, zinc, gold and silver. Also, the greenstone consists of silica, carbon dioxide, sulfur, and many elemental metals/metalloids, such as arsenic, antimony, silver, and gold. High temperature and pressure from tectonic activities in this area caused the migration of gold, silver, arsenic, sulfur, water, and carbon dioxide, from the greenstone to the shear zone. In the shear zone, chemical reactions between amphibolite rock reaction, carbon dioxide, and water resulted in chlorite and chlorite-carbonate sericite schist (Boyle 1961). At the shear zone (chlorite schist zone), elements and compounds such as silica, gold, iron, potassium migrated to dilatant zones and precipitated, creating gold-quartz lenses and veins (Boyle (1961). The same phenomena also happened in the sedimentary layer, where during the process of metamorphism, high pressure and heat caused the elements to migrate, and subsequently, precipitated in dilatant zones in faults, fractures, and drag folds.

One of the several Archean greenstone belts, which is located in the southern part of Slave Craton, Northwest Territories, is called The Yellowknife Volcanic Belt (YVB). The YVB belt has been subdivided into two groups, the Kam Group and the Banting Group (*Cousens, 2000;* Helmstaedt and Padgham 1986). The Kam Group is around 10 kilometers thick and is composed of tholeiitic mafic rocks and secondary felsic volcanic rocks (Cousens, 2000*;* Boyle, 1961). Giant Mine is within the Kam group (Figure 2.5).

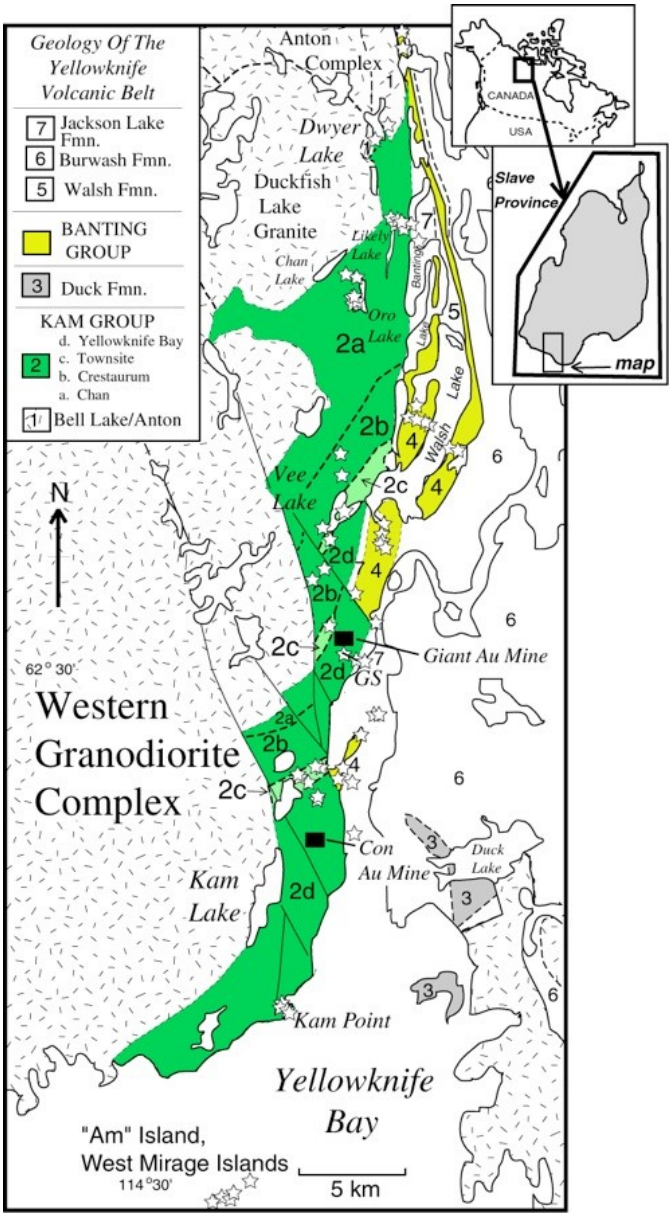

Figure 2.5. Geological map of the Yellowknife Volcanic Belt (Pahgham, 1987b).

2.10 Giant Mine

Giant Mine, is located 5 km north of the city of Yellowknife, NWT; 62°27'N, 114°26'W. According to Environment Canada the annual mean temperature in Yellowknife is minus -0.2 to -

9.0º C and the temperature during two months of July and August is between 10.2 to 21.3 º C (Figure 2.6).

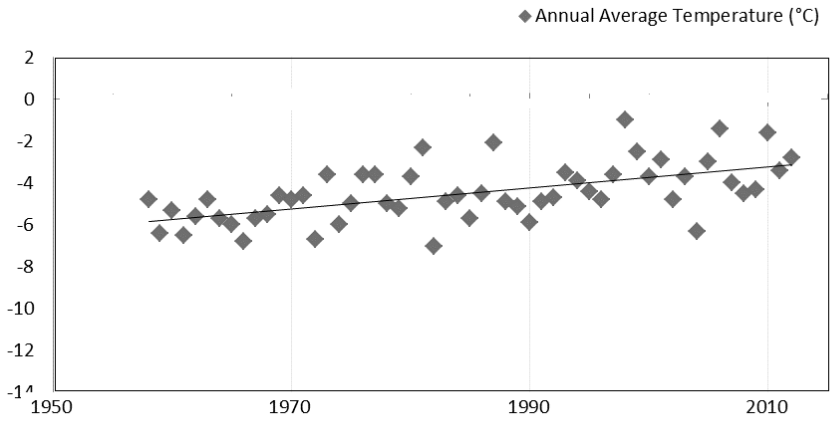

Figure 2.6. Annual Mean Temperatures in Yellowknife from 1958 to 2012 (Government of Northwest Territories. 2015)

Mine tailings from the former gold mine, Giant Mine (Yellowknife, NWT), fill up huge tailing ponds near the shores of the Great Slave Lake. It has been estimated that mine tailings produced during past mining activities at the Giant Mine in Yellowknife contain quarter-million tons of arsenic. The discharges from these tailing ponds enter a creek that brings them to Yellowknife Bay of Great Slave Lake (Mudroch et al., 1989). The concentration of heavy metals and metalloids in these mine tailings are significantly higher than the standard maximum limits for soil in industrial areas. The dispersion of these elements via fluvial or aeolian transportation poses severe environmental risks. There have been many reports on how heavy metals and metalloids from these mine tailings leak into local surface and groundwater.

Clark and Raven (2004) indicated that the seepage from underground chambers at Giant Mine contains arsenic concentrations higher than 4000 mg/L. It should be noted that there are 237,000 tons of arsenic trioxide dust stored inside the underground chambers in Giant Mine (Clark and Raven, 2004). There are many reports about the seepage of heavy metals and metalloids, especially arsenic, into The Great Slave Lake (Mudroch et al., 1989, Allan, 1979). Wallace and Hardin (1974) investigations showed that the seepage from mine tailing in Giant Mine brings a

significant amount of arsenic, cyanide, and other metals into Yellowknife Bay. When metalloids and heavy metals from the mine tailings spread to the surrounding environment, they enter and accumulate in animals and plants (Koch et al., 2000, Moore et al., 1979). This information draws attention to the threat that the abandoned mine tailings at Giant Mine pose for the region's environment, and to the importance of a plan to remediate these tailings. It also accentuates the fact that storing these hazardous by-products is not an ideal solution.

2.11 Mine tailings

Mine tailings are the residual product of the process of separating the valuable fractions from the by-products of ore. Their composition is directly dependent on the composition of the ore, and the process of mineral extraction used on the ore. Arsenic, mercury, cobalt, and nickel are considered common minerals and elements in mine tailings. In the past, tailings were discarded into low-lying areas or lakes and streams near the mines. As time passed, these tailings occupied larger areas around the mines and spilling pollution into the soil, air, and water. The heavy metals from these mine tailings could migrate into rivers and groundwater, threatening the health and well-being of inhabitants of even further areas. For example in Nova Scotia, the mine tailings containing arsenic released from the gold mines of the late 1800s and early 1900s, are still spread around the province and are one of the sources of arsenic in the groundwater in Nova Scotia, Canada (Government of Nova Scotia, 2010). Falk et al. (1973) reported on the biological effect of mine tailings in Canada's Northwest Territories, but after three decades the problem still exists.

2.11.1 History of Giant Mine

The first reports about the discovery of gold in Yellowknife were in 1896. The discovery of gold in Yellowknife led to the establishment of gold mines around the City of Yellowknife. Among these gold mines, the three main mines were The Discovery Mine, Con Mine, and Giant Mine (Galloway et al., 2012). The operation of extracting gold in Giant started at 1948 (AANDC, 2013). During the first seven months of Giant Mine's operation (May to December 1948), 49,985 tons of ore were used to extract 8,152 ounces of gold, and the rest were disposed of as mine tailings.

The magnitude of tailings which were produced in Giant mine during its half-century of activity (1948 to1999) can easily be estimated. According to reports, 7.6 million ounces of gold were produced during the lifetime of Giant Mine (AANDC, 2013).

In Yellowknife, gold is embedded in arsenopyrite ore. The first step ores go through is exposure to very high temperatures. The by-products of heating these ores are highly poisonous arsenic-rich fumes. Formerly, these poisonous fumes were released into the air via unfiltered stacks. In 1951, the installation of Cold Cottrell Electrostatic Precipitator (ESP) helped remove arsenic trioxide that was created by cooling the gas from the roasters. During the first decade of Giant Mine's operation, gold was separated by using a combination of mercury amalgamation and cyanidation, which can be found in the seepage from the tailings (Mudroch et al., 1989).

During Giant Mine's 50 years of operation, 237,000 tons of arsenic trioxide were produced and stored in underground stopes and chambers. Only 6,700 tons of this waste was sold for wood treatment, and the rest stayed in chambers. In the meantime, there have been reports about the malfunctioning of these chambers, and the seepage of water in and out of them, carrying dissolved arsenic to the surrounding area (AANDC, 2013).

2.11.2 Clean up plan for Giant Mine

Since 2005, Giant Mine was officially abandoned, and remediation activities began. One proposed plan that is being tested is to freeze the ground around the chambers via thermosyphons to prevent water seepage. Remediation plans also involve water and soil treatment or covering the tailing ponds (AANDC, 2013).

2.12 Remediation methods for arsenic contaminated soils and sediments

Over the years, different remediation methods have been developed for the treatment of contaminated soil and sediment. These methods can be categorized into three groups: a) physical, b) chemical and c) biological treatments. Despite these categories appearing entirely distinct in

their methods, in many cases, methods in one category overlap with those in other categories. In many cases, there is a need to combine two or more different methods to achieve the cleanup goal. Some of the common methods for treating heavy metal contaminated soil and sediment are phytoremediation, rhyzostabilization, soil amendments, soil capping, excavation and disposing of in landfills, thermal treatment, stabilization, solidification and chemical extraction.

Although some of these methods are successful in removing heavy metals from soil/sediments, most are not environmentally friendly, some are costly or time-consuming, and others require vast land areas. Some of the methods mentioned above, such as phytoremediation, are not effective on highly contaminated soils, as most plants are not able to grow in highly contaminated soils. There is a need for pre-treatment before the phytoremediation process. Also, in comparison with other remediation methods, the process of phytoremediation takes a long time to show any effect, and there is a chance of transport of the contamination out of the area, by groundwater or precipitation, before the process of phytoremediation can completely clean up the area. Other methods of remediation, such as soil capping, excavation, and disposing of in landfills, are costly and require extensive amounts of land area.

In the recent years, many researchers have studied the effectiveness of using environmentally friendly additives for metal extraction procedures. One of the promising methods is using biosurfactants to enhance the process of removing the contaminants from soil and sediment (Mulligan, 2005). Biosurfactants have been shown to be successful in removing hydrocarbons from soil. However, studies on the ability of biosurfactants to remove metals and metalloids from soil are still in the research phase. During the past decade, numerous researchers have studied the efficiency of various types of biosurfactants in removing heavy metals/metalloids from different media. Their findings confirm the effectiveness of these surface active agents in removing metals and metalloids (Mulligan, 2009). However, the success of a biosurfactant in removing metals from a medium is highly dependent on how strong they can bond with metals, which has to be stronger than the media-metal bond (Mulligan, 1998).

2.13 Soil washing and flushing

The process of soil washing and flushing mobilizes and separates contaminants from the medium by using a washing solution. The washing solution can be merely water or water with additives, such as solvents, acids, bases, surfactants, chelating or sequestering agents, which increases the efficiency of the washing solution (ITRC 1997; EPA, 1996).

2.13.1 In situ soil flushing

The in situ treatment has initially been designed for the treatment of groundwater. Palmer and Fish (1992) point out that the conventional pump-and-treat method is one of the most widely used techniques for the remediation of contaminated groundwater. Later researchers examined the possibility of using the in situ treatment of soil and sediments to decrease the cost of the remediation by avoiding costs related to ex-situ soil treatment, such as excavation and transportation.

In situ treatment reduces the possibility of spreading contamination beyond the contaminated area. According to the data provided in the 14th edition of the Superfund remedy report (EPA, 2013) during past three decades, soil flushing is considered one of the top four methods for soil and sediment remediation in the United States.

These emerging technologies can become more efficient by choosing suitable combinations of washing solutions for the type of contaminant. By introducing more bio-friendly and effective agents, soil flushing can become one of the top environmentally friendly methods. Soil flushing takes less time than the other two methods, bioremediation and phytoremediation. Nowadays, following the discovery of biosurfactants, biodegradable, low to non-toxic, bio-friendly, and efficient washing agent, a new venue in the remediation of soil and sediments, has been opened. At this stage, from the economical point of view, biosurfactants cannot compete with their rival, synthetic surfactants. According to Daverey et al. (2008), 75% of the manufacturing cost of these biosurfactants can be attributed to the raw material being used. By using low-cost raw materials such as soy molasses, sugarcane, beets, restaurants' leftovers and wastes, animal fat, and cheese whey, the cost of production could be significantly decreased.

2.13.2 Ex situ soil washing

Ex situ soil washing is one of the most common techniques for treating contaminated soil and sediment (Deshpande et al., 1998). In this technique, the contaminated soil is excavated and depending on the type of contaminant and the volume of the soil, it is either sorted so that the most contaminated fraction of the media is separated for further washing or disposal, or the contaminated matrix is washed using a suitable washing solution. By conducting a series of ex-situ soil washing tests prior to in situ soil washing, necessary information will be obtained for screening and choosing the most efficient combination of washing solutions for the given soil contamination.

Soil washing by using an adequate washing solution has shown to be an extremely effective method for simultaneous removal of organic contaminants and heavy metals. According to Guemiza et al. (2017), the efficiency of soil washing can be increased by accompanying it with other physical and chemical methods. The attrition process is a physical remediation method which significantly enhances the efficiency of the process of soil washing and decrease the cost of that process (Guemiza et al., 2017). The attrition method is used for coarser particles and the finer particles go through the process of soil washing (Metahni et al., 2017). In attrition, the coarser particles are broken down as the consequence of the collision between the particles and release the contaminants which concentrate in the finer particles (Metahni et al., 2017). Combining the process of soil washing with one of the physical separation methods, decreases the operational cost and increases the efficiency of the remediation (Metahni et al., 2017). According to Metahni et al. (2017), using attrition combined with alkaline leaching resulted in the simultaneous removal of heavy metals and organic contaminants from the soil. Their findings revealed that in the leaching part of their experiment, combining an amphoteric surfactant, Cocamidopropyl betaine (BW), to the leaching solution (NaOH), increases the removal of both inorganic and organic contaminants. Combining the washing process with one of the separations methods is very useful to reduce the cost of remediation. The reduction of the cost is very important in the case of remediating large quantities of contaminated soil and sediments, as well as mine tailings. Mercier et al. (2017) introduced a multi-step remediation process for decontaminating soils from inorganic and organic pollutants. In their proposed method, fractioning based on the size of the grains takes place, and

the courser particles are separated from the smaller particles. Then, the finer particles are treated in a leaching process by using a solution consisting of an inorganic base and a surfactant. The coarser particles are treated by attrition and sludge from this part is separated and goes through chemical leaching process. The effluents from these steps are treated through precipitation-coagulation, to be used in the process of leaching all over again. Their proposed method was not only successful in removing inorganic and organic contaminants, it was also more economically feasible than one step processes.

2.14 Biosurfactants

A variety of microorganisms produce a broad range of surface active agents called biosurfactants, which have great surface active properties, low toxicity, and they are biodegradable. Biosurfactants are amphiphilic molecules, which means they contain a hydrophilic head group and a hydrophobic tail group. These two moieties are responsible for the dual nature of these biomolecules. They adsorb at interfaces of two immiscible liquids, like oil and water, or at the interface water and solid surfaces or air. Therefore the presence of biosurfactants would reduce the interfacial energy, which makes these active agents, produced by bacteria or yeast, potentially useful in various applications.

The ability of these surface active agents to increase the solubility of the hydrophobic materials, and the fact that they are produced from renewable resources, are the main reasons that many researchers are interested in using these environmentally friendly surface active agents in environmental applications. They can be used for enhanced oil recovery, remediation of organic compounds from soil, and solubilization and removal of heavy metals from contaminated soil and sediments (Mulligan, 2005). Although biosurfactants are useful in the removal of heavy metals from contaminated soil and sediments, the mechanism of removal is different depending on the type of biosurfactant. According to Mudgil (2011), anionic biosurfactants, such as rhamnolipids, remove heavy metals from contaminated soils by forming ionic bonds complexes with cationic heavy metals, removing them from the solid phase and transferring them to the washing solution. However, cationic biosurfactants compete with the cationic heavy metals to replace the metal ions

on the negative surfaces through the ion exchange mechanism. According to Wang and Mulligan (2009a), increase in pH level cause the dissociation of carboxylic groups of biosurfactants (such as rhamnolipids) and increase the charge density of their head groups, consequently increasing the repulsiveness of the hydrophilic head group, and forming high-curvature micelles. Metal ions bind with polar groups of micelles and are mobilized and washed away from the soil (Gaspard & Ncibi, 2013).

With respect to their chemical compositions, biosurfactants are divided into groups, such as lipopeptides, glycolipids, fatty acids, polysaccharide-protein complexes, peptides, phospholipids, and neutral lipids (Banat *et al.*, 2010). They can also be classified according to their microbial origins, physiochemical properties, and mode of action (Banat et al., 2010; Nie et al., 2010). Generally, desirable properties of biosurfactants include solubility enhancement, surface tension reduction, and low critical micelle concentration (CMC) (Mulligan, 2005). Operational factors such as foam generation, and turbidity, as well as economic considerations, will be important in choosing a biosurfactant assisted remediation system.

Altogether, in the practical sense, they are divided into two main classes: low molecular weight and high molecular weight biosurfactants (Banat *et al.*, 2010, Franzetti *et al.*, 2010). The low molecular weight biosurfactants can reduce the surface tension at the air/water or oil/water interface, while the high-molecular-weight biosurfactants act as a bio-emulsifiers and can stabilize oil-in-water emulsions (Banat *et al.*, 2010). Most biosurfactants are either anionic or neutral, while only a few are cationic.

Although biosurfactants have shown excellent potential in various fields, their high cost of production has caused them not to have the same commercial success as synthetic rivals. Therefore, increasing the production of biosurfactants and decreasing the expenses related to production has been the focus of many investigations during the past decade. This objective can be achieved by choosing high-yield strains and inducing mutations in existing strains in order to produce the desired congeners and homologs. It can also be achieved by optimizing the condition of production, using low-cost substrates, developing economical methods for filtration, and by finding methods for recycling them.

2.14.1 CMC value of biosurfactants

At lower concentrations, biosurfactants exist merely as monomers which adsorb at interfaces. As the concentration of biosurfactants increase and interfaces become saturated, the concentration reaches a critical point, known as the critical micelle concentration, in which monomers start to form aggregates. The shape and the size of the aggregates are highly dependent on the concentration of biosurfactants, the temperature, the pH, their molecular structures, and the presence of additives (Li et al., 2015; Kim et al., 2011). The aggregate can be tube-shaped vesicles, spherical micelles, or rod-like micelles. The critical micelle concentration (CMC) of the biosurfactants is affected by temperature, pressure, as well, the presence and concentration of other surface-active substances, such as surfactants, biosurfactants, and electrolytes (Song et al., 2012, Song et al., 2013, Helvacı et al., 2004).

Moreover, the CMC of biosurfactants depends on the source of production and the type of bacteria used to produce them. For example, rhamnolipids produced by different strains of *Pseudomonas aeruginosa* display different CMC values. This confirms that the CMC is structure dependent. Different strains produce difference mixtures of compounds. It also depends on environmental conditions. According to Mulligan (2009), some strains of *Pseudomonas aeruginosa* were able to produce rhamnolipids that display critical micelle concentrations (CMC) ranging from 10 to 230 mg/kg and were able to decrease the surface tensions of water from 72.9 to 29 mN/m.

The critical micelle concentration (CMC) of a biosurfactant is the intercept of two straight lines from the concentration-dependent and concentration-independent sections of the graph of surface tension vs. logarithmic of biosurfactant concentration (Kim et al. 2001). Although this method is one of the easiest ways for measuring the quality of a biosurfactant, it should be noted that the presence of other components in the solution can cause errors in the results. Moreover, it should be pointed out that the CMC should be considered as a range of concentrations and not a point, as by changing the concentration, the size of aggregate changes and affects the CMC value. The other factors influencing the CMC are the presence of congeners and homologs of the

biosurfactant in the solution. As homologues and congeners have their CMC value, the CMC of the mixture depends on the ratio of each one. When biosurfactants are not homogenized thoroughly, the sample taken from the solution after dilution, may not retain the original ratios of congeners and homologues. Therefore the obtained CMC value cannot precisely determine the CMC value of the original sample.

According to Wilson (1989) solubilization happens in concentrations above the surfactant critical micelle concentration (CMC). Beyond the CMC concentration, the degree of the solubilization is a linear function of surfactant concentration. By determining the CMC of the biosurfactants, the minimum concentration that micelles would be formed, and the lowest concentration for the optimum performance of biosurfactant solution is determined. Furthermore, by measuring the CMC of the effluent from the experiment, biosurfactant concentration in the effluent can be determined, and the correlation of biosurfactant adsorption to the media to biosurfactant concentration can be determined.

There is a considerable difference between the values of the CMC of different types of biosurfactants. The lower the CMC value is, the less of the biosurfactant is a need. The cost of biosurfactants is a significant portion of the remediation cost, and it corresponds to the quantity of the biosurfactant being used. Therefore, one of the properties that makes a biosurfactant desirable is having a low critical micelle concentration (CMC) (Mulligan, 2005).

According to Wang and Mulligan (2009b), the efficiencies of biosurfactants in removing contaminants increase linearly as the surfactant concentration increases, until it reaches the CMC concentration. Beyond the CMC point, the effectiveness of biosurfactants remains moderately constant. The researchers above recommended using higher concentrations than the CMC concentration to overcome the effects of surfactant sorption by mine tailing particles (Wang and Mulligan 2009a).

2.14.2 Rhamnolipids

Rhamnolipids (Rh) are anionic glycolipid biosurfactants that are mainly produced by *Pseudomonas aeruginosa,* a pathogenic gram-negative bacterium that can be found in different environments. Figure 2.7 illustrates the structure of four different rhamnolipid congeners (Mulligan, 2005). Rhamnolipids were first isolated from *Pseudomonas aeruginosa* in 1949 by Jarvis and Johnson (Gunther *et al.*, 2005). In recent years, there have been many investigations to find new species of microorganisms that are also able to produce rhamnolipids. Based on these articles, it can be said that most rhamnolipid-producing strains were found and isolated from oil contaminated soil around refineries. In these harsh environments, with high salinity and a lack of other sources of carbon and nutrients, these microorganisms have evolved to survive by using hydrocarbons as a source of carbon. As well, they have adapted to survive in both aerobic and anaerobic environments. One of the survival strategies of these microorganisms consists of producing rhamnolipids. These organic compounds help the bacteria to move easily towards a source of nutrients, or away from a place where the level of nutrients is lower, and the level of toxins is higher. It also aids in eliminating competitors. Rhamnolipids solubilize hydrocarbons in order to be absorbed through the cell membrane of the bacterium. Furthermore, Kaczorek *et al.* (2012) reported that rhamnolipids change the cell surface of the bacteria by increasing the hydrophobicity of the cells, allowing them to absorb hydrophobic compounds such as petroleum hydrocarbons. This process enhances the biodegradation of these toxic compounds. Moreover, Kaczorek *et al.* (2012) reported that among all their chosen genera *Bacillus*, *Pseudomonas*, *Aeromonas*, *Achromobacter* and *Flavimonas*, the addition of rhamnolipids affected the cell membrane of the *Pseudomonas* genus more than any other genera. Their experiments showed that the *Pseudomonas* genus was the most effective genus in the bioremediation of petroleum. Rhamnolipids are effective agents for removal of heavy metals from soil and sediments (Mulligan, 1999). Rhamnolipids form stable complexes with cationic heavy metals, and the affinity value of rhamnolipids for metals has been shown to be higher or equal to many organic acids (Ochoa-Loza et al., 2001).

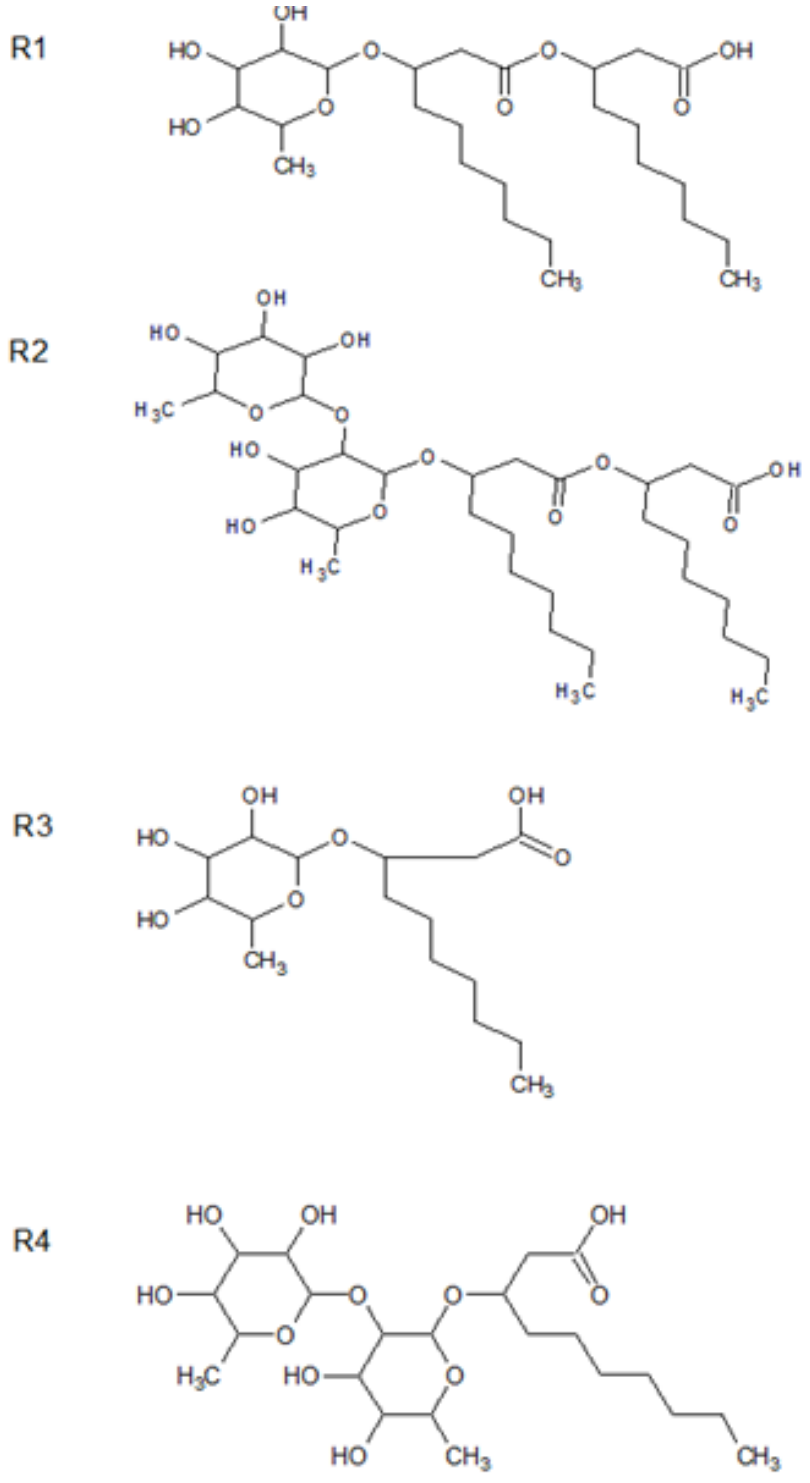

Figure 2.7. Structure of four different congeners of rhamnolipids (Mulligan, 2005)

Bergstrom (1946), Hauser and Karnovsky (1954), Jarvis and Johnson (1949) and Edwards and Hayashi (1965) were known as the pioneers in the research on rhamnolipids (Abdel-Mawgoud *et al.*, 2011). They took the first steps toward discovering the exact chemical nature of these biomolecules and their structural units. Due to rhamnolipids' significant tensio-active and emulsifying properties, it has shown a vast potential in diverse fields (Lotfabad *et al.*, 2010). There have been many investigations focused on this biosurfactant in order to decode its biosynthetic pathway (Abdel-Mawgoud *et al.*, 2011). In recent years, with the advancement of accurate methods of analysis, there have been significant advances in understanding these biomaterials.

Research on rhamnolipids and their production has resulted in the development of a range of techniques for isolating a few different rhamnolipid producing bacterial strains. As well as characterizing rhamnolipids homologs and congeners, and understanding of genetic details underlying rhamnolipid production in *Pseudomonas aeruginosa* (Abdel-Mawgoud *et al.*, 2010, Rezanka *et al.*, 2011). *Pseudomonas aeruginosa* is a common bacterium that is able to survive in a variety of environments. These bacteria are easy to cultivate, and after relatively short incubation periods, they are able to produce relatively high yields of rhamnolipids (Nguyen *et al.*, 2011).

However, in an acidic environment, rhamnolipids are separated from the solution and precipitate (Dahrazma et al., 2008). On the other hand, sophorolipids are acidic surfactants and are active at different pH levels, although according to the manufacturer (Ecover, 2014), the optimal pH level for these biosurfactants is between 6 and 10. Thus, there is no need for drastic pH adjustment in the sophorolipid solutions.

2.14.3 Sophorolipids

Sophorolipids (SL) are a mixture of anionic and nonionic glycolipid biosurfactants. Yeasts of *Candida* sp. are known as the primary producers of these biosurfactants. Among these yeasts, *Candida bombicola* has been known as the primary producer of SL. Two other members of the genus *Candida* that can produce sophorolipids are *Candida apicola* and *Candida bogoriensis* (Cavalero & Cooper, 2003). These non-pathogenic yeasts can produce high amounts of SL while using vegetable oils and sugars as their carbon source (Mulligan, 2005). *Candida bombicola*, under

optimum conditions, is able to produce levels as high as 400 g/L of sophorolipids (Van Bogaert, et al., 2011). The high production rate and thus lower production price make sophorolipids an eligible competitor with rhamnolipids for use in many applications.

The current production price of sophorolipids depend on the substrates being used and the scale of production, according to Van Bogaert et al. (2007) and ranges from 2 to 5 €/kg. According to a model developed by Ashby et al. (2013), using glucose and oleic sunflower oil/ oleic acid, the production rate could be 90.7 million kg/year, with a price of US$2.95/kg.

The sophorolipids' structure depends on the strain of the producer (Van Bogaert et al., 2011) and the substrate that the yeast grew on (Cavalero & Cooper, 2003). The findings of Cavalero and Cooper (2003) showed that, although these yeasts need carbohydrate substrates for their survival and sophorolipid production, by adding a hydrophobic substrate, the production rate increases. Raw sophorolipids are a mixture of acidic sophorolipids (anionic surfactant) and lactonic sophorolipids (non-ionic surfactant). The ratio between the two congeners depends on the substrate and environment conditions (Baccile et al., 2013; Weber et al., 2012; Hirata et al., 2009).

The types and ratios of the congeners dictate the physicochemical properties of the sophorolipid solutions. Acidic sophorolipids are composed of a glucose disaccharide head (sophorose), and the hydrophobic part is made of hydroxylated fatty acid (oleic acid) bonded together through an ether bond. This structure along with having free carboxylic acid groups, cause acidic SL to have higher rates of foam production and increased solubility. On the other hand, acidic sophorolipids are more susceptible to changes in the environment (Baccile et al., 2013). Lactonic sophorolipids form when the carboxylic group of its hydrophobic tail esterifies to the hydroxyl group of its hydrophilic head (Morya and Kim, 2014). Lactonic sophorolipids display a superior surface tension lowering ability, and show more antimicrobial and anti-fungal activity (Van Bogaert et al., 2011; Yuan et al., 2011). Lactonic sophorolipids have been shown to efficiently inhibit the growth of various types of cancer cells, such as leukemia inducing cells (K562 cells) (Chen et al., 2015). Figure 2.8 illustrates the structure of both types of sophorolipids produced by *C. bombicola.* The sophorolipids produced by *C. bombicola* are a mixture of several kinds. Their

fatty acids have different lengths, saturation, positions of hydroxylation, and different lactonization and acetylation patterns.

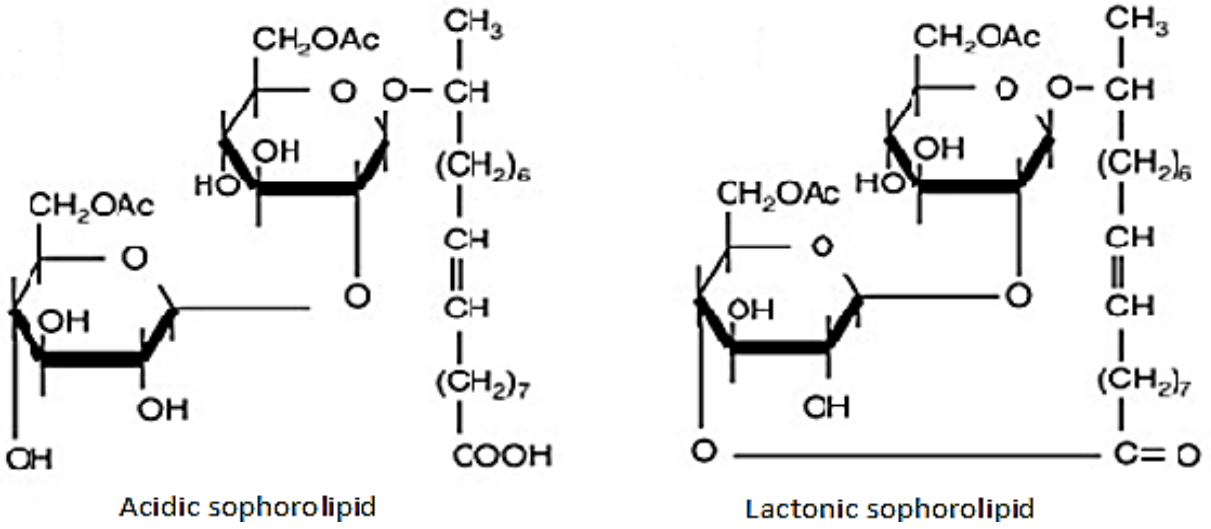

Figure 2.8. Structure of two primary types of sophorolipids produced by *C. bombicola* (Rau et al., 2001).

Sophorolipids have been observed to show antimicrobial activities, mostly against gram-positive bacteria strains (Ashby et al., 2011). This property opens a new venue of applications for this biosurfactant. Sophorolipids have shown success in several industrial applications, but the higher cost of sophorolipid production compared to the cost of synthetic surfactant production is the main reason preventing them from being used in industries (Ashby et al., 2013). According to Hirata et al. (2009), sophorolipids display remarkably low toxicity and high biodegradability. Their experiments showed that 61% of the sophorolipids degraded after eight days of cultivation, according to the standard biodegradation test. These results placed sophorolipids in the class of readily biodegradable substances (Hirata et al., 2009).

Sophorolipids lower the surface tension of water at 20ºC from 73 mN/m to 30–40 mN/m, depending on the ratio of the congeners and the length of their hydrophobic tails. They are able to withstand high salinity without changing their properties, and they are active in a variety of temperatures, and acidic to neutral environments (Van Bogaert et al., 2011). These properties

combined with sophorolipids' low critical micelle concentration (CMC), their high production rate, high biodegradability, and their low toxicity make these biosurfactants ideal candidates for being used in a wide range of applications and different industries.

2.14.4 Fourier transform infrared spectroscopy (FTIR) analysis

The wave numbers corresponding to the functional groups within the sophorolipid structure depends on both the species being used and the substrate on which the fungi grew on. For instance, the sophorolipids used in the present study (SL 18), *Candida bombicola* ATCC 22214 were cultured on a substrate consisting of rapeseed oil and glucose. As it can be seen the FTIR spectrum for SL 18, the O-H stretch is at 3323 cm^{-1}. On the other hand, Bajaj and Uday (2015) analyzed the spectrum of sophorolipids produced by *Starmerella bombicola* NRRL Y-17069, which used castor oil as a secondary carbon source, and determined that the O-H stretch was at 3419 $cm^{-1.}$ Also, as shown in Table 2.2, in lactonic sophorolipids analyzed by Daverey and Pakshirajan (2010) and Daverey and Pakshirajan (2010) and acidic sophorolipids analyzed by Baccile et al. (2013), the functional groups differ by both their wavenumbers and their presence and absence.

Chandran and Das's (2011) experiments showed that *Candida rugosa* and *Rhodotorula muciliginosa* were able to produce diacetate acidic sophorolipids and monoacetate lactonic sophorolipids. By comparing the FTIR spectra from these strains to the FTIR spectrum of SL18, a mixture of acidic and lactonic sophorolipids produced by *Candida bombicola*, it was shown that the structure and wave number of functional groups within the sophorolipids is dictated not only by the substrate being used but also by the strain of the microorganism which produces them. Table 2.2 summarizes a comparison between the functional groups of SL18 and other sophorolipids.

Table 2.2: Summary of a comparison between the functional groups in SL18 with a few other types of sophorolipids, produced by using different substrates or by various species than *Candida bombicola*.

Functional group / References	O-H	$\upsilon_{as}CH_2$	υ_sCH_2	C＝O	C=C	COOH	C-O	C(=O)–O–C	C-O-H
	Wave no. (cm^{-1})	Wave no. (cm^{-1})	Wave no. (cm^{-1})	Wave no. (cm^{-1})	Wave no. (cm^{-1})	Wave no. (cm^{-1})	Wave no. (cm^{-1})	Wave no. (cm^{-1})	Wave no. (cm^{-1})
Arab & Mulligan (2017)	3323	2930	2853	1636		1412	1078		1033
Bajaj & Uday (2015)	3419	2925	2853	1742			1240	1036 1080	
Daverey & Pakshirajan (2010)	3403	2926	2854	1747	1624		1157		1035
Chandran & Das (2011)	3410 - 3434	2920-2926		1620-1627 1744			1157		1048
Shah & Prabhune (2007)				1744		1048	1157	1445	1048
Daverey & Pakshirajan (2009).	3,403	2,926	2,854	1744	1624			1157	1035
Baccile et al. (2013)	3490	3004 2950	2850	1535 (υ_{as}) 1418 (υ_s)	1705		1024		1069
Hu & Ju (2001)	3433	2926	2857	1744	1624	1445	1157 1247		1048

2.15 Summary and conclusions

Abandoned mine tailings are a significant threat to the environment. Despite the many reports about their impact on the environment during the years, there has not enough action towards

the remediation of these tailings. These reports also stress the fact that storing these hazardous by-products is not an ideal solution.

Biosurfactants have shown promise in being a suitable candidate for use in the process of contaminated soil and sediment remediation. They can be utilized for removing both oil and heavy metals/ metalloids from the contaminated medium. Wang and Mulligan (2009)'s research demonstrated the effectiveness of rhamnolipids in removing arsenic and heavy metals from mine tailings. Previous research has shown that there is a need for further research on the efficiency of less costly biosurfactants which can remove pollutants from soil and sediment. Furthermore, there is also a need for further investigation on the effects of these biosurfactants on the medium, and on the mechanism of heavy metal/ metalloid removal.

The present study focuses primarily on the physiochemical properties of the mine tailing sample to elucidate the depth of the problem. The high concentration of the heavy metals/ metalloids on these tailings is not the only property that is discussed. Other properties such as size, organic content and cation exchange capacity of the samples which affect the retention of elements is investigated and discussed. For instance, the total surface area of the medium per unit mass or specific surface area (SSA) is one of the significant factors which affect the adsorption capacity of the sample. The specific surface area of a medium is correlated to the clay-size fraction of the medium and has a negative correlation with the total organic matter. The specific surface area affects the medium's cation exchange capacity, water retention, movement within the medium, and the medium's ability to adsorb heavy metals and other contaminants (Petersen et al., 1996). The cation exchange capacity (CEC) of a medium is another important factor which represents the number of negativity-charged sites on the medium (Astera, 2010). The cation exchange capacity is a measure of a medium's ability to retain or release different elements. Furthermore, by measuring the pH level of the mine tailing, the heavy metal/metalloid retaining capability of the medium is determined. Also, the quantity of the organic matter within the medium is a major factor, a medium with a higher ratio of organic matter can retain a greater quantity of metals/ metalloids. Finally, by investigating the elemental composition of the sample, the bioavailability of the heavy metals and metalloids within the mine tailing sample can be determined.

The next step is to focus on the effect of sophorolipid biosurfactants on mine tailings, and its efficiency for removing arsenic from mine tailings. Additionally, the effect of the sophorolipids on metalloids and metals, as well as, on different fractions of a mine tailing sample, and the mechanism of arsenic removal by sophorolipids were investigated and discussed.

CHAPTER THREE: MATERIALS AND METHODS

This study was done in two phases. Phase one of this study consisted of investigating the physiochemical properties of the mine tailing sample. In the second step, the effects of sophorolipids on the removal of arsenic and other metal/ metalloids from the mine tailings were evaluated.

3.1 Analytical apparatus

The analytical apparatus used in this research were: ICP mass spectrometer (ICP-MS) Agilent 7700 (Tokyo, Japan) equipped with a plasma frequency-matching RF generator and an octopole reaction collision cell and with detection limit of 0.1 ppb for arsenic, Niton XLp 700 cadmium base X-ray Fluorescence Analyzer (XRF) Laser Scattering Particle Size Distribution Analyser (Horiba Partica, LA950V2- Kyoto Japan), SEM/ EDS-SEM: JEOL 35-cf equipped with EDAX system for elemental analysis (Hitachi S-3400N), Fisher Scientific Tensiomat model 21 which uses du Noüy ring method for direct results and has an accuracy equal data from capillary-height or drop-weight measurements to within ±0.25%, Philips X'Pert Pro Multipurpose X-ray Diffractometer (XRD), Aokton Electronic pH meter, and Denver Analytical Balance (Denver Instrument, SI 234; NY, USA), Brookfield digital viscometer, model DV-II (Brookfield AMETEK Middleboro, Massachusetts, USA), Dynamic Light Scattering (DLS) NanoS90 with red laser of 632.8 nm (Malvern Instruments Ltd, Malvern, UK), Fourier transform infrared spectroscopy (FTIR), Thermo Scientific, 4700 (Thermo Fisher Scientific Waltham, MA USA), Zeta-Meter System 3.0+ (Zeta-Meter Inc., Staunton, VA, USA).

3.2 Experimental apparatus

The setup of the continuous experiment, as seen in Figure 3.1, is composed of two Plexiglas columns (length: 15 cm and inner diameter: 1.5 cm), a column holder, tubing, a peristaltic pump (Cole Parmer Instrument Company, Montreal Canada), and volumetric and Erlenmeyer flasks for preparing and storing the inlet and outlet streams.

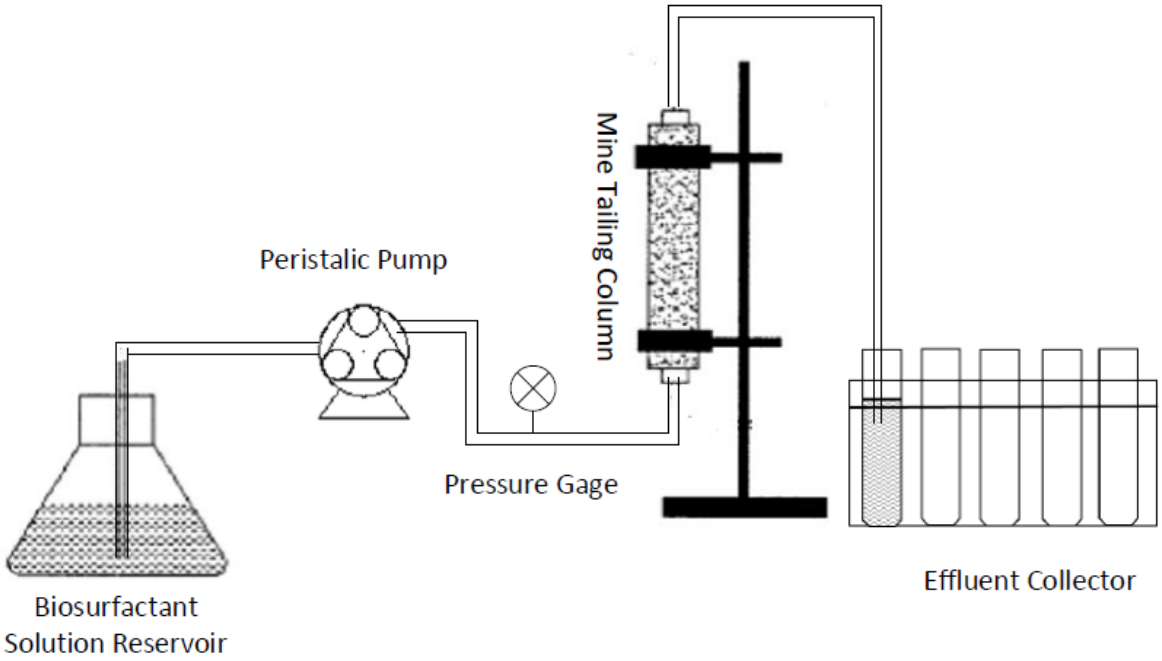

Figure 3.1. Schematic of the experimental setup.

Although filters used in continuous systems are usually chosen to have openings smaller than the grain size, preliminary experiments showed that filters smaller than the grain size were not permeable enough. When filters with pore sizes larger than the grains were used, it has been demonstrated that finding an optimal size is crucial for the experiment, as filters with smaller openings get clogged and cause interruptions. On the other hand, larger filters cause the loss of the sample during the experiment. In this study, the filters used in the continuous operation were three layers of unwoven geotextile (TE-GTN350), supplied by Titan Environmental Containment Ltd, and aerator air stones which were bought from Uxell, Hong Kong. The unwoven geotextile had a 75 µm pore size and was made from long fibers of polyester. The second filter was an air stone, which was made from glass and plastic and had an effective pore size of 50 µm.

3.3 Statistical analysis

For the first part, one-way analysis of variance (ANOVA) was used to investigate the result of measuring the concentration of heavy metals/ metalloids untreated and sample treated with

sophorolipids and DI water in batch and continuous experiments, to make sure that the p-value is less than 0.05, to confirm the reliability of the results. In this study, both linear and nonlinear regression models were fitted. A line of best fit with the highest coefficient of determination (R^2) for linear one and the adjusted coefficient of determination for nonlinear regression model were created. For determining the correlation between the removals of elements, the Pearson correlation coefficient (r) was obtained.

$$r = \frac{\sum(x_i - \bar{x})(y_i - \bar{y})}{\sqrt{(x_i - \bar{x})^2 \ \ (y_i - \bar{y})^2}}$$

Statistical analysis was conducted in Excel and STATA (version 12).

3.4 Materials

The materials used for the experiments were the following:

Nitric acid (HNO_3), calcium chloride ($CaCl_2$), hydrochloric acid (HCl), sodium hydroxide (NaOH), ethylene glycol monoethyl ether (EGME), potassium acetate (KCH_3COO) and sodium dodecyl sulfate (SDS) were purchased from Fisher Scientific Co. (Canada). Arsenic trioxide (As_2O_3), disodium hydrogen arsenate heptahydrate ($Na_2HAsO_4 \cdot 7H_2O$) and dimethyl arsinic acid (DMAA) were purchased from Sigma-Aldrich, USA. Disodium methyl arsenate (DSMA) was Supelco-PS281 fromSigma-Aldrich, Bellefonte, PA, USA. Sodium cacodylate trihydrate was Sigma-C0250 from Sigma-Aldrich, Bellefonte, PA, USA. The reagents were of analytical grade.

The deionized water used in this study was prepared by the Milli-Q® Integral Water Purification system (MilliporeSigma, Darmstadt, Germany). The DI water had an internal specific resistance of 18.2 MΩ, and the conductivity was 0.055 microsiemens.

3.5 Biosurfactants

In the experiments, two glycolipid biosurfactants were used, rhamnolipids and sophorolipids. The rhamnolipids utilized in this research, JBR425, are a mixture of mono-

rhamnolipids and di-rhamnolipids. It was purchased from JENEIL Biosurfactant Co. (Saukville, WI, USA). The critical micelle concentration (CMC) of this biosurfactant was found to be 35.7 mg/L equal to 0.003% rhamnolipid (Arab & Mulligan, 2014).

Sophorolipids (SL) are the other biosurfactants being used in this study. The high production rate, and thus lower production price make sophorolipids an eligible competitor with Rhamnolipids for being used in many applications. The sophorolipids used in this experiment were Ecover 41% sophorolipids (SL18), high lactonic SL, donated by Ecover Co., Belgium (Figure 3.2). It was a mixture of 30% acidic sophorolipids and 70% lactonic SL. These sophorolipids were produced by yeast *Candida bombicola* growing on a mixture of vegetable oil (rapeseed oil) and glucose (Develter and Lauryssen, 2010).

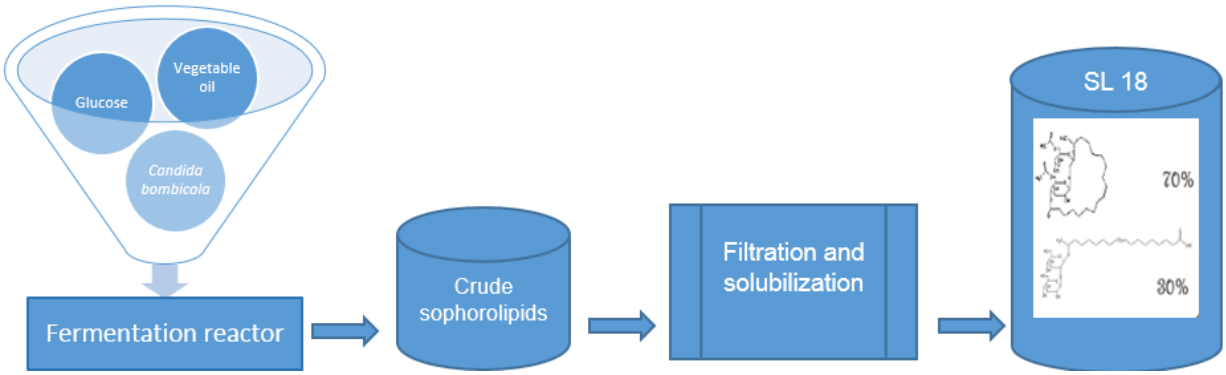

Figure 3.2. SL18 production diagram (Ecover, Belgium 2014).

The critical micelle concentration (CMC) of this biosurfactant was measured before starting the experiment to ensure its quality. The results are discussed in the next chapter. Table 3.1 summarizes the SL18 information.

Table 3.1. General specifications of the high lactonic sophorolipids SL18 (Ecover, Belgium 2014).

Parameter	Value
Active matter	41%
Appearance	Dark colored liquid solution
pH	4.9 ±0.5
Minimum surface tension	32-34 mN/m
Foaming capability	Low
Wetting properties	High, fast

3.6 Mine tailings sample

Mine tailing samples were taken from Giant Mine (formally Royal Oak Mines), a former gold mine located within the City of Yellowknife, Northwest Territories, Canada. The samples were collected from the south pond, which is one of the older tailing ponds. The sample is a mixture of mine tailings taken from different depths of the pond, from the surface to a depth of 1.2 m. The sample was brought to the laboratory and was kept in an air-tight container to preserve the physical and chemical qualities of the mine tailings. The main physicochemical properties of the mine tailings sample, such as water content, organic content, pH, particle size distribution and metalloid/ heavy metal content of the samples, when it was received in the laboratory, were measured.

3.7 Overview of the first phase of experiments

- Experiments in phase one consisted of different tests to investigate the physiochemical properties of the mine tailings sample (Figure 3.3).

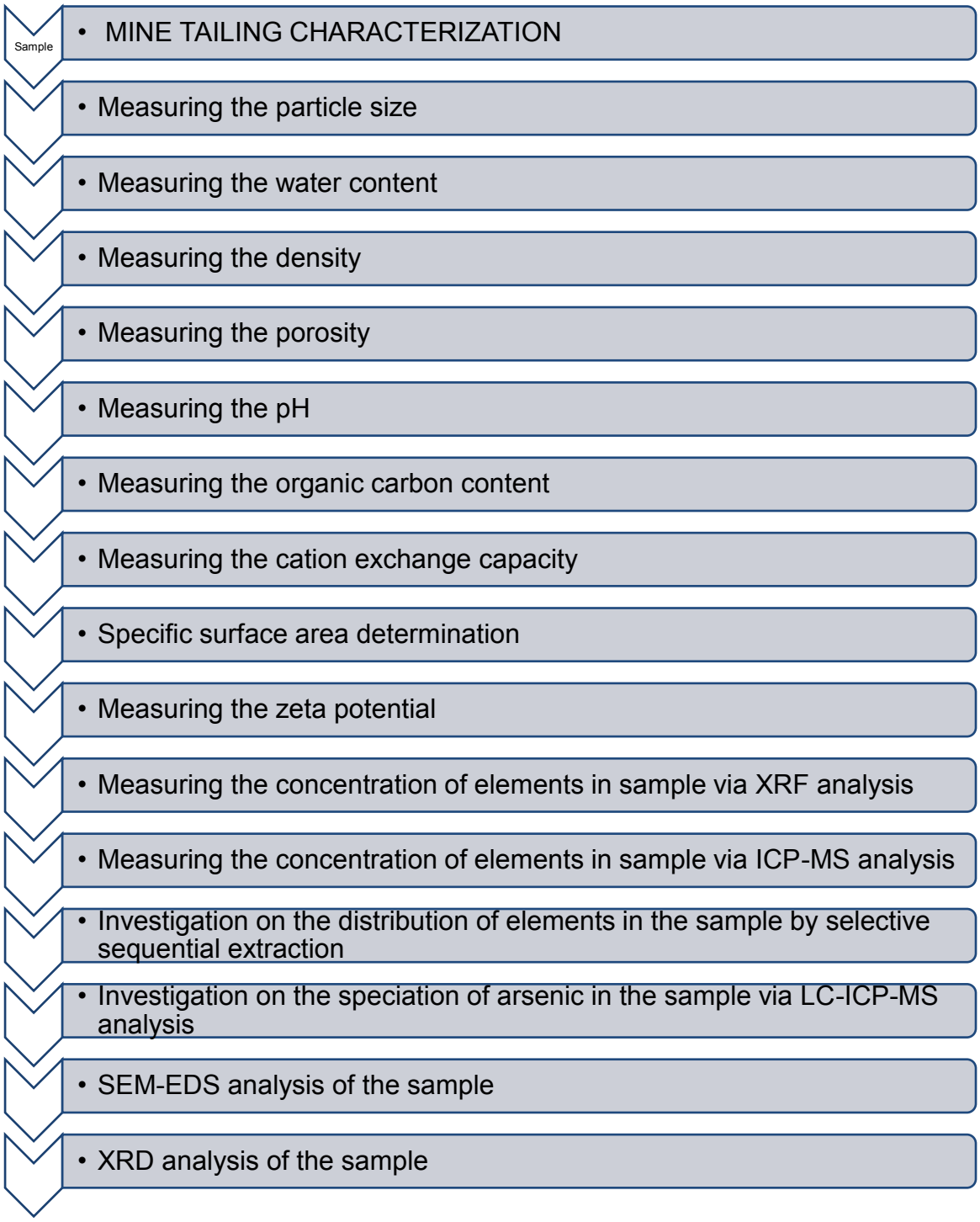

Figure 3.3. Diagram of phase one of the research.

3.9 Preliminary measurement of element concentration

In the first step, the Niton X-ray fluorescence (XRF) analyzer was used to detect the presence and the relative concentration of elements within the sample. Air-dried samples were sieved through a 250 μm sieve. The sample was placed in the sample holder to be analyzed by the XRF.

3.10 Measurement of element concentration with ICP-MS analyzer

The ICP-MS (Agilent 7700) was used to determine the exact concentration of target elements within the sample. This technique enabled us to measure trace metals in the sub-parts per trillion range. In this simultaneous multi-element analytical tool, samples are broken down to ions in a high-temperature argon plasma, and then analyzed based on their mass-to-charge ratio. The process was completed in three modes; without gas, with helium, and with hydrogen.

To analyze the sample with the ICP-MS, elements that are to be measured (arsenic, iron, molybdenum, antimony, and chromium) should be in a soluble form. Therefore, samples were digested in several steps, using different reagents (concentrated HNO_3, 30% H_2O_2, concentrated HCl, deionized water) according to EPA Method 3050B, and then filtered through Whatman No. 1 filter paper into a sample container.

Samples were then further filtered through a 0.2 μm filter, diluted to make sure the concentration of arsenic in the sample is in the range of 1 to 50 ppb (μg/L) for more accurate analysis by ICP-MS. Then the diluted samples were acidified further by using nitric acid (1%) and hydrochloric acid (0.5%) to be analyzed with ICP-MS to measure the concentration of the elements in the solution. The nitric acid and hydrochloric acid is used in this part of the experiments are high purity trace metal acids. Using the correction equation (Equation 3.1), the interference of argon and chlorine is accounted for, and a more realistic arsenic concentration is obtained (Neubauer, 2010).

$$^{75}As = ^{75}As - [3.127 \times (77Se - (0.322 \times {}^{78}Se))] \quad \textbf{Equation 3.1}$$

Which can be interpreted as:

^{75}As signal = total signal in mass 75 – (3.127 x (signal in mass 77 – (0.322 x signal in mass 78)).

3.11 Particle size distribution

To determine the particle size distribution of the mine tailings, they were analyzed with a Laser Scattering Particle Size Distribution Analyzer (Horriba, LA-950), in the Department of Building, Civil and Environmental Engineering (BCEE), Concordia University. This laser diffraction analyzer is able to accurately determine particle size and reveal the mean diameter of particles from 0.1 to 3000 μm. The particle size distribution was calculated based on the number of particles.

3.12 Coefficient of uniformity (Cu), coefficient of gradation (Cc) and sorting index (So)

The coefficient of uniformity (Cu) of the mine tailings was calculated according to Equation 3.2:

$$\mathbf{Cu = D_{60} / D_{10}} \qquad \textbf{Equation 3.2}$$

Where D_{60} and D_{10} are the diameters, corresponding to the 60% and 10% finer in the particle-size distribution. The higher the value of Cu is, the larger the range of particle sizes in the soil is. A Cu greater than 4 represents a well-graded soil, and a Cu less than 4 indicates r a poorly graded soil. A Cu of ~ 1 represents a uniformly graded soil.

The coefficient of gradation (Cc) was calculated via the equation:

$$\mathbf{Cc = (D_{30})^2 / (D_{10} * D_{60})} \qquad \textbf{Equation 3.3}$$

Where D_{30}, D_{10}, and D_{60} are the diameters corresponding to 30%, 10% and 60% finer in the particle-size distribution. A Cc in the range of 1 to 3 represents a well-graded soil (Ameratunga et al., 2016).

The sorting index (So) shows how uniform the grains of soil and sediments are. According to Task (1932), a So less than 2.5 represents a well-sorted soil, a So value between 2.5 to 3.5 represents a normally sorted soil, if 3.5<So<4.5, this means the soil is somehow sorted, and when So is greater than 4.5 the soil is poorly sorted. Calculation of the sorting index of the untreated specimen and a sample treated with a 1% sophorolipid solution in a continuous setup, was done by following the Trask (1932) method:

$$\mathbf{So = (Q_3/Q_1)^{1/2}} \qquad \textbf{Equation 3.4}$$

Q_3 and Q_1 refer to quartiles (75% and 25%) on the cumulative frequency curves.

Furthermore, to obtain a better understanding of these samples, the sorting coefficient was also calculated according to the methods described by Folk and Ward (1957):

$$\mathbf{\sigma = [(Ø_{84}-Ø_{16})/4] + [(Ø_{95} – Ø_5)/ 6.6]} \qquad \textbf{Equation 3.5}$$

A comparison between the sorting classifications of Task (1932) and Folk and Ward (1957) can be seen in Table 3.2. The phi value represents the cumulative frequency at a particular percentile level. To translate the diameter from millimetre to phi the following equation is used:

$$Ø = - \log 2 \text{ (particle diameter (mm))} \qquad \textbf{Equation 3.6}$$

Table 3.2. Sorting classification according to Task (1932) and Folk and Ward (1957).

Task (1932)	Folk and Ward (1957)	Classification
$So = (Q_3/Q_1)^{1/2}$	$\sigma = [(Ø_{84}-Ø_{16})/4] + [(Ø_{95} – Ø_5)/ 6.6]$	
$So < 2.5$	$\sigma < 0.35$	Very well sorted
	$0.35< \sigma <0.50$	Well sorted
$2.5< So <3.5$	$0.50 < \sigma <1.00$	Moderately sorted
$3.5 < So <4.5$		Somehow sorted
$So > 4.5$	$1.00 < \sigma <2.00$	Poorly sorted
	$2.00 < \sigma <400$	Very poorly sorted
	$\sigma >4.00$	Extremely poorly sorted

3.13 Moisture content

The moisture content of the sample was calculated according to the ASTM method D2216. For this method, after weighing three separate samples of mine tailing, they were placed in an oven at 105^{o}C for 24 hours. Then, after oven drying the samples, they were kept in a desiccator, in order to prevent any absorption of humidity from the air during the cooling down period. At the end of this step, the weights of the dried samples were measured and recorded. The percentage of water content was calculated according to the following equation:

$$\textbf{Moisture content (\%)} = \frac{(Ww - Wd)}{Ww} \times 100 \qquad \textbf{Equation 3.7}$$

W_w: weight of the fresh sample (g)

W_d: weight of the dried sample (g)

3.14 Organic content

The organic content of soil and sediment greatly contributes to the absorption of heavy metals and arsenic. The experiments of Wang (2006) showed that the organic content of mine

tailings has a direct correlation with arsenic concentration. In acidic environments, H^+ binds to negatively charged sites on the organic matter, and in alkaline environments, the H^+ ions are released. The organic content of the sample was measured according to EPA Method 160.4**.** It was calculated by measuring the lost mass of the sample after calcination.

In this technique, the total solid mass of the samples was measured after drying in an oven at 103-104^{0}C. The samples were then placed in a muffle furnace for 50 minutes to be ignited at a temperature of 550^{0}C. After ignition, the mass of solid material combustible at 550^{o}C is calculated by subtracting the mass of the sample after calcination from the mass of the dried sample before going through ignition. The loss of mass is equal to the volatile residue of the sample and a rough approximation of the amount of organic matter present in the sample.

3.15 pH of the sample

The pH of the mine tailing samples was measured according to the method described by Schofield & Taylor (1955). It was done by measuring the pH of a mixture of 4 grams of the sample in 10 ml of 0.01M calcium chloride (1g per 2.5 ml solution) using an electronic pH meter.

3.16 Porosity of the sample

Porosity is one of the main factors affecting the permeability of a medium. It indicates how quickly a washing solution (with a known viscosity) can pass through the medium in a continuous experiment. For determining the porosity of the mine tailing sample, the known volume of the air-dried mine tailing sample (V_t) was added to the known volume of the water (V_w). By subtracting the volume of the water from the volume of the mixture (V_{w+b}), the volume of the grains (V_b) is obtained. By subtracting this value from the volume of the air-dried sample, the total pore volume of the sample (V_p) was calculated.

$$V_{w+b} - V_w = V_b \qquad \textbf{Equation 3.8}$$

$$V_p = V_t - V_b \qquad \textbf{Equation 3.9}$$

Total porosity (P_t) is calculated from the following equation:

$$P_t = \frac{V_p}{V_t} \times 100 \qquad \textbf{Equation 3.10}$$

The density of the grain (ρb) was calculated by dividing the mass of grains (M_b) by the volume of the grains (V_b).

$$\rho b = \frac{M_b}{V_b} \qquad \textbf{Equation 3.11}$$

3.17 Specific surface area of the sample

In this study, by measuring the specific surface area, the affinity of the mine tailing to adsorb heavy metals and metalloids can be predicted. One of the most accurate methods of measuring specific surface area is by using ethylene glycol monoethyl ether (EGME) (Yukselen & Kaya, 2006). In this approach, ethylene glycol monoethyl ether (EGME) was added to the specimen (3 ml of EGME per each gram of sample), and then the excess EGME was removed by evaporation under vacuum and weighed. The procedure is repeated until the mixture reaches a constant mass. In the next step, the mixture goes through drying at 105^0C for 24 hours. After that, the total mass is measured. By subtracting the mass of the mine tailings sample from the total, the mass of added EMGE is calculated. In this method, it is assumed that the EMGE forms monolayers covering the surface of every grain. Also, the amount of EGME required to form a monolayer on a square meter of surface is equal to 0.000286 g/m^2 (Liu, 1998).

The SSA of the specimen can be calculated by using the following equation:

$$SSA = \frac{W_a}{Ws \times 0.000286} \qquad \textbf{Equation 3.12}$$

SSA=Specific surface area (m^2/g)

W_a=Weight of added EGME (g)

W_s= weight of mine tailing sample (g)

3.18 Zeta potential and the isoelectric point of the sample

The zeta potential of the mine tailing particles were measured by using Zeta-Meter System 3.0+ (Zeta-Meter Inc., Staunton, VA, USA) and the isoelectric point of the mine tailing sample before and after treatment by sophorolipids, were determined. In this part of the investigations, 0.1 g of sample was placed in 50 mL centrifuge tubes and DI water or the sophorolipid solution was added. Solutions in each tube were adjusted to different pH levels. Measurements for the samples from each tube were repeated five times.

3.19 Hydraulic conductivity of the sample

One of the major parameters affecting the migration of heavy metals and one of the main parameters in planning for remediation is the hydraulic conductivity. The hydraulic conductivity is a measure of how easily and rapidly a fluid can pass through a medium. The presence of fractures and a high effective porosity of the sample will ease the flow and increase the permeability of the media and its hydraulic conductivity. On the other hand, the viscosity of the fluid determines how easily fluid can pass through the pores. The higher the viscosity of the fluid, the lower is the hydraulic conductivity. Lower hydraulic conductivities result in delays in flushing and passing the contaminated solution through the medium. Therefore, some of the heavy metals and metalloids, which were released by the media, will re-adsorb to the medium or will precipitate.

There are two approaches to determine the hydraulic conductivity of a medium. The first approach is the empirical approach, in which the hydraulic conductivity is calculated via data related to the particle size distribution of the medium and the pore ratio (Hazen equation) according to Equation 3.13:

$$K = cD_{10}^2 \qquad \textbf{Equation 3.13}$$

Where:

K is hydraulic conductivity (cm/s)

c is Hazen constant, $1 \leq c \leq 1.5$

D_{10} is the grain size corresponding to 10% by weight passing, also referred to as the effective size (mm)

The other approach is the experimental approach, which is conducted by measuring the flow rate through the medium and applying Darcy's equation to find the hydraulic conductivity of the sample. Testing can be done in situ or in a laboratory setting.

In a laboratory setting, there are two standard methods for measuring the hydraulic conductivity of a given sample, the 'constant head method' and the 'falling head method.' Since the mine tailing sample was categorized as silt, the method of choice is the falling head method (Figure 3.4). In this approach, a mass balance approach was taken to calculate the hydraulic conductivity of mine tailing sample in the column which was being used in the continuous experiment.

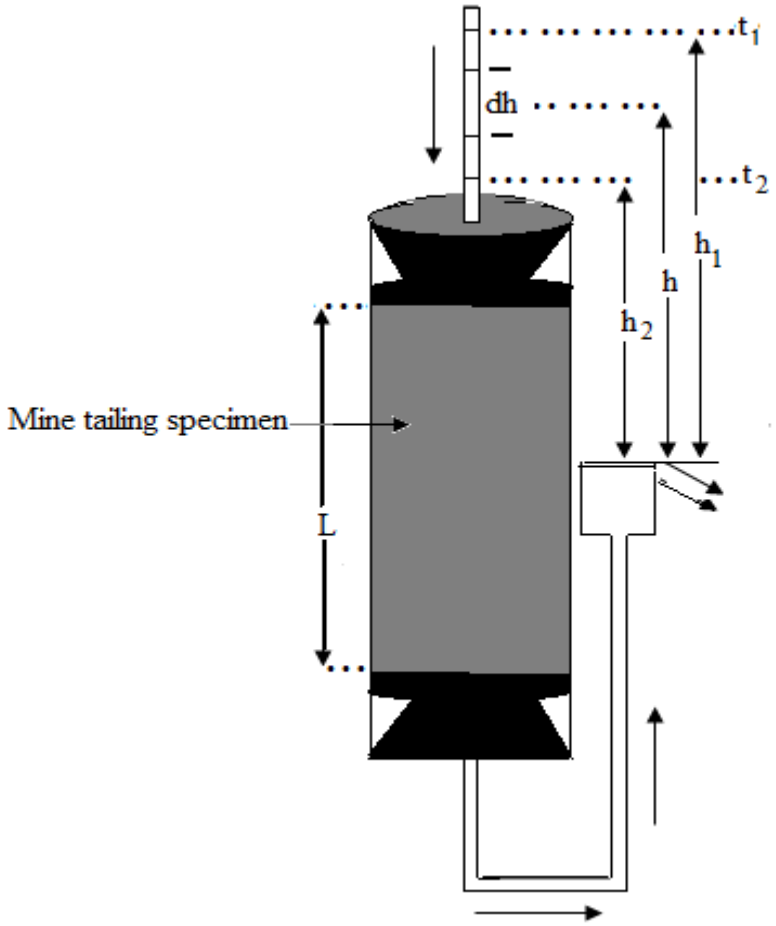

Figure 3.4. Falling-head test setup

First, h_1 was recorded at the time $t_{1\,=\,0,}$ after allowing the fluid to flow out of the system when head reached to $h_{2,}$ time t_2 was recorded.

$$Q_{column} = -a\frac{dh}{dt} = Q_{tube} \qquad \textbf{Equation 3.14}$$

Where:

a is cross-sectional area of the tube

dh/dt is the rate of fluid movement through the tube

$$\boldsymbol{Q_{column} = K\frac{h}{L}A} \qquad \textbf{Equation 3.15}$$

Where:

K is the sample hydraulic conductivity

h is the total head loss

L is the length of mine tailing column

A is column cross-sectional area

According to the law of continuity:

$$\boldsymbol{Q_{in}} = \boldsymbol{Q_{out}}$$ Equation 3.16

Therefore, K for mine tailing can be calculated as follows:

$$-\boldsymbol{a}\frac{\boldsymbol{dh}}{\boldsymbol{dt}} = \boldsymbol{KA}\frac{\boldsymbol{h}}{\boldsymbol{L}}$$ Equation 3.17

$$\boldsymbol{K}\frac{\boldsymbol{A}}{\boldsymbol{L}}\boldsymbol{dt} = -\boldsymbol{a}\frac{\boldsymbol{dh}}{\boldsymbol{h}}$$ **Equation 3.18**

$$\boldsymbol{Kdt} = -\boldsymbol{L}\,\frac{\boldsymbol{a}}{\boldsymbol{A}}\frac{\boldsymbol{dh}}{\boldsymbol{h}}$$ **Equation 3.19**

$$\boldsymbol{K}\int_{\boldsymbol{t_1}}^{\boldsymbol{t_2}}\boldsymbol{dt} = -\boldsymbol{L}\,\frac{\boldsymbol{a}}{\boldsymbol{A}}\int_{\boldsymbol{h_1}}^{\boldsymbol{h_2}}\frac{\boldsymbol{dh}}{\boldsymbol{h}}$$ **Equation 3.20**

$$\boldsymbol{Kt} = -\boldsymbol{L}\,\frac{\boldsymbol{a}}{\boldsymbol{A}}\,(\ln \boldsymbol{h_2} - \ln \boldsymbol{h_1}) = -\boldsymbol{L}\,\frac{\boldsymbol{a}}{\boldsymbol{A}}\,(\ln\frac{\boldsymbol{h_2}}{\boldsymbol{h_1}})$$ **Equation 3.21**

$$\boldsymbol{Kt} = \boldsymbol{L}\,\frac{\boldsymbol{a}}{\boldsymbol{A}}\,(\ln\frac{\boldsymbol{h_1}}{\boldsymbol{h_2}})$$ Equation 3.22

$$\boldsymbol{K} = \frac{\boldsymbol{aL}}{\boldsymbol{At}}\ln\frac{\boldsymbol{h_1}}{\boldsymbol{h_2}}$$ **Equation 3.23**

$$\boldsymbol{K} = \frac{\boldsymbol{Ld_{tube}^2}}{\boldsymbol{td_{column}^2}}\ln\frac{\boldsymbol{h_1}}{\boldsymbol{h_2}}$$ **Equation 3.24**

3.20 Cation Exchange Capacity

The cation exchange capacity of a medium is determined by measuring the ability of the medium to retain or release cations. Many researchers have proposed numerous methods for measuring the cation exchange capacity (CEC; measured in milligram equivalents, meq/100g) (Ciesielski et al., 1997; Ross, 1995; Sumner et al., 1996). Some researchers, such as Mulligan et al. (1999) and Van Reeuwijk (1992), have used the silver-thiourea method for measuring the cation exchange capacity of soil and sediment. In this experiment, three of the common methods for measuring CEC, the silver-thiourea and potassium acetate methods were applied, and the results were compared.

According to Mulligan et al. (1999), one of the methods that can be used for measuring CEC is a modified method based on the method purposed by Chhabra et al. (1975). In this method, a mixture of 15 g of thiourea and ammonium acetate 0.1 M is dissolved in 0.5 l of water and is gradually added to silver nitrate. The final concentration is 0.01 M, and the pH value is adjusted between 3 and 8. The above researchers noted that they used acetic acid (0.1 M) or sodium hydroxide (0.1 M) for adjusting the pH value. The mixture was then added to the specimen in a ratio of 25ml to 1g and was shaken by a reciprocating shaker for 4 hours. The supernatant was separated by using a centrifuge, 5000 rpm, and was analyzed for the silver content (Mulligan et al. 1999).

The potassium acetate method has been described as an effective method for measuring the CEC value of soil and sediment (Wang, 2003). For this method, a mixture of potassium acetate (1 M) and the specimen with a ratio of 4 ml per gram of sample was prepared. The pH value of the mixture was adjusted to 7. The mixture was shaken for 5 minutes. The supernatant was separated by centrifuging the mixture for 15 minutes at 3000 rpm and then discarded. In the second step, 1M potassium acetate was added a second time to the solid part in the same ratio as before, shaken, then centrifuged, and its supernatants are then discarded. In the third step, methanol was added to the solid, then shaken, and then centrifuged for 15 minutes at 4500 rpm. The supernatant was discarded. In the fourth step, step 3 was repeated. In the fifth step, 1 M ammonium acetate at a ratio

of 5 ml per gram of solid was added to the solid part, and then the mixtures were shaken and centrifuged for 15 minutes at 3000 rpm. The supernatant was collected. On the sixth step, the solid part was mixed with ammonium acetate, shaken and centrifuged again, the supernatant collected and added to the supernatant from step five. The supernatants were diluted to be analyzed with the ICP-MS to measure the concentration of potassium ions in the supernatant. Using this value, the amount of potassium which can be adsorbed to 100 g of the mine tailing sample (C_{K^+}) was calculated. Potassium is a monovalent cation. Therefore, the equivalent mass of K^+, which is calculated by dividing the molar mass by the number of valence electrons, is 39.1 mg/meq. The CEC of the dry mine tailing was determined in meq/100g or $cmol_c$/kg (centimoles of charge per kg) using the following equation:

$$CEC\ (\frac{meq}{100g}) = \frac{K^+(\text{mg}/100\text{g})}{39.1\ (\frac{mg}{meq})} \qquad \textbf{Equation 3.25}$$

It should be noted that 1 meq/100g is equal to 6.022 x10^{20} electron charges.

One of the most accurate methods for measuring the cation exchange capacity of mine tailings is the sodium acetate (NaOAc) method, Method 9081 (EPA, 1986). In this approach, 4g of the mine tailing sample were put in a 50 ml centrifuge tube. Then 35 mL 1 N NaOAc was added to the tube, and the tube was vigorously shaken, so the sample was mixed with sodium acetate solution, and they were put on the shaker for 5 minutes. Afterward, the tube was transferred to centrifuge for 10 minutes at 10000 rpm. At that point, the supernatant was discarded. The steps of adding NaOAc and shaking and centrifuging and discarding the supernatant were repeated three more times. Next, the samples were washed with isopropyl alcohol three times, by adding 35 mL of 99% isopropyl alcohol to the tube, shaking it for 5 min, and centrifuging and discarding the supernatant.

Next, 35 ml of ammonium acetate (NH_4OAc) solution were added to the tube. It was shaken for 5 minutes and then centrifuged. The supernatant from this part of the experiment was collected in a volumetric flask. NH_4OAc was then added to the tube. The tube was then shaken, and the supernatant was collected via centrifuge. These steps were repeated two more times. The collected

supernatants were diluted and analyzed by atomic absorption spectroscopy (AA) to determine the concentration of Na^+ in the solution. Using this value, the CEC of the mine tailing sample was calculated according to the method that was used for the potassium acetate method. Therefore:

$$CEC = \frac{\mathbf{C}Na^{+}\mathbf{(mg/100g)}}{\mathbf{10}*\mathbf{23}\ (\frac{mg}{meq})} \qquad \textbf{Equation 3.26}$$

3.21 Investigation with scanning electron microscope (SEM) and energy dispersive X-ray analysis (EDXA)

To obtain a better understanding of the elemental composition of the samples and to obtain a clear image of the sample in nano-scale, the untreated and treated samples were analyzed by SEM-EDXJEOL (35-cf) equipped with EDAX (Hitachi S-3400N) in the Department of Mechanical and Industrial Engineering, Concordia University.

3.22 Mineralogical analysis by X-ray diffraction

The crystalline structures of the minerals within the mine tailing samples were investigated by the X-ray diffractometer (Philips X'Pert Pro Multipurpose X-ray Diffractometer) in the Thermodynamics of Materials Research (TMG) laboratory at Concordia University. In the XRD, the sample was mounted and bombarded with X-rays of wavelengths of 0.01 to 100 Å. The analysis was Cu-based radiation at 50 kV, 260 mA, a step-scan of 0.02º, and the scan rate was at 1º per minute in 2Θ from 10º to 120º. The angle and intensity of the diffracted beams depend on the minerals within the medium and the distinct interatomic distances within their planes. By measuring the diffracted beams, minerals within the medium can be distinguished.

The obtained XRD results were interpreted by comparing with data from the International Centre for Diffraction Data (ICDD) (Hubbard and O'Connor, 2002) at the Department of Mining and Materials Engineering, McGill University. The ICDD database has diagrams for each

composition. By comparing the spectra from the XRD with the diagrams for each composition, the presence or absence of that composition was determined.

3.23 Critical micelle concentration (CMC)

One of the standard methods used for measuring the critical micelle concentration (CMC) of biosurfactants is by measuring the surface tension of the surfactant in various concentrations. The surface tension of sophorolipids in different concentrations was measured by using a tensiometer according to the Du Nouy method (Fisher Scientific, Tensiomat model 21) in the Department of Building, Civil and Environmental Engineering (BCEE), Concordia University. A tensiometer measures the force needed to pull up a thin metal ring (platinum ring) out of the surface of the solution. For the first step, the torsiometer was calibrated by measuring the surface tension of DI water to ensure the accuracy of the measurements. to determine the critical micelle concentration (CMC) of the sophorolipids, the solution was consecutively diluted. After each step of dilution, the surface tension of the solution was measured by submerging a platinum ring in the solution. The sample mount is then gradually lowered, so the liquid film produced beneath the ring is stretched until it breaks and the ring is released. In the Tensiomat Model 21, the value of the surface tension can be read directly in mN/m. Afterward, surface tension plotted against the logarithm of concentration. By studying the curve, it can be seen, at a lower concentration, increasing the concentration of the sophorolipids, results in decreasing the surface tension up to the point that increasing the concentration of sophorolipids has no effect on the surface tension, this point is called the CMC.

3.24 Concentration of sophorolipids in the effluent

Investigation of the concentration of sophorolipids concentration in the effluent from washing the mine tailing was done by measuring the surface tension of the effluent as it was diluted consecutively and comparing the calibration curve and using Gibbs Adsorption Isotherm. The calibration curve was made by measuring the surface tension of sophorolipid solution as it was sequentially diluted, from 0.01 SL to 10^{-7}, and deionized water as the point 0% SL. Then plotting

γ vs. log C, in which gamma represents surface tension (mN/m) and C is the sophorolipid concentration. Based on the reference curve regression function, the concentration of sophorolipids in the effluents can be determined.

The surface excess (Γ) was determined from the calibration curve by using the following equation:

$$\frac{d\gamma_{\left(\frac{N}{m}\right)}}{d\ log C} = -\Gamma_{\left(\frac{mol}{m^2}\right)} RT \qquad \textbf{Equation 3.27}$$

3.25 Viscosity measurement

The viscosity of the sophorolipid solution was determined using a Brookfield digital viscometer (model DV-II) in the environmental engineering laboratory, Concordia University. For this investigation, after calibration by a conventional fluid, 2 mL of the 5%, 4%, 3%, 2% and 1% sophorolipid solutions were placed inside a chamber within the instrument. The device was set to rotate at 12 rpm and at 0.4% torque. The experiment was conducted twice for each concentration. The temperature at the time of operation was 23ºC.

3.26 Digestion

To analyze the sample with ICP-MS and to measure the quantity of arsenic and other metals or metalloids in the sample, these elements should be in a soluble form. Therefore, dried untreated samples and dried treated samples were placed in four small beakers (two grams of the specimen in each beaker) and a beaker without any specimen as the blank. Samples went through acid digestion according to EPA method 3050B. Figure 3.5 illustrates the step by step process of digestion.

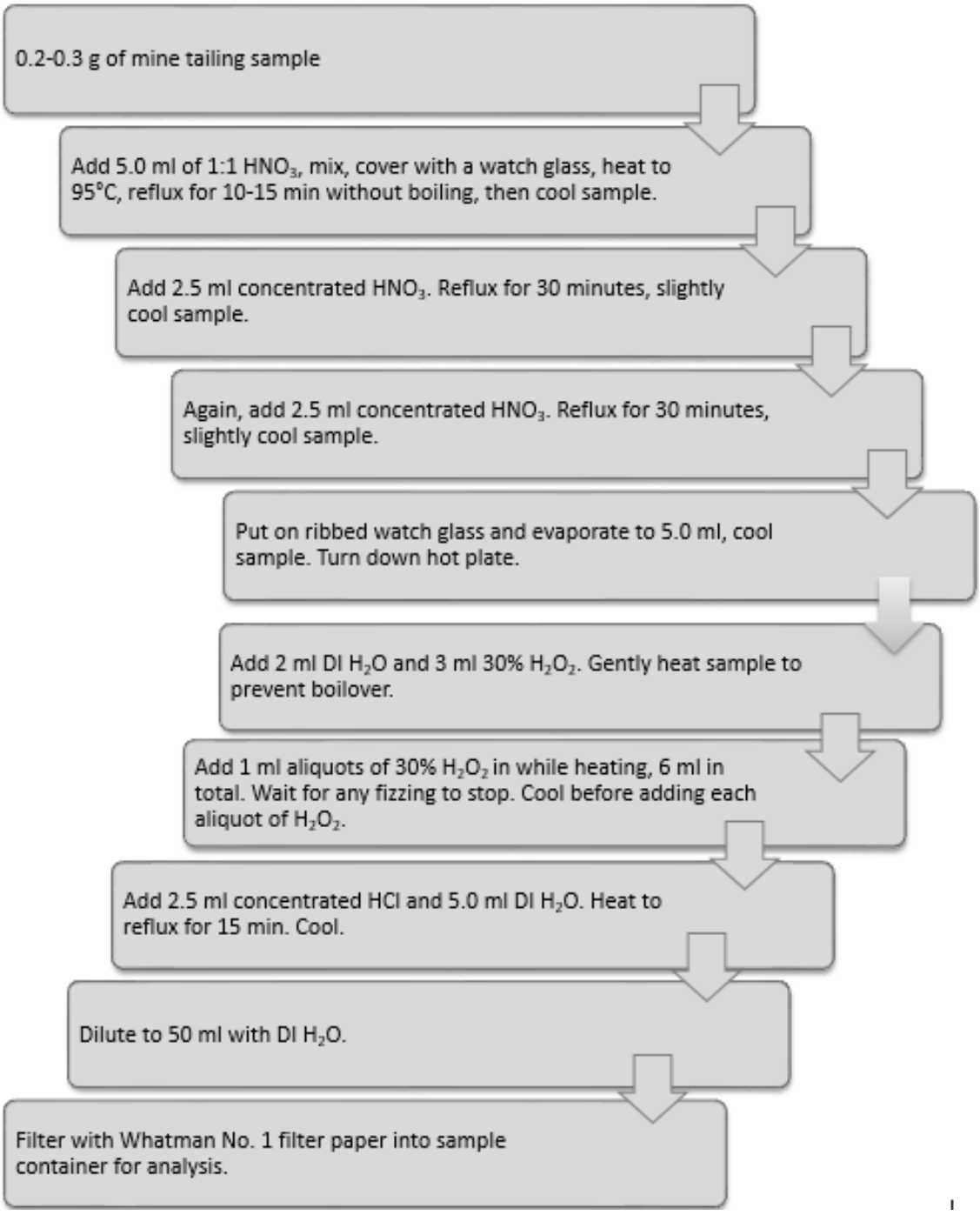

Figure 3.5. Digestion according to EPA Method 3050b.

3.27 Overview of the second phase of experiments

Experiments in phase two focused on the removal of arsenic and studied the interaction of biosurfactants on arsenic and heavy metals in the medium. These experiments were done in two phases, batch and continuous (Figure 3.6). They involved measuring the concentration of arsenic and other heavy metals released from the mine tailing specimen, using different solvents. The speciation of arsenic and other metals/metalloids in the supernatants from the mine tailings and the effect of biosurfactants on the speciation of these elements were studied. After the metal extractions with various concentrations of biosurfactants or DI water, the remaining arsenic and other metal/ metalloids in the mine tailings were measured. The goal of the experiments was to develop environmentally friendly and cost-effective cleanup strategies for heavy metal contaminated soil and mine tailings.

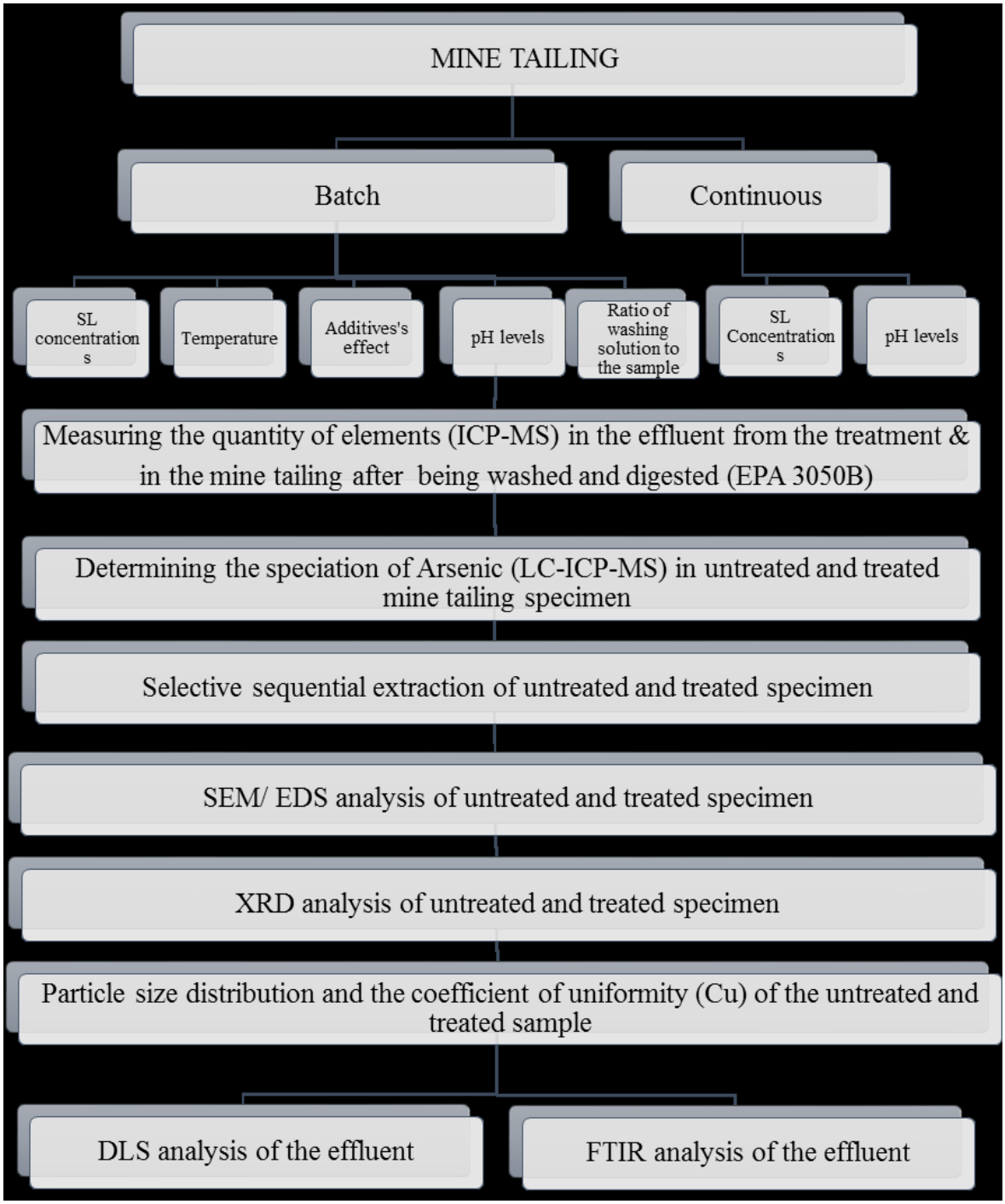

Figure 3.6. Schematic diagram of experimental procedures in phase 2.

3.28 Batch experiments

In the first phase, samples were placed in fifteen 50 ml centrifuge tubes (1 g per tube) and were mixed with the washing solution: a mixture of rhamnolipids or SL, and deionized water in different ratios. 36 tubes were prepared by placing 1g of mine tailings into the tubes with the various concentrations of both biosurfactants and different volume of surfactants per gram of sample (10 or 20 ml per gram). The concentrations of the sophorolipids and rhamnolipids in each tube were: 0% biosurfactant, 0.1 % Rh, 0.5% Rh, 1% Rh, 5% Rh, 0.1% SL, 0.5% SL, 1% SL, 2% SL, 3% SL 4% SL and 5% SL. The tubes were kept at room temperature on a shaker with a speed of 60 rpm for seven days. After that, the pH of each tube was adjusted to 6 or 11, by adding NaOH or HCl. A sample was taken from the supernatant of each tube every 24 hours to observe the effect of the type of biosurfactants, biosurfactant concentrations, pH level, and time of the concentration of released arsenic into the supernatant. The effect of the type of biosurfactants used, and the different pH levels, on arsenic speciation was also noted. Supernatants from each tube were filtered by 0.2 μm filters and were diluted 10,000 and 100,000 times (until the concentrations of the target elements reached to 10 to 70 μg/kg). Next, their pH was lowered using a solution of 1% HNO_3 and 0.5% HCl, to be analyzed by the ICP-MS for measuring the concentration of target elements. Percentage of desorption for each element (% D) was calculated using Equation 3.28:

$$\%\mathbf{D} = \frac{\mathbf{C_S}}{\mathbf{C_0}} \times \mathbf{100} \qquad \textbf{Equation 3.28}$$

Where: $C_{s\ (mg/kg)}$ represent the quantity of the element removed from one kilogram of mine tailing sample and $C_{0\ (mg/kg)}$ represent the concentration of the same element in the mine tailing sample before the process of mobilization. In this experiment, the original concentration for rhamnolipids was 25%, and sophorolipids were at 41%. All experiments were conducted at room temperature (22 ± 1˚C), and each experiment was duplicated. Lastly, the filtered samples were diluted 10,000 and 100,000 times (for samples which have been adjusted to pH 11) and were analyzed by the LC-ICP-MS. It should be noted that the pH of the samples, which were prepared for the speciation analysis, were not altered.

3.29 Arsenic speciation

Arsenic speciation of the mine tailing samples was conducted by using the LC-ICP-MS (Agilent 7700) and the column G3288A (Main Column: G3288-80000, Guard Column: G3154-65002). For this stage of the experiment, the mine tailing samples were placed in 20 tubes (one gram per tube), 20 ml of washing solution (0.5% and 1% SL, 0.5% and 1% Rh, and deionized water) was added to each tube, and the pH of the tubes were adjusted to 6 or 11 in order to compare the changes in speciation of arsenic by adding different concentrations of sophorolipids and rhamnolipids. The tubes were kept at room temperature on a shaker with a speed of 60 rpm for 7 days. A sample was taken from each tube every 24 hours to observe the effect of the concentration of biosurfactants and time on arsenic speciation at two different pH levels. Samples were filtered by 0.2 μm filters and were diluted and acidified to be first analyzed by ICP-MS for their total concentration of arsenic and to determine how many times the effluent should be diluted before analyzing with LC-ICP-MS. Then, to obtain information about the arsenic species in the effluent and to ascertain the concentration of each oxidation state of arsenic in the samples, the supernatant from the batch experiments were diluted and filtered with 0.2 micron Teflon syringe filters and were placed into the 1 ml vials to be analyzed by the LC-ICP-MS. LC-ICP-MS separates arsenic species, such as arsenite [As(III)], arsenate [As(V)], monomethyl arsonic acid (MMAA), dimethyl arsinic acid (DMAA), trimethylarsine oxide (TMAO), tetramethylarsonium (TeMA), arsenobetaine (AsB) and arsenocholine (AsC).

In this part of the experiment, the effect of adding sophorolipids and rhamnolipids with different concentrations and different pH levels, on the speciation of the arsenic present in the extracted supernatant, and the ratio of As (V) versus As (III) released by each washing solution, was determined. The results from this study have shown the interaction of these two biosurfactants with arsenic in the medium, and it has been determined whether the change in the speciation causes the release of this metalloid into the solution.

3.30 Column experiments

To compare the effectiveness of sophorolipids in mobilizing the arsenic from mine tailings in continuous flow configuration, 50 g of dried mine tailing sample were passed through a 100 μm sieve and were compacted into a Plexiglas column (length: 15 cm and inner diameter: 1.5 cm). During the first step, DI water was pumped to the column, into the sample, from the inlet in the base of the column at the flow rate of 0.1 mL/min. When the sample in the column was saturated, the water started to appear at the top of the sample. Immediately the pump was stopped. From the time that the water reached the inlet and started entering the column until the water began to appear on the top of the sample, the time was measured with a digital stopwatch. By calculating the volume of the water that was passed through that time frame the pore volume was calculated. This procedure was repeated 3 times to ensure the accuracy of the obtained value.

In the column experiments, the mine tailing samples were flushed with different concentrations of sophorolipids (0.1%, 0.05% and 1% SL) at various pH. In this part of the experiments, samples were taken from the effluent after a specific number of pore volumes of the solution were passed through the column. The washing solution in the column flowed upward to minimize errors arising from bubble entrapment. Different flow rates were examined to find the optimal flow rate for this part of the experiment. It has been found that the optimal flow rate was 0.74 ml/s when using aerator air stone and 1.19 ml/s when using geotextile filter. As a control, the experiments were repeated by using deionized water adjusted to the same pH level as the sophorolipid solutions which were utilized in the continuous experiment.

Each run consisted of washing the sample with 50, 65 or 100 pore volumes of sophorolipid solution or deionized water at selected pH levels (2.5, 5, 6, 7 and 11) to measure the arsenic being extracted by sophorolipids during flushing with each pore volume. The solutions pass through a column containing a mine tailing sample, at a flow rate of 40 ml/min to minimize pressure buildup and channeling through the sample. This flow rate was found to be suitable for the setup, and it was chosen after repeated attempts and testing with a few different flow rates. After each pore volumes, a sample was collected from the effluent and was filtered and diluted to be analyzed by

the ICP-MS for arsenic concentration. All experiments were conducted at room temperature and were duplicated.

Column experiments were performed in two stages: in the first part of experiments, the effluent was passing a 75 μm filter, and in the second part, the effluent was passing a 50 μm filter. At the end of the experiments, the residues that had settled on in the bottom of collection tubes were collected. These residues and the remaining mine tailing samples from the columns were air dried, and their weight was measured. The particle size distribution of these residues was measured. The concentrations of the remaining elements within these residues were measured via digestion according to the EPA 3050 method and analysis by the ICP-MS. Then, these residuals went through sequential extraction to determine which fraction of the mine tailings were more affected by biosurfactants. It should be noted that the initial sophorolipid concentration was 41% before dilution. Also, all experiments were conducted at room temperature, and each experiment was duplicated to ensure the repeatability of the results.

3.31 Mass balance investigation in batch experiments

Results from analyzing the effluent from a batch experiment using deionized water and sophorolipid solutions at different pH levels and the results from the digestion of the untreated and treated samples were used to compare the quantity of the arsenic in effluent and in the treated mine tailing sample with the quantity of arsenic in the untreated sample. The value of the mass balance coefficient was calculated according to the following equation:

$$\boldsymbol{MB = \frac{M_{r\,(mg)} + M_{out\,(mg)}}{M_{in\,(mg)}}} \qquad \textbf{Equation 3.29}$$

In which:

MB denotes the mass balance coefficient

M_{in} denotes the mass of arsenic in the untreated sample (mg)

M_r denotes the mass of arsenic in the treated sample (residues from tubes) (mg).

M_{out} denotes the total mass of arsenic extracted from the sample by washing solution (mg).

3.32 Mass balance investigation in column experiments

The mass balance coefficient in the column experiment was determined using the results from analyzing the effluent from the column experiment using deionized water and sophorolipid solution, and the results from digestion of the untreated and treated sample, as well the residues which settle down from the effluent in the collecting vials. The value of the mass balance coefficient was calculated according to the following equation:

$$MB = \frac{M_{r\,(mg)} + M_{rv\,(mg)} + M_{out\,(mg)}}{M_{in\,(mg)}} \qquad \textbf{Equation 3.30}$$

In which:

M_{in} denotes the mass of arsenic in the untreated sample (mg)

M_r denotes the mass of arsenic in the treated sample (residues from the column) (mg).

M_{rv} denotes the mass of arsenic in residues which settle from the effluent (residues from collecting vials) (mg).

M_{out} denotes the total mass of arsenic extracted from the sample by washing solution (mg).

First, the quantity of arsenic in the untreated sample was calculated based on the concentration of arsenic in the sample and its total mass (e.g. 50 g). The mass of the treated mine tailing sample from the column was then determined by adding the mass of residues remaining inside the column (after drying) and the mass of the sample adsorbed to the outlet filter (the difference of the filter's mass before and after treatment). To measure the quantity of residues in the collecting vials, after the residues were settled, the supernatants in the vials were separated, and the residues were collected in a container then air dried. After 1 gram of each sample was digested and analyzed by the IC-PMS, the concentration of arsenic was calculated, and, based on the total mass, the mass of arsenic in each sample was calculated.

3.33 Selective sequential extraction

For the sequential extraction of the samples (both untreated and treated samples), the sequential extraction procedure described by Yong et al. (1993) was applied. Dried untreated mine tailing samples and treated mine tailing samples (washed by biosurfactants and dried) were put in six separate 50 mL centrifuge tubes (1 g of sample in each tube). In each step of extraction, the specimens in the tubes and the control tubes were subjected to different solutions, from deionized water, magnesium chloride ($MgCl_2$), sodium acetate (NaOAc), hydroxylamine hydrochloride ($NH_2OH \cdot HCl$), acetic acid (CH_3COOH), to nitric acid (HNO_3), hydrogen peroxide (H_2O_2) and ammonium acetate (NH_4OAc) and finally to aqua regia. At the end of each step, the supernatant was collected and analyzed to determine the percentage of target elements that were washed with each solution, or, the concentration and the proportion of elements associated with each portion of the medium. Figure 3.7 illustrates the step by step process of sequential extraction.

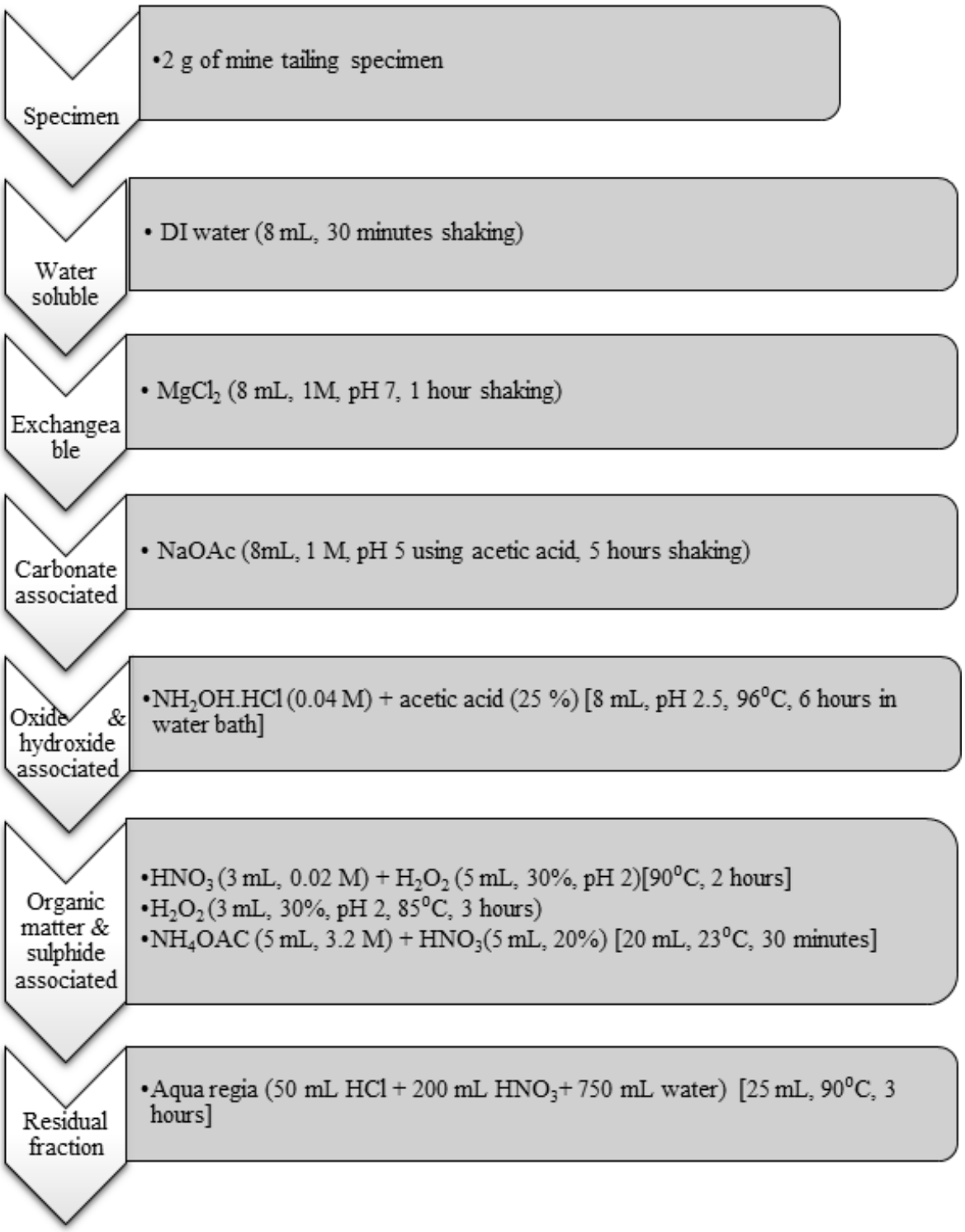

Figure 3.7. Selective sequential extraction diagram.

3.34 FTIR analysis

Fourier transform infrared spectroscopy (FTIR) is one of the most widely used techniques to study the structure of molecules. It is based on the fact that different molecules absorb different wavelengths of infrared light, thus causing the excitement energy emitted from the bonds to differ. The raw data, energy received by the detector, is converted to the absorbance and transmission spectrums using the Fourier transform function. These recordings are in three ranges of the near (NIR) (760-1500 nm), mid (MIR) (1400-3000 nm) and far (FIR) (3000- 10^6 nm) infrared spectrum. By comparing the obtained data with data available in spectra databases, the data is interpreted, and changes in the composition of the sophorolipids are determined.

It should be noted that in spectroscopy, the x-axis represents the wave number ($\tilde{\nu}$) cm^{-1}. The following equations describe the relationship between the wave number and frequency:

$$\tilde{\nu} = \frac{\mathbf{1}}{\boldsymbol{n\lambda}} \qquad \textbf{Equation 3.31}$$

$$\tilde{\nu} = \frac{\boldsymbol{\nu}}{\boldsymbol{C}} \qquad \textbf{Equation 3.32}$$

Where λ represents the wavelength (cm), n represents the medium reflective index, ν denotes frequency (s^{-1}) and c is the speed of light which is $2.99792458 \times 10^{10}$ $cm.s^{-1}$.

To study the effect of the presence of arsenic and other heavy metals in the mine tailing sample on the oscillation frequency of functional groups of the sophorolipid at different pH levels, a series of analyses were conducted using Fourier transform infrared spectroscopy (FTIR) at Centre de Recherche NanoQAM. The samples which were analyzed in this part of the experiments were:

- Series of samples with five different concentrations of sophorolipid, 0.5 to 5% SL.
- Samples of 1% sophorolipid adjusted to different pH (2, 4, 6, 8, 10 and 12).
- Samples of 1% sophorolipid and disodium hydrogen arsenate (Na_2HAsO_4), in which pH as adjusted to pH 2, 4, 6, 8, 10 and 12.

- Samples of 1% sophorolipid, disodium hydrogen arsenate (Na_2HAsO_4) and ferric oxide (Fe_2O_3), in which pH was adjusted to pH 2, 4, 6, 8, 10 and 12.
- Samples of 1% sophorolipid and 1g mine tailing, in which pH was adjusted to pH 2, 4, 6, 8, 10 and 12.

3.35 Dynamic Light Scattering (DLS) analysis

Dynamic Light Scattering (DLS) works based on the principle of dynamic and static light scattering. A beam from a 4 mW laser passes through the sample, and the scattered rays are detected by photon detectors, measuring the diffusion of the particles. Finally, the obtained data is converted to particle size and size distribution using the Stokes-Einstein equation.

$$D_h = \frac{k_B T}{3\,\pi\eta\,Dt} \qquad \textbf{Equation 3.33}$$

D_h: Particle size

k_B: Boltzmann's constant

T: Thermodynamic temperature

η: Dynamic viscosity

D_t: The translational diffusion coefficient

To investigate the effect of arsenic and other heavy metals in the mine tailing sample on the size of sophorolipid micelles at different pH levels, a series of analysis was conducted by Dynamic Light Scattering (DLS) NanoS90 at Centre de Recherche NanoQAM. The minimum detection size of the particles was 0.3 nm. The instrument can work between the temperatures of 0°C and 90°C. For the DLS analysis, the same samples which were prepared for the FTIR analysis was used. The measurements were conducted three times for each sample. Each time, there were 25 runs, and each run lasted for 10 seconds.

CHAPTER FOUR: RESULTS AND DISCUSSION

4.1 Physiochemical characteristics of the mine tailing specimen

The results of the investigation on the physiochemical characteristic of the mine tailing samples are as follows:

4.1.1 Main physicochemical properties of the mine tailings sample

Table 4.1 summarizes the main physicochemical properties of the mine tailings sample.

Table 4.1. Main physicochemical properties of the mine tailings sample.

Characteristics	Value		
Organic matter content	2.8%		
Water content	19.7%		
pH	7.61		
Moisture content	19.8 %		
Bulk density	1.43 g/cm^3		
Grain density	2.37 g/cm^3		
Type of the sample	Silt*	Median Size	9.55 μm
		Mean Size	13.42 μm
		Std. Dev	12.73 μm
		Mode Size	9.44 μm

*Categorized based on the size of the particle in mine tailing specimen.

As shown in Table 4.1, the moisture content of the sample upon arrival was 19.8 %, and the pH of the sample was alkaline (7.61 ± 0.3). The mass of the volatile residues of the sample is a rough approximation of the amount of organic matter present in the sample and was calculated to

be 0.82 ± 0.07%. This falls within the range of organic matter in mine tailings (0 to 5.8%) reported by previous researchers (Pepper et al., 2012; Wu et al., 2006).

4.1.2 Particle size distribution

The results of the analysis of the mine tailing samples, using a Laser Scattering Particle Size Distribution Analyzer showed that mean size of the grains in the sample were 13.42 μm. The measurements were volume-based. These results indicate that the size of the grains in the mine tailing sample and their homogeneity place them in the same category as silt (4 to 62 μm) according to the classification by Wentworth (1922). The coefficient of uniformity (Cu) of the mine tailing sample was: 2.38 [$Cu=D_{60}/D_{10}$; Cu= 9.29/3.91= 2.38] that indicates the uniformity of the sample. The results for the sorting coefficient of the untreated and treated sample are summarized in Tables 4.2 and 4.3. As it can be seen, treatment of the mine tailings resulted in uniformity within the grains of the residual. The Sorting Coefficient (S_o) of the untreated and treated samples were determined according to the method described by Folk and Ward (1957). σ for the untreated sample was 1.02, which indicates a poorly graded sample. The sample treated by 1% sophorolipids was well graded (σ =0.41).

Table 4.2. Sorting coefficient of untreated and treated sample according to Trask (1932)'s method.

Percentiles	Particle diameter in untreated (on the phi scale)	Particle diameter in treated (on the phi scale)
Q75	6.32	6.58
Q25	7.5	7.46
$(Q75/Q25)^{0.5}$	0.92	0.94

*** Phi = - log 2 (particle diameter (mm))**

Table 4.3. Sorting coefficient of untreated and treated sample according to Folk and Ward (1957)'s method.

phi values	Untreated sample	Treated sample
Ø84	6	6.39
Ø16	8	7.8
Ø95	5.3	6.04
Ø5	8.7	6.39
$\sigma = \frac{\phi_{84} - \phi_{16}}{4} + \frac{\phi_{95} - \phi_5}{6.6}$	1.015	0.41
Result	poorly sorted	well sorted

* The phi values represents the cumulative frequency at a particular percentile level.

The results of the mine tailing sample particle size analysis are illustrated in Figure 4.1. The smaller grain size results in the higher total surface area, and it is expected to adsorb the higher quantity of trace elements on the surface of grains. On the other hand, sometimes when the sizes of the grains are so small, they cement together and form aggregates, so the surface area decreases (Horowitz and Elrick, 1987). The presence of organic matter or clay, as well, results in cementing the grains together, reducing the effective surface area. Lower effective surface area results in a lower adsorption rate.

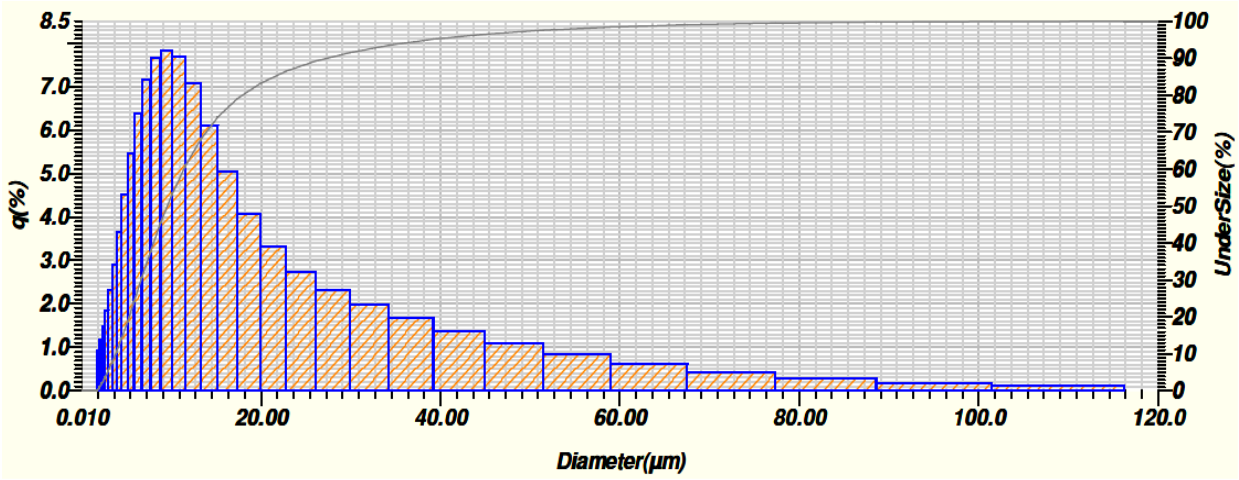

Figure 4.1. Particle size distribution of mine tailing sample (q% represents amount of each size by volume).

As it can be seen in Figure 4.1, the distribution of the grains is skewed and the majority of the grains are in the range of fine silt. There is a small percentage of clay, and the skewness is toward the larger grains.

4.1.3 Preliminary measurement of elemental concentrations

The results of the preliminary measurement of elements in the mine tailing sample with the Niton X-ray fluorescence analyzer (XRF) showed all the elements present in the media, which have a concentration higher than the XRF detection limit for that element (for example > 0.1 µg/kg for arsenic). These results show that iron and calcium have the highest concentrations of the elements which were measured by the XRF device. The presence of elevated levels of arsenic and chromium is an indication that these tailings are highly toxic. The results from the XRF measurement revealed the presence of high concentrations of valuable elements such as titanium (4.1 g/kg). Extracting these elements from the tailings can partially cover the cost of the remediation.

Titanium alloys are used in different industries and have found many applications, from water/air purification, solar cells, aircrafts, to medical applications (Takizawa et al., 2017; Alkan et al., 2017; Dimiduk, 1999). One of the titanium alloys, titanium aluminide, with its remarkable properties, such as its low density, resistance to oxidation, resistance to high temperature, and its high stiffness can solve many engineering problems (Dimiduk, 1999; Kothari et al, 2012). It has been predicted that titanium aluminide, which is currently used in different parts of aircrafts, can replace nickel-base superalloys (Inconel) in aerospace industry (Dimiduk, 1999). According to Alkan et al. (2017), by expansion in the applications of titanium alloys and depletion of its primary resources, there is a need for finding new resources for this valuable material. Mine tailings with high concentrations of titanium can be an excellent resource for this valuable metal.

4.1.4 Results of measurement of element concentration with ICP-MS analyzer

To obtain more accurate values of the concentration of the target elements in the specimen, the specimen was digested with strong acids according to the guidelines of the method EPA 3050B. The supernatant was diluted and analyzed by using an Agilent ICP-MS. Results from analysis of

the sample with ICP-MS for a few elements in the untreated mine tailings and their acceptable threshold limit are shown in Table 4.4. As it can be seen, the concentration of heavy metals/ metalloids within the mine tailings are a few times higher than the maximum acceptable limit for these elements within industrial areas based on the Canadian Environmental Protection Act (CEPA, 1991 to 2015). For instance, the maximum level of inorganic arsenic recommended for soil in a residential area is 32 mg/kg. Likewise, the highest recommended level of inorganic arsenic for a commercial area is 640 mg/kg of the soil's dry weight (Canadian Environment Agency, 2009) or 12 mg/kg of the soil's dry weight according to Canadian Council of Ministers of the Environment Guidelines (CCME, 1997). Therefore the results obtained from this study point out the urgency of a cleanup plan for these tailings.

Table 4.4. Concentration of elements targeted in this study in untreated mine tailing sample.

Element	Percentage	Concentration (mg/kg)	Maximum acceptable limit in industrial areas (mg/kg dry weight) (CEPA)
As	0.26	2567	12 (1997)
Cr	0.02	220	1.4 (1999)
Mn	0.46	4577	-
Fe	21.26	212633	-
Ni	0.04	396	89 (2015)
Cu	0.06	649	91 (1999)
Zn	5.63	56296	360 (1999)
Mo	0.003	28	40 (1991)
Sb	0.02	219	40 (1991)

4.1.5 X-ray diffraction analysis (XRD)

Arsenic is usually found in association with minerals such as arsenopyrite (FeAsS) and pyrite (FeS_2), or absorbed within goethite (FeO (OH)) or hematite (Fe_2O_3). The result of the study with the SEM-EDS analysis of the samples (treated and untreated) showed that arsenic was mainly associated with silicon, aluminum, iron, potassium, calcium, and magnesium. These combinations

predict the presence of minerals such as quartz (SiO_2), different types of silicates, goethite, sulfates, and sulfides.

Figure 4.2 illustrate the result of XRD analysis of the mine tailing sample. The spectra obtained from the XRD were compared to the standards from the International Centre for Diffraction Data (ICDD). The result of the comparison the data from XRD analysis with ICDD database revealed the presence of high counts of quartz crystals in the sample. Furthermore, arsenopyrite (FeAsS), limestone ($CaCO_3$) and ferric sulfate ($Fe_2(SO_4)_3$) crystals were identified. The presence of high levels of ferric sulfate, which is a secondary mineral, point toward the oxidation of sulfide minerals in the mine tailings. On the other hand, unlike the other secondary minerals, such as jarosite, which could assist the immobilization of arsenic, the ferric sulfate plays a role in the production of acid mine drainage (AMD) and mobilizing the elements in the mine tailing. Then again, the presence of limestone in the sample helps in stabilizing arsenic through neutralizing the pH (Mahoney et al., 2005, Langmuir et al., 2006). Therefore, there is an equilibrium in the sample, which is susceptible to changes by any of the controlling parameters.

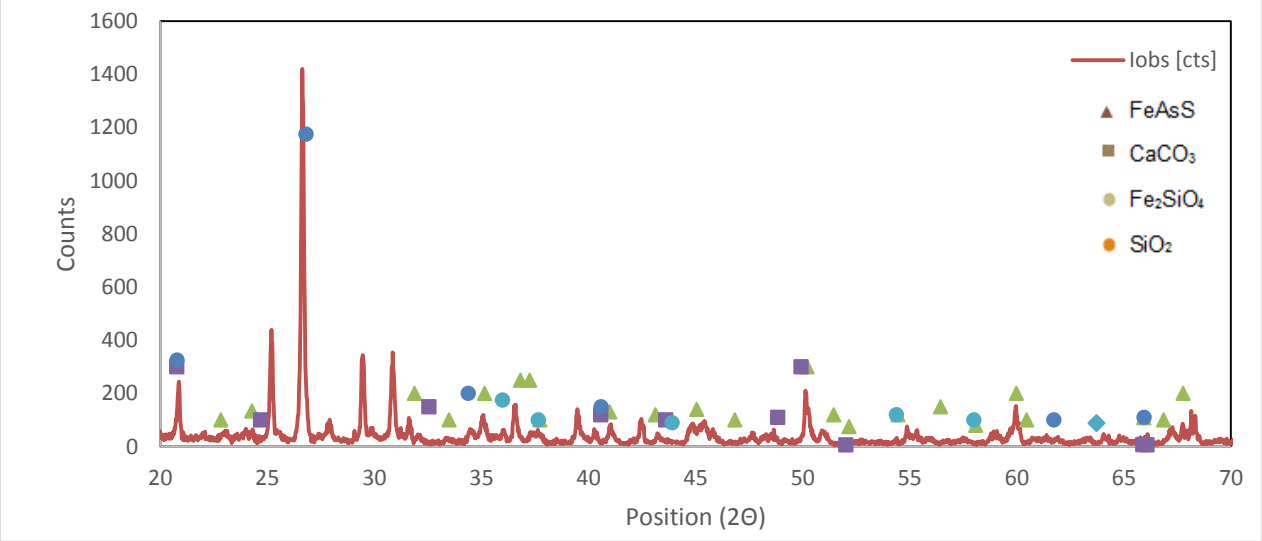

Figure 4.2. XRD spectrum of mine tailing sample.

The XRD was not able to detect the minerals with concentrations lower than the detection limit of the XRD, and only one run of counting was completed. For further investigation and obtaining more precise results, there is a need for repeating the experiments with the XRD to get more counts. The other option is analysis with a Micro-XRD and also studying samples with a petrographic microscope to gain a better understanding of the composition of the present mine tailing samples.

4.2 CHARACTERISTICS OF SOPHOROLIPIDS (SL18)

4.2.1 Critical micelle concentration (CMC) of sophorolipids SL18 and the effect of the addition of electrolytes on the CMC level

The critical micelle concentration (CMC) of the sophorolipids which were used in the present study was found to be 10 mg/L, and the surface tension at that point was 40.5 mN/m. The addition of only 2 g/L of sodium chloride decreased the surface tension of the sophorolipids at the CMC point to 40. Figure 4.3 shows a comparison between the surface tension and sophorolipid concentration in both saline and non-saline solutions. Additional experiments were conducted to examine the effect of adding salt to the sophorolipid solution, on micelle size and the ability of the sophorolipids in the removal of arsenic (both in continuous and batch experiments). This part of the study was crucial as the goal of this research is to develop an efficient method for removing arsenic and heavy metals from not only mine tailing, also from soil and soil and sediments. As in some parts of the world, fresh water is not as abundant as in Canada; it was important to investigate the effect of using saline water for the efficiency of the sophorolipids.

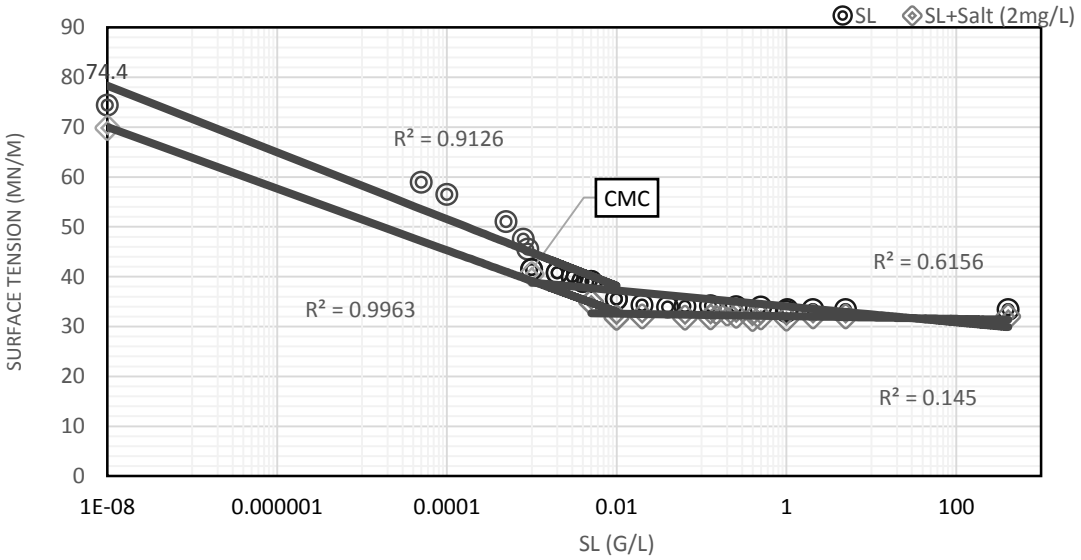

Figure 4.3. Surface tension of sophorolipids at pH 6 and the effect of adding NaCl (2 g/L).

Furthermore, an investigation of the micelle size of sophorolipids at pH 5 via with dynamic light scattering (DLS; Zetasizer Nano s90), revealed that the addition of sodium chloride or arsenate causes an increase in the size of the micelles. The average micelle size increased from 70 µm to 90 µm after the addition of salt.

Other researchers obtained similar results on micelles from other surfactants. Song et al. (2012) reported that the addition of sodium chloride causes only a slight decrease in the CMC of sophorolipids. Likewise, the investigations of Mitra and Dungan (1997) showed that adding sodium chloride decreases the CMC of the biosurfactant saponin, even though adding salt did not change the size of the micelles. In the past, studies of Corrin and Harkins (1947) on the effect of salt on a surfactant's micelles, showed that adding salt, even at concentrations as low as 0.1 M, substantially increased the number of positive ions. Thus increasing the concentration of counterions, resulted in a lower critical concentration for forming micelles. Moreover, investigations of Cates and Candau (1990) on the effect of salts on micelles of a cationic surfactant showed that different salts at a particular concentration have different effects on the micelles. For example, NaBr, at a concentration of 0.006 M, was able to increase the micelle size. On the other hand, NaCl, at the above-mentioned concentration, had no effect on the micelle size. NaCl can

promote an increase in the size of micelles only in concentrations greater than 1 M. Varade et al. (2005)'s investigations on the effect of salts on cationic surfactants had similar results. Their studies showed that increasing the concentration of salt results in decrease of the CMC of the surfactant.

According to Baccile et al. (2012), acidic sophorolipids are sensitive to pH, temperature, and electrical fields. This can result in changes in their efficiency. By altering the pH level, different aggregate states of sophorolipids can be obtained (Baccile et al., 2013). In similar investigations, Mitra and Dungan (1997) have shown that increasing the pH level causes an increase in the CMC value of the biosurfactant saponin. However, they also reported that changes in pH had no effect on the size of saponin micelles. Investigations of Daverey and Pakshirajan (2009) showed that changing the pH affected the performance of sophorolipids. At neutral pH levels, sophorolipids show high emulsifying activity. However, increasing pH increased the stability of the emulsion formed. In the next phase of the current study, the effect of pH on the CMC level of sophorolipids, the size of their micelles, and the viscosity of the solution was investigated.

After washing mine tailings with the 1% sophorolipid solution, there was a slight change in the surface tension of the effluent, although the CMC level stayed the same. This difference may be caused by the introduction of ions from mine tailing sample into the solution, which affect surface tension and also the adsorption of sophorolipids to the tailings. Figure 4.4 illustrates the surface tension of sophorolipids (SL18) in effluent at pH 4 and at different concentrations.

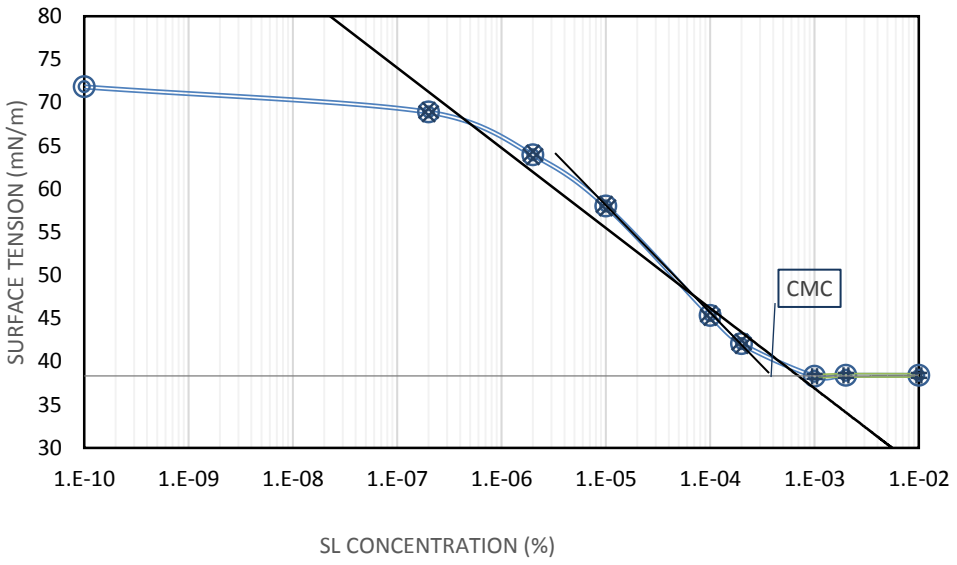

Figure 4.4. Surface tension of sophorolipids in the effluent at pH 5.

The surface excess (Γ) concentration at pH 5 was calculated from the slope of the concentration-dependent region of the curve (the region with concentration less than CMC point) and by using the following equation (Equation 4.1) and found to be 1.64 $\times 10^{-6}$ mole.m^{-2}.

$$\frac{d\gamma_{(\frac{N}{m})}}{d\ lnC} = -\Gamma_{(\frac{mol}{m^2})}\ RT \qquad \textbf{Equation 4.1}$$

$\Gamma = (4.032*10^{-3})/(8.314*295.15)$

Further investigations on the concentration of sophorolipids in the effluent following the Anthrone method, and using a spectrophotometer, showed a decrease in the concentration of sophorolipids in the effluent. The decrease in alkaline environments (pH 10 and 12) was much more than the decrease in acidic environments (pH 2 and 4). Observations in the laboratory showed that increasing the pH intensified the emulsifying ability of sophorolipids, which is caused by the adsorption of sophorolipids on mine tailing surfaces.

4.2.2 Viscosity of sophorolipid solution

Investigations on three concentrations of sophorolipids showed that the dynamic viscosity of sophorolipids increased with the increase of concentration (Table 4.5).

Table 4.5. Viscosity of sophorolipids in different concentrations at 23 °C.

Temperature (ºC)	Solution	Dynamic Viscosity (cp)
23	DI water	0.93
23	1% SL	1.15
23	2% SL	1.23
23	5% SL	2.35

Hydraulic conductivity of the washing solution depends heavily on its viscosity, and its value shows the ease with which the washing solution can move through pore spaces of the media. Increasing the viscosity of the solution, in a given media, results in decreasing the hydraulic conductivity as:

$$K = \frac{k\rho g}{\mu}$$ **Equation 4.2**

Where:

- K is the hydraulic conductivity, m/s
- k is the permeability, m^2
- μ is the dynamic viscosity of the fluid, kg/(m·s)
- ρ is the density of the fluid, kg/m^3
- g is the acceleration due to gravity, m/s^2.

Therefore, increasing the concentration of the sophorolipids in the washing solution from 1% to 5%, not only escalates the expense of the remediation process, but it also makes the in situ washing difficult and more time-consuming. Also, lower hydraulic conductivity results in delays

in flushing and passing the contaminated solution through media, thus showing some of the heavy metals/metalloids which were released from the media to re-adsorb or precipitate.

4.2.3 Result from DLS analysis

Effect of concentration on the average size of micelle

Investigations on the impact of concentration on micelle size, using 1%, 2%, 3%, 4% and 5% sophorolipid solutions (SL 18), showed that an increase in the concentration of sophorolipids resulted in an increase in the average micelle size (Figure 4.5).

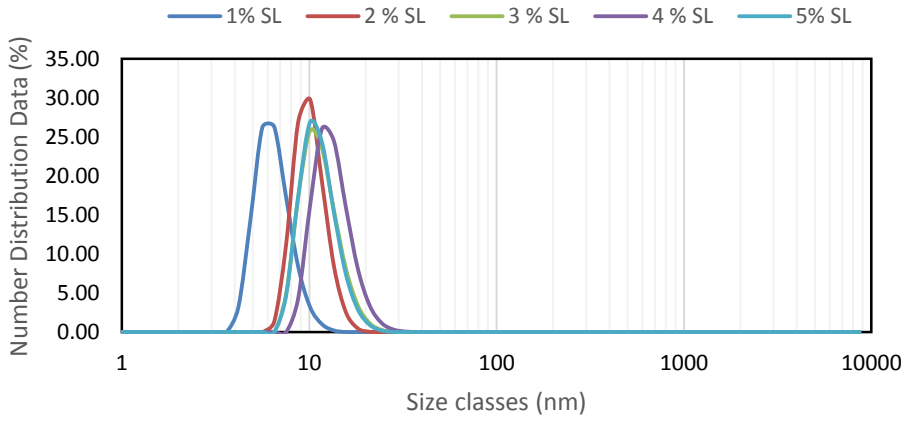

Figure 4.5. Size distributions of micelles in sophorolipid solutions with different concentrations.

Based on the results of these measurements, increasing the concentration from 1% SL to 2, 3, 4, and 5 wt % sophorolipids caused an increase of 55%, 80%, 108% and 80% in average diameter of the micelle, correspondingly. It should be noted that the highest concentration available in this experiment was 41 wt % (410 mg/mL), which was a thick and viscous solution that forms worm-like aggregates instead of spherical micelles. Within the range that was investigated, the data followed a logarithmic trend (Figure 4.6):

$$\text{Average diameter of micelles (nm)} = 7.51 + 3.16 \ln(\%\,\text{SL}); R^2 = 0.84.$$

In which % SL represents the sophorolipid concentration within the solution. The increase in the average size of the micelles may be due to transformations in the shape of micelles. As sophorolipid concentration increases, the spherical shaped micelles transform into long, rod-shaped micelles (Cates and Candau, 1990; Aswal and Goyal, 2003).

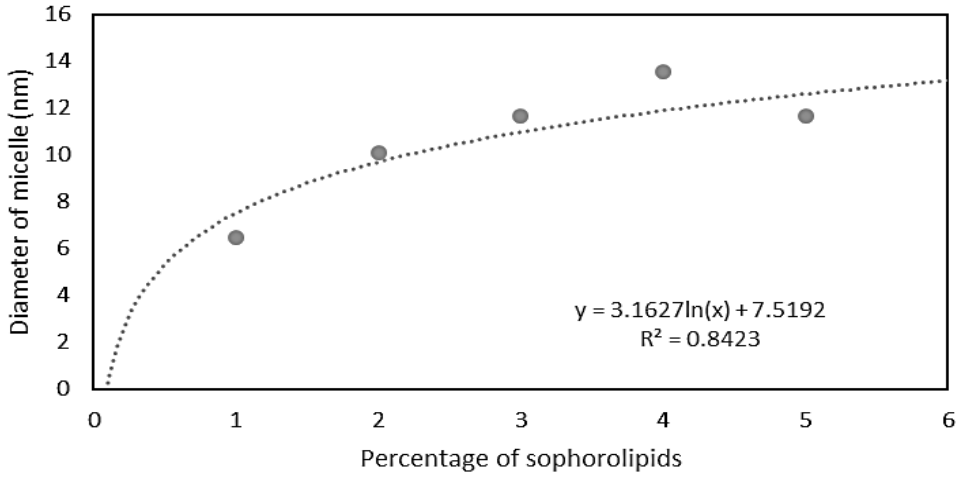

Figure 4.6. Average diameter of sophorolipid micelles at different concentrations.

Effect of pH on the average size of micelle

Investigations on the impact of pH on the size of micelles showed that the size of a micelle is highly pH dependent. This statement agrees with the Baccile et al. (2013)'s investigation on sophorolipids using Small Angle Neutron Scattering (SANS), which determined that shape and surface charges of sophorolipid micelles are profoundly affected by pH and the base being used for pH adjustment. Present DLS investigations on samples of 1% sophorolipids at pH 2, 4, 6, 8, 10, and 12, show that increasing pH up to pH 6 resulted in a decrease in the size of sophorolipid micelles (Figure 4.7).

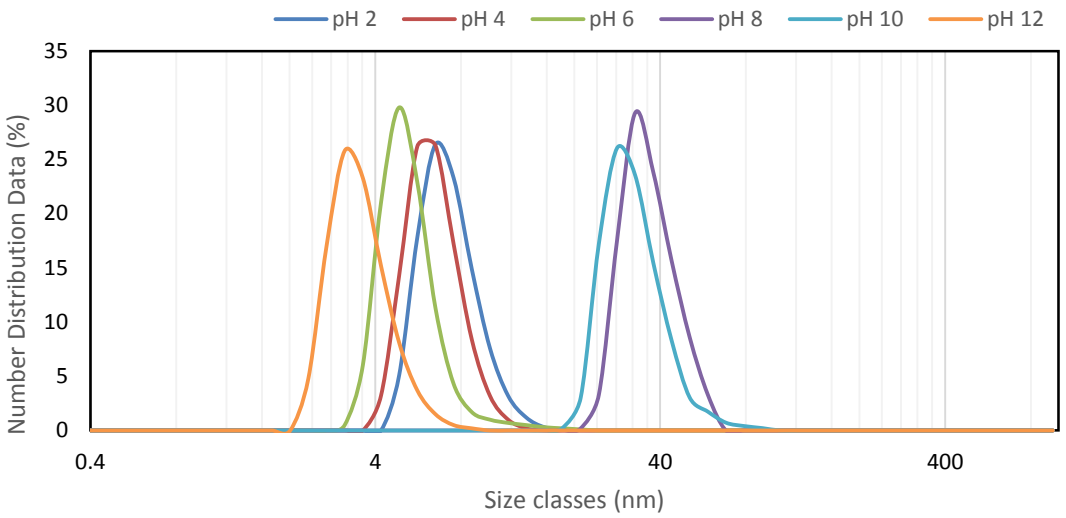

Figure 4.7. Micelle size (DLS result) in a solution of SL18 at pH 2, 4, 6, 8, 10 and 12.

As it can be seen in Figure 4.8, the average diameter of sophorolipid micelles at pH 2 was 7.63 nm. When the pH increased to 4, the average micelle diameter decreased to 6.51 nm. Further increase of pH resulted in reducing the average micelle diameter to 4.49 nm at pH 6. At pH 8 and 10, the charge density on carboxylic groups increases, packing parameter (CPP), changes the shape of aggregates from micelles to vesicles, bilayers, or inverted micelles. The critical packing parameter determines the geometry of biosurfactant aggregates (Figures 4.8 and 4.9). CPP is calculated according to the following equation:

$$CPP = \frac{V}{L\,a} \qquad \textbf{Equation 4.3}$$

Where:
V represents volume of a chain
L represents the length of the tail
a represents the cross-sectional area of head group

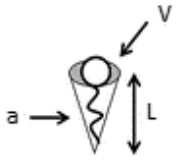

Previous researchers also stated that the size and the shape of aggregates of biosurfactants are pH dependent (Cantor and Schimmel, 1980, Dahrazma, 2008). The size and shape of biosurfactant aggregates is highly pH dependent. The diameters of aggregates vary from less than 5 nm diameter (micelles) to a diameter of greater than 500 nm (vesicles) (Miller, 1995). Mulligan

(2009) stated that changes in pH caused changes in rhamnolipid aggregates. It was shown that by increasing pH, the diameter of rhamnolipid aggregates decreased, reforming them from large vesicles (D = 60 nm) to smaller vesicles, which further increase in pH transformed them into micelles (D =1.5 to 1.7 nm).

According to Baccile et al. (2012), the overall degree of ionization of free functional groups such as COOH, which is caused by increasing pH, drives the self-assembly of sophorolipids. Baccile et al. (2012) stated that, by increasing the ionization degree of functional groups, the curvature of the aggregates increases. Therefore, cylindrical aggregates were transformed into ellipsoid/sphere micelles.

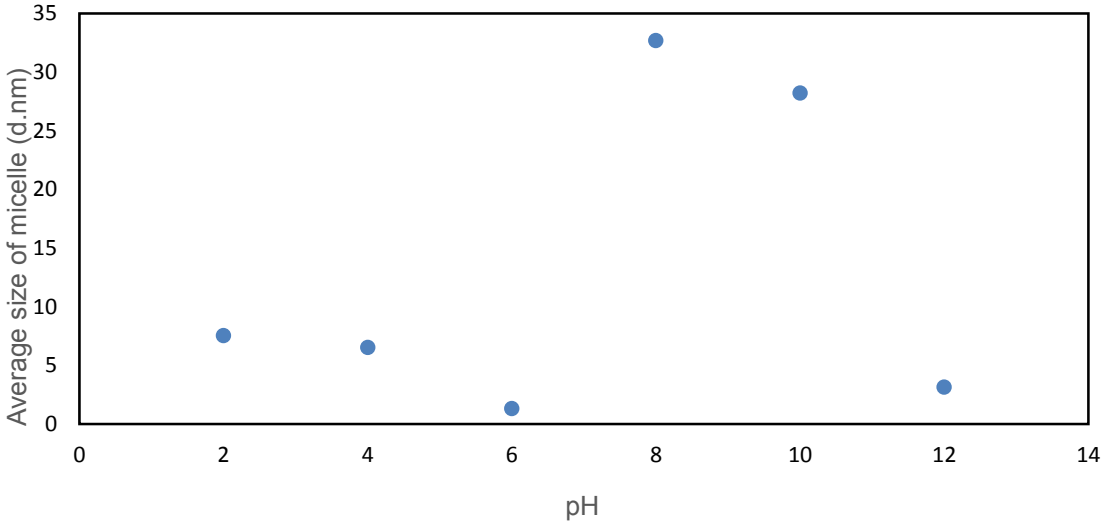

Figure 4.8. Average diameter of sophorolipid micelles at pH 2, 4, 6, 8, 10 and 12.

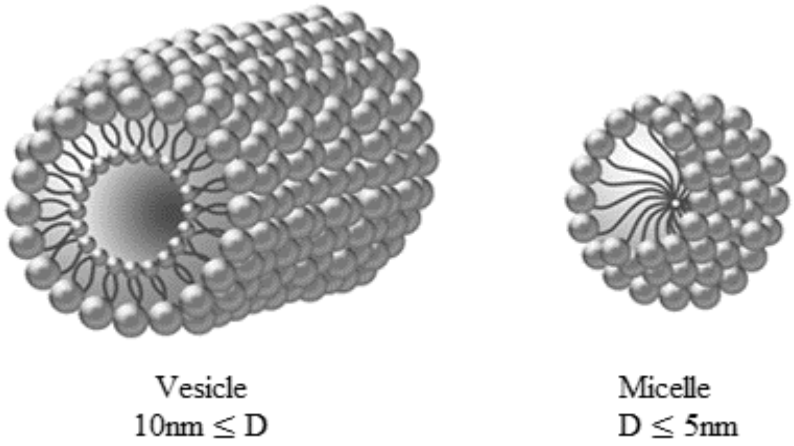

Figure 4.9. Effect of changes in pH on the shape of aggregates in a sophorolipid solution.

As it can be seen in Figure 4.10, there are some considerable changes in the diameter of the particles, resulting from pH-related changes in the structure and morphology of particles. As was noted before, the negative charges on the surface of sophorolipid aggregates increases by increasing pH, and at pH levels higher than 5, the surface of the aggregates become negatively charged. As Manet et al. (2017) stated, as pH increases, the boundary between the three regions of the micelle became less defined, therefore the shape and size of the micelle changes. Likewise, Ishigami et al. (1987) described the effect of pH on the size and shape of aggregates in rhamnolipid solutions (Figure 4.10). Their report shows that by increasing pH, the surfactant particles change from vesicle to lamellar, and finally, when pH is higher than 6.8, micelles are formed. It can be assumed that in a sophorolipid solution, changes in pH cause changes in the shape and size of aggregates.

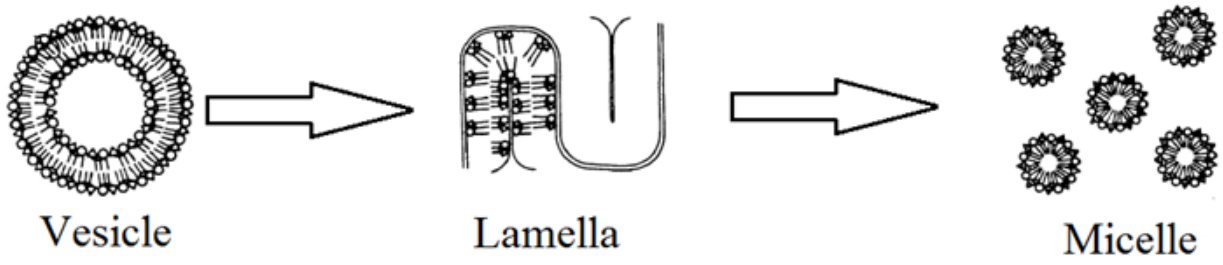

Figure 4.10. Effect of increasing pH on the morphology of rhamnolipid aggregates (Ishigami et al., 1987).

Zhou et al. (2004)'s investigation on aggregates in an acidic sophorolipid solution by microscope showed that, at pH 2, sophorolipid monomers rapidly start producing small ribbons, which, after 20 minutes, start to form flowerlike supramolecular aggregates (30-50 μm). By increasing the pH to 3.6, they developed more twisted ribbons, and at pH 4.1, the process of creating ribbons became slow, and the solubility decreased. Their investigation showed that at pH 5.1 and 5.9, the solubility of sophorolipids increased and the surface of micelles became negative. Finally, at pH 7.8 (in a solution of 0.2% SL), soluble micelles of SL-COONa with hydrodynamic radii as large as 100 nm were formed. As the sophorolipids used in the present study are highly lactonic, some differences are expected. Currently, there are no investigations on the micelle formation of lactonic sophorolipids, so there is a need to investigate this matter closely.

Sophorolipids has been known to be stable in wide range of pH levels, from 2 to 12 although investigations of Al-Jasim et al. (2016) showed that in highly alkaline environments (pH 12, 50˚ C), the production of small quantities of sucrose, sophorose, and other disaccharides were detected, which correspond to hydrolysis of a sugar. Increasing the pH to 12 caused the average diameter of micelles to decrease significantly (3.605 nm). A smaller micelle diameter can be interpreted as fewer monomers in each micelle. Because smaller micelles form in alkaline solutions, it is expected that in highly alkaline (pH 12) solutions with the same concentration of sophorolipids as an acidic solution, the number of micelles would be greater.

The more micelles are in the solution, the greater the solution's effectiveness. The current study showed that sophorolipids were most effective at removing arsenic in both acidic and highly alkaline environments. Moreover, the lowest sophorolipid assisted arsenic removal was observed at pH 8 and 10. Furthermore, investigation of the spectra of sophorolipids at different pH showed that sophorolipids have more affinity to adsorb arsenic in highly acidic environments. To further understand the relation between pH and sophorolipid aggregates, further investigation on micelles at different pH, through SANS and TEM is needed.

Effect of adding arsenic on the average size of micelle at various pH

To investigate the effect of adding arsenic to the micelle size, a mixture of 1% sophorolipids and arsenate (2 g/L) was prepared. Figure 4.11 illustrates the results of measuring the size of micelles in sophorolipid and arsenic mixtures (SL-As), at pH 2 to pH 12.

Figures 4.11 shows that by increasing the pH, the average diameter of micelles decreases, except in pH 6 and 8, where a sudden increase was seen because of changes in the shape of micelles. This increase is a result of increasing negative charge on the SL-COO^- and expansion of the micelle caused by repulsive inter-micellar interactions induced by NaOH. As the concentration of NaOH increases, it is expected that the interruption increases. On the other hand, the value of the average diameter at pH 10 and 12, shows an exception and these two points show a decrease in the size of micelle which is aligned with the result from pH 2 and 4 (Figure 4.12). The further microscopic investigation can elucidate the reason behind these abnormalities.

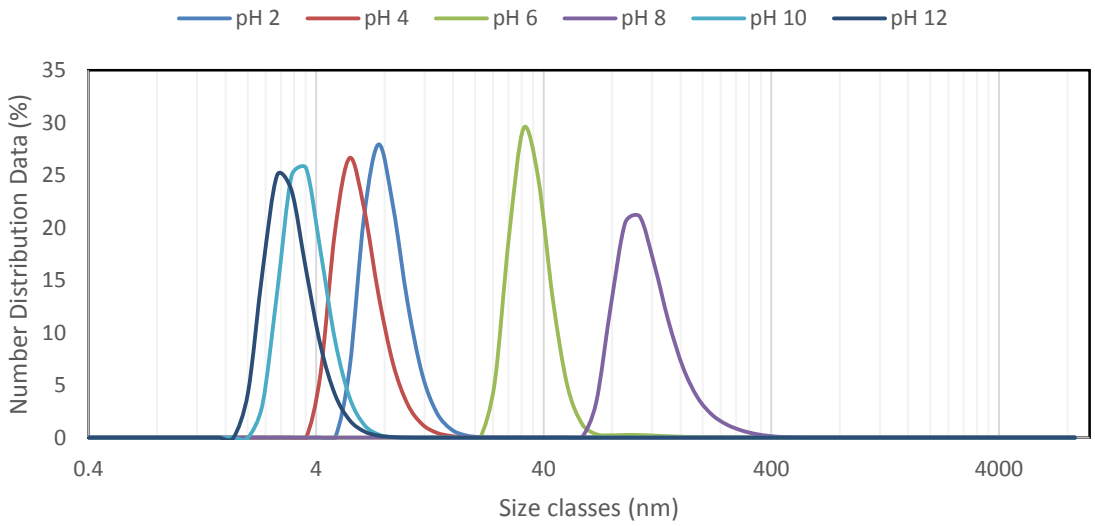

Figure 4.11. Micelle size (DLS result) in a solution of sophorolipids and arsenic at different pH.

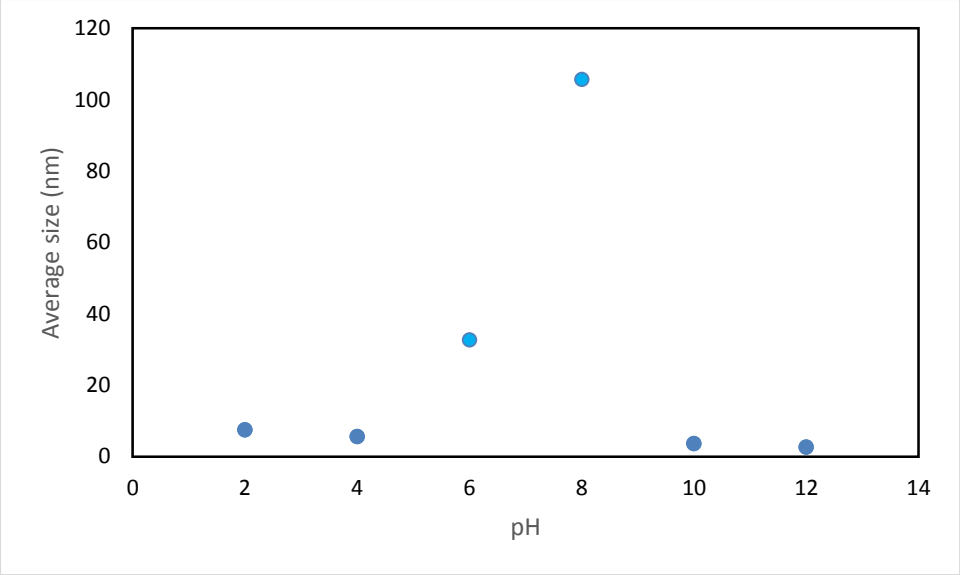

Figure 4.12. Average diameter of micelles in a solution of sophorolipids and arsenic at different pH.

Effect of adding iron on the average size of micelle at pH 2

To investigate the effect of adding iron and arsenic to sophorolipid solution on the size of micelles, a mixture of 1% sophorolipids and iron and arsenic was prepared. Figure 4.13 shows a comparison between the distribution of micelle size in a sophorolipid solution and solutions of sophorolipids with iron, arsenic and mine tailings at pH 2. As it can be seen, adding iron (SL-Fe-As), arsenic (SL-As) and mine tailings (SL-MT) caused increases of 18.5%, 15.7%, and 31.2%, respectively, in the average size of micelles. FTIR investigation on the effect of the presence of Fe, As and mine tailing on sophorolipid structure showed changes on the wave numbers of functional groups of sophorolipids which signify complexation with ions in the solution (Table 4.6).

Table 4.6. Average diameter of aggregates in solutions of sophorolipids, SL-As, SL-Fe-As, and SL-MT at pH 2

Solution	Average diameter size (nm)
SL	6.507
SL-As	7.531
SL-Fe-As	7.712
SL-MT	8.539

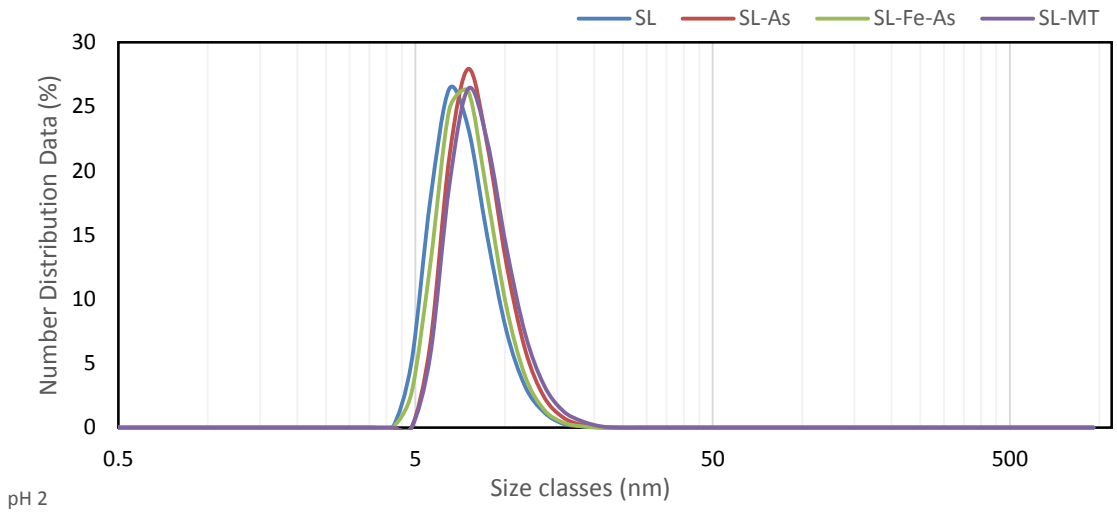

Figure 4.13. Size distributions of micelles in sophorolipid, SL-As, SL-Fe-As, and SL- MT solutions at pH 2.

Effect of adding mine tailings on the average size of micelle at different pH

In an investigation on the effect of the presence of mine tailing on sophorolipids, micelles showed that an increase in the pH of a mixture of sophorolipids and mine tailings (SL-MT) causes a decrease in the average diameter of micelles (Figure 4.14).

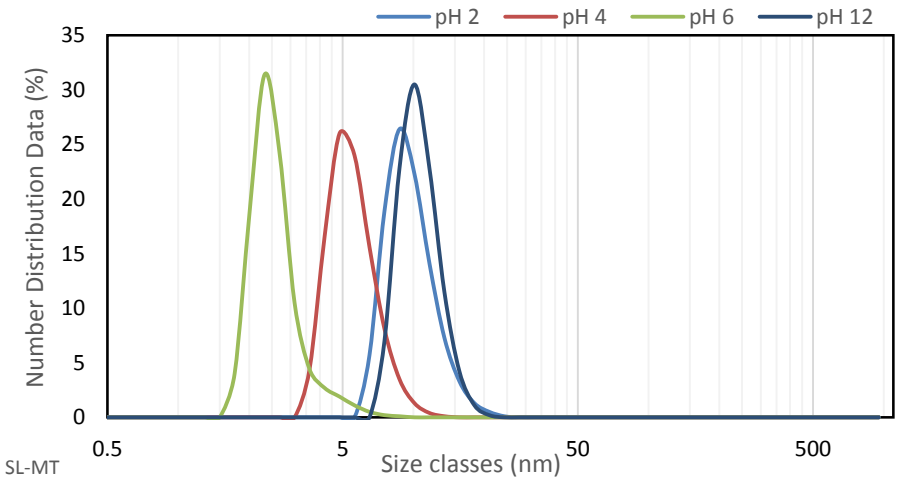

Figure 4.14. Size distributions of micelles in solutions of sophorolipid with mine tailing at different pH.

At the same time, the presence of mine tailings at each pH slightly increased the average diameters of the micelles as micelles solubilize the sample's constituents and bond to metals/metalloids. A comparison between the effect of pH on the size of micelles in sophorolipids, SL-As and SL-MT, shows that, by introducing arsenic and mine tailings, the size of micelles at pH 8 and 10 increased substantially which confirms the transformation of aggregates from micelles to vesicles at these two pH levels (Figure 4.15).

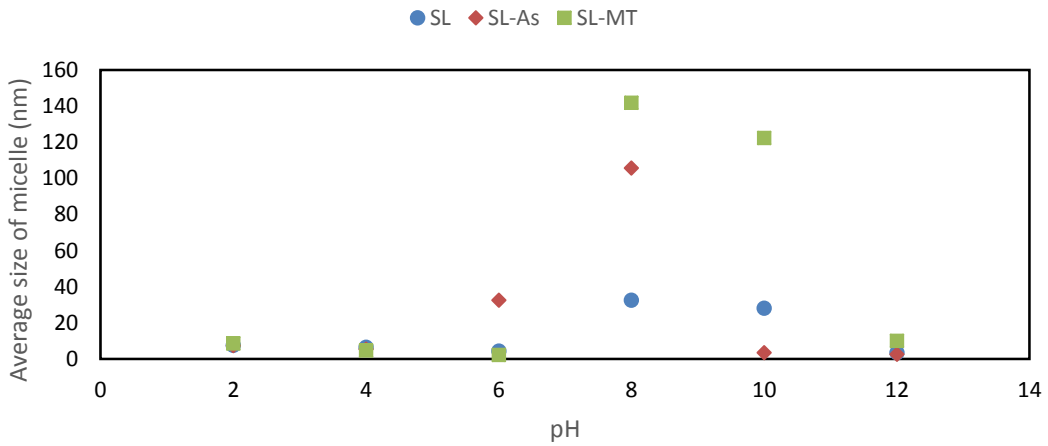

Figure 4.15. Average diameter of micelles in a solution of SL, SL-As, and SL- MT solutions at different pH.

In conclusion, investigations on the effect of concentration of sophorolipids on the size of micelles showed that an increase in the sophorolipid concentration resulted in an increase in the average size of micelles. It should be noted that the concentrations of the solutions which were used in this part of the experiment, 1%, 2%, 3%, 4% and 5% SL, were at least 4 orders of magnitude more concentrated than the CMC level of sophorolipids.

The current investigation showed that the pH has a greater impact on the micelle size than any other factor. These results are in agreement with the results of the investigations conducted by Dahrazma et al. (2008) on the effect of pH and additives on the rhamnolipid aggregates using small angle neutron scattering (SANS). Their results revealed that pH is an important factor affecting the size and morphology of rhamnolipid aggregates. It was also shown that pH has a stronger impact on the size and morphology of aggregates than the presence of additives, as variations in pH change

the charge density on carboxylic groups, influencing the effective size of aggregates' head group, affecting the size and shape of micelles from (Dahrazma et al., 2008). However, the results reported on the impact of pH on rhamnolipid aggregates are different from the results obtained in the present study on pH-induced changes in sophorolipid aggregates.

The investigations on the effect of pH on micelle size showed that in acidic environments, increasing the pH resulted in a decrease in the average micelle size, in medium alkaline environments, aggregates tend to be larger, which confirm the transformation of micelles to vesicles. As the size of vesicles is up to 100 times larger than micelles, the ability of the biomolecules to penetrate pores decreases. On the other hand, at any concentration above the CMC level, more monomers are used for creating these bilayers aggregate (vesicle) than what is used for creating micelle, thus there would be fewer aggregates in the solution compared to a sophorolipid solution composed of micelles. Therefore, less removal of elements is expected at these pH levels. The result from the batch and continuous experiments supported this statement. In highly alkaline (pH 12) environments, a substantial reduction in micelle size was observed.

Further investigations on the samples using Nuclear Overhauser Spectroscopy (2D NOSEY) can help with understanding the reason for these discrepancies at higher pH levels (8 and 10). Additionally, a close examination of the sample using small angle neutron scattering (SANS), and TEM techniques can shed light on the SL micelle behavior and their shape in solution at different pH.

4.3 RESULT OF THE REMOVAL OF ELEMENTS FROM MINE TAILING SAMPLE

In the first stage, a series of batch experiments was conducted to evaluate the feasibility of sophorolipid assisted arsenic removal from mine tailings. During this stage, the optimal condition for sophorolipid assisted removal of elements was investigated by changing factors such as pH, temperature, concentration of sophorolipids and the ratio of washing solution to one gram of sample. The second stage consisted of column experiments (continuous soil washing). During this stage of the experiment, in a bench top column, the removal of elements in a continuous system was investigated.

4.3.1 Batch experiments

The batch experiments were conducted in three segments. The first phase of the research focused on comparing the efficiency of sophorolipids and rhamnolipids in the removal of arsenic and heavy metals from mine tailings; the second part consisted of investigation on the effectiveness of sophorolipids at three different temperatures, and different pH levels, with the various concentrations of sophorolipids. The third phase of the study consisted of observing the effect of biosurfactants on different fractions of mine tailings and the speciation of arsenic.

The results of the analysis of the amount of arsenic removed during preliminary batch tests by using different concentrations of biosurfactants, sophorolipids (SL) or rhamnolipids (Rh), at various pH levels, showed that the removal of arsenic has a positive correlation with the concentration of the biosurfactants. Increasing the concentration of the biosurfactants, for both rhamnolipids and sophorolipids, resulted in a higher removal (Arab and Mulligan, 2013). This result is in agreement with observations of Guemiza et al. (2017) on the removal of contaminant from soil by using cocamidopropylbetaine-BW (CAPB) at a pilot scale test. During the experiment conducted by Guemiza et al. (2017), the contaminated soil was subjected to a zwitterionic surfactant (CAPB) in a 10L reactor equipped with a mechanical stirrer, to investigate the effect of temperature, concentration of surfactant and pulp density in removal of contaminants such as heavy

metals and polychlorinated dibenzodioxins (PCDDs).Their result showed that the concentration of surfactants was the main factor controlling the efficiency of surfactant in the removal of contaminants from soil.

In a comparison between rhamnolipids and sophorolipids, it was observed that in an alkaline environment, the concentration of arsenic removed by the rhamnolipids was higher than the concentration removed by the sophorolipids at the same pH. It has been observed that the rhamnolipids at pH 11 were able to remove a greater amount of arsenic than at pH 6. At pH levels lower than pH 6, the rhamnolipids started precipitating and lost their effectiveness (Arab and Mulligan, 2013). The experiments conducted by Wang (2010) and Dahrazma (2005) showed that rhamnolipids are able to remove higher quantities of heavy metals in highly alkaline environments than at lower pH levels. Rhamnolipids have been proven as an effective agent for the removal of heavy metals, by previous researchers. Despite results from the current study, which shows that, in highly alkaline environments, rhamnolipids are more efficient than sophorolipids in the removal of arsenic and heavy metals (Arab and Mulligan, 2013), the economic feasibility and effectiveness of sophorolipids at lower pH levels make them an excellent substitute to other washing solutions in the soil washing process.

Figure 4.16 illustrates the results of the batch experiments using different concentrations of sophorolipids. These results have shown that the increase in the sophorolipid concentration enhanced the removal of all of the target elements. Similarly, experiments conducted by Mulligan (1998) showed that the removal of copper, zinc, and cadmium increased by increasing the sophorolipid concentration in acidic and alkaline environments and a mixture of sophorolipids and Triton X-100.

However, the correlation between the sophorolipid solution concentration and the removal of elements is not linear for all elements. For example, the removal of arsenic follows a power regression model:

$$As = 28 + 1.43\sqrt{SL} \qquad (R^2 = 0.97) \qquad \textbf{Equation 4.4}$$

In which:

As represents the concentration of arsenic removed (mg/kg)

SL represents the concentration of sophorolipid in solution (mg/kg)

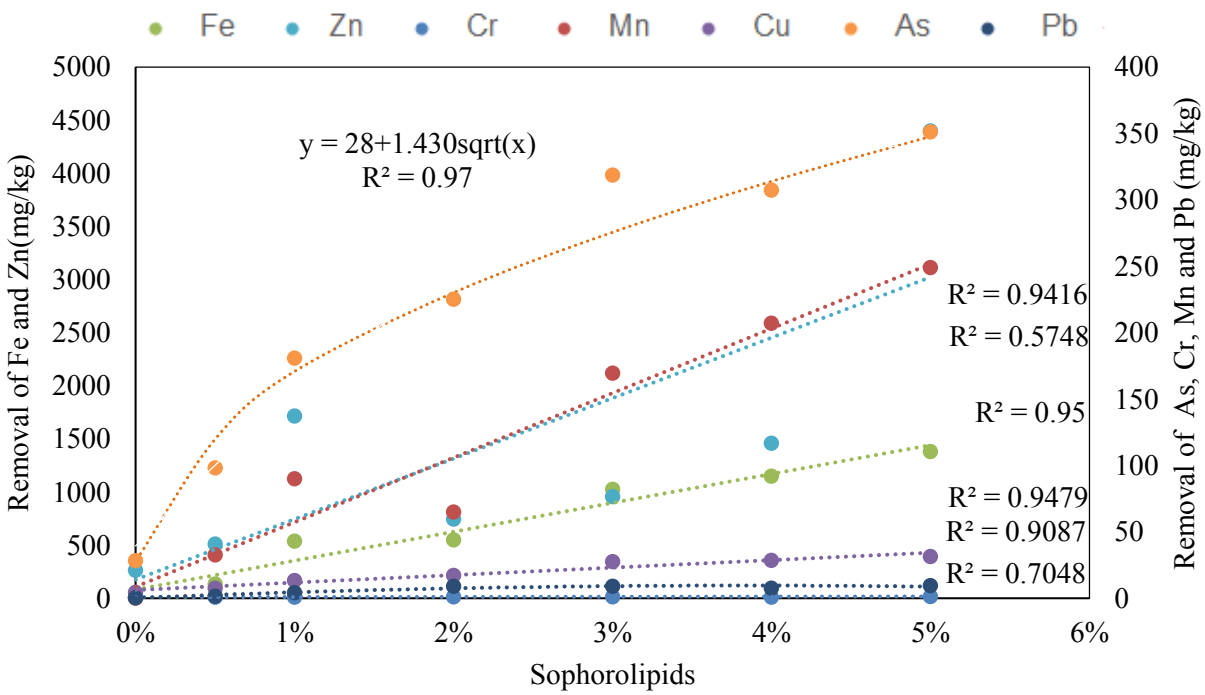

Figure 4.16. Removal of Mn, Fe, As, Cr, Ni, Cu, and Pb during the batch experiment using different concentrations of sophorolipids (20mL per gram of sample) at pH 5.

As it can be seen in Figure 4.16, the removal of elements in batch experiments using DI water (at 0 % SL) was much lower than the removal of elements using sophorolipids. For example, in these experiments, the removal of chromium during the batch experiment by using DI water was very low. Further investigations by digestion of the residual from the tubes showed that the amount of the chromium in the residual was very close to the concentration of chromium in the untreated sample.

Figures 4.17 and 4.18 illustrate a comparison between the removal of target elements by using 0.5 % SL and 1% SL at two different temperatures (15˚C and 23˚C) and the ratio of 20 mL

sophorolipids per gram of mine tailing. As it can be seen, the solution of 1% sophorolipids was more effective in removing elements from mine tailing than 0.5% sophorolipid solution during the seven-day experiment at both temperatures (Figures 4.17 and 4.18). For instance, it was shown that in batch experiments at 23ºC after 24 h removal of arsenic, 1% SL was 9.1% more efficient than 0.5% SL and was 164 % more effective than DI water. In the removal of iron also it was observed that 1% was 14% more effective than 0.5% SL and was 1510 % more effective than DI water.

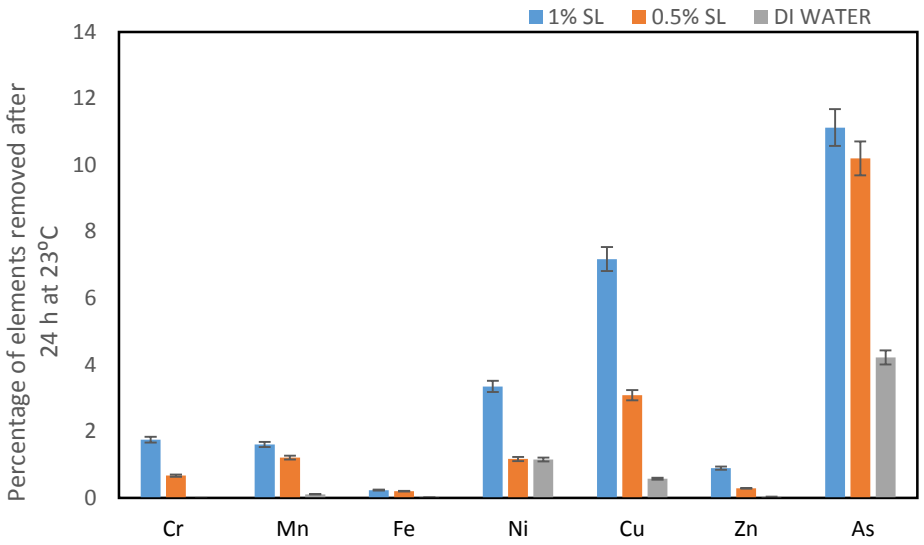

Figure 4.17. Percentage of elements released by a solution of 1% sophorolipids vs. 0.5% sophorolipids and deionized water at 23 ºC.

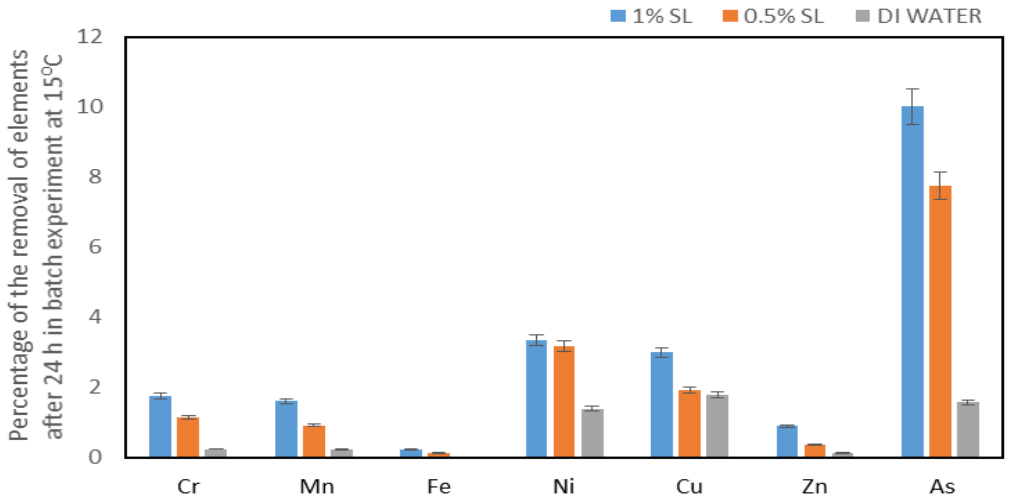

Figure 4.18. Percentage of elements released by a solution of 1% sophorolipids vs. 0.5% sophorolipids and deionized water at 15ºC.

The effect of the ratio of the washing solution to the dry sample on the removal of 10 different elements from the mine tailing sample has shown that increasing the volume of washing solution causes a substantial increase in the release of elements from mine tailing sample. During these experiments, samples of 1g of the mine tailing sample were subjected to 30, 20 and 10 ml of 1% sophorolipids, and 30, 20 and 10 ml deionized water during a batch experiment at 23ºC and 15 ºC (Figure 4.19 and 4.20). In these experiments, it was shown that sophorolipid solutions were much more efficient in removing arsenic and heavy metals from mine tailings than deionized water with the same volume. These experiments have shown that an increase in the volume of 1% SL from 10 to 20 mL of a washing solution causes an increase in the removal rate of arsenic after 24 hours, 48 hours and 7 days by 36%, 59%, and 90%, respectively.

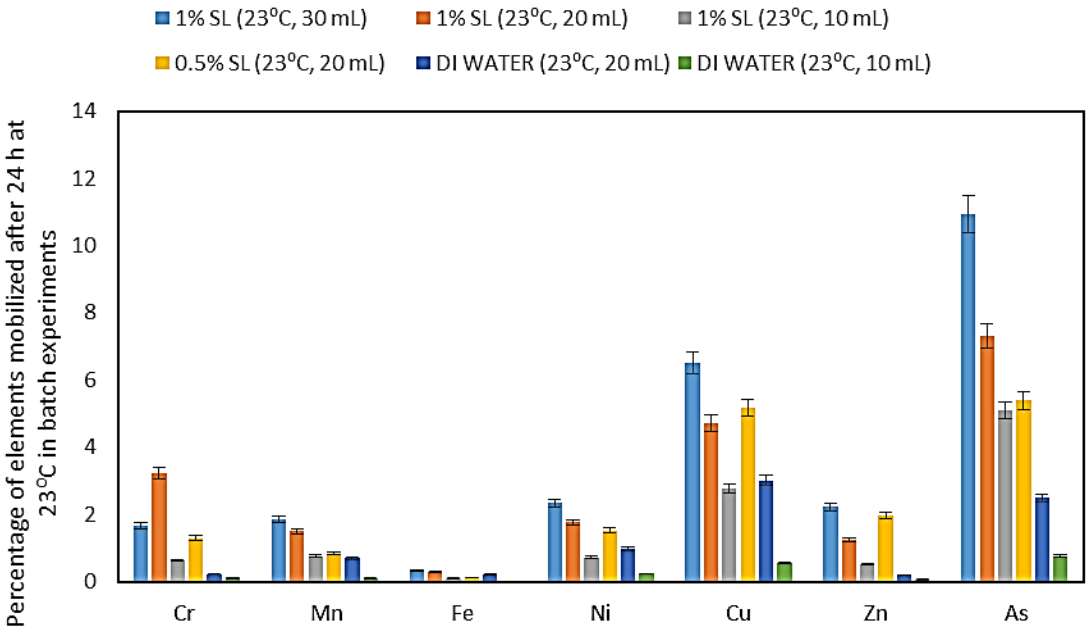

Figure 4.19. Arsenic released by different volumes of 1% SL solution and different volumes of washing solutions at 23ºC.

A comparison between the removal arsenic at 23ºC, using 1% SL (20 mL per 1 g sample), and 0.5% SL (40 mL per 1 gram of sample) proves that the concentration of biosurfactants has a more significant impact on their effectiveness in removing elements from the sample.

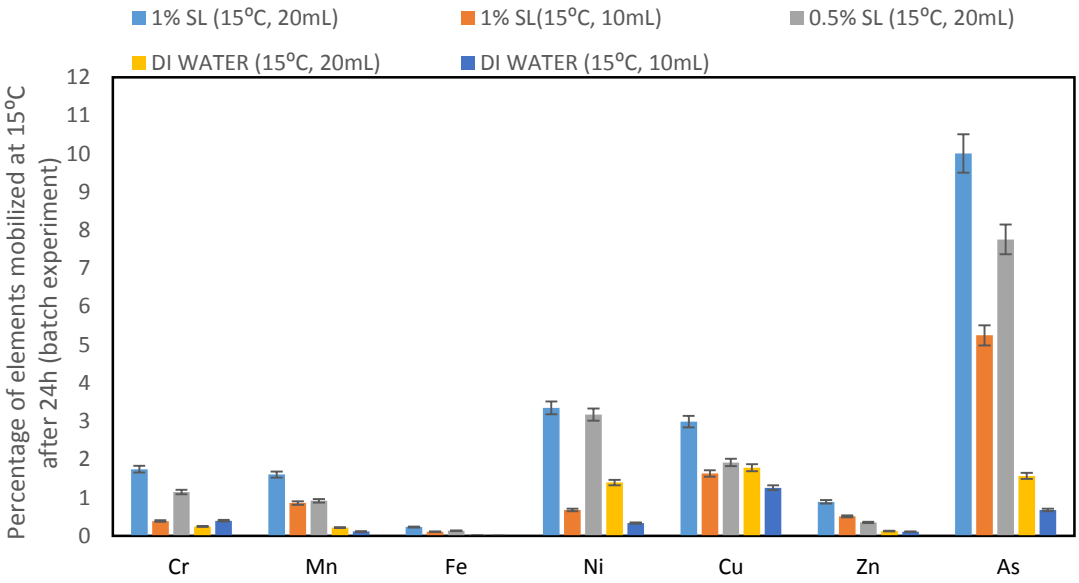

Figure 4.20. Arsenic released by different volumes of 1% SL solution and different volumes of washing solutions at 15°C.

Figures 4.21 and 4.22 illustrate the result from the batch experiments using DI water and 1% sophorolipids as the washing solution, at different pH levels ranging from 2 to 12, despite the fact that these extreme pH levels (pH 2 and 12) are not expected in typical environments. However, to predict the inevitable effect of presence acid mine drainage (AMD), acid rain or some other unpredicted extreme environmental conditions, the experiments were expanded. Throughout these experiments, the stability of sophorolipids and their effectiveness in various pH levels were investigated.

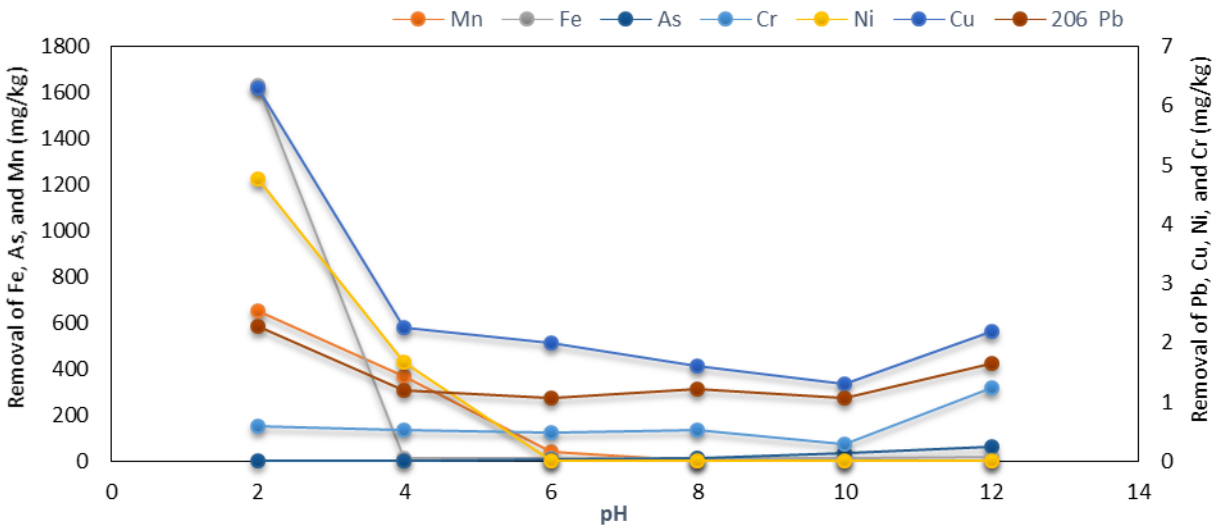

Figure 4.21. Removal of elements with DI water at different pH.

As it can be seen in Figure 4.21, in the leaching with DI water, for copper, iron, nickel, lead, and manganese the highest quantity of removal were in the acidic environment, and their removal has a negative correlation with pH. Although a small increase in the removal of Cu, Fe, Mn at pH 12 was observed, that could be the result of the dissolution of some fractions of tailing samples, such as organics, in an extreme alkaline environment. It can be assumed that at acidic conditions, iron oxide/hydroxide and carbonates react with acid (HCl) and produce two species of iron chloride, ferrous chloride, and ferric chloride, both of which are soluble in water. According to Sidho et al. (1961), the presence of HCl in the solution increases the dissolution rate of iron oxides. Also, the size of crystals of iron oxide is an important factor governing its dissolution rate (Schwertmann, 1991). On the other hand, the pH of the environment has a significant effect on the charge of the multivalent metal oxy/hydroxides, as they act as buffers in solution (Stumm and Morgan, 1996). Therefore the higher solubility of these metal oxide/hydroxides at acidic environment and precipitation of them as hydroxide in alkaline environment is the result of compensation for higher H^+ or OH^- in the solution. At neutral pH, hydroxides of aluminum and transition metals such as iron have very low solubility. For example, the solubility product (K_{sp}) for $Fe(OH)_3 = 6 \times 10^{-38}$ and $Fe(OH)_2 = 4.1 \times 10^{-15}$; and in high alkaline environments, iron II hydroxide and iron III hydroxide accept OH^- and forming the soluble ion of $Fe(OH)_4^-$ (Figure 4.22).

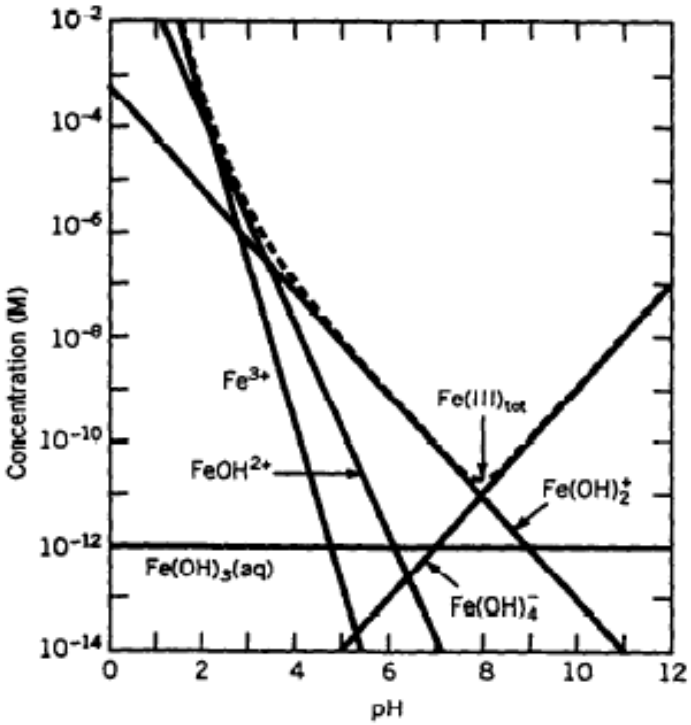

Figure 4.22. The effect of hydrolysis in the solubility of amorphous FeOOH (Stumm and Morgan, 1996).

Chromium and arsenic removal with DI water was low and had a slight increase at pH 12. This result is consistent with observations of Reynier et al. (2013) on the comparison between the efficiency of inorganic acids and bases in the process of removal of arsenic from contaminate soil. According to Reynier et al. (2013), sodium hydroxide (1N) was far more efficient than hydrochloric acid (1N) in removing arsenic from the soil. It should be noted that the presence of buffers in the sample made increasing the pH beyond 10 challenging, it was achieved by adding a solution of NaOH and stirring numerous times until the pH reaches 12, which also contributed to the breakdown of some of the fractions of the sample and releasing elements. Based on these experiments, transition metals have the highest removal in acidic environments, and that their release had a linear correlation with each other, except chromium. Chromium, unlike other transition metals, shows lower mobility in its lower oxidation state and (Cr (III)) and has higher mobility in its higher oxidation state (Cr (VI)) (Geelhoed et al., 2003).

At low pH, sulfide minerals are oxidized more rapidly than in alkaline solutions. Oxidizing the sulfide minerals results in releasing sulfate ions, which with metal ions in the media form metal sulfate. In washing with sophorolipids, clusters of particles were broken down, thus more surfaces of minerals were exposed and subjected to oxidation. Washing with DI water couldn't break down clusters and expose more surfaces in the sample.

The low removal of arsenic, when washing with DI water, in both acidic and alkaline environment can be due to the low quantity of this metalloid presence in the water-soluble fraction of mine tailing. The increase at pH 12 was due to the release of arsenic from other fractions such as the organic fraction of the mine tailing (Masscheleyn et al., 1991; Azouzi et al., 2015).

However, in the process of removal by using 1% SL (Figure 4.23), arsenic was removed in both acidic and alkaline environment, and the removal of arsenic by sophorolipids was much higher than removal with DI water. The lowest removal of arsenic happened at pH 8, from pH 4 to pH 8, there was a negative correlation between the pH and removal. After pH 8, this correlation became positive. By comparing the removal of arsenic from the acidic and alkaline environment, it can be assumed that the sophorolipid solution was most effective at removing arsenic in acidic and highly alkaline conditions.

The highest chromium and zinc removal were at pH 8 and 10, respectively. Decreasing or increasing the pH caused a reduction in the removal of both chromium and zinc. The greatest copper removal occurred at pH 2 and 10, although results show that changes in pH level insignificantly affected the copper removal. The removal of iron, manganese, nickel, and lead had negative correlations with pH. The highest removal for Fe, Mn, and Ni occurred at pH 2, and the maximum removal for Pb was observed at pH 2 to 4, and beyond these peaks, increasing pH resulted in a decrease in the removal of these elements.

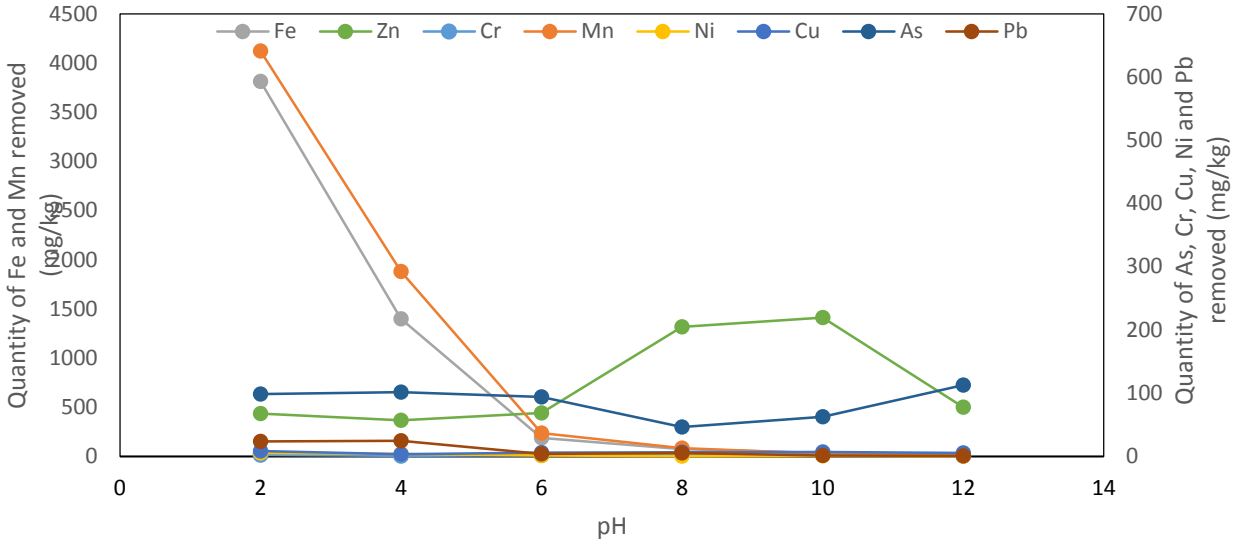

Figure 4.23. Removal of elements with 1% SL at different pH.

It was shown that the release kinetics of iron from mine tailing in the batch experiment by using 20 ml/g of 1% SL solution, were described by the power function equation (Figure 4.24). These results were expected, as iron is soluble in acidic environment and precipitate as pH increases. Moreover, at lower pH levels, the number of negatively charged sites for absorption of cations on the media decreases. Also, there would be a competition between cations and H^+ ions. On the other hand, in an alkaline environment, there are plenty of negatively charged sites available in the medium for iron to be adsorbed (Moghimi et al., 2013; Qafoku et al., 2004, Smith, 1999).

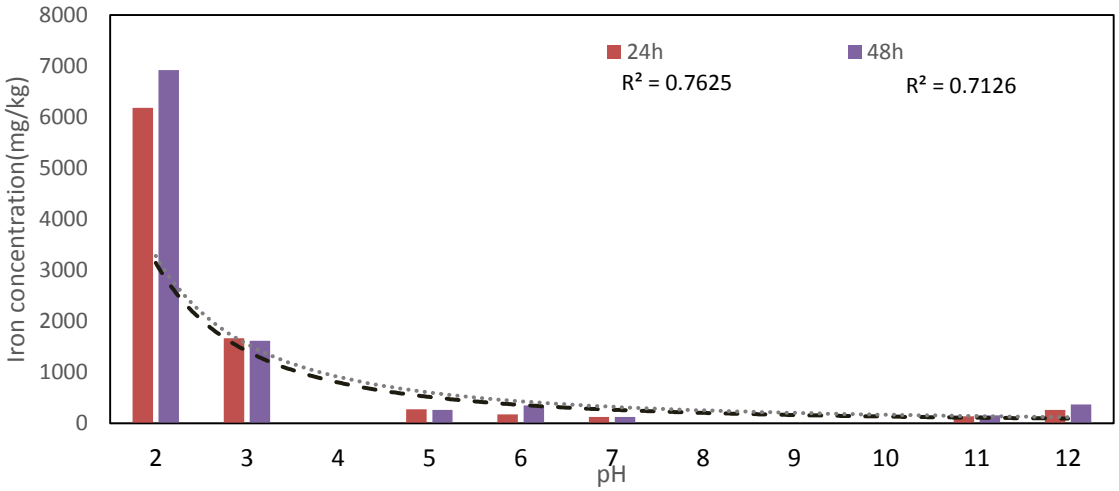

Figure 4.24. Release of iron after 24 hours vs. 48 hours in batch experiments using a solution of 1% SL.

The results from this part of the study show that transition metals such as manganese, iron, and nickel are more mobile in the acidic environments, and can be washed away with acid mine drainage (AMD). These transition metals and aluminum are the main adsorption sites for arsenic anions, therefore dissolving these elements results in the release of arsenic anions into the effluent. Therefore, the increased removal of arsenic in low pH levels can be attributed to the release of cations such as iron and aluminum and bonding with a sophorolipid micelle through metal bridging (Figure 4.25).

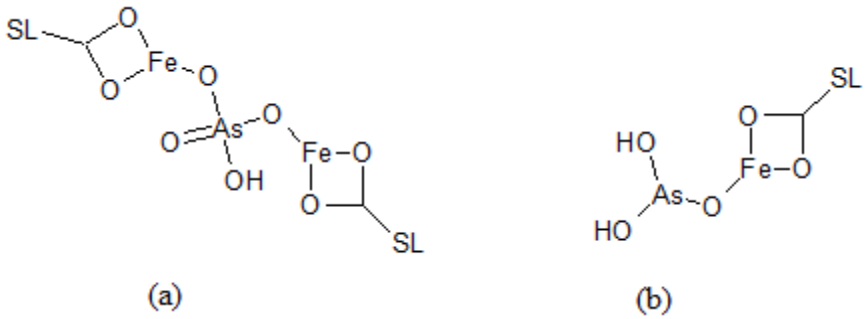

Figure 4.25. Adsorption of arsenate (a) and arsenite (b) to sophorolipid surface through metal bridging.

The release of arsenic from mine tailings decreases as the environment goes toward neutral pH. This phenomenon could be the result of co-precipitation of arsenic and iron oxide/ hydroxide in neutral pH. At alkaline conditions, the arsenic release is increasing by pH rise. However, the release of arsenic at alkaline environments is not correlated to the release of metals such as iron and manganese. Figure 4.26 shows a comparison between the removal of iron and arsenic by DI water (DIW) and a 1% SL solution at different pH levels.

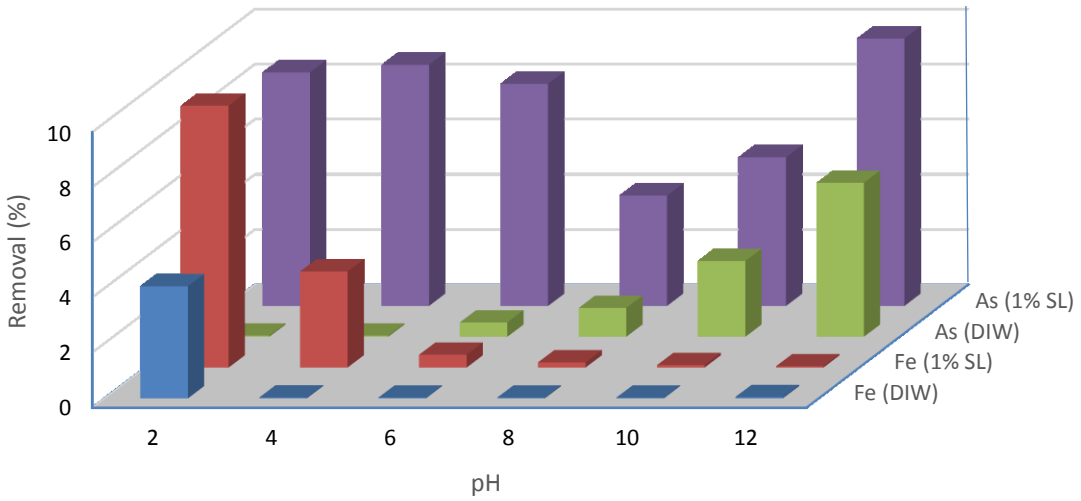

Figure 4.26. Removal percentage of iron and arsenic with 1% SL DI water at various pH

In alkaline environments, the increased solubility of arsenic is the result of the release of hydrogen, from hydroxides in the media into the solution, resulting in increasing the negative charges on the surface of minerals, therefore repelling the arsenic anions. According to Dzombak and Morel (1990), and Manning and Goldberg (1997), the adsorption of arsenic ions to iron oxide is pH dependent. In an acidic to a neutral environment, iron oxide surfaces are positive and adsorb arsenate and arsenite. However, if the pH is increased above the point zero charge (PZC), for example above pH 7.5 - 8 for goethite (Rong et al., 2009; Kosmulski, 2004), iron oxide surfaces become negatively charged, and thus repel arsenite and arsenate ions. Another mechanism that explains the increase in solubility of arsenic in alkaline environments is that in alkaline environments, there is a high concentration of OH^-, therefore, H^+ is consumed. This causes the equilibrium state of the reaction of $FeAsO_4.2H_2O + H_2O \rightleftharpoons H_2AsO_4^- + Fe(OH)_3 + H^+$ to shift towards the right, since H^+ is consumed, lowering the concentrations of the products, thus decreasing the rate at which the backward reaction occurs.

According to Baccile et al. (2013), sophorolipid micelle effectiveness is pH dependent. Considering the Le Chatelier's Principle, and the fact that when the environment becomes more alkaline, the number of negative ions will be increased, for carboxyl groups from pH 6 they start donating protons to the effluent (Figure 4.27).

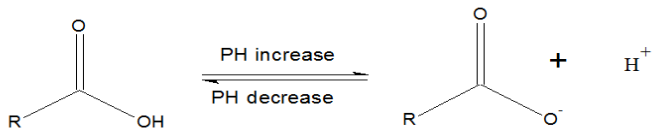

Figure 4.27. Effect of changes in pH level on carboxyl groups.

In an alkaline environment, the carboxyl groups of sophorolipids have more negative charges and thus bind more strongly with cations from the effluent. The increase in the release of arsenic at alkaline environment cannot be attributed to the process of metal bridging with SL-Fe. In an alkaline environment, the organic portions of mine tailings were more susceptible to decay and are eroded away by washing with sophorolipid solution, which consequently results in a decrease of the available complex-formation sites for arsenic. An alternative explanation for the increased release of arsenic in an alkaline environment is that higher pH levels reduce the arsenic oxidation state and convert it to a more soluble state of arsenic (As III) (Theis and Singer, 1974, Dixit and Hering, 2003, Masscheleyn et al., 1991, Frost and Griffin, 1977).

As it has been shown in previous research (Wang and Mulligan, 2009), rhamnolipids are able to remove high concentrations of arsenic at higher pH levels. However, Rh precipitates at acidic pH levels (Dahrazma et al., 2008). Sophorolipids show satisfactory performance at a variety of pH levels, and the concentration of arsenic released was much higher than the concentration of arsenic released with deionized water.

As it can be seen in Figure 4.28, in an acidic environment (pH 2.5), a strong linear correlation between the release of iron and arsenic was observed ($r = 0.97$). On the contrary, there was no correlation between the release of iron and arsenic in the slightly acidic environment (pH 5) ($r = 0.17$). In the alkaline environment (pH 8) there was a strong correlation between the release of these two elements ($r = 0.81$).

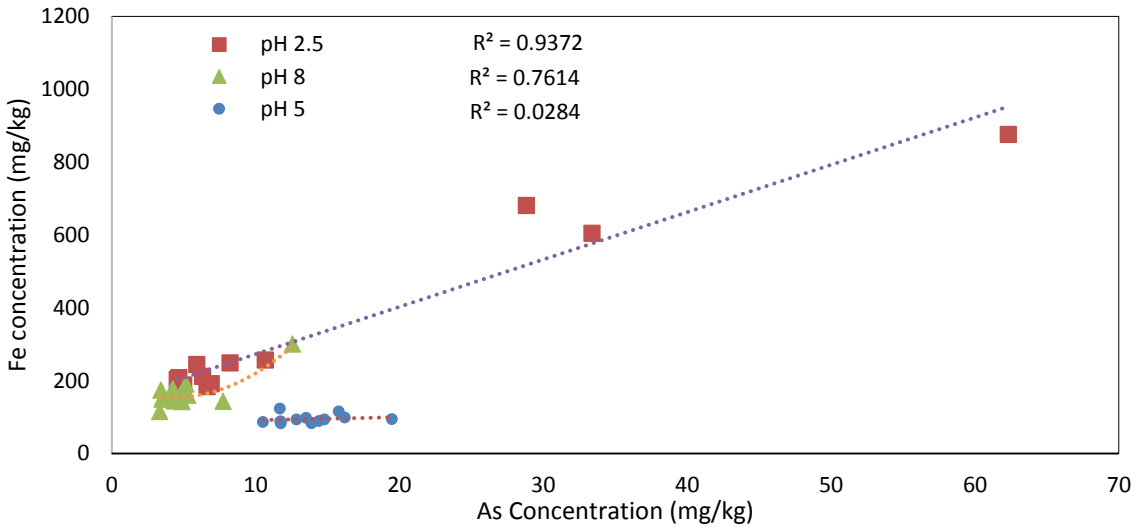

Figure 4.28. Correlation between the release of arsenic and iron at pH 2.5, 5, and 8 using 0.5% sophorolipids at 23^{0}C.

At this stage of the research, the removal of arsenic during batch tests at three different temperatures, 15ºC, 23 ± 1ºC, and 35ºC was compared. As temperature decreased from 15 °C, the solubility of sophorolipids and their efficiency was decreased and at temperatures below 10 °C, they started to precipitate. The sophorolipids used in this study, SL18, was highly lactonic sophorolipid. It was a mixture of lactonic sophorolipids (nonionic) and acidic (anionic) sophorolipids. Lactonic sophorolipids are more effective than acidic sophorolipids in lowering surface tension (Van Bogaert, 2011). On the other hand, acidic sophorolipids are much more effective in solubilizing metal ions. Baccile et al. (2013) described the effect of temperature and pH on the affinity of these biosurfactants toward cations. Acidic sophorolipids are more susceptible to temperature (Webera et al., 2012; Rau et al., 2001). At temperature below 10˚C, sophorolipids started to precipitate. For this reason, the efficiency of sophorolipids decreased substantially in temperatures lower than 10˚C and the removal by using a sophorolipid solution was in the same range as the removal by DI water. Figure 4.29 shows the solubility of sophorolipids in aqueous phase at different temperatures. As it can be seen, the maximum solubility was at 20˚C, which agrees with the results of the efficiency of sophorolipids in removal of heavy metals/ metalloids at different temperatures.

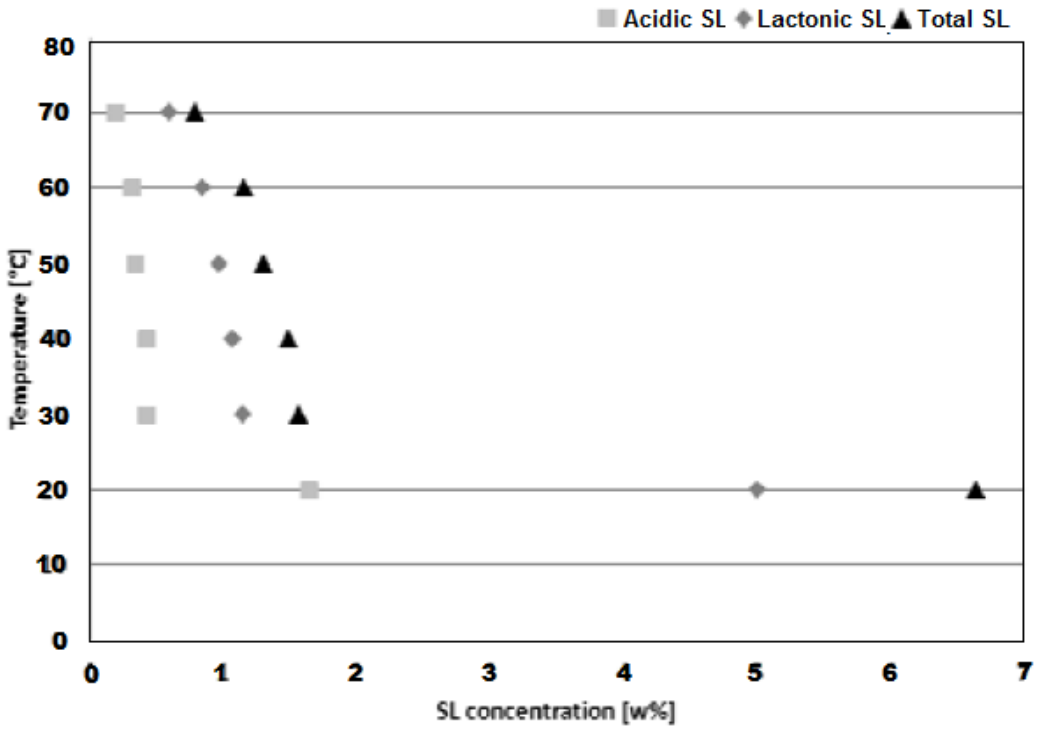

Figure 4.29. Solubility of SL in aqueous phase at different temperatures (Webera et al., 2012).

These experiments confirmed the importance of temperature in the removal of arsenic from mine tailings. As it can be seen in Figure 4.30, increasing the temperature from 15^0C to 23^0C resulted in a 36% increase in the removal of arsenic from the mine tailing specimen when using 1% sophorolipids. At the same time, results demonstrated that, when using deionized water (DIW), an increase in temperature from 15^0C to 23^0C led to an average of 16% increase in arsenic removal. The same experiments showed that increasing the temperature from 15^0C to 23^0C, affected iron removal significantly, and resulted in a 48% increase in the removal of iron from the mine tailing specimen by washing with 1% sophorolipids. On the other hand, when deionized water was used as the washing solution, the increase in temperature from 15^0C to 23^0C resulted in only a 24 % increase in iron removal.

In the batch experiments when 1% sophorolipids were used as the washing solution, by increasing temperature from 23 ºC to 35ºC, 22% decrease in the removal of arsenic and 11% reduction in the removal of iron was observed. At the same time using DI water as a washing

solution showed that by increasing temperature from 23 ºC to 35ºC, 2.9 times more arsenic was released.

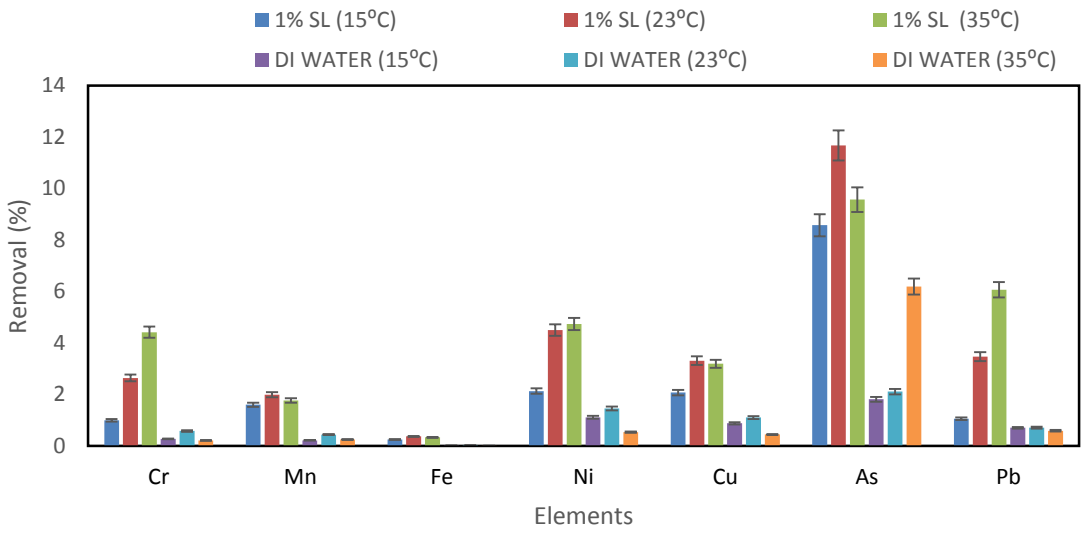

Figure 4.30. Release of elements from mine tailing by using sophorolipids and DI water at 15˚C, 23˚C and 35˚C.

The current experiments confirmed the importance of temperature in the efficiency of sophorolipids in the removal of arsenic from mine tailings. As shown in the Figure 4.30, sophorolipids assisted removal of all elements tested were higher than the removal by using DI water. Increasing the temperature from 15^{0}C to 23^{0}C resulted in an increase in the removal of all the elements, although the changes in the temperature had more effect on the sophorolipids assisted removal of elements than DI water removal. On the other hand, it was shown that, although the solubility of elements increases with increasing temperature, the efficiency of sophorolipids in removing elements from mine tailings at 35ºC was less than its efficiency at 23ºC.

In the seven-day batch experiments using a solution of 1% sophorolipids at pH 5, it was shown that at 15ºC a weak negative correlation (r = - 0.36) between arsenic and iron was observed. Likewise, at 23ºC and a weak correlation between the release of arsenic and iron was found (r = 0.17) (Figure 4.31).

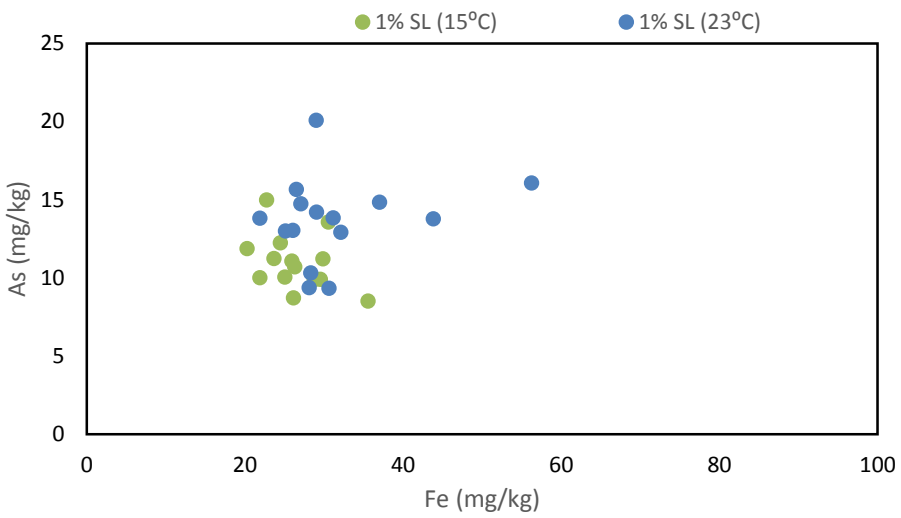

Figure 4.31. Release of arsenic vs. iron in batch experiments using 1% sophorolipids at pH 5 at 15°C and 23°C

The results from the seven-day batch experiments using 1% sophorolipids at pH 5 at 15º C and 23º C showed that there was a weak positive or weak negative correlation between the removal of arsenic and majority of elements being tested. At 15ºC there was a negative correlation between arsenic and other elements. Results from the release of manganese, zinc, and arsenic at pH 5 and at 23ºC showed a strong correlation between arsenic and these two elements.

Results from the batch experiments at 23ºC, using deionized water as the washing solution, showed that there was a strong positive correlation between the arsenic removal with Cr, Fe, Pb, and Mn. The R^2 for their best fit were 0.91, 0.77, 0.76, and 0.63 respectively. This demonstrates that the release of arsenic associated with the water-soluble section of the mine tailings is linked to the release of iron and other metals. As arsenic has a strong affinity to adsorb on the surface of metal oxide/hydroxides, this affinity is intensified for iron oxide/hydroxide (Smedley & Kinniburgh, 2001). Figure 4.32 illustrates the correlation between arsenic and iron at 23˚C by using DI water and different concentrations or volumes of sophorolipids.

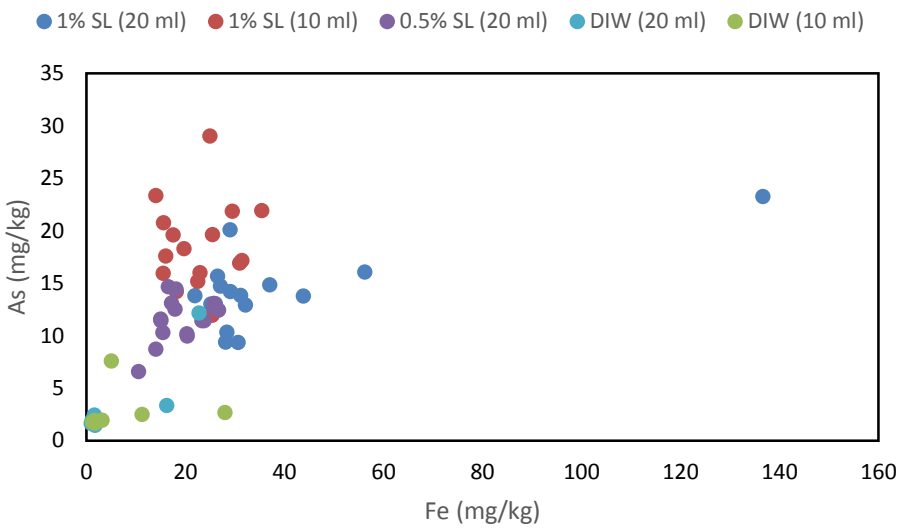

Figure 4.32. Correlation between the release of arsenic and iron at pH 5 at 23^{0}C.

The batch experiments with deionized water at 15ºC, removal of iron and manganese had a moderate positive correlation with arsenic. As predicted, at 15 ˚C, the release of arsenic and other elements was much lower than the removal at 23 ˚C or 35 ˚C. As the removal of these elements using DI water was highly temperature dependent, the removal increased by increasing the temperature. Figure 4.33 illustrates the correlation between arsenic and iron at 15˚C by using DI water and different concentrations or volumes of sophorolipids.

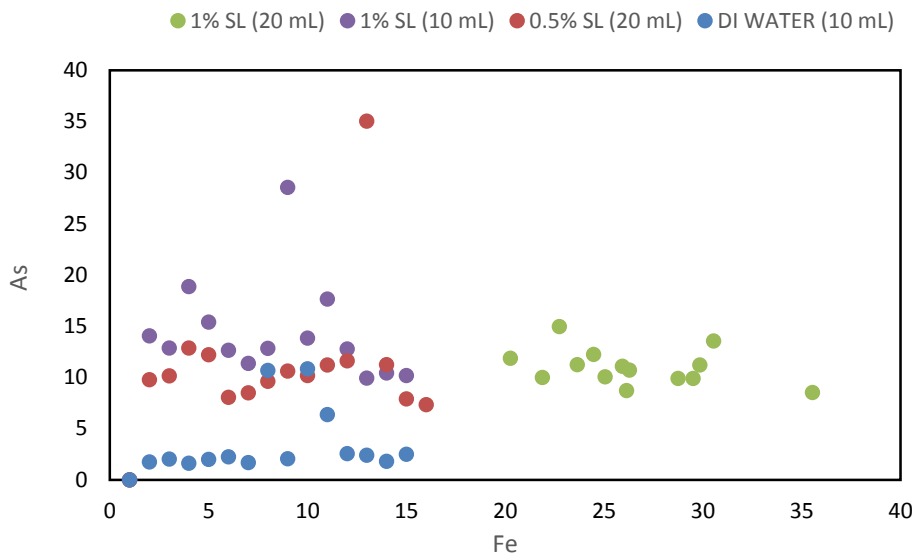

Figure 4.33. Correlation between the release of arsenic and iron in batch experiments at pH 5 at 15^{0}C

The result from the study of mobilization of arsenic and other elements by using sophorolipids in batch experiments showed that mobilization of arsenic and mobilization of iron had a strong correlation at acidic and high alkaline pH. The increase in the mobilization of iron in very acidic and highly alkaline environments shows that the presence of iron and other transition metals could assist in the removal of arsenic through co-mobilization from the media and metal bridging to micelles. On the other hand, in sophorolipid assisted removal of arsenic and other elements at pH 5, the removal of all elements was minimal but higher than the removal by deionized water. At pH 5, as the environment gets closer to a neutral environment, iron starts precipitating as ferric hydroxide. The removal of arsenic at this pH was not as high as in lower pH levels, as it adsorbed to Iron hydroxide.

By investigating the effect of temperature on the removal of elements by using deionized water, it was proven that the solubility and removal of elements has a positive correlation with the temperature. On the other hand, in sophorolipid assisted removal, increasing the temperature from 23ºC to 35ºC resulted in a decrease in the removal of elements, which points out that efficiency of sophorolipids is highly temperature dependent. In the current study, by comparing the results from the seven-day batch experiments at 10, 12.5, 15, 23, 35ºC, it was shown that peak performance of sophorolipids in removing elements from the medium was at 23 ºC.

Results from analyzing the effluent from a batch experiment by using deionized water and 1% sophorolipids, at different pH and from digestion of untreated sample and treated sample were used to compare the concentration of arsenic in effluent and in treated mine tailing sample with the concentration of arsenic in the untreated sample. It has been demonstrated that the mass balance of arsenic was maintained and the variation from 1 was minimal which points toward the analytical and operational errors and loss of elements during filtering the sample.

4.3.2 Column experiments

To investigate the efficiency of sophorolipids in mobilizing arsenic from mine tailings, specimens were subjected to the process of soil washing in a continuous flow configuration by using biosurfactants and deionized water as washing solution and by using two types of exit filters. Experiments were conducted at room temperature (22 ±1ºC), and all experiments were duplicated.

The hydraulic conductivity of the mine tailing, measured using the falling head method and calculated by using Darcy's equation, was 3.17×10^{-7} m/s. It should also be noted that, since the mine tailing specimen was transported from the site to the lab, this number is not an accurate representation of the hydraulic conductivity of the mine tailings at the tailing ponds.

The first step of the column experiments consisted of washing the mine tailings with different concentrations of sophorolipid solutions at pH 7. The washing solutions utilized in this part of the experiment were 0.1 % (1 g/L), 0.5% (5 g/L) and 1% (10 g/L) sophorolipids, as well as, deionized water (Figure 4.34). It should be noted that density of SL 18 was 1 g/cm^3. The removal increases with the increase in sophorolipid concentration. As all concentrations used in this study (except DI water) were at least a thousand times higher than the critical micelle concentration (CMC) of sophorolipids, it can be concluded that as sophorolipid concentration increases, the number of micelles in the solution increases. Therefore solubilization of the various fractions of arsenic rises. Although higher concentrations of sophorolipids are more efficient in the removal of metals/ metalloids from mine tailing, the experiments by using higher concentrations of sophorolipids cause the particles in mine tailings to form floating clusters/colloids and clog the outlet filter. The sophorolipid's viscosity increases by increasing its concentration. As the viscosity

increases, the hydraulic conductivity for the solution decreases, the flow rate of the solution decreases, and its movement through pores become more difficult. Also, there would be a need for higher pressures which in turn can be greater than the pressure which the outlet gauge can handle.

Increasing the concentration of the sophorolipids in the washing solution from 1% to 5% not only increases the cost of the remediation process, it also makes the in situ washing difficult and more time-consuming. Also, the lower hydraulic conductivity results in delays in flushing and passing the contaminated solution through the medium, thus slowing some of the heavy metals/metalloids which were released from the media, allowing them to re-adsorb or precipitate.

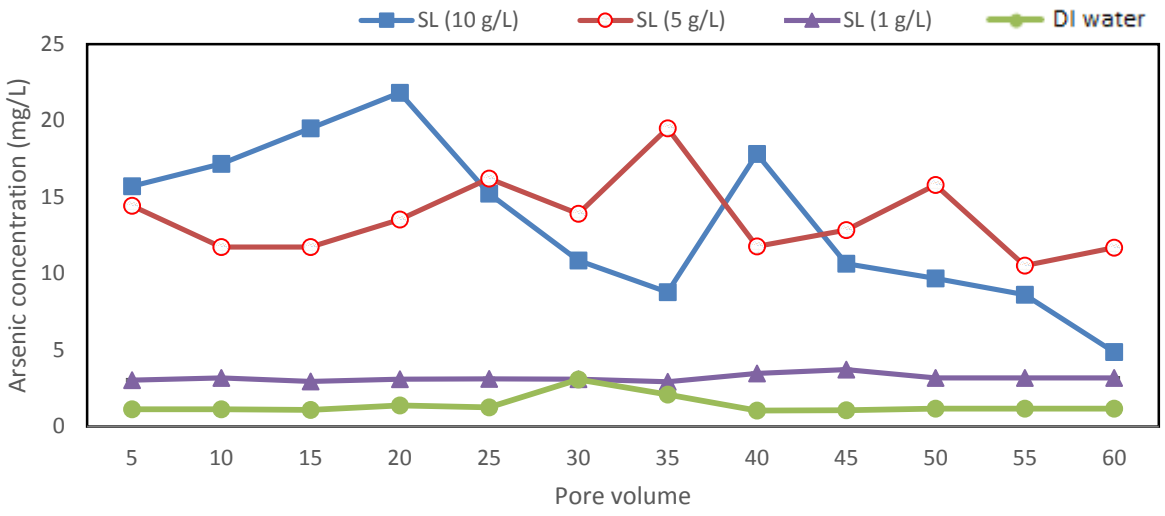

Figure 4.34. Removal of arsenic from mine tailings using SL with different concentrations in a column experiment at 23^{0}C at pH 5.

As it was shown In Figure 4.34, the concentration of the arsenic in the samples obtained from the effluent, after every pore volume, increases until it reaches a maximum removal, and then there is a decrease in arsenic removal until the removal reached a constant value. The fluctuations in the removal of arsenic are the result of changes in the condition inside the column, caused by the release some of the fractions such as organic matter or carbonates, along with the inhomogeneity of the sample.

In this part of experiments, the maximum number of pore volumes was 60. The obtained data shows that not only higher concentrations resulted in the greater removal of arsenic, but also, the solution with a higher concentration of sophorolipids reached its peak of removal in fewer pore volumes of washing. Altogether, although sophorolipids with the concentration of 1% sophorolipids are more efficient in removal of arsenic from mine tailings, by comparing the quantity of sophorolipids used and total removal, 0.5% sophorolipids are a more economically feasible choice. In comparison with the CMC level of sophorolipids (0.001 to 0.003%), the concentration of the 1% and 0.5% sophorolipids were one thousand times higher. The reason for that was that sophorolipids act as a wetting agent, is adsorbed to solid-liquid interfaces and the air-liquid interface, lowering the interfacial tension. Above the CMC level, micelles are formed, and by increasing the concentration, the number of micelle increases, therefore the solution becomes more effective at solubilization.

In comparison between iron and arsenic release by sophorolipid solutions, it was shown that the quantity of iron removed is much higher than arsenic (Figure 4.35). It was expected due to the presence of higher concentrations of iron in the medium.

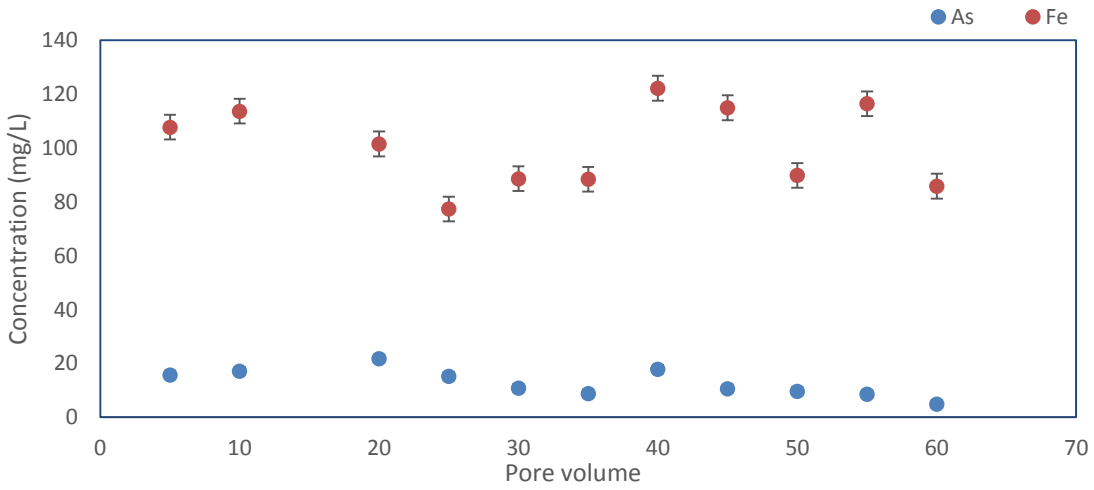

Figure 4.35. Removal of iron and arsenic from mine tailings using 1% SL at pH 5.

A comparison between the data obtained from the column experiment at pH 2.5 versus pH 8 shows at the lower pH; there was higher arsenic removal when SL or deionized water (Figure

4.36) was used as the washing solution. The total removal of arsenic with 0.5% SL at the pH 2.5 was 3.7 times more than the total removal at pH 8. Although when a sophorolipid solution at pH 2.5 was used, the release of arsenic, as well as iron, displayed a high number of rapid fluctuations. This phenomenon could be the result of dissolving different fractions of the mine tailings during soil washing at different pH, and the effect of dissolved materials on the pH level, and the effect of pH on each fraction of media.

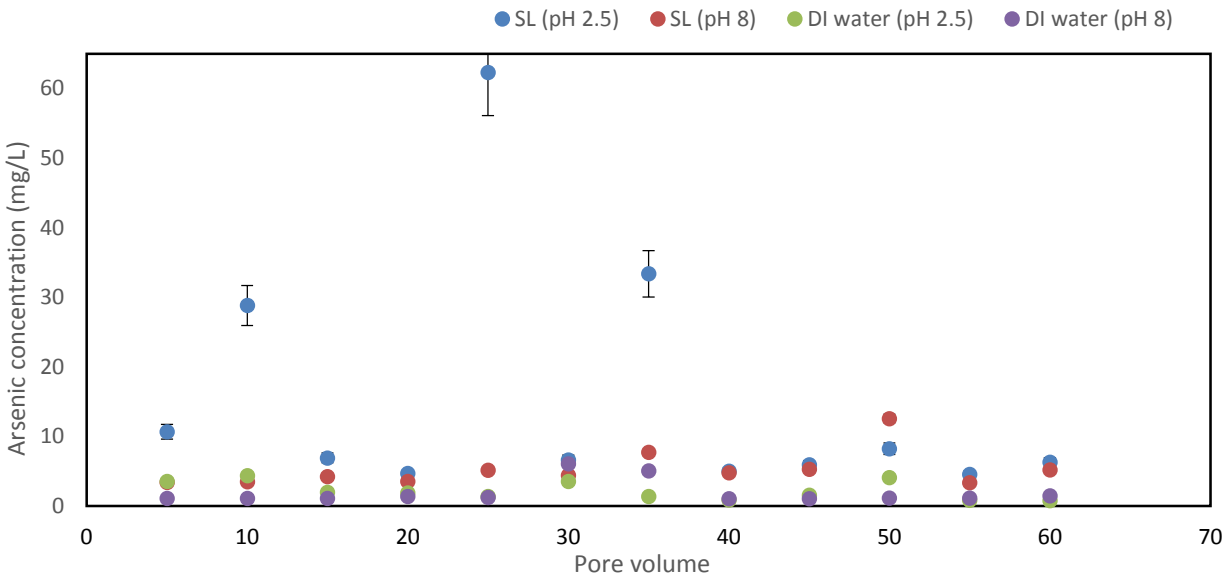

Figure 4.36. Concentration of arsenic released from the mine tailings in the column experiments, using 0.5% SL and DI water at pH 2.5 and 8 as the washing solution.

Comparing the removal of arsenic in column test by using 0.5% SL and deionized water at pH 2.5 and 8 shows that the sophorolipid solution was much more efficient than deionized water. Also, it has been demonstrated that changes in pH of the sophorolipid solution had a significant impact on the iron and arsenic removal. On the other hand, the changes in the pH of DI water made a slight change in the iron and arsenic removal.

Further experiments for removal of arsenic, iron and six other heavy metals, in the continuous configuration by using 0.5% SL solution and without altering the pH (at pH 4.20), through a 100 pore volume wash, were conducted. In this part of the experiments, measuring the pH of the effluent after each pore volume shows that there was a minimal fluctuation (Figure 4.37).

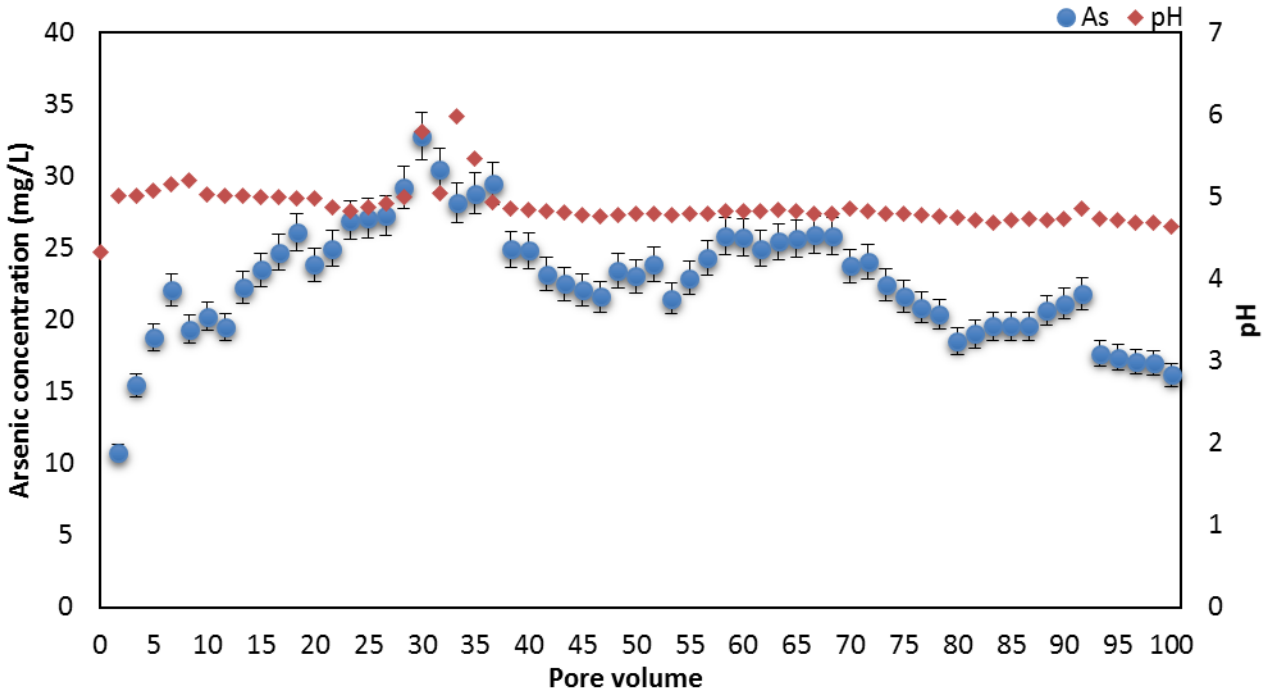

Figure 4.37. Concentration of arsenic and pH of the effluent after each pore volume, during 100 pore volume wash with 0.5% SL.

Figure 4.38 shows the release of arsenic and iron during sophorolipid assisted removal through 100 pore volume showed a weak positive and the Pearson correlation coefficient was 0.23. Closer investigations revealed that the release of arsenic vs. iron in the first 50 pore volumes had a positive correlation (r = 0.67), on the contrary, the correlation between iron and arsenic from 50 to 100 pore volume wash was negative (r = - 0.63).

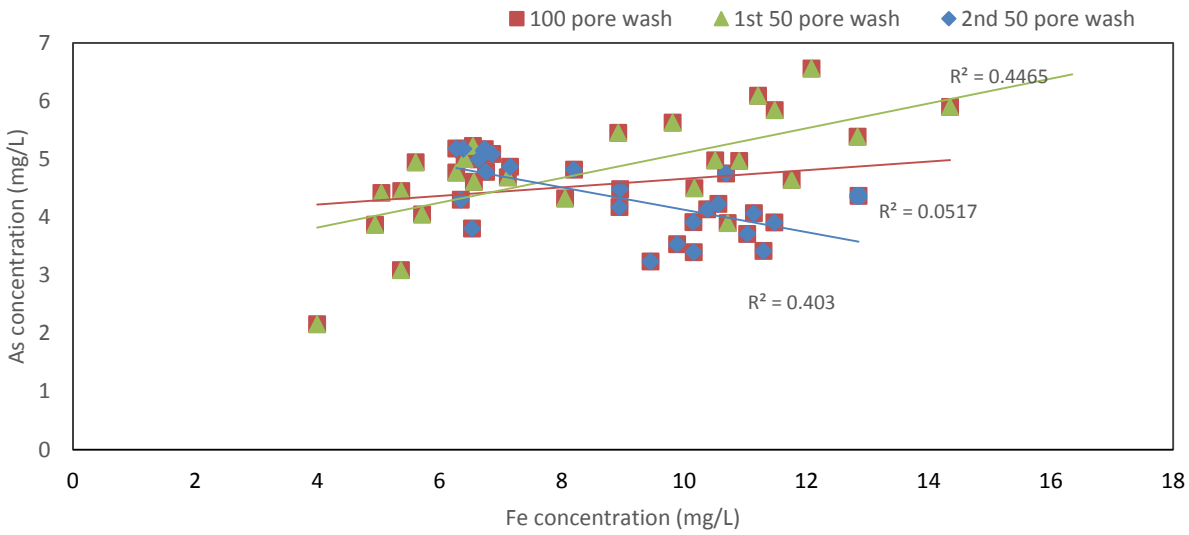

Figure 4.38. Correlation between the release of iron and arsenic in column experiments after 100 pore volume wash by using 0.5% SL at pH 4.33 (no alteration in the initial pH of the solution).

Figure 4.39 illustrates the comparison of concentrations of iron and arsenic in untreated mine tailing sample versus treated mine tailing sample. This comparison between the result of analysis of untreated mine tailing versus the treated mine tailing (remaining residue in the column) shows that there was a substantial decrease in the concentration of all elements. This decrease is the result of the separation of these elements from the mine tailings by the washing solution, as well as, the separation of fine-grained particles (with the mean size of 3.70 μm) from the specimen.

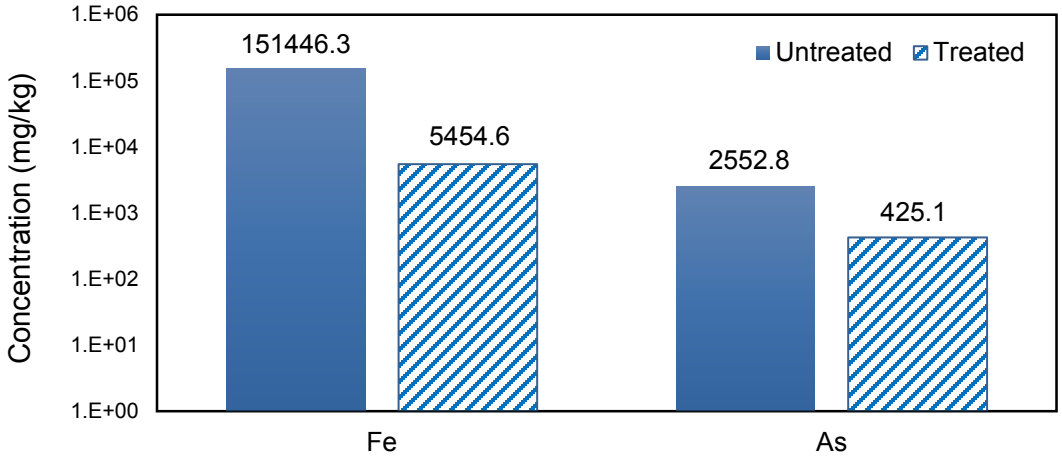

Figure 4.39. Comparison between the total arsenic and iron extracted from the untreated sample and the sample washed with 1% sophorolipids in the column test after a 60 pore volume wash by using a column with a geotextile filter.

In the previous parts of the column study, an unwoven geotextile (TE-GTN350) was used as the outlet filter and collecting of the sample was done manually. At this section of a study for outlet filter, an air stone was used, and an automatic sample collector collected the samples after each pore volume. Figure 4.40 illustrates the results from column experiments that were performed using a 1% sophorolipid solution and DI water at pH 5. As it can be seen, the peak removal of arsenic using sophorolipids was during the first 11 pore volume wash. After this point, the removal decreased steadily. Conversely, the removal of arsenic using DI water in was very low and was constant. When sophorolipids were used, there was a sharp reduction in the removal of arsenic. Further investigations showed that the release of arsenic after 60 pore volumes was low, so continuing the experiment and the expenses related to the operation and cost of the sophorolipid solution cannot be justified for continuation of the process after the 60th pore volume wash.

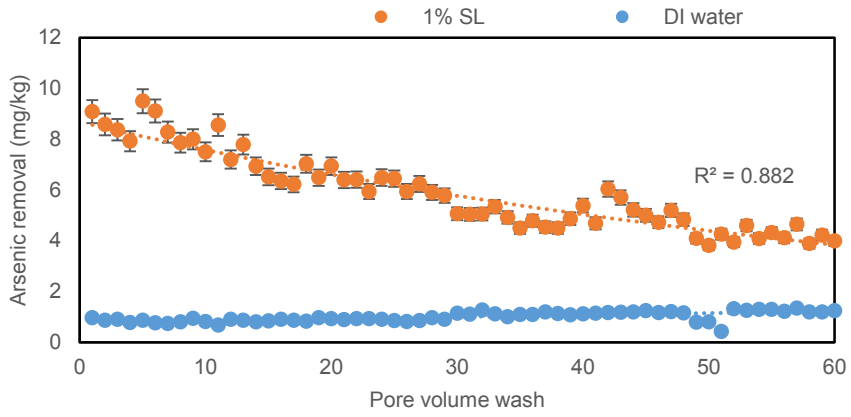

Figure 4.40. Removal of arsenic from mine tailings in the continuous setup using 1% sophorolipids and DI water at pH 5 by using an air stone filter.

Results from the current column experiments using 1% sophorolipids shows that there was no correlation between arsenic and iron mobilization at pH 5 (r = 0.12). However, there was a moderate correlation between the release of iron and arsenic by and DI water (r=0.53) (Figure 4.41).

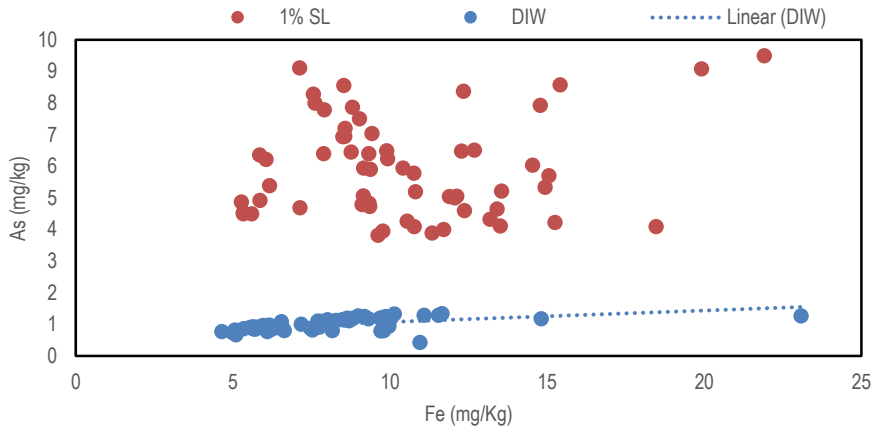

Figure 4.41. Correlation between the release of arsenic and iron from mine tailings, by using DI water and 1% sophorolipids, at pH 5 in a continuous experiment.

Figures 4.42 to 4.45 represent a comparison between the removal of selected elements (Fe, Cr, Cu, and Mn) by using 1% sophorolipids versus DI water (DIW).

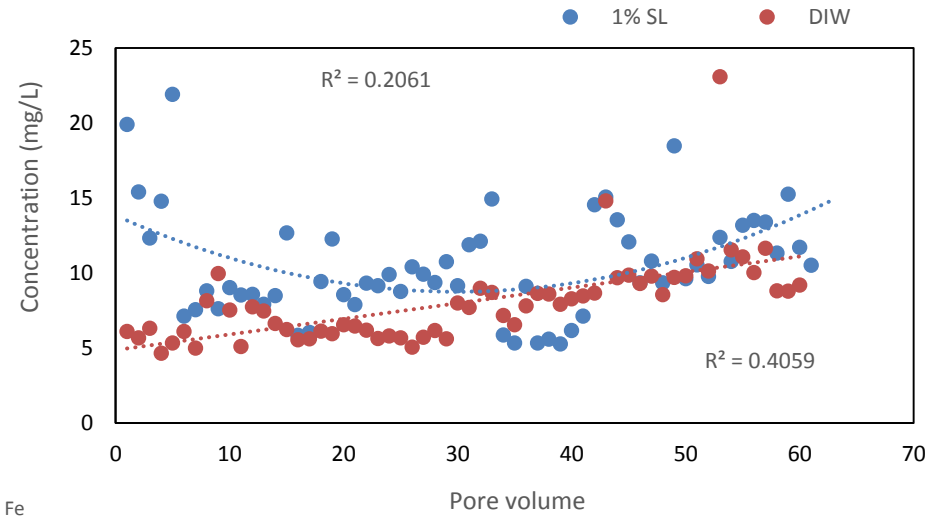

Fe

Figure 4.42. Removal of iron from mine tailings in the continuous setup using 1% sophorolipids at pH 5 by using a column with an air stone filter.

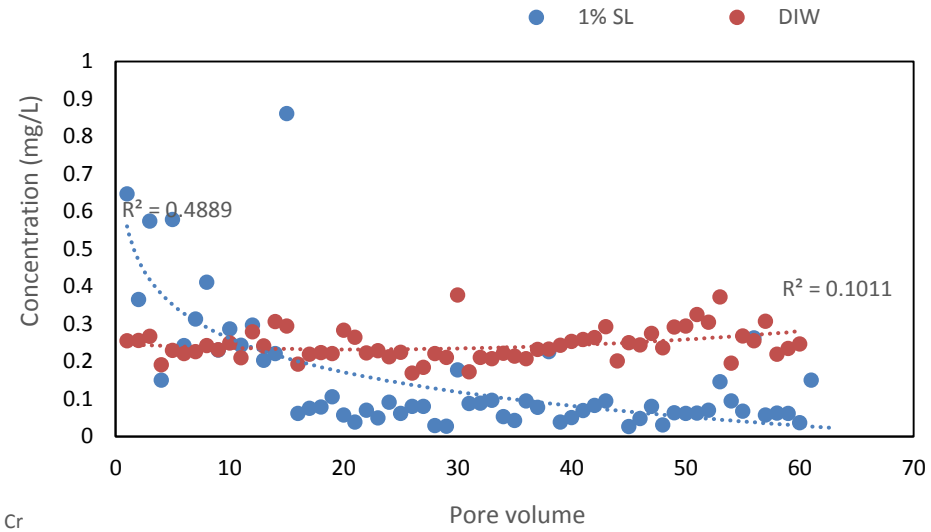

Cr

Figure 4.43. Removal of chromium from mine tailings in the continuous setup using 1% sophorolipids at pH 5 by using a column with an air stone filter.

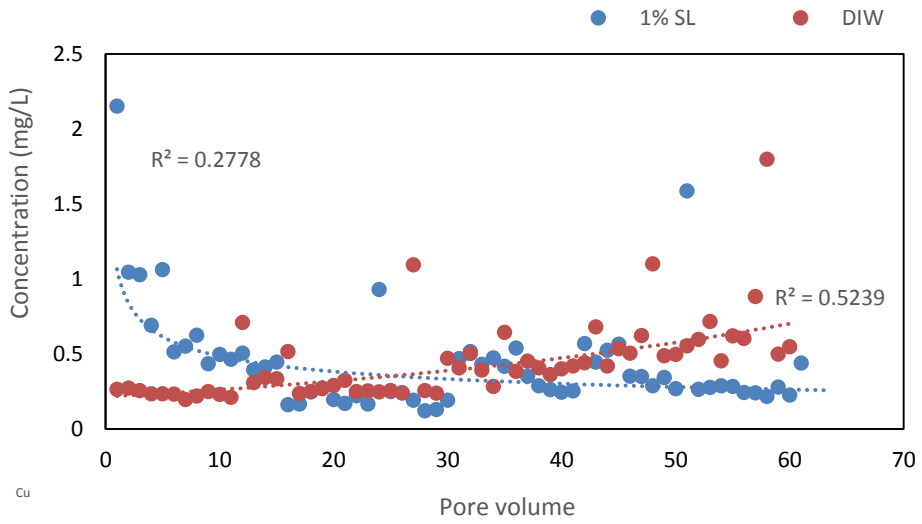

Figure 4.44. Removal of copper from mine tailings in the continuous setup using 1% sophorolipids at pH 5 by using a column with an air stone filter.

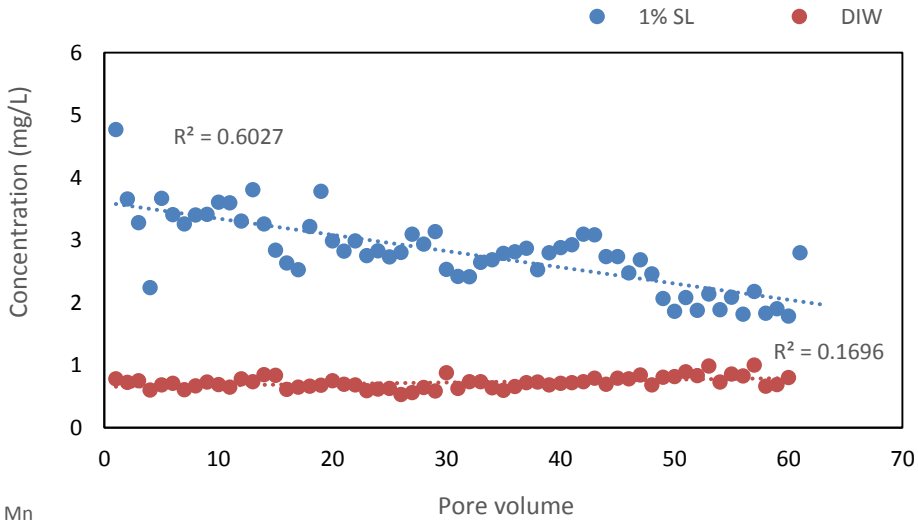

Figure 4.45. Removal of manganese from mine tailing in the continuous setup using 1% sophorolipids at pH 5 by using a column with an air stone filter.

To determine the concentration of target elements in the untreated mine tailing sample and the residues inside the column were digested following the procedure described in EPA method 3050B.The result from the digestion is shown in Figure 4.46.

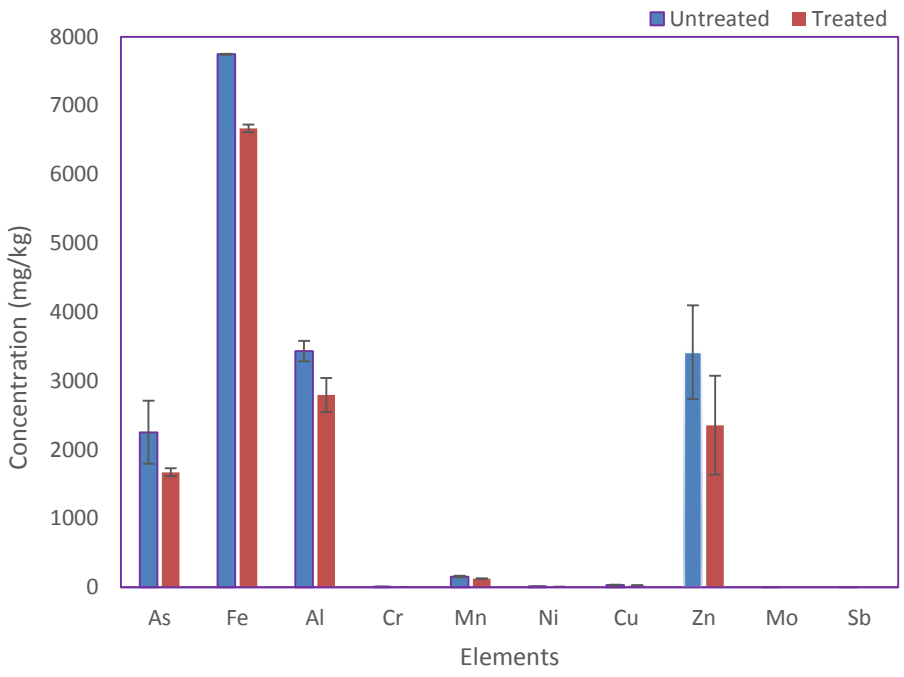

Figure 4.46. Concentration of elements in untreated and treated mine tailing sample.

Figure 4.47 compares the concentrations of arsenic in the untreated and treated mine tailing samples. This comparison between the arsenic concentrations of untreated mine tailings versus treated mine tailings, and the remaining residue in the column shows that although there was a substantial decrease in the concentration of all elements, the removal of elements using air stone filters was far less than the removal using geotextile filters. The high removal of arsenic during the process of soil washing when there was a geotextile filter was not only the caused by the removal of arsenic from the mine tailings by the washing solution, it is also the resulted from the separation of very fine-grained particles from the specimen, as geotextile filter allows very fine particles (with the mean size of 3.70 μm) to exit from the column. The eluted residues settled in the collecting vials. The settled residues were composed of very fine silt, clay, and colloids, and sophorolipids were adsorbed to their surfaces.

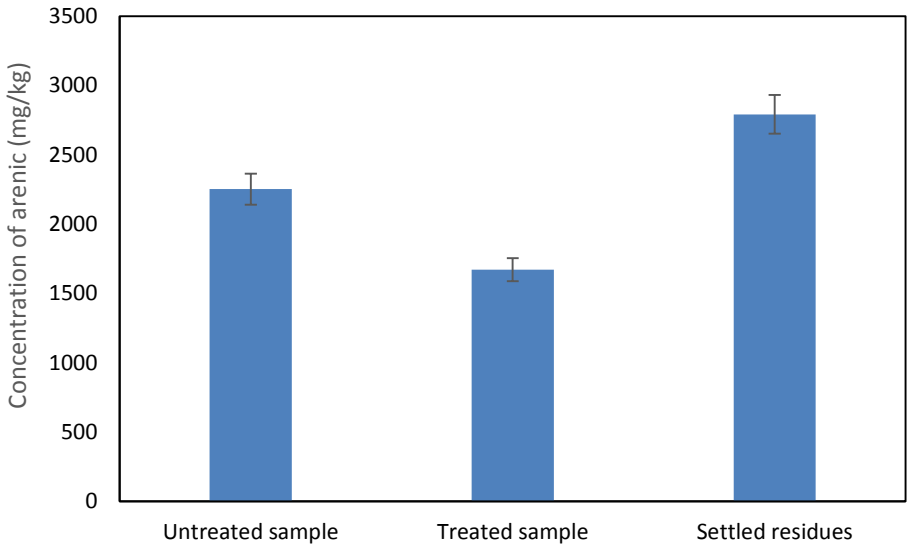

Figure 4.47. Comparison between the total arsenic extracted from the untreated sample and the sample washed with 1% sophorolipids in the column test after 60 pore volume wash by using a column with an air stone filter.

Despite the fact that the mass of the total residue in the collecting vials was 90% less than the weight of the sample, the concentration of arsenic in the settled residues was much higher (Figure 4.47). This can be due to the high concentration of arsenic in the very fine particles. Also, it may result from the precipitation of arsenic with iron from the solution. Observation in the laboratory showed a high concentration of magnetite in these residues. Table 4.7 displays the result from particle size analysis of untreated samples, residues in the column after being washed with sophorolipids (1% SL) by using geotextile (GT) or air stone (AS).

Table 4.7. Summary of particle size characteristics of the untreated samples, residues in the column and the residues settled in the collecting vials.

Sample	Median (μm)	Mean (μm)	Variance (μm^2)	Mode (μm)
Untreated	7.95	10.07	72.07	8.22
Treated (1% SL, GT)	7.60	8.17	14.87	8.23
Treated (1% SL, AS)	9.04	9.08	0.89	9.10
Residues in collecting vials	3.52	3.70	2.19	3.66

The result from particle size analysis showed that the mean size of the sample was decreased with the washing with sophorolipids as larger particles within the sample were broken down. Also decreasing the standard deviation of the untreated sample from 8.49 to 3.86 and 0.94 μm in the treated samples shows that the sample became more homogeneous with regards to the size of particles. During the process of continuous flushing with sophorolipids, a portion of very fine silt, clay and colloids were separated and removed by the washing solution (Table 4.8).

Table 4.8. Composition of the untreated, treated sample and residues from collecting vials (volume-based percentage).

Classification	Diameter (μm)	Untreated sample (%)	Treated sample (%)	Residues from vials (%)
Very fine sand	< 125.00	0.4	0	0
Coarse silt	< 62.50	2.5	0	0
Medium silt	< 31.25	10.1	4.9	0
Fine silt	< 15.63	38.1	44.2	1.2
Very fine silt	<7.81	36.6	42.4	38.3
Clay	< 3.91	12.3	8.5	60.1
Colloid	< 0.98	0	0	0.3

The mass balance coefficient in the column experiment was found by using the results from analyzing the effluent from column experiment by using 1% sophorolipids, and the result from digestion of the untreated and treated sample, as well the residues which settled in the effluent in the collecting vials.

In the first part of the study, collection of the effluent was conducted manually. By collecting effluents in centrifuge tubes for each pore volume, mass balance investigations showed a loss of target elements. This loss of elements is attributed to the loss of effluent between collecting in vials. Therefore, mass balance investigations were based on the results from part two of study which an automated collecting system was used. It was shown that the coefficient of mass balance for arsenic removal when 1% sophorolipids was used as the washing solution was 0.9933. When deionized water was used the coefficient of mass balance was 1.0197. The variation of mass balance coefficients from 1 was less than 1% for sophorolipids assisted removal and 2% for

removal with deionized water. These variations are due to inevitable analytical and operational errors. Following graphs shows the particle size distribution in the residues from the column after treatment with 1% sophorolipids (Figure 4.48) and the particle distribution in the effluent from the column test (Figure 4.49).

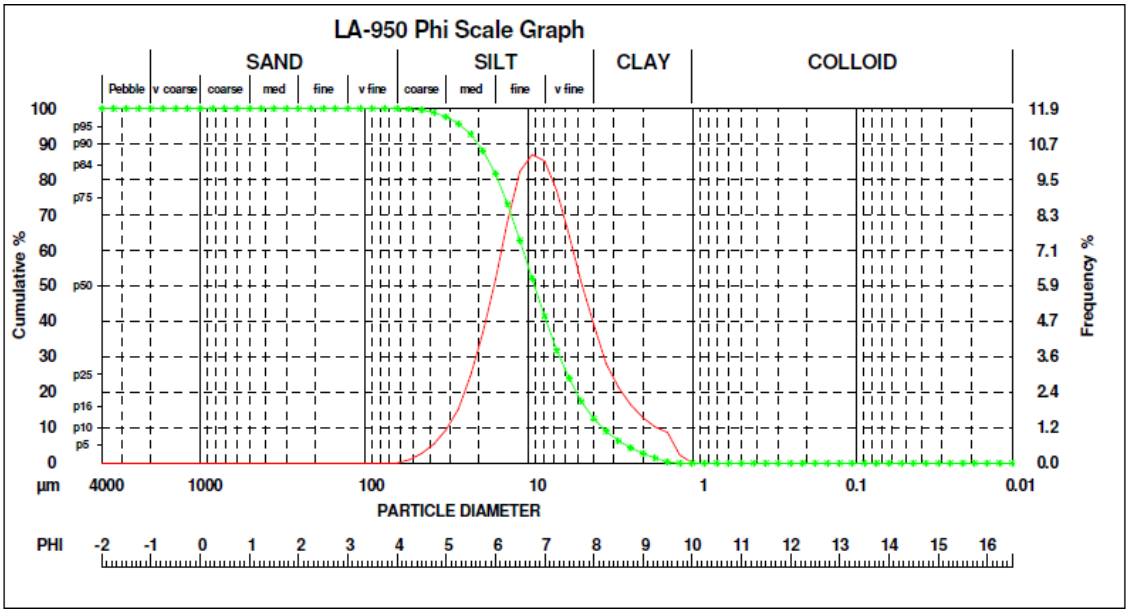

Figure 4.48. Particle size distribution of mine tailing sample after 60 pore volume wash by 1% sophorolipids in the column test.

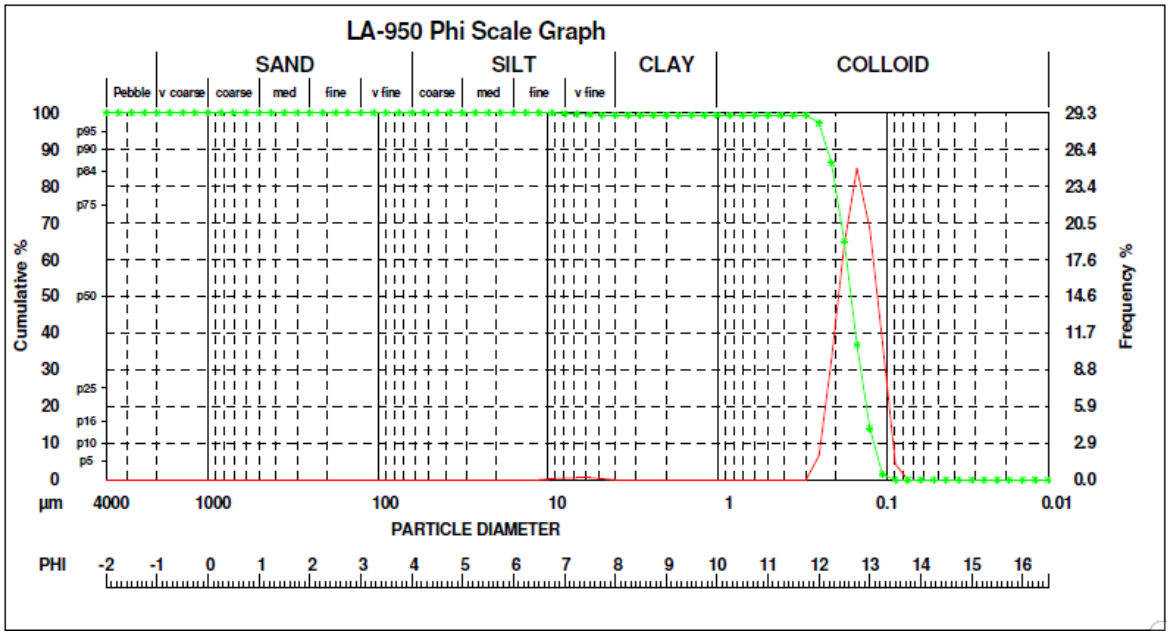

Figure 4.49. Particle size distribution in the effluent from column experiment

In summary, during the seven-day batch experiments, it was shown that the maximum removal of arsenic happened during the first 24 hours. The concentration of arsenic and other target elements in the effluent after the first 24 hours stayed in a range and fluctuations were minimal compared to the concentration of elements in solution. In batch experiments, the concentration of arsenic and other elements in the solid phase and solution remains in equilibrium, and at any time there is a fluctuation, and the concentration of any element surpasses the equilibrium level, the element starts to precipitate, so the concentration in the solution returns to the equilibrium level.

It was shown that, despite the fact that the solubility of arsenic increases with increasing temperature, as observed while washing with deionized water, the removal of arsenic using sophorolipids was highest at 23±1˚C. Increasing the temperatures from 23˚C to 35˚C or decreasing the temperature to 15˚C caused a substantial reduction in the removal of arsenic by sophorolipids.

A comparison between these results from the batch experiments revealed the parameters which have an impact on the removal of sophorolipids assisted removal of elements from mine tailing. These results show that removal of arsenic and other elements, by using a sophorolipid solution, not only depends on pH, temperature, the volume of washing solution, and the biosurfactant concentration; the effect of sophorolipids on elements also varies depending on the types of elements present.

The removal of arsenic in a continuous set up has shown to be more efficient when a filter which could separate very fine grains (clay particles and colloids) was used. Although, the results of analyzing effluents using larger pore filters fluctuated more compared to the results from analyzing the effluents which passed through the sand filter, there was a consistent decrease in the concentration of arsenic in each passing pore volume. It was shown that the fluctuations in the concentration of arsenic in the effluent are not caused by changes in pH, as pH during the 100 pore volume wash did not vary significantly. It was shown that the removal reached a minimum at 60 pore volume wash, and after this point changes in the concentration of arsenic in the effluent from 60 to 100 pore volumes were minimal. For this reason, during the rest of study, only the effluent from the first 60 pore volumes in the continuous experiments was analyzed.

During the process of continuous experiments, 0.9 L of 1% sophorolipids flushed 60 pore volume of sophorolipid solution through 50 g mine tailing specimen (180g SL per kilogram of mine tailing sample). In the in situ treatment with sophorolipids, the price of sophorolipids is one of the limiting factors. The cost of and the volume of sophorolipids can be reduced by combining the process of sophorolipids assisted removal of contaminants with adequate physical technologies, to enhance the removal of contaminants and reduce the cost of remediation. The other limting factor in situ remediation is changes in the permeability at different depths, and the fact that the temperature of the environment changes the outcomes of the remediation.

The concentration of arsenic in the effluent from the column experiments was gradually decreasing from 22 to 4.8 mg/L. Many methods has been developed in the past for the removal of arsenic and other heavy metals from water that can be used for removing arsenic and other toxic elements from these effluents. One of the effective methods is using granular activated carbon embedded with nanoscale zero-valent iron (Chowdhury, 2015).

4.4 MECHANISM OF THE SOPHOROLIPID ASSISTED REMOVAL OF ARSENIC

Arsenic is the twentieth most abundant element in the earth's crust (Centeno et al., 2007). The release of this element to the environment, caused by weathering the host rocks or human activities, puts the life of inhabitants in polluted areas at risk. The mobilization and immobilization of arsenic compounds are highly dependent on their speciation, pH, reduction/oxidation potential of the environment and presence of organic matter in the media or decomposition of it, as well as the coexistence of minerals such as iron oxide/ hydroxide in the media or dissolution of them.

In Giant mine, gold is embedded in arsenopyrite (FeAsS). In arsenopyrite (FeAsS) the oxidation states of elements are Fe^{+2}, As^{-}, S^{-} (Jones and Nesbitt, 2002). Arsenopyrite oxidized in the presence of oxygen, releasing arsenic (As (V) and As (III)), Fe(III) oxide, SO^{-2}_3 and SO^{-2}_4, result in the production of acid mine drainage (Corkhill and Vaughan, 2009). The mobilization or retention of the released arsenic is highly pH dependent. Experiment conducted by Beattie and Poling (1987) showed that oxidation of arsenopyrite at pH higher than 7 resulted in formation of iron layers on the surface of mineral and the released arsenate deposited and formed complexation with these iron oxides. On the other hand, sulfur portion of arsenopyrite was oxidized into sulfate and went into the solution. Beattie and Poling (1987) reported that at pH below 7, iron tends to be soluble releasing the arsenic associated with it. Different species of arsenic show different solubilities at certain pH as their dissociation constants vary, for example, pKa for As (V) (2.20) is much lower than pKa for As (III) (9.22). The redox potential of the environment is the other important parameter which governs the solubility of arsenic. According to Masscheley et al. (1991) at reducing environment As (V) acts as an electron acceptor thus reducing to the more mobile and toxic As (III) species, though the presence of competing ions could slow this process. One of the main factors governing the mobility or retardation of solubilized arsenic is the presence or absence of binding sites such as iron oxide/hydroxides. Masscheley et al. (1991) observation showed that by dissolution of iron hydroxides, the arsenic concentration in solution increased. As speciation and solubility of arsenic is highly governed by pH and redox status, any changes in the environment could promote the release of the arsenic from the mine tailing.

The focus of this study was to find an environmentally friendly and efficient agent for the process of soil washing. Afterwards, the mechanism of mobilization of arsenic was investigated.

In the past, researchers used different techniques such as octanol-water partitioning, ultrafiltration, ion exchange, sequential extraction, scanning electron microscopy, monitoring pH levels and measuring zeta potential, to determine the mechanism for metal removal by rhamnolipids (Mulligan 1998, Dahrazma, 2006, and Wang, 2009). They concluded that sorption of biosurfactants on the soil interphase, lowering the interfacial tension between media and solution, therefore, desorption of metal and solubilization of the metal within the micelle are the main mechanisms for the removal of metals from soil and sediments. Sophorolipids used in this study was highly lactonic sophorolipids according to Glenns (2003) are more effective in lowering surface tension than acid sophorolipids. In this study, to identify the mechanisms governing the sophorolipids removal of arsenic from mine tailing sample, series of tests was conducted to examine the effects of sophorolipids on different fractions of mine tailing sample, the surface charge of the medium, and the speciation of arsenic. Also, the effects of mine tailing constituents on the structure of sophorolipids were investigated.

4.4.1 Results from the SEM analysis

This part of study is divided into three sections, Secondary Electron Imaging (SEM), Backscattered (BSE) and Energy-dispersive X-ray spectroscopy (SEM-EDS).

Secondary electron imaging

In the first step, the Secondary Electron Imaging (SEM) analysis was used to obtain a visualization of the morphology of the mine tailing specimen, before and after treatment, using different concentrations of sophorolipids (1% and 0.5% SL), and deionized water. In this step, the SEM analyzed with the secondary electrons received by the detector showed the surface morphology of the samples. Figures 4.50 a and b display the secondary electron image of the mine tailing particles from a non-treated sample compared with a treated sample.

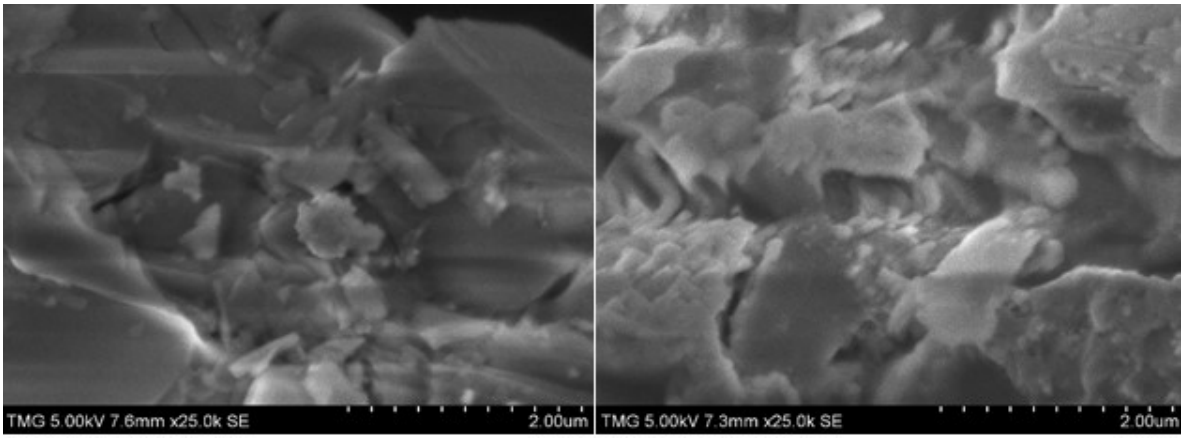

a **b**

Figure 4.50. Secondary electron image of an untreated (a) and treated (treated by using 1% SL) (b) mine tailing sample with the magnification of 25 thousand times.

As it can be seen in the images, after treatment by sophorolipids, the grain sizes became more homogenous, and the texture on the surface of the grains changed. The surface of the grains in the untreated samples looked smooth. On the other hand, at the surface of treated samples, a porous structure was observed (Figure 4.51). This could be the result of the removal of some fragments of the grains that were solubilized by sophorolipids. The remaining insoluble fragments are minerals such as silicates and quartz. The data from EDS confirmed this statement. In the experiments conducted by Dahrazma (2006), washing with rhamnolipids had no effect on the texture of grains. Therefore, it can be stated that sophorolipids had a higher wetting ability than rhamnolipids, and not only covered the surfaces of grains, it can penetrate in pores and fractures, break down the particles and remove constituents.

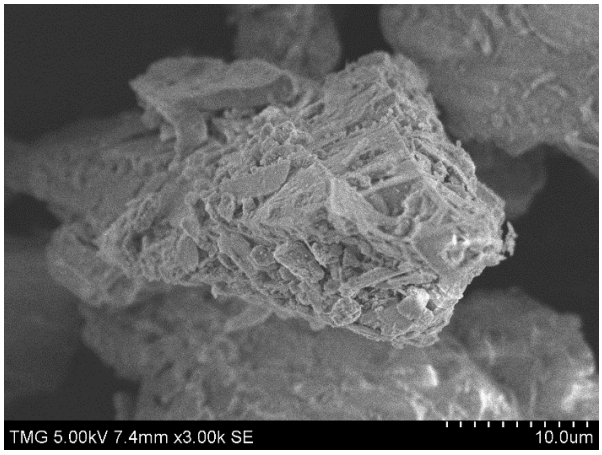

Figure 4.51. Image of a grain of treated mine tailing specimen at 3000 x magnification and voltage of 5kV.

Backscattered electron imaging

The analysis of the backscattered electrons from the samples displays the composition image of the samples. Figures 4.52 and 4.53 show the backscattered images of untreated samples and samples which have been treated by using different solutions: 1% SL, 0.5% SL, and deionized water. The backscattered image of the untreated mine tailing sample in Figure 4.52a illustrates the compositional heterogeneity of the sample. There are crystals with the metallic sheen that seem like pyrite crystals, while the white amorphous matter in the center of the image resembles a calcium compound. As it was mentioned before, during the analysis of the untreated mine tailing sample, the high metal content of untreated samples limited the ability to increase the magnification. By increasing the magnification or voltage, the grains were charged, which resulted in blurred pictures. For obtaining a more accurate understanding of the composition of the grains, the sample was analyzed by the SEM-EDS that will be discussed in the next section.

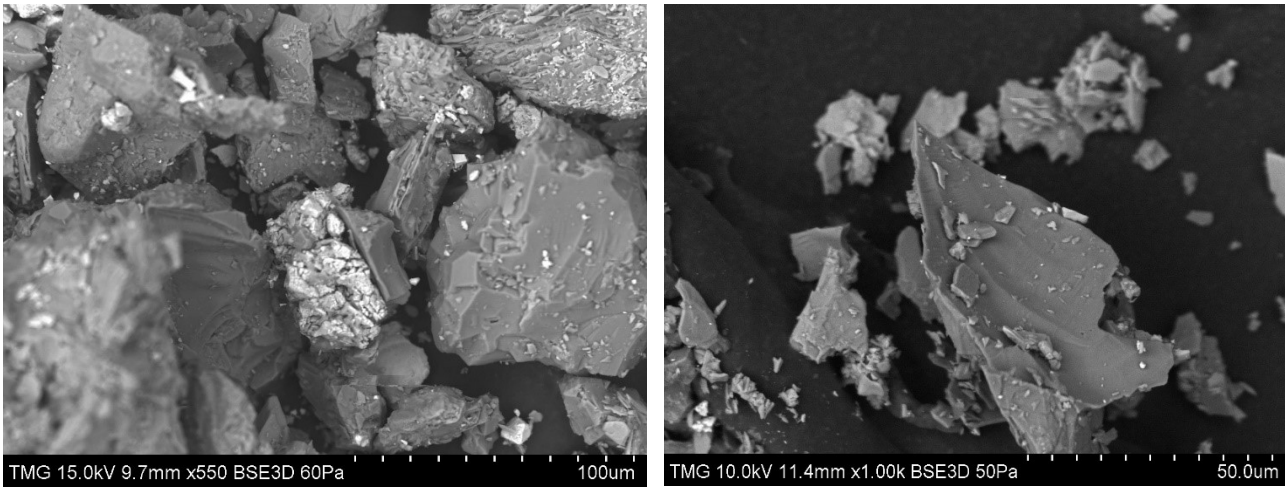

a b

Figure 4.52. Backscattered image of an untreated mine tailing sample (a) and a treated sample with 1%SL (b).

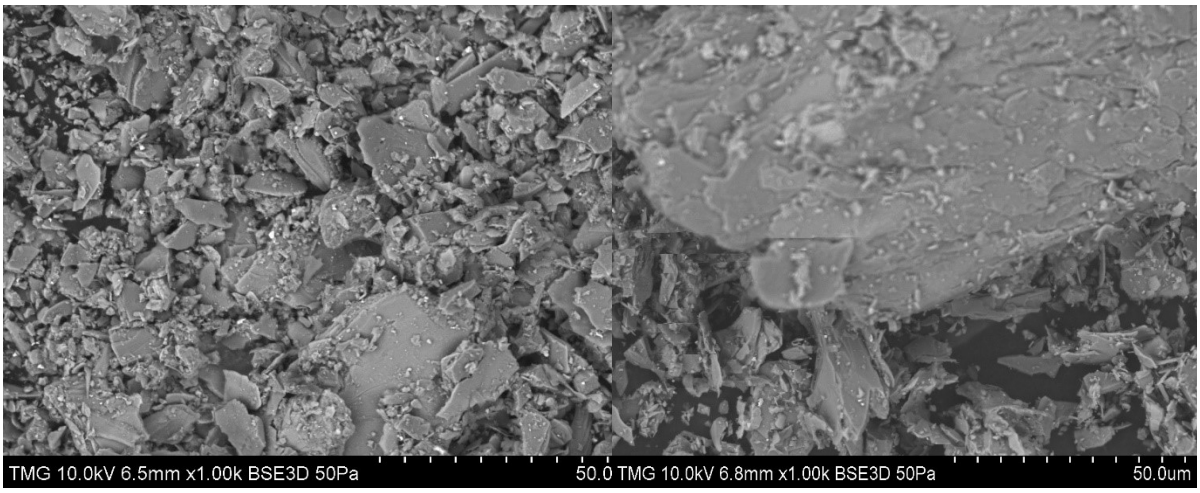

a b

Figure 4.53. BSE image of a treated sample with 0.5% SL (a) and treated with deionized water (b).

A comparison between the images of the samples treated by 0.5% SL vs. samples treated with 1% SL shows that in the samples which were treated with 0.5% SL, a greater variety of grain sizes and grain compositions were observed. On the other hand, in the backscattered image of specimens which was treated with deionized water, various grain types and grain sizes were observed.

Analysis of the samples with SEM-EDS

By analyzing the X-rays emitted by electrons striking a sample, the composition of a sample can be determined. The SEM-EDS analysis can be used for both performing the average composition analysis across an area of the sample, and also to perform point analysis on selected points of interest. The results from the EDS analysis were obtained from random points on the specimen. The X-rays reflected from target points showed the elemental composition on each point. This helped to understand the co-occurrence of elements in the grains, and which elements are associated with arsenic in the samples. Table 4.9 displays the concentrations of elements in 5 selected points on the untreated mine tailing specimen (Figure 4.54).

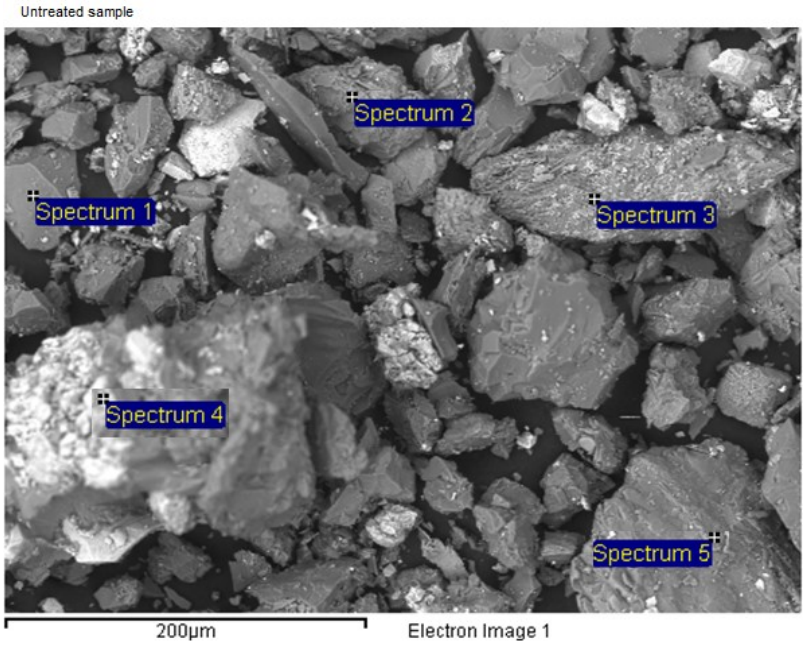

Figure 4.54. Locations of target points on the untreated sample.

Table 4.9. Average of elements in selected points (which had different morphology and color) in the untreated mine tailing sample (EDS analysis).

	1		2		3		4		5	
Element	Weight%	Atomic%	Weight%	Atomic%	Weight%	Atomic%	Weight%	Atomic%	Weight%	Atomic%
C	14.5	22.99	7.64	13.39	2.13	3.6	6.28	12.96	7.61	12.3
O	42.17	50.19	42.01	55.24	54.94	69.61	37.75	58.46	49.87	60.49
Na	0	0	0.23	0.21	0.15	0.13	0	0	0.17	0.14
Mg	0.67	0.53	1.29	1.11	1.09	0.9	0.69	0.7	0.47	0.37
Al	1.03	0.73	9.2	7.17	2.05	1.54	1.31	1.2	2.5	1.8
Si	34	23.05	17.76	13.3	26.64	19.23	5.39	4.75	33.24	22.96
S	0.2	0.12	0.21	0.14	0	0	1.13	0.87	0	0
K	0.36	0.18	8.54	4.59	0.54	0.28	0.35	0.22	0.91	0.45
Ca	1.67	0.79	2.09	1.1	0.78	0.4	2.35	1.46	0.91	0.44
Ti	0	0	0.5	0.22	7.13	3.02	0	0	0	0
Fe	3.63	1.24	8.82	3.32	3.14	1.14	41.6	18.46	2.23	0.77
Zn	0	0	0	0	0	0	0.41	0.16	0	0
As	0	0	0	0	0	0	1.98	0.65	0.33	0.08
W	1.76	0.18	1.71	0.2	1.41	0.16	0.76	0.1	1.76	0.19
Totals	100		100		100		100		100	

Table 4.10 shows the concentrations of elements in 7 selected points on the treated mine tailing specimen (Figure 4.55). The SEM-EDS analysis of the target points showed that the particles in both samples (untreated and treated) were highly variable in composition.

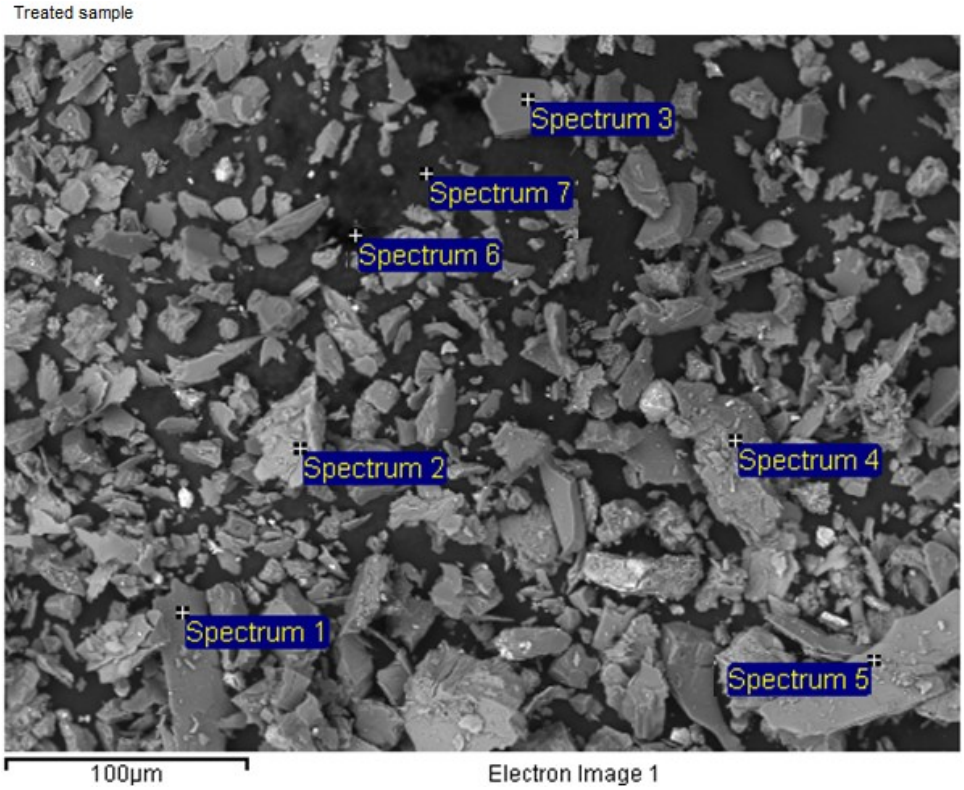

Figure 4.55. Selected points for analysis of the treated sample.

High percentages of silicon in both untreated and treated samples points toward the presence of quartz, and the presence of aluminum, iron, magnesium, and potassium indicate the presence of silicates. The presence of calcium could be an indication of the presence of a form of calcium-bearing silicate, or the result of adding calcium carbonate to the mine tailings. Although these data are from random points and areas in the sample and don't represent the whole sample, a reduction in the concentration of many elements was observed.

Table 4.10. EDS analysis of 7 selected points in the treated mine tailing sample with 1% sophorolipids.

	1		2		3		4		5		6		7	
Element	Weight%	Atomic%	Weight%	Atomic%	Weight%	Atomic%	Weight%	Atomic%	Weight%	Atomic%	Weight%	Atomic%	Weight%	Atomic%
C	15.22	23.43	15.54	23.68	24.28	34.21	11	17.28	14.12	21.5	61.33	70.86	69.56	77.36
O	46.98	54.31	50	57.2	47.1	49.81	51.5	60.7	52.13	59.56	28.72	24.92	23.9	19.96
Na	0.69	0.55	0	0	0.09	0.06	0.33	0.27	0	0	0	0	0	0
Mg	0.47	0.36	4.85	3.65	0.32	0.22	0.78	0.6	5.04	3.79	0.68	0.39	0.4	0.22
Al	11.54	7.91	7.54	5.11	0.66	0.42	10.83	7.57	7.56	5.12	1.6	0.82	1.04	0.52
Si	15.29	10.07	9.16	5.97	24.19	14.57	14.62	9.82	9.7	6.31	3.95	1.95	2.73	1.3
S	0	0	0	0	0	0	0	0	0	0	0	0	0	0
K	4.45	2.11	0.31	0.14	0.21	0.09	4.16	2.01	0.8	0.38	0.42	0.15	0.31	0.11
Ca	0.86	0.4	0.86	0.39	0.39	0.16	0.69	0.33	0.73	0.33	0.94	0.33	0.53	0.18
Ti	0	0	0	0	0	0	0.23	0.09	0	0	0	0	0	0
Fe	1.71	0.57	11.75	3.85	0.91	0.28	2.92	0.99	8.63	2.82	2.36	0.59	1.52	0.36
Zn	0	0	0	0	0	0	0	0	0	0	0	0	0	0
As	0	0	0	0	0	0	0.25	0.06	0.4	0.1	0	0	0	0
Yb	1.58	0.17	0	0	0.57	0.06	1.51	0.16	0	0	0	0	0	0
W	1.2	0.12	0	0	1.29	0.12	1.19	0.12	0.89	0.09	0	0	0	0
Total	100		100		100		100		100		100		100	

Based on the data provided in Tables 8.1 and 8.2, Figure 4.56 was prepared to illustrate the average concentration of elements in untreated samples vs. treated samples. As it can be seen a reduction in the concentration of many elements is observed. It was shown that treatment with the sophorolipid solution caused a substantial decrease the percentage of arsenic, iron and other heavy metals in the particles in the sample. Although, the relative percentage of some of the metals, which were not considered among the major elements such as zinc, following the treatment of the sample and reduction in the percentage of the main elements, increased.

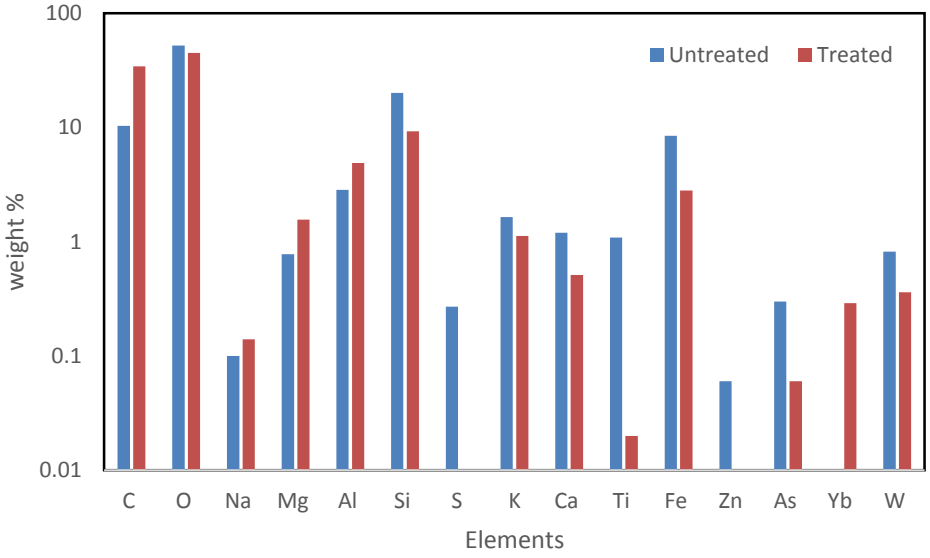

Figure 4.56. Average elemental composition of selected points on untreated sample vs. the points on treated sample.

In the next part of the EDS analysis, the average composition of elements over an area of the sample was determined. Figure 4.57 shows the area selected in a sample treated with a solution of 1% sophorolipids. The following images (Figure 4.58 a, b, c and d) represent the elemental concentration in the area selected on the samples treated with solutions of 1% sophorolipids, 0.5% sophorolipids, deionized water, and hydrogen peroxide (50 µM).

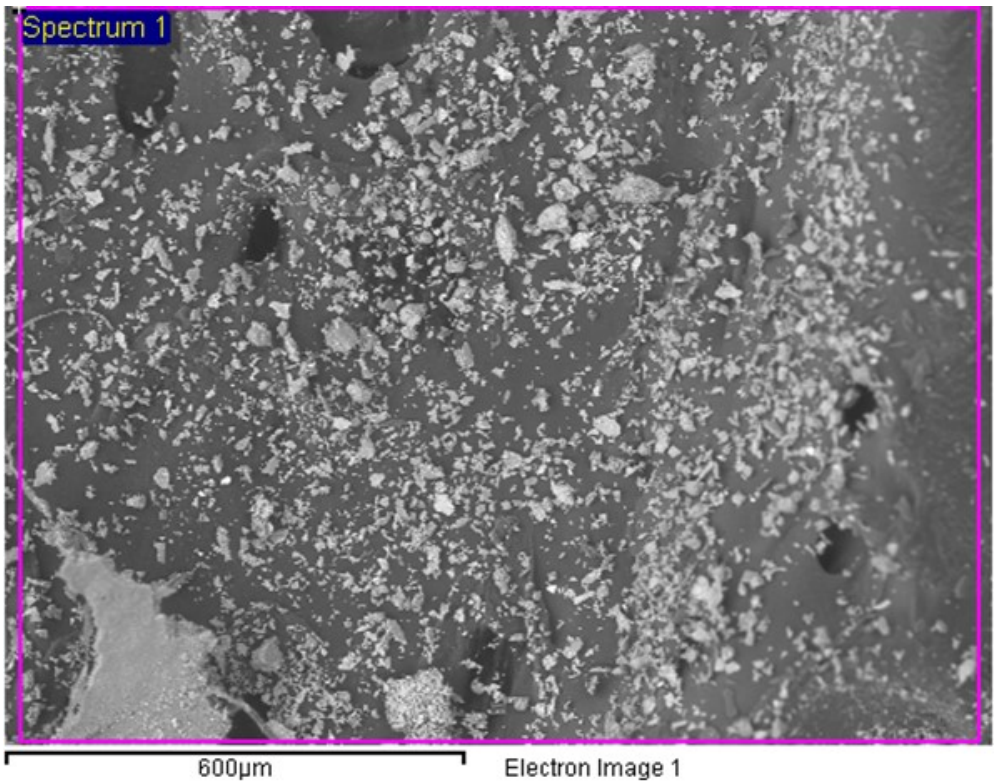

Figure 4.57. Area selected on a sample treated with a solution of 1% sophorolipids.

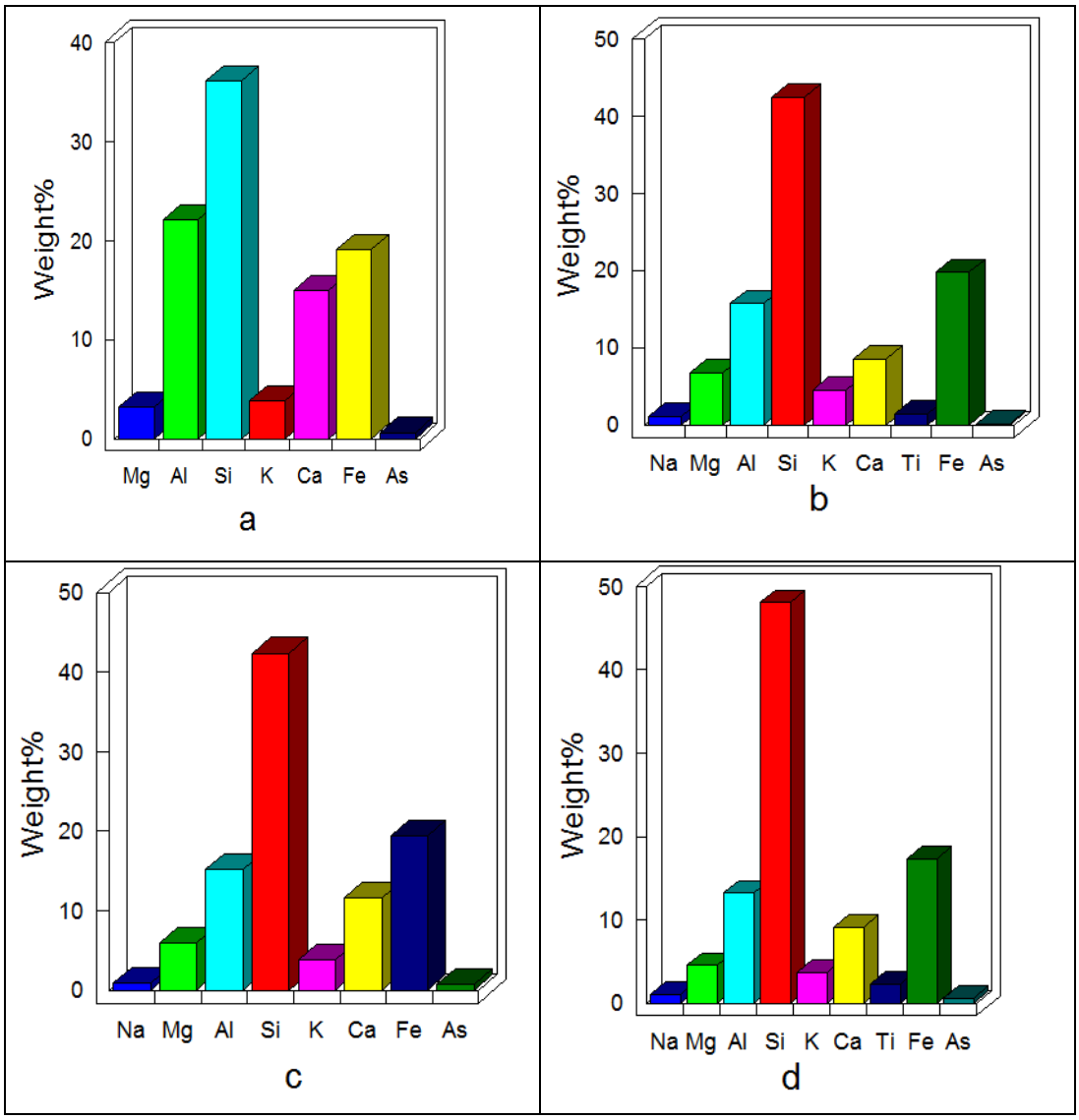

Figure 4.58. EDS spectrum of a sample treated with 1%SL (a) 0.5% SL (b), D water (c) and 50 µM H_2O_2.

Although the EDS has the ability to accurately detect and collect data within the span of a few seconds, the heterogeneity of the mine tailing sample reduces the accuracy of the data. By studying the spectra and graphs of each sample, the difference between the compositions of samples treated with different solutions can be observed. The data showed that the solution of 1% sophorolipids was more efficient in removing metals/metalloids than 0.5% sophorolipids. Hydrogen peroxide was more efficient in removing metals/metalloids than DI water. The fact that hydrogen peroxide is present in rainwater (up to 200 µM) (Willey et al., 1996; Ma et al., 2014),

shows the vulnerability of these minerals to rainfall, and how easily acid rain can cause the weathering of arsenic-bearing minerals in mine tailings and release arsenic to the surface and groundwater. During the past decades, there have been a few reports about the presence of hydrogen peroxide in the atmosphere and the effect of precipitation containing H_2O_2 on mobilizing heavy metals and metalloids (Gonçalves et al., 2010; Ma et al., 2014).

A comparison between the data from the analysis of sample treated with 0.5% SL and sample treated by H_2O_2 showed that the percentage of aluminum, magnesium, potassium, and iron in the sample treated with 0.5% sophorolipids was higher than the one treated by H_2O_2, the removal of arsenic was far greater in the sample treated by 0.5% sophorolipids. It can be due to the fact that hydrogen peroxide is an oxidizing agent and could break down organic matter, and affect the oxide/ hydroxide fraction of the mine tailing, releasing metals associated with them. On the other hand, hydrogen peroxide had no effect on the residual part of the sample, which contains the highest percentage of arsenic in the sample. Then again, sophorolipids not only mobilized the arsenic associated with amorphous iron oxides in the sample, but they are also able to affect all fractions of mine tailing sample by wetting the surfaces of the grains, seep into the pores, dissolve and wash out some fractions.

4.4.2 Speciation of arsenic in untreated and treated mine tailing sample

The results of the analysis show that, among the extractable arsenic species from mine tailing samples, using deionized water at pH 6 as the washing solution, As (V) was the only species of arsenic detected. After washing with deionized water at pH 11, 0.7% of the extracted arsenic was As (III), and 99.3% were As (V). The reason for this occurrence is that the majority or all of the arsenic was associated with the exchangeable and water-soluble fractions of mine tailings are As (V). As the mine tailing specimens that were used have been stored in tailing ponds for over ten years, it was expected that arsenic and other metals/ metalloids were oxidized. Then again, by increasing the pH of the deionized water, the organic fraction of the mine tailings was subjected to being partially washed, therefore releasing the arsenic associated with the affected parts. Therefore the presence of As (III) in the solution with pH 11 shows (Table 4.11) that some of the arsenic is associated with the organic fraction of mine tailing are in the lower oxidation states, As (III). The presence of As (III) in the effluent from arsenic removal with DI water at pH 11 also could be the result of the reduction of arsenic at the high alkaline environment. Besides, as the environment becomes more alkaline, the surface of oxides in the media become more negative and consequently repels and releases arsenic into the solution (Masscheleyn et al., 1991).

Further investigations on the effect of the biosurfactant on the oxidation state of arsenic have shown that the arsenic extracted by using a 1% rhamnolipid solution was a mixture of As (V) and As (III), although, the majority of the arsenic removed with the rhamnolipids was As (V). It was shown that at pH 6, only 1% of extracted arsenic was As (III), but at pH 11 this ratio was increased to 5%. The increase in the concentration of arsenic extracted at pH 11 can also be the effect of increasing pH on the organic fractions of the mine tailings. The result of analyzing the extracted arsenic from the mine tailing samples by using a solution of 1% sophorolipids showed that 79% of the extracted arsenic was in the form of As (III) (the more mobile state of arsenic). On the other hand, the arsenic released by a solution of 0.1% sophorolipids was in the form of As (V). Table 4.11 displays the result of analyzing the extractable arsenic species from the batch experiments.

Table 4.11. Extractable arsenic species in the mine tailing by using sophorolipid and rhamnolipids

Biosurfactant	%	pH	Total As (mg/L)	As(III) + DMA* (mg/L)	As(V) (mg/L)
SL	0.1	6	4.87	0	4.8
SL	1	6	23.51	18.6	4.91
Rh	0.1	6	4.78	0.16	4.62
Rh	1	6	19.73	0.26	19.47
Rh	1	11	35.56	1.74	33.82
Control	NA	6	2.27	0	2.27
Control	NA	11	36.32	0.25	36.07

*DMA: Dimethylarsonic acid

This data shows that the concentration of particular arsenic oxidation states mobilized from the samples depends on both the biosurfactant used and the biosurfactant concentration. Furthermore, the 3-week batch experiment, performed by using sodium arsenate at different concentrations of sophorolipids (0.1, 0.5, 1, 5 %) at two pH levels (6 and 11) showed that sophorolipids had no effect on the oxidation state of arsenic (Table 4.12). Hence, the reasons behind the release of arsenic (III) from the mine tailing samples in the presence of biosurfactants, is the presence of As (III) in non-water soluble fractions of mine tailings, and the effectiveness of the biosurfactants in releasing arsenic from non-water soluble fractions of the specimen.

Table 4.12. Effect of sophorolipids on the speciation of As (V).

Solution	%	pH	Total As (mg/L)	As(III) + DMA* (mg/L)	As(V) (mg/L)
SL	0.1	11	10.2	0	10.2
SL	0.5	11	36.8	0	36.8
SL	0.5	11	32.1	0	32.1
SL	1	11	399.9	0	399.9
SL	1	11	36.5	0	36.5
SL	5	11	36.5	0	36.5
SL	5	11	41.6	0	41.6
DI water	NA	11	23.5	0	23.5
SL	0.1	6	41.9	0	41.9
SL	0.5	6	41.4	0	41.4
SL	0.5	6	48.7	0	48.7
SL	1	6	37.7	0	37.7
SL	1	6	45.5	0	45.5
SL	5	6	52.0	0	52.0
SL	5	6	45.9	0	45.9
DI water	NA	6	48.2	0	48.2

Further investigation focused on the effect of sophorolipids at different pH on the mine tailing which has been kept in a closed container at room temperature (22±1˚C) for three years (Figure 4.59). At this part of experiments, the samples with pH 2 and 12 were not analyzed, as these extreme pH levels could affect the instrument. The results from this part of the study show that the presence of sophorolipids increased the removal of total arsenic substantially. For instance, 1% sophorolipids at pH 6 were able to remove 11.6 times more arsenic than DI water at the same pH. Sophorolipids also increased the percentage of As (III) removal significantly. As it can be seen, the ratio of As (III) to the total extracted arsenic at pH 6 was 38 to 88 percent. On the other hand, the ratio of As (III) to the total arsenic removed by DI water at pH 6 was from 1% to 4.8%, which shows the slight increase in the quantity of As (III) in the water-soluble fraction of mine

tailing sample, which points to the susceptibility of these tailings to the weathering and microbial activities.

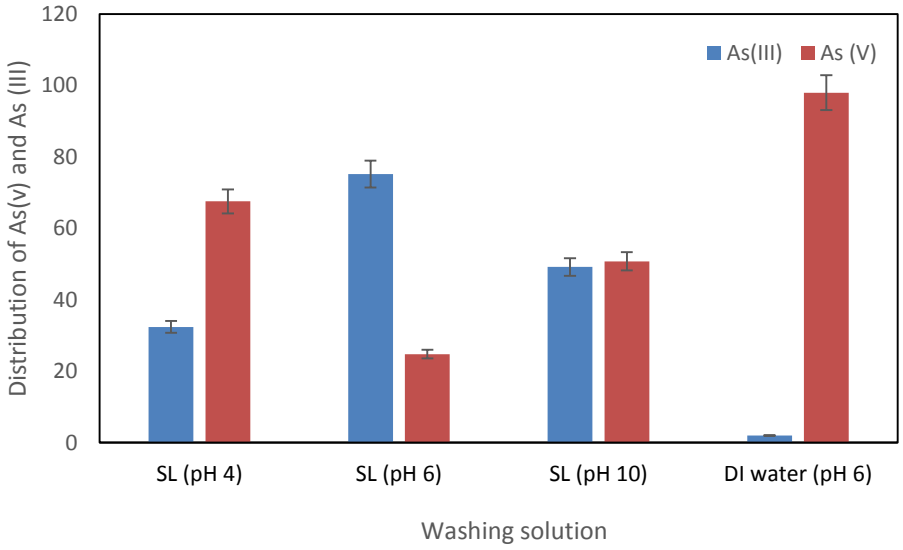

Figure 4.59. Distribution of As (III) and As (V) in the effluent from washing mine tailings with DI water and SL at different pH.

4.4.3 Zeta potential and isoelectric point of the specimen

Measuring the zeta potential of mine tailing sample showed that in alkaline and neutral environment, the particle net charge is negative. The isoelectric point (PI) of the mine tailings specimens were 1.95 ± 0.03. Below this point (pH ≤ 1.92), the zeta potential of the particles are positive. By increasing pH, the zeta potential of the particles becomes more negative. Investigations on the zeta potential of mine tailing sample in the presence of sophorolipids showed that the presence of sophorolipids causes an increase in the net negative charge (zeta potential) of particles. This illustrates the sorption of sophorolipids on the mine tailing particle which in return could increase the mobilization of arsenic from mine tailings. Further investigation on these samples showed that further flushing of the samples, which had sophorolipids adsorbed on the surface of their particle, restores the original zeta potential. This indicates that, after the process of sophorolipids-assisted soil washing, the sophorolipids adsorbed on the particles can be washed away by flushing the sample with water.

4.4.4 Results from FTIR analysis

The FTIR spectrum in the mid-infrared region (600-4000 cm^{-1}) was used to identify various functional groups present in sophorolipids SL18, at pH 5 (the non-altered pH for SL18). Figure 4.60 represents the FTIR spectra of sophorolipids (SL 18) which was interpreted according to the available data on the infrared absorption frequencies of functional groups in organic materials (Pretsch et al., 2013, Silverstein et al., 2014). This spectrum reveals a broad band at 3323 cm^{-1} corresponding to O-H, while bands at 2930 and 2853 cm^{-1} correspond to $CH_{2(\upsilon_{as})}$ (asymmetric stretching) $CH_{2\ (\upsilon_{s})}$ (symmetric stretching) of methylene (bands of the aliphatic backbone), respectively. The band at 1636 cm^{-1} was due to C=O stretching, which may include a contribution from that of lactones, esters or acids. The alkyne group (C≡C) peak was at $\tilde{\nu}$ = 2157 cm^{-1}. The bands at 1412 correspond to the C – O –H bending of carboxylic acid (-COOH). Furthermore, the band at 1033 and 1078 was due to C-O and C (=O)-O-C stretching of sophorose. The stretch at 668 (cm^{-1}) was identified as C-H bond which is due to the vibration of the C_1H of glucose (Silverstain, 1981; Weissenborn et al., 1995; Mantsch and Chapman, 1996; Baccile et al., 2013).

All of the structural details of SL 18 were similar to the sophorolipid structure in the literature, although it should be noted the wave number corresponding to functional groups within the sophorolipid structure is highly dependent on the substrate and the species being used.

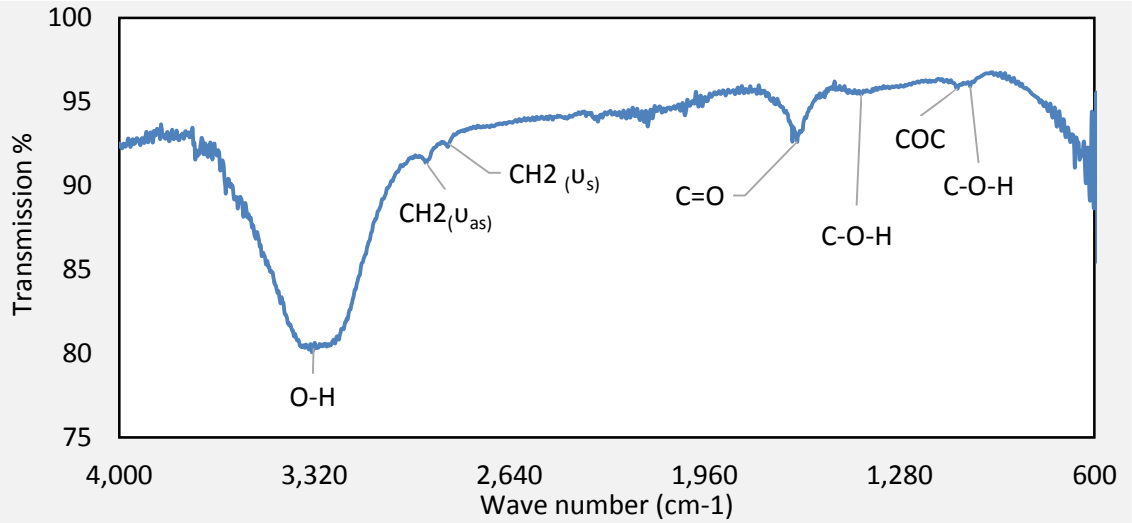

Figure 4.60. FTIR spectra of sophorolipids (SL 18).

Effect of concentration on the sophorolipid spectrum

Further investigations using different concentrations of sophorolipids determined that the changes in the concentration of sophorolipids had no effect on the spectrum and wave numbers corresponding to functional groups. The only difference was in the amplitude of the stretches; as the concentration increases, the amplitude increases (Figure 4.61).

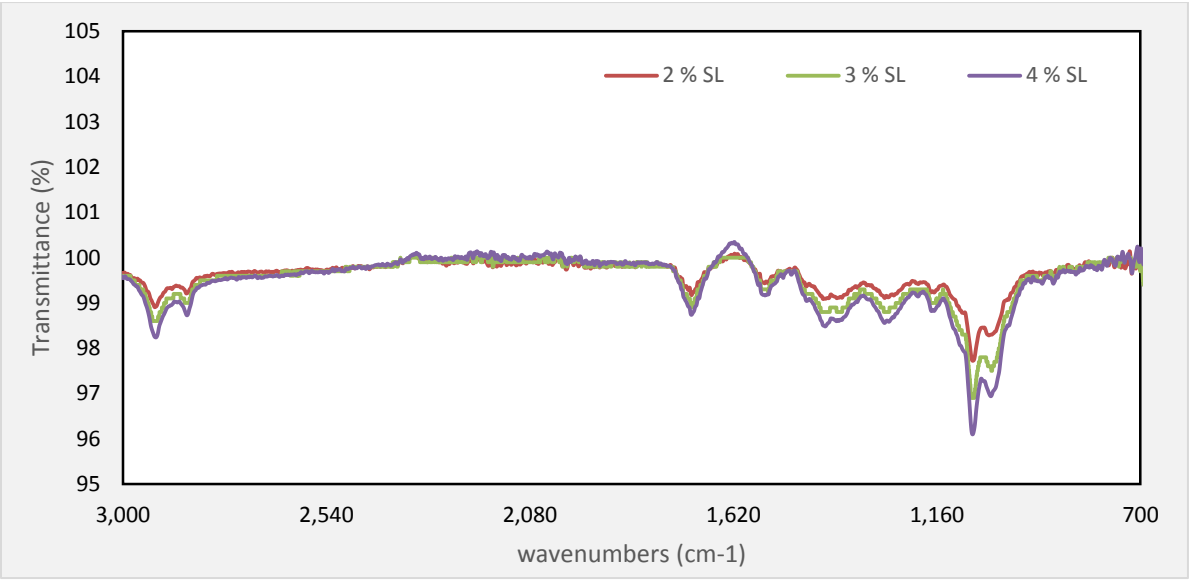

Figure 4.61. Comparison between the transmittance spectra of 2 %, 3 %, and 5 % sophorolipids.

Effect of pH on the sophorolipid spectrum

A comparison between the FTIR spectrum of a 1% sophorolipid solution (SL 18) at pH 2, 4, 6, 8, 10 and 12 (Figure 4.62), illustrates the effect that the pH level (addition of HCl and NaOH) has on the wavenumber and amplitude of functional groups on sophorolipid spectrum. As it can be seen, at pH 2 and 4, the OH group showed lower transmittance and was stretched downward at $\tilde{\nu}$ =3308 cm^{-1}. From pH 6 to 12, which was more alkaline than the natural pH of the sophorolipid solution, the OH band was eliminated. This may be caused by OH losing a proton to become O^-, and O^- binding with sodium ions. The removal of the OH bond at pH 6 is a result of adding NaOH, causing competition between H^+ and Na^+ to bond with R- O^-.

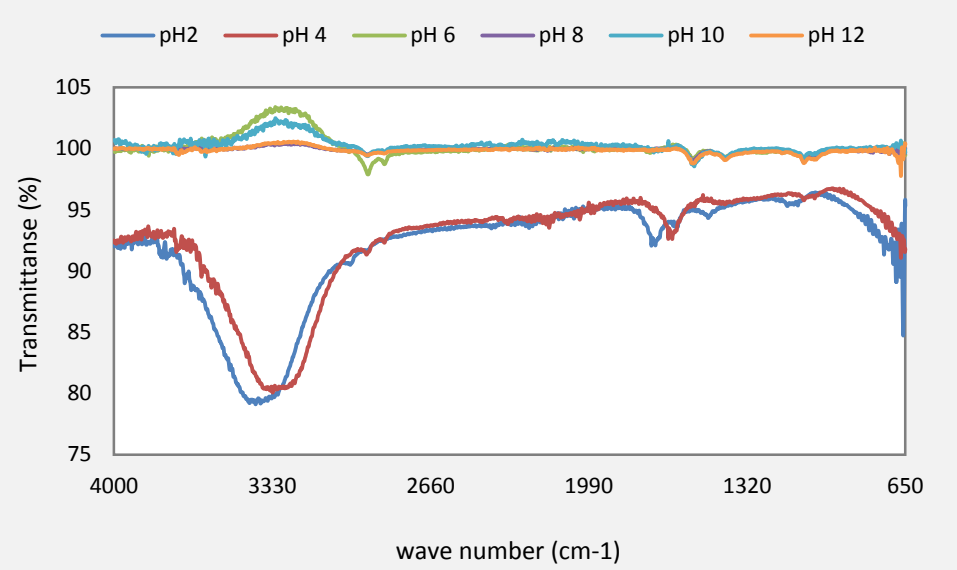

Figure 4.62. Comparison between the transmittance of spectra of sophorolipids at different pH levels.

Effect of adding arsenic, iron and mine tailing on the sophorolipid spectrum at pH 2.

A comparison between the FTIR spectrum of a solution of 1% sophorolipids SL 18 at pH 2 with the same solution in the presence of mine tailings (MT), arsenic (As) and arsenic-iron (As-Fe) shows that there were significant differences in the intensity of the sophorolipid spectrum and the SL-Fe-As / SL- MT spectra (Figure 4.63). The spectra of the four solutions at pH 2 show that the transmittance spectrum of SL-Fe-As and SL-MT are similar. At pH 2, iron cations are soluble, and based on the similarity of the Fe-As-SL and SL- MT spectra, the ions from the mine tailing sample caused the same changes on the sophorolipid spectra as ions in the SL-Fe-As solution (Tables 4.13 and 4.14).

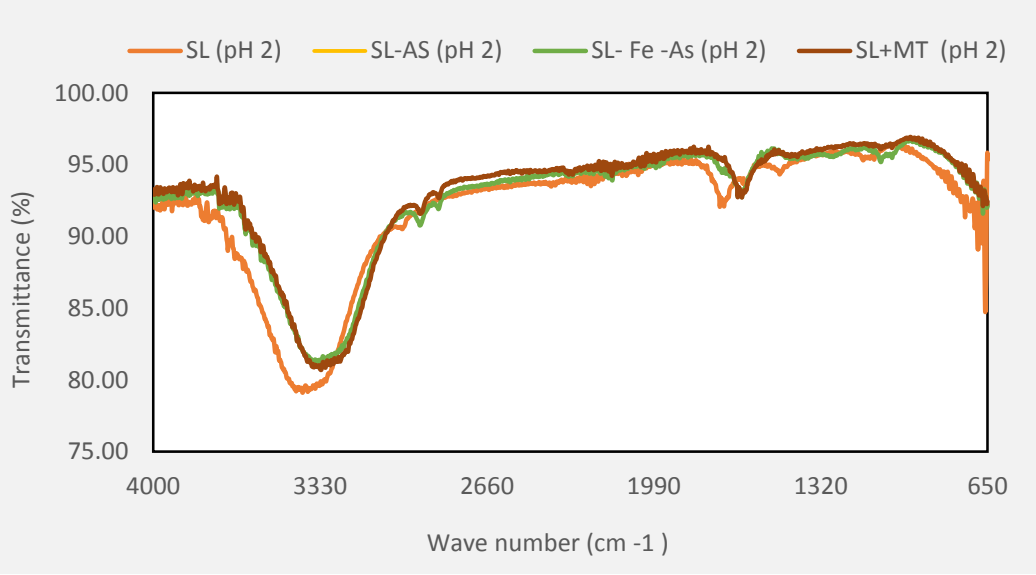

Figure 4.63. FTIR spectrum of sophorolipids and its spectra by adding As, Fe and mine tailing at pH 2.

Table 4.13. Wave number attributed to each functional group in sophorolipid solution and sophorolipids plus iron, arsenic and mine tailing at pH 2.

Solution	OH (cm^{-1})	CH_2 (v_{as}) (cm^{-1})	CH_2 (v_s) (cm^{-1})	C≡C (cm^{-1})	C=O (cm^{-1})	C-O-O-H (cm^{-1})	C-O-C (cm^{-1})	C-OH (cm^{-1})
SL	3402	2997	-	2241	1708	1482	1146	1082
SL-As	-	2920	2852	-	1712	-	1079	1030
Sl-Fe-As	3287	2924	2851	-	1635	-	1076	1029
SL- MT	3287	2919	2851	-	1635	-	1063	1029

Table 4.14. Shifts observed in wave number attributed to each functional group in sophorolipid solution with addition of iron, arsenic and mine tailings at pH 2.

Solution	OH (cm^{-1})	CH_2 (v_{as}) (cm^{-1})	CH_2 (v_s) (cm^{-1})	C≡C (cm^{-1})	C=O (cm^{-1})	C-O-O-H (cm^{-1})	C-O-C (cm^{-1})	C-OH (cm^{-1})
SL-As	-	-77	2852	-2241	4	-1482	-67	-52
Sl-Fe-As	-115	-73	2851	-2241	-73	-1482	-70	-53
SL- MT	-115	-78	2851	-2241	-73	-1482	-83	-53

As can be seen in Figure 4.61, the absorbance of the hydroxyl group (O-H) was at $\tilde{\nu}$ = 3402 cm^{-1}. The addition of iron and arsenic (SL-Fe-As) or mine tailings (SL-MT) to the sophorolipid solution caused a significant shift in the position of the O-H peak, $\tilde{\nu}$ = 3287 cm^{-1}, which was attributed to the complexation of the OH group with iron ions.

The asymmetric CH_2 stretch in pure SL at $\tilde{\nu}$ = 2997 cm^{-1}, reduced to 2920, 2924 and 2919 cm^{-1} in SL-As, SL-Fe-As and SL- MT, respectively. At pH 2, the symmetric CH_2 stretch in pure SL was absent. However, in SL-As, SL-Fe-As and SL- MT, it was at 2852 cm^{-1} (for SL-As) and 2851 cm^{-1} (for SL-Fe-As and SL-MT). The C≡C peak in pure SL which was at $\tilde{\nu}$ = 2241 cm^{-1}, was absent in the SL-As, SL-Fe-As, and SL- MT spectra.

The FTIR spectra showed that the wave number of the C=O bond in the sophorolipid solution decreased from $\tilde{\nu}$ =1708 cm^{-1} to 1635 and 1635 cm^{-1} in SL-Fe-As and SL- MT, respectively. The carbonyl bond C=O in sophorolipids, which is attributed to the lactonic and carboxylic groups, has a significant role in the complexation of iron ions to sophorolipids. The carbonyl band's shift in the presence of both iron and mine tailings, 73 cm^{-1}, was substantial (more than 40cm-1), and points towards complexation. Decreases in the stretching frequency of carbonyl indicate that the carbonyl oxygen is involved in metal coordination (Harris et al., 1997, Raymond et al., 1984, Borsari et al., 2001). These results point to the existence of a complexation between iron ions and carbonyl groups in solutions above, which results from the affinity of the C=O bond in lactonic and carboxylic acids to iron, and the formation of a bidentate bond with iron. This frequency change is in agreement with values previously reported for C=O-Fe coordination (Borsari et al., 2001).

The C-O-H bond in the SL spectrum is attributed to the carboxyl group (COOH) of the sophorolipids. At pH 2, the COH peak of sophorolipids was at $\tilde{\nu}$ = 1482 cm^{-1}. This peak was absent in SL-As, SL-Fe-As, and SL- MT spectra. The absence of the COH peak, in the presence of As-Fe and mine tailings, signify the complexation of COO- with iron ions at pH 2. This agrees with previous results, as carboxylic groups have been reported to display a high affinity towards iron ions (Baccile et al., 2013).

The wave number of the C-O-C glucosidic linkage stretch on sophorolipid spectrum decreased from 1146 cm-1 to 1079 cm^{-1} in SL-As, 1076 cm^{-1} in SL-Fe-As and 1063 cm^{-1} in SL-MT respectively. The COH peak in pure SL decreased from 1082 to 1030 cm^{-1} in SL-As, 1029 cm^{-1} in SL-Fe-As and 1029 cm^{-1} in SL- MT. These significant shifts in the COC and COH stretch may be the result of arsenic and iron bonding to the sophorose functional groups at pH 2.

Effect of adding arsenic and mine tailings on the sophorolipid spectrum at pH 4.

Adding arsenic, iron, and mine tailings to the sophorolipid solution at pH 4 did not alter the sophorolipid spectrum (Figure 4.64). It can be concluded that at pH 4, arsenic was not removed from medium by bonding with sophorolipids, rather it was released because of the sophorolipids' effect on mine tailings, washing away the organic fraction of mine tailing, loosening the bonds between the particles and breaking down the particles in the process of soil washing. It should be noted that our observation showed that the removal of arsenic decreased the closer the environment's pH gets to neutral pH. Although, even in neutral conditions, where the least arsenic removal happened, the removal of arsenic using sophorolipids was significantly higher than when DI water was solely used.

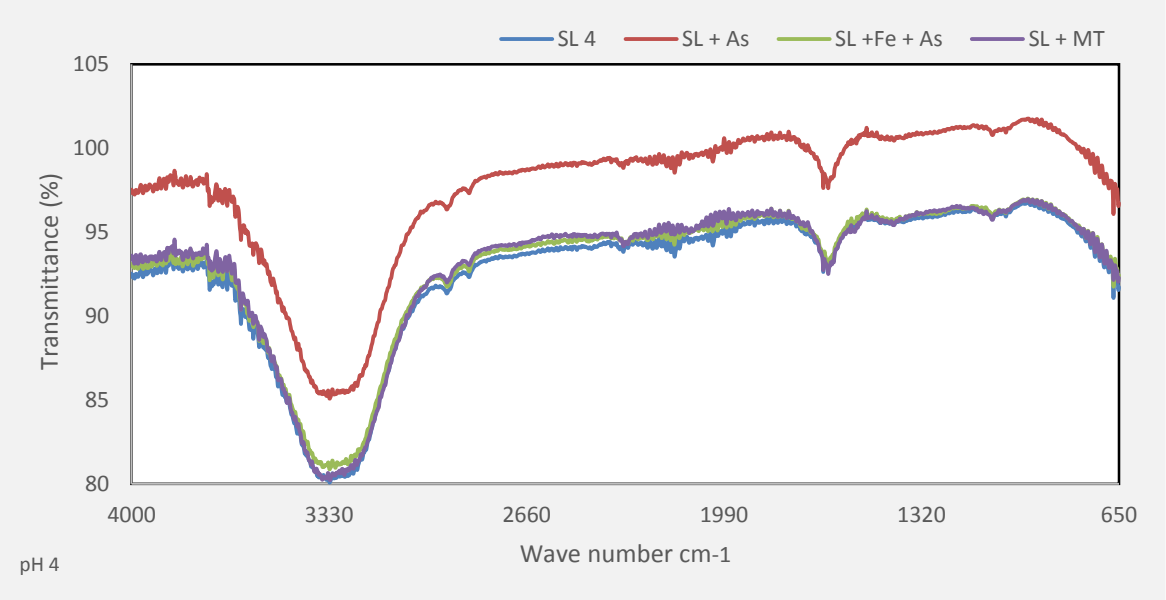

Figure 4.64. FTIR spectra of sophorolipids (SL 18) at pH4.

Effect of adding arsenic and mine tailing on the sophorolipid spectrum at pH 6.

At pH 6, the IR spectra of the sophorolipid solution, SL-Fe-As, and SL- As were comparable, and adding iron or arsenic had no effect on the sophorolipid structure. On the other hand, the spectrum of sophorolipids and mine tailings showed that the stretching of COOH at 1416 cm^{-1}, two peaks of C-O at 1249 and 1132 cm^{-1}, and sophorose's COC stretch at 1035 cm^{-1} and its COH stretch at 1024 cm^{-1} were not present in SL-MT spectrum, which can be explained by the presence of numerous types of ions in the mine tailing sample (Figure 4.65).

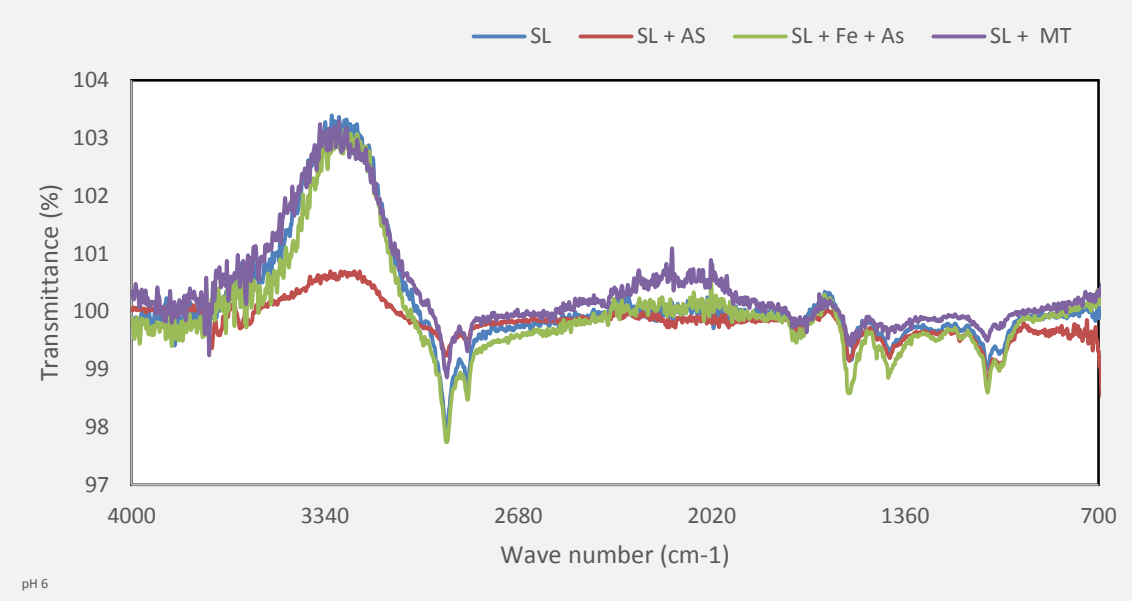

Figure 4.65. FTIR spectra of sophorolipids (SL 18) at pH 6.

Effect of adding arsenic and mine tailing on the sophorolipid spectrum at pH 8.

At pH 8, the only noticeable change in the sophorolipid spectra was the absence of peaks at wave numbers of 1409 cm^{-1} and 1037 cm^{-1}, which show that carboxylic (COOH) groups and COH groups interacted with cations in mine tailing sample (Figure 4.66). In an alkaline environment, iron precipitates as iron hydroxide, therefore the changes in COOH and COH were

caused by the interaction of these two functional groups with cations in mine tailing (excluding iron or aluminum), cations such as K^+ and Na^+.

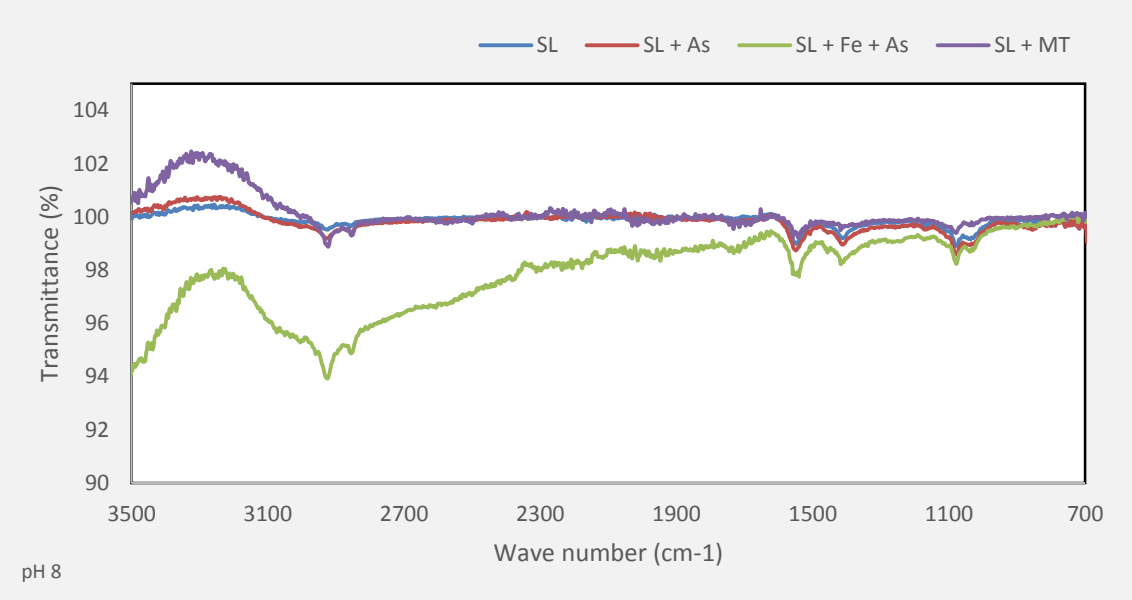

Figure 4.66. FTIR spectra of sophorolipids (SL 18) at pH 8.

Effect of adding arsenic and mine tailing on the sophorolipid spectrum at pH 10.

At pH 10, when arsenic or mine tailings were added to the sophorolipid solution, the absorbance peaks increased drastically. The carbonyl stretch (C = O) in the sophorolipid solution was at 1684, which shifted to 1714 in SL-As and SL-MT solutions. Because this shift is less than 40 cm^{-1}, no conclusion can be currently made, and there is a need for more investigation. As seen within the spectrum and from observations of the sample in the laboratory, at pH 10, iron precipitated as iron hydroxide, and this precipitant, which was visible in the samples, adsorb arsenic from the solution. As it can be seen in Figure 4.67, the solution of SL-Fe-AS at pH 10 did not affect any functional groups in the sophorolipids. The reason for this phenomena is that, as iron precipitated at pH 10, the high affinity of arsenic to iron and the strong bond between them (Frazer, 2005) cause arsenic to precipitate with the iron hydroxide. This, in return, emphasizes the importance of iron presence in the metal bridging process of sophorolipid assisted arsenic removal.

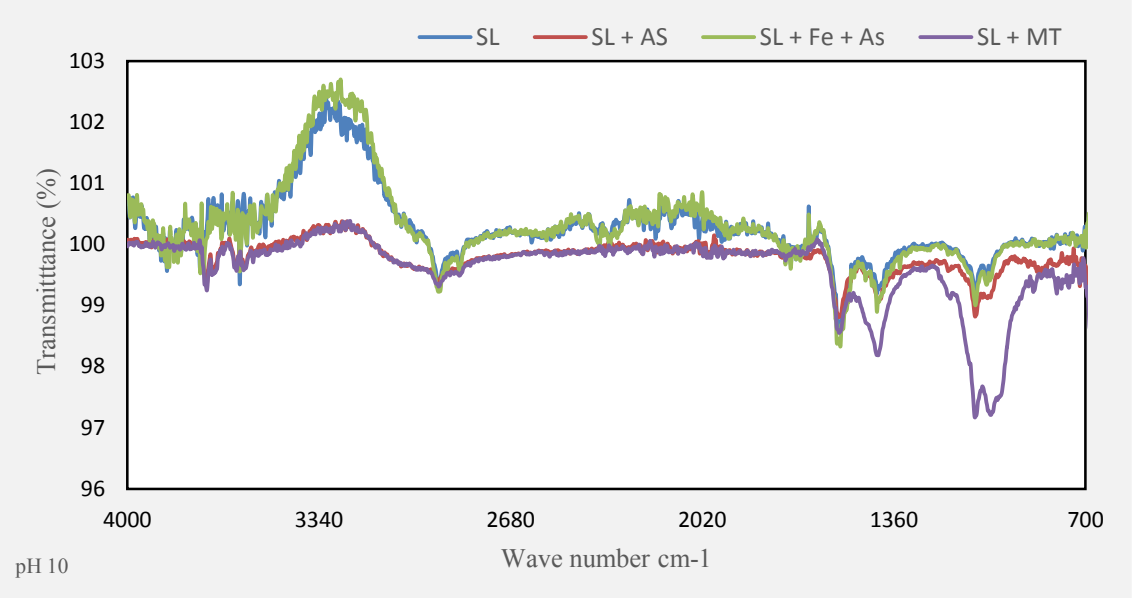

Figure 4.67. FTIR spectra of sophorolipids (SL 18) at pH 10.

Effect of adding arsenic and mine tailing on the sophorolipid spectrum at pH 12.

At pH 12, the addition of mine tailings or iron increased the intensity and absorbance of functional groups. The only shift was at the OH peak at $\tilde{\nu}$ =3253 cm^{-1}, which was reduced to 3286 cm^{-1} by adding mine tailings. This is not a substantial shift to represent a complexation (Figure 4.68).

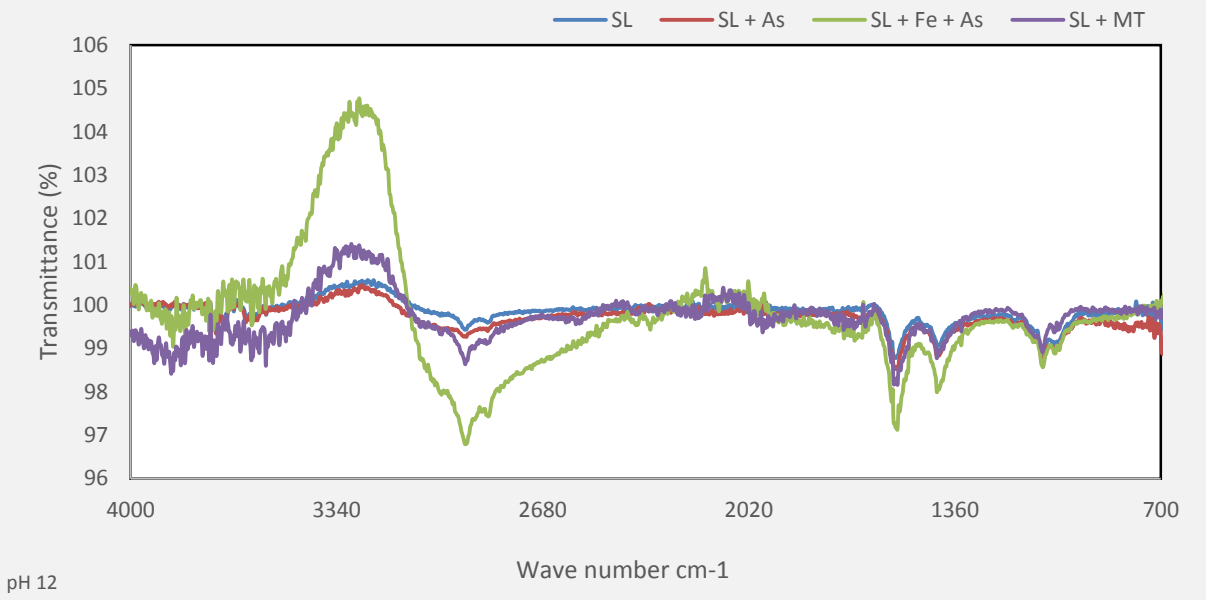

Figure 4.68. FTIR spectra of sophorolipids (SL 18) at pH 12.

In conclusion, the mechanism of arsenic removal using sophorolipids is complex which is affected by multiple parameters, such as pH, concentration, duration of contact, and temperature. It was shown that the complexation of metalloids and heavy metals to sophorolipids is highly pH dependent. At higher pH than neutral pH of the sophorolipids (4.5), the presence of sodium ions prevents the adsorption of iron to hydroxyl and carboxylic groups. The highest engagement between sophorolipids and ions occurred at pH 2. The magnitude of shifts and a comparison between the shift in functional groups in different solutions, and comparing the results with the literature, assisted in identifying the cause of each shift and detect the elements which were involved.

Finally, it should be noted that the concentration of sophorolipids was the same (1% SL) in all solutions in this investigation. Also, As (V) was used to prepare the SL-As and SL-Fe-As solutions. Therefore, the results of this study highlight the interaction of As (V) and sophorolipids. As the functional groups of sophorolipids engage differently toward arsenite (As (III)), there is a need for further investigations on the effect of As (III) on different functional groups in sophorolipids at various pH levels.

4.4.5 Results from sequential extraction

In this part of the experiments, the treated mine tailing sample which was washed with a solution of 1% sophorolipids in a column experiment was dried. It was then subjected to the sequential extraction procedure. Table 4.15 illustrates the distribution of arsenic and iron content of mine tailing specimen in different fractions of untreated mine tailing samples. As shown, most of the iron and arsenic contents of mine tailings are associated with the residual fraction. The higher ratio of arsenic associated with the residual fraction of mine tailing can be interpreted as lower mobility, lower toxicity and lower bioavailability of the arsenic in these tailings. However, the high quantity of arsenic in these tailings, which is distributed within other fractions of the sample, points towards the urgency of cleaning up of these tailings. Also, since the small size of grains in these tailings makes these tailings more susceptible to weathering, arsenic from residual fraction will eventually be released to the environment.

The result shows that the arsenic and iron content of the specimen was distributed differently between different fractions of the specimen. As it is presented in Table 4.15, washing with sophorolipids at pH 5 not only caused a decrease in the quantity of arsenic and iron, it also changed the distribution of arsenic and iron within the fractions of mine tailing. The higher percentage of arsenic compared to the total arsenic in the water-soluble and exchangeable fractions means that the arsenic has been extracted by the sophorolipid from the various fractions.

Table 4.15. Total iron and arsenic associated with different fractions of the untreated and treated mine tailing sample from column washing.

	Fe (mg/kg)		As (mg/kg)	
Fraction	Untreated	Treated	Untreated	Treated
Water soluble	25.87	26.46	8.06	7.07
Exchangeable	147.59	160.73	8.68	9.55
Carbonate	1049.88	1124.68	104.55	115.36
Oxide/hydroxide	992.94	613.78	15.71	21.32
Organic	59.03	55.97	2.58	2.70
Residual	70299.01	18856.93	2435.22	682.33

As it can be seen in the Figure 4.69, the sophorolipid solution affected all fractions of the mine tailings, mobilizing arsenic from all fractions of the specimen and redistributing them among all fractions. As it can be noticed, arsenic was mainly mobilized from oxide/hydroxide and residual fractions. Arsenic concentration was slightly increased in organic, carbonate, and water-soluble fractions and the highest increase in arsenic concentration was in the exchangeable fraction of the sample. This shows that sophorolipids can redistribute the arsenic in the sample and make them more bioavailable. It should be noted that the organic content of samples after being treated by sophorolipids has shown a substantial increase due to the presence of absorbed sophorolipids. Measuring the zeta potential of the sample before and after treatment and measuring the concentration of sophorolipids in the effluent confirmed the adsorption of sophorolipids on the surface of grains.

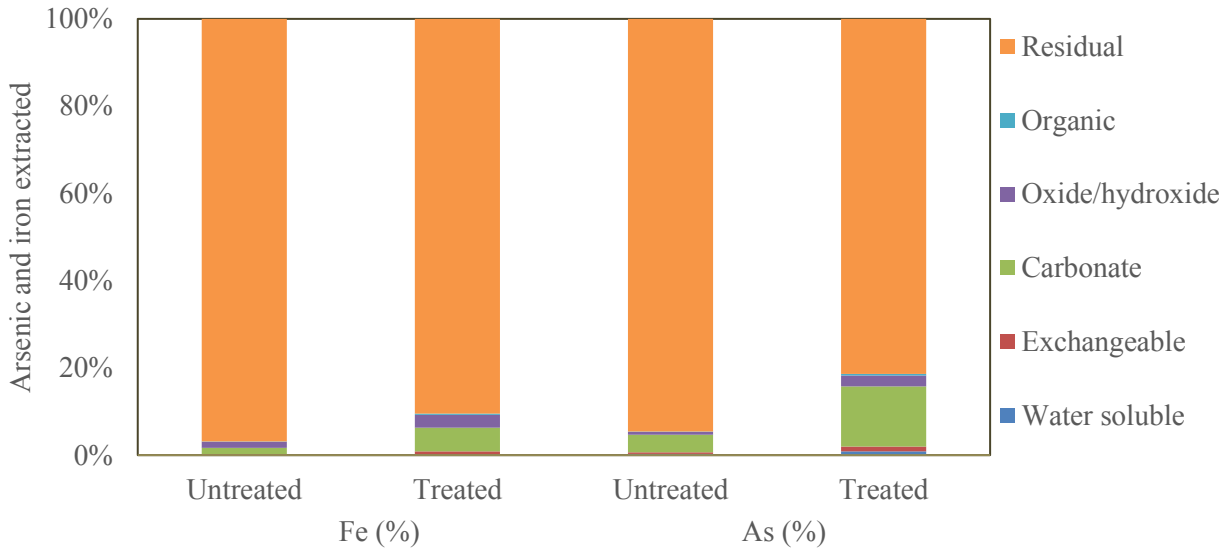

Figure 4.69. Arsenic and iron extracted during SSE process from different fractions of untreated and treated mine tailing using 1% SL at pH 4.

The results from the sequential extraction of untreated and treated samples (Figure 4.67) illustrate that all fractions of mine tailing sample were affected by sophorolipid assisted soil washing. It was shown that the affinity of sophorolipids toward different elements and their fractions varies, and sophorolipids act selectively in the sophorolipid assisted release of elements

from each fraction of the mine tailing. This part of the experiments showed that the relative percentage of arsenic in exchangeable and water-soluble fraction of mine tailing sample increased. Since these two fractions are thermodynamically unstable and are easily leachable, further flushing with water can remove arsenic from these fractions.

The presence of a high ratio of arsenic in the residual fraction of mine tailing prolongs the process of remediation, and the number of soil flushings required. In addition, a complementary process, such as particle separation to separate the colloid and clay size particles and attrition, is needed. On the other hand, the arsenic and heavy metals associated with the residual fraction of mine tailing will gradually be released to the surrounding environment due to the weathering process. Therefore, remediation or separations of heavy metals and metalloids from the mine tailing are crucial. The result from sequential extraction shows that the relative percentage of arsenic attributed to the residual fraction of the untreated sample decreased from 94% to 81% in the treated sample. The reason for this phenomenon was that sophorolipids can decrease the interfacial tension, wet the surfaces of minerals, penetrate fractures and openings in the framboidal structure of arsenopyrite, breaks down the particles and separates the segments. Clay size crystals of arsenopyrite passed through the outlet filter and later settled in the sampling tubes. Measuring the particle size of these deposits on the bottom of sampling tubes using PSA showed that these deposits are composed of colloids and clay size particles. Close examination and analysis of the composition of the deposits through digestion shows that they contain high concentrations of iron and arsenic.

4.4.6 Summary

Using sophorolipid solutions in a continuous setup led to a substantial decrease in the concentration of heavy metals and metalloids in the sample. These results show that sophorolipids are efficient in the removal of elements at a wide pH range, from 2 to 12. However, the maximum arsenic removal occurred in acidic and highly alkaline environments. A comparison between the removal of heavy metals, metalloids at different temperatures (10, 15, 23 and 35˚C) revealed that the highest removal using sophorolipid solutions was at 23˚C. In contrast, when deionized water

was used as the washing solution, the optimal temperature was at 35˚C. It should be noted that 23 ˚C was the optimum temperature for sophorolipid assisted heavy metal/metalloid removal. And the maximum solubility of sophorolipids was at 23˚C. For the removal of other contaminants, the optimum temperature may be different. For instance, rhamnolipids have shown to be more effective in the removal of crude oil from soil at 50˚C (Urum et al., 2003). Using different outlet filters, a geotextile and an air stone showed that the higher pore size filter (geotextile) not only filters out the effluent and colloids, it also separates very fine particles. The residuals from the collecting vials contained a high level of magnetite and a high concentration of arsenic.

SEM and EDS analysis of the samples before and after treatment showed that treatment of the sample by using 1% sophorolipids caused some drastic changes in the structure and composition of the sample. These investigations showed that break down of particles, dissolution of segments of particles, removal of metal oxide/ hydroxide are among of the main reasons for the removal of arsenic through sophorolipid assisted soil washing.

Using hydrogen peroxide following the method described by Robinson (1927) to measure the quantity of the organic matter in untreated and treated samples shows an increase in the organic matter in the treated mine tailing sample, which is attributed to the adsorption of sophorolipids to the surface of grains. Measuring the zeta potential of the sample before and after treatment, and measuring the concentration of sophorolipids indirectly by measuring the CMC of the effluent, and by using UV-Vis spectroscopy confirmed the adsorption of sophorolipids on the surface of grains. It was found that the maximum adsorption of sophorolipids on mine tailing surfaces happened at high alkaline and acidic environments which indicates the conclusion that sophorolipids competition with arsenic ion for binding sites on the surface of media, therefore decreasing or even inhibiting the re-adsorption of arsenic ions into media is one of the main mechanism for the removal of arsenic. These results are in agreement with the findings of previous researchers who have studied the effect of organic acids and organic matter on the release of arsenic from soil and sediments (Bauer and Blodau, 2006; Shi et al., 2008). Experiments of Bauer and Blodau (2006), by using dissolved organic matter as extractant to mobilize arsenic from soil, showed that the main factor which controlled the mobilization of arsenic from solid phases was the competition between

organic matter and arsenic for sorption sites. Further investigation of Bauer and Blodau (2006) revealed that although reduction of arsenate to the more mobile form arsenic, arsenite, in the presence of dissolved organic matter, was observed, albeit they stated that the redox activity had a minor role in the release of arsenic into the solution. It should be noted that further flushing of the sample with water washes adsorbed sophorolipids. As sophorolipids are nontoxic and biodegradable, the remaining sophorolipids would not have any adverse effect on the ecology of the area and its flora and fauna.

FTIR investigation showed that in an acidic environment, complexation of arsenic with sophorolipids' functional groups is one of the key factors in the removal of arsenic from the mine tailing sample. Furthermore, investigation of untreated and treated mine tailing samples through sequential extraction showed that all the fractions of mine tailing were affected by sophorolipids soil washing, and arsenic was removed or redistributed among the sample's fraction.

In the process of soil washing, it was shown that sophorolipids were able to release a high quantity of arsenite, the more mobile form of arsenic, from non-water-soluble fractions of mine tailing sample at all different pH being tested. Further investigations on the effect of sophorolipids on the speciation of arsenic to this point of time showed that addition of sophorolipids to a sodium arsenate solution had no effect on the speciation of arsenic. On the other hand, increasing pH to high alkaline level affected the speciation of arsenic in the solution. Therefore it can be stated that the reduction of arsenic is not a significant factor in the sophorolipid assisted arsenic mobilization.

Altogether, sophorolipid assisted soil washing in a continuous setup has been shown to be an effective method for removing heavy metals and metalloids from mine tailings and a potential efficient candidate for the treatment of mine tailings as well as contaminated soil and sediments. Summary of the mechanisms of the mobilization of heavy metals/ metalloids by sophorolipids is illustrated in Figure 4.70.

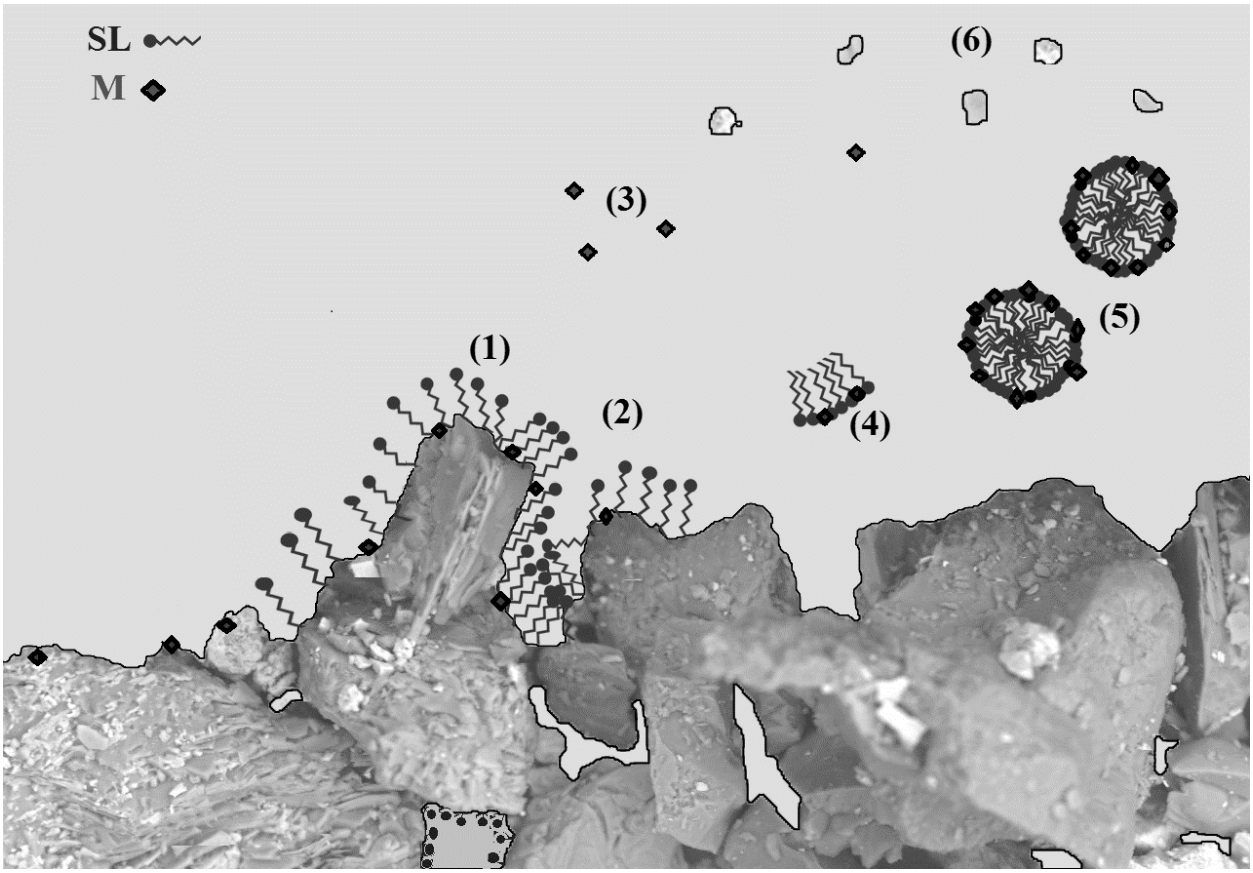

Figure 4.70. Schematic of the mechanisms of the mobilization of heavy metals/ metalloids (M) by sophorolipids

(1) Sorption of sophorolipid molecules at the interface between the media and water and lowering interfacial tension, wetting the surfaces, and letting solution to enter pores and fractures in the media.

(2) Solubilization of some fractions of the sample.

(3) Release of ions caused by diffusion, being repelled from surfaces (electrostatic interaction) by sophorolipids and competition of ions and sophorolipids for adsorption sites.

(4) Sophorolipid complexation with the elements, and desorption of SL-metal/metalloid complexes.

(5) Formation of micelles and complexation with heavy metals/ metalloids in the solution,

(6) Breakdown of the sample, dissolution of some fractions of media, and release of some minerals from media into solution.

CHAPTER FIVE: CONCLUSIONS AND RECOMMENDATIONS

5.1 Concluding remarks

The presence of elevated levels of heavy metals and metalloids indicate that the mine tailings from Giant Mine are highly toxic and are a major threat to the surrounding environment. In Yellowknife, gold is embedded in arsenopyrite ore. When arsenopyrite is enclosed in rock, its oxidation is minimal. After the rocks were crushed to extract gold, the remaining constituents, such as arsenopyrite, are exposed to air and water. It was found that mean size of the particles within the mine tailings were 13.42 μm. The small size of the particles means that they have a large surface area, making them more susceptible to weathering. Oxidation of arsenopyrite releases constituents such as arsenic and eventually results in the production of acid mine drainage (AMD). X-ray diffraction (XRD) analyses of the mine tailing samples showed that minerals such as quartz, arsenopyrite (FeAsS), limestone ($CaCO_3$) and ferric sulfate ($Fe_2(SO_4)_3$) are the main components of the tailings. Oxidation of sulfide minerals produces iron sulfate, and further oxidation of iron sulfate turns the ferrous ions in the solution into ferric ions. These ferric ions can cause further oxidation of sulfide minerals (Akcil and Koldas, 2006). Thus, the presence of a high concentration of ferric sulfate in the tailings indicates the start of the process of AMD production in these tailings. The presence of acid-buffering minerals, such as limestone, neutralizes the environment and can mask AMD production. During the warm season, heavy metals/ metalloids are removed by rain and runoffs from the tailing ponds and are discharged to Baker Creek, then transported into the Great Slave Lake, which signifies the importance of the remediation of these mine tailings.

Investigations on the removal of metal and metalloids during the batch experiments showed that increases in sophorolipid concentration resulted in an increase in the removal of all elements being measured. Using a 1% sophorolipid solution in a continuous setup resulted in the removal of up to 83% of the arsenic. These results show that sophorolipids are efficient in the removal of elements in a wide pH range, from 2 to 12. However, the maximum arsenic removal occurred in acidic and highly alkaline environments.

Further investigations on the mechanism of arsenic removal by sophorolipids were conducted by analyzing the structure of sophorolipids and the effect of the presence of arsenic, iron, and mine tailings on its spectrum and functional groups. Studies on the sophorolipid spectrum through Fourier transform infrared spectroscopy (FTIR), showed that, in an acidic environment, complexation is one of the main mechanisms of the arsenic removal by sophorolipids. The FTIR investigations shed light on the importance of the presence of iron in the solution and its role in metal bridging for binding arsenic to sophorolipid micelles during the process of sophorolipid assisted arsenic removal.

In acidic to neutral environments (from pH 2), iron oxide surfaces are positive and adsorb arsenate and arsenite. However, if the pH is increased above the isoelectric point (PI) (7.7 goethite and 8 for ferrihydrite) iron oxide surfaces become negatively charged, and thus repel arsenite and arsenate ions. Moreover, iron in the medium provides the majority of binding sites for arsenic. Therefore, in an acidic environment, the release of iron reduces the binding sites in the medium for arsenic.

In neutral environments, the higher removal of arsenic by sophorolipids in comparison to with DI water may be attributed to the fact that sophorolipids lower the interfacial between the solid phase and solution, thus allowing the solution to permeate the media, increase the wettability of the solid phase and enter the pores and break down the particles, separate the constituents, solubilize some fractions and reduce the size of the particles. Also, when sophorolipids cover the surfaces of particles, they change the surface charge and cation exchange capacity of grains. Moreover, sophorolipids bonds with the free metal/ metalloids in the solution, which causes a decrease in the number of the metal/ metalloids in the solution, which in turn promote desorption of metals to retain the equilibrium.

The decrease in the efficiency of sophorolipids in removing arsenic in neutral and low alkaline environment in comparison to acidic or high alkaline environment not only caused by precipitation of iron and other transition metals, it also caused by changes in the size, shape, and number of the aggregates in the solution.

Investigations on the zeta potential of mine tailings in the presence of sophorolipids showed that the presence of sophorolipids causes increases in the net negative charge (zeta potential) of particles, which consequently results in the repulsion of arsenic anions and prevents the re-adsorption of the released anion to the surface of the medium.

In alkaline environments, the increased removal of arsenic results from of the release of hydrogen ions from minerals in the media into the solution, resulting in an increased negative charge on the surface of the minerals, which repels the arsenic anions. Alkaline environments also favor the dissolution, desorption, and dispersion of organic matter, causing the release of arsenic associated with the organic fraction of the mine tailings. A decrease in the amount of organic matter in the medium reduces the number of sites on which arsenic can reabsorb. In alkaline solutions, iron hydroxides accept OH^- and turn to soluble $Fe(OH)^-_4$. This process reduces the OH^- concentration. Following the dissolution of iron hydroxide, arsenic adsorbed to these iron hydroxides is released to the solution.

Investigations on the effects of sophorolipids on the speciation of arsenic showed that the release of arsenic by sophorolipids in acidic and neutral environments was not related to the reduction of arsenate. However, alkaline solutions cause a reduction in the arsenic's oxidation state, converting it to a more soluble state of arsenic (As III) (Theis and Singer, 1974, Dixit and Hering, 2003, Masscheleyn et al., 1991, Frost and Griffin, 1977). Results from the speciation of arsenic removed from mine tailing by using deionized water at pH 11, agree with these researchers' statement.

Analyses of the elemental distribution of untreated and treated samples, via sequential extraction, showed that the increase in the release of arsenic from mine tailings by sophorolipids was caused by the ability of this biosurfactant to release arsenic from most fractions of mine tailing sample, and not only the arsenic associated with the water-soluble and exchangeable fractions.

Sophorolipids not only change the elemental composition of the sample, they also reduce the interfacial tension between the washing solution and mine tailings, accumulate at the solid-solution interface thus increasing the wettability of the medium. The washing solution covers the

surfaces of grains, enter pores and break down particles, separating the constituents and reducing the size of particles. This gives the biosurfactant to have direct contact with the elements in the media. In XRD investigation of samples which were treated by sophorolipids, no detectable crystalline structures were found. Selectivity of biosurfactant toward arsenic than other competing ions increase the efficiency of sophorolipids in the removal of arsenic. This research showed that sophorolipids are more effective in removing arsenic than other heavy metal/metalloids (remove a higher percentage of total arsenic). The results illustrate the selectivity of sophorolipids toward arsenic.

In summary, sophorolipids have been shown to be an effective agent for the process of removal of heavy metals and metalloids from contaminated sites. They are biodegradable and environmentally friendly. Due to the high rate of production of sophorolipids by yeasts of *Candida* sp., sophorolipids are more cost-effective than the other biosurfactants which are used for remediation of soil and sediments. The findings of this research showed that the process of arsenic removal using sophorolipids is a complex process which takes place through several mechanisms. Investigations on the mechanism of sophorolipid assisted arsenic removal showed that solubilization, complexation, and ion exchange are the main mechanisms and that the impact of each mechanism is chiefly governed by the pH. The results from this study shed light on the mechanism of arsenic removal by biosurfactants, which can aid in the development of a sustainable and environmentally friendly solution for mine tailing remediation.

5.2 Contributions to knowledge

The original contribution of the present study to scientific knowledge can be summarized as follows:

- For the first time, the effect of an inexpensive (in comparison with the other biosurfactants), degradable, environmentally friendly biosurfactant produced by yeast *Candida bombicola,* sophorolipids, was investigated in the process of heavy metals/ metalloid removal in a continuous setup.

- Investigations of the physiochemical characteristics of the mine tailing specimen from Giant Mine were conducted, along with the effect of different environmental conditions and solvents on the composition of these mine tailings.
- The mechanism of arsenic removal by sophorolipids was explored.
- The effect of environmental conditions, such as temperature and pH, on the structure, characteristics, and efficiency of sophorolipids were explored.

5.3 Publications based on the present research

- Arab, F., & Mulligan, C. N. (2014). Chapter three: Rhamnolipids Biosurfactants: Research Trends and Applications. C. N. Mulligan, S. K. Sharma, A. Mudhoo (1 edition ed., pp. 49-104): CRC Press.
- Arab, F., & Mulligan, C. N. (2016). The efficiency of sophorolipids for arsenic removal from mine tailings. *Environmental Geotechnics*. DOI: 10.1680/jenge.15.00016
- Arab, F., & Mulligan, C. N. (2013), Evaluating the use of biosurfactants in the removal of arsenic from mine tailings, GeoMontreal, Sep. 29 to Oct. 2, 2013, Montreal, Canada.
- Arab, F., & Mulligan, C. N. (2014). On the effect of sophorolipids on different fractions of mine tailing and the speciation of arsenic, GeoQuebec Sept. 20 to 23, 2015, Quebec, Canada.
- Arab, F., & Mulligan, C. N. (2014). The efficiency of sophorolipids for removal of arsenic from mine tailings. GeoRegina, Sep. 28 to Oct. 1, 2014, Regina, Canada.
- Arab, F., & Mulligan, C. N. (2015). An investigation into the efficiency of sophorolipids in mobilizing arsenic from mine tailings. Geo-Environmental Engineering. May 21-22, 2015, Montreal, Canada.
- Arab, F., & Mulligan, C. N. (2016). An eco-friendly method for heavy metal removal from mine tailings. Goldschmidt2016, June 26 to July 1, 2016, Yokohama, Japan.
- Arab, F., & Mulligan, C. N. (2017). An investigation on the mechanism of removal of heavy metals/ metalloids from mine tailings by sophorolipids. GeoOttawa 2017, Oct. 1 to Oct. 4, 2017, Ottawa, Canada.

5.4 Recommendations for future studies

- Investigation on the microbial population present in mine tailings and their role in oxidation/ reduction of mine tailing constituents.
- Evaluation of in situ production of biosurfactants to enhance metal removal from mine tailings.
- Development of applicable technologies for the treatment of effluent from the sophorolipid assisted soil washing.
- Carrying out a pilot-scale column test for sophorolipid assisted removal of heavy metals/ metalloids to validate the results from benchtop column experiments.
- Combining the process of sophorolipids assisted removal of contaminants with adequate physical technologies, to enhance the removal of contaminants and reduce the cost of remediation.

REFERENCES

Akcil, A., & Koldas, S. (2006). Acid Mine Drainage (AMD): causes, treatment and case studies. *Journal of Cleaner Production*, 14(12), 1139-1145.

Alkan, G., Srecko Stopic, & Friedrich, B. (2017). Titanium extraction from red mud via hydrometallurgical treatment. European Metallurgical Conference, June 25 to June 28, 2017, Leipzig, Germany. DOI: 10.13140/RG.2.2.17939.78886.

Allan, R. 1979. Heavy metals in bottom sediments of Great Slave Lake (Canada): A reconnaissance. *Environmental Geology,* 3**,** 49-58.

Ameratunga, J., Sivakugan, N., & Das, B. M. (2016). *Correlations of soil and rock properties in geotechnical engineering* (pp. 8-9). Springer.

Ammar, A. J., Davis, M., Cossar, D., Miller, T., Humphreys, P., & Laws, A. P. (2016). Isolation of sophorose during sophorolipid production and studies of its stability in aqueous alkali: epimerisation of sophorose to 2-O-β-d-glucopyranosyl-d-mannose. *Carbohydrate Research*, *421*, 46-54.

Andrade, C. F., Jamieson, H. E., Kyser, T. K., Praharaj, T., & Fortin, D. (2010). Biogeochemical redox cycling of arsenic in mine-impacted lake sediments and co-existing pore waters near Giant Mine, Yellowknife Bay, Canada. *Applied Geochemistry*, *25*(2), 199-211.

Arab, F., & Mulligan, C. N. (2014). Chapter three: Rhamnolipids Biosurfactants: Research Trends and Applications. C. N. Mulligan, S. K. Sharma, A. Mudhoo (1 edition ed., pp. 49-104): CRC Press.

Arab, F., & Mulligan, C. N. (2016). The efficiency of sophorolipids for arsenic removal from mine tailings. *Environmental Geotechnics*. DOI: 10.1680/jenge.15.00016

Arab, F., & Mulligan, C. N. (2013), Evaluating the use of biosurfactants in the removal of arsenic from mine tailings, GeoMontreal, Sep. 29 to Oct. 2, 2013, Montreal, Canada.

Aswal, V. K., & Goyal, P. S. (2003). Role of different counterions and size of micelle in concentration dependence micellar structure of ionic surfactants. *Chemical Physics Letters*, 368(1), 59-65.

Azouzi, R., Charef, A., & Hamzaoui, A. H. (2015). Assessment of effect of pH, temperature and organic matter on zinc mobility in a hydromorphic soil. *Environmental Earth Sciences,* 74(4), 2967-2980.

Baccile, N., Babonneau, F., Jestin, J., Pehau-Arnaudet, G., & Van Bogaert, I. (2012). Unusual, pH-induced, self-assembly of sophorolipid biosurfactants. *ACS Nano*, *6*(6), 4763-4776.

Baccile, N., Nassif, N., Malfatti, L., Van Bogaert, I. N., Soetaert, W., Pehau-Arnaudet, G., & Babonneau, F. (2010). Sophorolipids: a yeast-derived glycolipid as greener structure directing agents for self-assembled nanomaterials. *Green Chemistry*, *12*(9), 1564-1567.

Baccile, N., Noiville, R., Stievano, L., & Van Bogaert, I. (2013). Sophorolipids-functionalized iron oxide nanoparticles. *Physical Chemistry Chemical Physics*, *15*(5), 1606-1620.

Baccile, N., Pedersen, J. S., Pehau-Arnaudet, G., & Van Bogaert, I. N. (2013). Surface charge of acidic sophorolipid micelles: effect of base and time. *Soft Matter*, *9*(19), 4911-4922.

Bajaj, Vinit Kamalkishor, & Uday S. Annapure. "Castor Oil as Secondary Carbon Source for Production of Sophorolipids Using *Starmerella bombicola* NRRL Y-17069." *Journal of Oleo Science* 64, no. 3 (2015): 315-323.

Beattie, M. J. V., & Poling, G. W. (1987). A study of the surface oxidation of arsenopyrite using cyclic voltammetry. *International Journal of Mineral Processing*, *20*(1-2), 87-108.

Blais, J.F., REYNIER, N., & Mercier, G. (2013). Process for decontamination of soils polluted with metals, pentachlorophenol, dioxins and furans and contaminants removal from leachates: Google Patents.

Bodner, G. M., May, M. P., & Mckinney, L. E. (1980). A Fourier transform carbon-13 NMR study of the electronic effects of phosphorus, arsenic, and antimony ligands in transition metal carbonyl complexes. *Inorganic Chemistry*, *19*(7), 1951-1958.

Borsari, M., Gabbi, C., Ghelfi, F., Grandi, R., Saladini, M., Severi, S., & Borella, F. (2001). Silybin, a new iron-chelating agent. *Journal of Inorganic Biochemistry*, 85(2), 123-129.

Boyle, R. W. (1960). The Geology, Geochemistry, and Origin of the Gold, Deposits of the Yellowknife District. Department of Mines and Technical surveys.

Bowell, R. J. (1994). Sorption of arsenic by iron oxides and oxyhydroxides in soils. *Applied Geochemistry*, *9*(3), 279-286.

Bowell, R., Alpers, C., Jamieson, H., Nordstrom, K., & Majzlan, J. (Eds.). (2014). *Arsenic: Environmental Geochemistry, Mineralogy, and Microbiology* (Vol. 79). Walter de Gruyter GmbH & Co KG.

Canadian Council of Ministers of the Environment (CCME). 1997. Recommended Canadian Soil Quality Guidelines. Winnipeg, Manitoba, Canada.

Cantor, C. R., & Schimmel, P. R. (1980). Part III: The behavior of biological macromolecules. Biophysical Chemistry, WH Freeman and Company, New York.

Cates, M. & Candau, S. 1990. Statics and dynamics of worm-like surfactant micelles. *Journal of Physics: Condensed Matter,* 2**,** 6869.

Chandran, P., & Das, N. (2011). Characterization of sophorolipid biosurfactant produced by yeast species grown on diesel oil. *Int J Sci Nat*, *2*, 63-71.

Chowdhury, A. M. R. 2004. ARSENIC CRISIS. *Scientific American*.

Chowdhury, M.R. I. (2015). *Removal of Arsenic from Contaminated Water by Granular Activated Carbon Embedded with Nano scale Zero-valent Iron* (Doctoral dissertation, Concordia University).

Clark, I. D. & Raven, K. G. 2004. Sources and circulation of water and arsenic in the Giant Mine, Yellowknife, NWT, Canada. *Isotopes in Environmental and Health Studies,* 40**,** 115-128.

Constantine, T., & Price, L. (1983). Removal of cyanide and arsenic from tailings decant water at giant-Yellowknife-mines, Yellowknife, NWT. *The Canadian Institute of Mining Bulletin, 76*(851), 56-56.

Corkhill, C. L., & Vaughan, D. J. (2009). Arsenopyrite oxidation–A review. *Applied Geochemistry*, *24*(12), 2342-2361.

Cornell, R. M., & Schwertmann, U. (2003). *The iron oxides: structure, properties, reactions, occurrences, and uses*. John Wiley & Sons.

Corrin, M. L. & Harkins, W. D. 1947. The Effect of Salts on the Critical Concentration for the Formation of Micelles in Colloidal Electrolytes1. *Journal of the American Chemical Society,* 69**,** 683-688.

Cotton, F. A. (1964). Vibrational spectra and bonding in metal carbonyls. III. Force constants and assignments of CO stretching modes in various molecules; evaluation of CO bond orders. *Inorganic Chemistry*, *3*(5), 702-711.

Cousens, B. L. (2000). Geochemistry of the Archean Kam Group, Yellowknife Greenstone Belt, Slave Province, Canada. *The Journal of Geology*, *108*(2), 181-197.

Cuvier, A. S., Berton, J., Stevens, C. V., Fadda, G. C., Babonneau, F., Van Bogaert, I. N., ... & Baccile, N. (2014). pH-triggered formation of nanoribbons from yeast-derived glycolipid biosurfactants. *Soft Matter*, *10*(22), 3950-3959.

Czaplicki, L. M., Cooper, E., Ferguson, P. L., Stapleton, H. M., Vilgalys, R., & Gunsch, C. K. (2016). A New Perspective on Sustainable Soil Remediation—Case Study Suggests Novel Fungal Genera Could Facilitate in situ Biodegradation of Hazardous Contaminants. *Remediation Journal*, *26*(2), 59-72.

Dahrazma, B., Mulligan, C. N., & Nieh, M. P. (2008). Effects of additives on the structure of rhamnolipid (biosurfactant): A small-angle neutron scattering (SANS) study. *Journal of Colloid and Interface Science*, 319(2), 590-593.

Das, Dilip Kumar, Garai, TK, Sarkar, S, & Sur, Pintu. (2005). Interaction of Arsenic with Zinc and Organics in a Rice (Oryza sativa L.)–Cultivated Field in India. *The Scientific World Journal, 5*, 646-651.

Daverey, A., & Pakshirajan, K. (2009). Production of sophorolipids by the yeast *Candida bombicola* using simple and low cost fermentative media. *Food Research International*, *42*(4), 499-504.

Daverey, A., & Pakshirajan, K. (2009). Production, characterization, and properties of sophorolipids from the yeast *Candida bombicola* using a low-cost fermentative medium. *Applied Biochemistry and Biotechnology*, *158*(3), 663-674.

Daverey, A., & Pakshirajan, K. (2010). Sophorolipids from Candida bombicola using mixed hydrophilic substrates: production, purification, and characterization. *Colloids and Surfaces B: Biointerfaces*, *79*(1), 246-253.

Davis, A. P., & Singh, I. (1995). Washing of zinc (II) from contaminated soil column. *Journal of Environmental Engineering*, *121*(2), 174-185.

Dermont, G., Bergeron, M., Mercier, G., & Richer-Laflèche, M. (2008). Soil washing for metal removal: a review of physical/chemical technologies and field applications. *Journal of Hazardous Materials*, *152*(1), 1-31.

Deshpande, S., Shiau, B. J., Wade, D., Sabatini, D. A., & Harwell, J. H. (1999). Surfactant selection for enhancing ex situ soil washing. *Water Research*, *33*(2), 351-360.

Develter, Dirk WG, & Lauryssen, Luc ML. (2010). Properties and industrial applications of sophorolipids. *European Journal of Lipid Science and Technology, 112*(6), 628-638.

Dhasaiyan, P., Banerjee, A., Visaveliya, N., & Prasad, B. L. V. (2013). Influence of the Sophorolipid Molecular Geometry on their Self-Assembled Structures. *Chemistry–An Asian Journal*, *8*(2), 369-372.

Dimiduk, D. M. (1999). Gamma titanium aluminide alloys—an assessment within the competition of aerospace structural materials. *Materials Science and Engineering: A*, *263*(2), 281-288.

Dixit, S. and Hering, J. G. 2003. Comparison of arsenic (V) and arsenic (III) sorption onto iron oxide minerals: Implications for arsenic mobility. *Environmental Science & Technology,* 37**,** 4182-4189.

Dos Santos, E. C., Lourenço, M. P., Pettersson, L. G., & Duarte, H. A. (2017). Stability, Structure, and Electronic Properties of the Pyrite/Arsenopyrite Solid–Solid Interface–A DFT Study. *The Journal of Physical Chemistry C*, *121*(14), 8042-8051.

Dove, P. M. & Rimstidt, J. D. 1985. The solubility and stability of scorodite, $FeAsO_4$. $2H_2O$. *American Mineralogist*, 70 (7), 838-844.

Dushenko, W. T., Bright, D. A., & Reimer, K. J. (1995). Arsenic bioaccumulation and toxicity in aquatic macrophytes exposed to gold-mine effluent: relationships with environmental partitioning, metal uptake, and nutrients. *Aquatic Botany, 50*(2), 141-158.

Dzombak, D.A., Morel, F.M.M., 1990. Surface Complexation Modeling: Hydrous Ferric Oxide. John Wiley & Sons, Toronto, Canada.

Ecover. 2014. Price Quotation for Sophorolipids (SL) [Online]. Available: http://www.agrobiobase.com/base/data/f_283/p_509/documents/product%20information%20for%20ecover%20sl18.pdf 2014].

Environment Canada, 2017, 1981-2010 Climate Normals & Averages. Website: http://climate.weather.gc.ca/climate_normals/ (accessed Nov. 2017).

Environmental Protection Agency (EPA) 1996. A Citizen's Guide to Soil Washing. OSWER. April. EPA 542-F-96-002.

Environmental Protection Agency (EPA), 2009. Contaminants in soil: updated collation of toxicological data and intake values for humans. *Inorganic arsenic. Science Report SC050021/SR TOX1*.

Fawcett, S. E., Jamieson, H. E., Nordstrom, D. K., & McCleskey, R. B. (2015). Arsenic and antimony geochemistry of mine wastes, associated waters and sediments at the Giant Mine, Yellowknife, Northwest Territories, Canada. *Applied Geochemistry*, *62*, 3-17.

Frazer, L. (2005). Metal Attraction An Ironclad Solution to Arsenic Contamination? *Environmental health perspectives*, 113, no. 6 (2005): A399-A401.

Frost, R. & Griffin, R. 1977. Effect of pH on adsorption of arsenic and selenium from landfill leachate by clay minerals. *Soil Science Society of America Journal,* 41**,** 53-57.

Gaspard, S., & Ncibi, M. C. (Eds.). (2013). *Biomass for Sustainable Applications: Pollution Remediation and Energy* (Vol. 25). Royal Society of Chemistry (chapter 4).

Geelhoed, J. S., Meeussen, J. C., Roe, M. J., Hillier, S., Thomas, R. P., Farmer, J. G., & Paterson, E. (2003). Chromium remediation or release? Effect of iron (II) sulfate addition on

chromium (VI) leaching from columns of chromite ore processing residue. *Environmental Science & Technology*, *37*(14), 3206-3213.

Gómez-Bombarelli, R., Calle, E., & Casado, J. (2013). Mechanisms of lactone hydrolysis in neutral and alkaline conditions. *The Journal of Organic Chemistry*, *78*(14), 6868-6879.

Government of Northwest Territories. 2015. Climate observations in the Northwest Territories (1957-2012). Website: http://www.enr.gov.nt.ca/sites/enr/files/page_3_nwt-climate-observations_06-13-2015_vf_1_0.pdf (retrived: Nov. 2017).

Grantham, D. A., & Jones, J. F. (1977). Arsenic Contamination of Water Wells in Nova Scotia (PDF). *Journal-American Water Works Association*, *69*(12), 653-657.

Guemiza, K., Coudert, L., Tran, L. H., Metahni, S., Blais, J. F., Besner, S., & Mercier, G. (2017). Optimizing removal of arsenic, chromium, copper, pentachlorophenol and polychlorodibenzo-dioxins/furans from the 1–4 mm fraction of polluted soil using an attrition process. *Environmental Technology*, *38*(15), 1862-1877.

Guemiza, K., Coudert, L., Metahni, S., Mercier, G., Besner, S., & Blais, J. F. (2017). Treatment technologies used for the removal of As, Cr, Cu, PCP and/or PCDD/F from contaminated soil: A review. *Journal of Hazardous Materials*. Volume 333, 5 July 2017, Pages 194-214.

Harris, W. R., Carrano, C. J., & Raymond, K. N. (1979). Spectrophotometric determination of the proton-dependent stability constant of ferric enterobactin. *Journal of the American Chemical Society*, *101*(8), 2213-2214.

Hayter, R. G. (1963). Phosphorus-and Arsenic-Bridged Complexes of Metal Carbonyls. II. Cyclopentadienylnickel, molybdenum, and tungsten Complexes. *Inorganic Chemistry*, *2*(5), 1031-1035.

Hayter, R. G. (1964). Phosphorus-and Arsenic-Bridged Complexes of Metal Carbonyls. VI. Reactions of Tetrasubstituted Biphosphines and a Biarsine with Monomeric Metal Carbonyls. *Inorganic Chemistry*, *3*(5), 711-717.

Holm, T. R., & Wilson, S. D. (2006). Chemical Oxidation for Arsenic Removal from Drinking Water. Illinois State Water Survey, Midwest Technology Assistance Center for Small Public Water Systems (MTAC).

Horowitz, A. J. & Elrick, K. A. 1987. The relation of stream sediment surface area, grain size, and composition to trace element chemistry. *Applied Geochemistry,* 2**,** 437-451.

Hu, Y., & Ju, L. K. (2001). Purification of lactonic sophorolipids by crystallization. *Journal of Biotechnology*, *87*(3), 263-272.

Hubbard, C. & O'connor, B. 2002. International Centre for Diffraction Data (ICDD).

Interstate Technology & Regulatory Council (ITRC). 1997. Technical and Regulatory Guidelines for Soil Washing. Metals in Soil Workgroup. Washington, D.C. December. MIS-1.

Ishigami, Y., Gama, Y., Nagahora, H., Yamaguchi, M., Nakahara, H., & Kamata, T. (1987). The pH-sensitive conversion of molecular aggregates of rhamnolipid biosurfactant. *Chemistry Letters*, *16*(5), 763-766.

Ismail, M. 2008. Mathematical correlations between the effective diameter of soil and other properties. *Engineering and Technology,* 26**,** 1274-1281.

Jain, C. K., & Ali, I. (2000). Arsenic: occurrence, toxicity and speciation techniques. Water Research, 34(17), 4304-4312.

Jamieson, H. E., Walker, S. R., & Parsons, M. B. (2015). Mineralogical characterization of mine waste. *Applied Geochemistry*, *57*, 85-105.

Jones, R. A., & Nesbitt, H. W. (2002). XPS evidence for Fe and As oxidation states and electronic states in loellingite (FeAs2). *American Mineralogist*, *87*(11-12), 1692-1698.

Kasture, M., Singh, S., Patel, P., Joy, P. A., Prabhune, A. A., Ramana, C. V., & Prasad, B. L. V. (2007). Multiutility sophorolipids as nanoparticle capping agents: synthesis of stable and water dispersible Co nanoparticles. *Langmuir*, 23(23), 11409-11412.

Kim, I. S., Park, J. S., & Kim, K. W. (2001). Enhanced biodegradation of polycyclic aromatic hydrocarbons using nonionic surfactants in soil slurry. *Applied Geochemistry*, *16*(11), 1419-1428.

Kim, J., & Vipulanandan, C. (2006). Removal of lead from contaminated water and clay soil using a biosurfactant. *Journal of Environmental Engineering*, *132*(7), 777-786.

Kim, T. H., Han, Y. S., Seong, B. S., & Hong, K. P. (2011). Thermally responsive vesicles based on a mixture of cationic surfactant and organic derivative below the CMC. *Soft Matter*, *7*(21), 10070-10075.

Koch, I., Wang, L., Ollson, C. A., Cullen, W. R. & Reimer, K. J. 2000. The predominance of inorganic arsenic species in plants from Yellowknife, Northwest Territories, Canada. *Environmental Science & Technology,* 34**,** 22-26.

Kołodyńska, D., Krukowska, J., & Thomas, P. (2017). Comparison of sorption and desorption studies of heavy metal ions from biochar and commercial active carbon. *Chemical Engineering Journal*, *307*, 353-363.

Kothari, K., Radhakrishnan, R., & Wereley, N. M. (2012). Advances in gamma titanium aluminides and their manufacturing techniques. *Progress in Aerospace Sciences*, *55*, 1-16.

Kosmulski, M. (2004). pH-dependent surface charging and points of zero charge II. Update. *Journal of Colloid and Interface Science*, 275(1), 214-224.

Lang, S. (2002). Biological amphiphiles (microbial biosurfactants). *Current Opinion in Colloid & Interface Science*, *7*(1), 12-20.

Li, W., Yang, Y., Liu, L., Tan, X., Luo, T., & Shen, J. (2015). Dual stimuli-responsive self-assembly transition in zwitterionic/anionic surfactant systems. *Soft Matter*, *11*(21), 4283-4289.

Mandal, B. K. & Suzuki, K. T. (2002). Arsenic round the world: a review. *Talanta,* 58**,** 201-235.

Manet, S., Cuvier, A. S., Valotteau, C., Fadda, G. C., Perez, J., Karakas, E., Stéphane Abel & Baccile, N. (2015). Structure of bolaamphiphile sophorolipid micelles characterized with SAXS, SANS, and MD simulations. *The Journal of Physical Chemistry B*, *119*(41), 13113-13133.

Manning, B.A., Goldberg, S., 1997. Arsenic (III) and arsenic (V) adsorption on three California soils. *Soil Sci*. 162, 886–895.

Masscheleyn, P. H., Delaune, R. D., & Patrick Jr, W. H. (1991). Effect of redox potential and pH on arsenic speciation and solubility in a contaminated soil. *Environmental Science & Technology*, *25*(8), 1414-1419.

Mattson, E. C., Aboualizadeh, E., Barabas, M. E., Stucky, C. L., & Hirschmugl, C. J. (2013). Opportunities for live cell FT-infrared imaging: macromolecule identification with 2D and 3D localization. *International Journal of Molecular Sciences*, *14*(11), 22753-22781.

Mazumder, D. N. G., Haque, R., Ghosh, N., Binay K. D., Santra, A., Chakraborty, D. & Smith, A. H. (1998). Arsenic levels in drinking water and the prevalence of skin lesions in West Bengal, India. *International Journal of Epidemiology, 27*, 871-877.

Mercier, G., Blais, J.F., Guemiza, K., Metahni, S., Mercier, G., Chartier, M., . . . Besner, S. (2017). Decontamination process of soils and effluents polluted by inorganic and/or organic contaminants: Google Patents.

Metahni, S., Coudert, L., Chartier, M., Blais, J. F., Mercier, G., & Besner, S. (2017). Pilot-Scale Decontamination of Soil Polluted with As, Cr, Cu, PCP, and PCDDF by Attrition and Alkaline Leaching. *Journal of Environmental Engineering*, *143*(9), 04017055.

Miller, R. M. (1995). Biosurfactant-facilitated remediation of metal-contaminated soils. Environmental Health Perspectives, 103(Suppl 1), 59.

Milton, A. H., Smith, W., Rahman, B., Hasan, Z., Kulsum, U., Dear, K., Rakibuddin, M. & Ali, A. 2005. Chronic arsenic exposure and adverse pregnancy outcomes in Bangladesh. *Epidemiology,* 16**,** 82-86.

Mitra, S. & Dungan, S. R. (1997). Micellar properties of Quillaja saponin. 1. Effects of temperature, salt, and pH on solution properties. *Journal of Agricultural and Food Chemistry,* 45**,** 1587-1595.

Moghimi, A. H., Hamdan, J., Shamshuddin, J., Samsuri, A. W., & Abtahi, A. (2013). Physicochemical properties and surface charge characteristics of arid soils in Southeastern Iran. *Applied and Environmental Soil Science*, Volume 2013, Article ID 252861, pages 1-11. DOI: http://dx.doi.org/10.1155/2013/252861

Moore, J. W., Beaubien, V. A. & Sutherland, D. J. (1979). Comparative effects of sediment and water contamination on benthic invertebrates in four lakes. *Bulletin of Environmental Contamination and Toxicology,* 23**,** 840-847.

Morales, K. H., Ryan, L., Kuo, T. L., Wu, M. M. & Chen, C. J. (2000). Risk of internal cancers from arsenic in drinking water. *Environment Health Perspectives, 108*(7), 655-661.

Morya VK, Kim EK (2014) Sophorolipids: characteristics, production and application (chapter 4). In: Mulligan CN, Sharma SK, Mudhoo A (1th Ed.) Biosurfactants: Research Trends and Application. CRC Press, 105-124.

Mudgil, P. (2011). Biosurfactants for soil biology. In A. Singh, N. Parmar, & R. C. Kuhad (Eds.), *Bioaugmentation, Biostimulation and Biocontrol*. DOI:10.1007/978-3-642-19769-7_9

Mudroch, A., Joshi, S., Sutherland, D., Mudroch, P. & Dickson, K. (1989). Geochemistry of sediments in the back bay and Yellowknife Bay of the Great Slave Lake. *Environmental Geology and Water Sciences,* 14**,** 35-42

Mulligan, C. N. (2005). Environmental applications for biosurfactants. *Environmental Pollution, 133*(2), 183-198.

Mulligan, C. N., Yong, R. N., & Gibbs, B. F. (2001). Remediation technologies for metal-contaminated soils and groundwater: an evaluation. *Engineering Geology*, *60*(1), 193-207.

Mulligan, C. N. (1998). On the capability of biosurfactants for the removal of heavy metals from soil and sediments, (PhD Dissertation). McGill University, Montreal, QC.

Nakamoto, K. (1986). *Infrared and Raman spectra of inorganic and coordination compounds*. John Wiley & Sons, Ltd.

Neubauer, K. (2010). Reducing the Effects of Interferences in Quadrupole ICP-MS. Retrieved from http://www.spectroscopyonline.com/reducing-effects-interferences-quadrupole-icp-ms.

Nordstrom, D. K. (2002). Worldwide occurrences of arsenic in ground water. *Science, 296,* 2143-2145.

Ochoa-Loza, F. J., Artiola, J. F., & Maier, R. M. (2001). Stability constants for the complexation of various metals with a rhamnolipid biosurfactant. *Journal of Environmental Quality*, *30*(2), 479-485.

O'Day, P. A. (2006). Chemistry and mineralogy of arsenic. *Elements*, *2*(2), 77-83.

Pacwa-Płociniczak, M., Płaza, G. A., Piotrowska-Seget, Z., & Cameotra, S. S. (2011). Environmental applications of biosurfactants: recent advances. *International Journal of Molecular Sciences*, *12*(1), 633-654.

Panagiotaras, D., & Nikolopoulos, D. (2015). Arsenic Occurrence and Fate in the Environment; A Geochemical Perspective. *Journal of Earth Science & Climatic Change*, *6*(4), 1.

Papageorgiou, S. K., Kouvelos, E. P., Favvas, E. P., Sapalidis, A. A., Romanos, G. E., & Katsaros, F. K. (2010). Metal–carboxylate interactions in metal–alginate complexes studied with FTIR spectroscopy. *Carbohydrate Research*, *345*(4), 469-473.

Pepper, IL, Zerzghi, HG, Bengson, SA, Iker, BC, Banerjee, MJ, & Brooks, JP. (2012). Bacterial populations within copper mine tailings: long-term effects of amendment with Class A biosolids. *Journal of Applied Microbiology, 113*(3), 569-577.

Pretsch, E., Clerc, T., Seibl, J. & Simon, W. 2013. Tables of spectral data for structure determination of organic compounds, Springer Science & Business Media.

Qafoku, N. P., Van Ranst, E., Noble, A., & Baert, G. (2004). Variable charge soils: their mineralogy, chemistry and management. *Advances in Agronomy*, 84, 159-215.

Qiang, T., Xiao-quan, S., & Zhe-ming, N. (1994). Evaluation of a sequential extraction procedure for the fractionation of amorphous iron and manganese oxides and organic matter in soils. *Science of the Total Environment*, *151*(2), 159-165.

Rahman, P. K. S., Pasirayi, G., Auger, V., & Ali, Z. (2010). Production of rhamnolipid biosurfactants by *Pseudomonas aeruginosa* DS10-129 in a microfluidic bioreactor, *Biotechnology and Applied Biochemistry*, 55 (1), pp.45-52.

Rau, U., Heckmann, R., Wray, V., & Lang, S. (1999). Enzymatic conversion of a sophorolipid into a glucose lipid. *Biotechnology Letters*, *21*(11), 973-977.

Rau, U., Hammen, S., Heckmann, R., Wray, V., & Lang, S. (2001). Sophorolipids: a source for novel compounds. *Industrial Crops and Products*, *13*(2), 85-92.

Raymond, K. N., Müller, G., & Matzanke, B. F. (1984). Complexation of iron by siderophores a review of their solution and structural chemistry and biological function. In *Structural Chemistry* (pp. 49-102). Springer Berlin Heidelberg.

Reynier, N., Blais, J. F., Mercier, G., & Besner, S. (2013). Optimization of arsenic and pentachlorophenol removal from soil using an experimental design methodology. *Journal of Soils and Sediments*, *13*(7), 1189-1200.

Robinson, W. O. (1927). The determination of organic matter in soils by means of hydrogen peroxide. *Journal of Agricultural Research,* 34, 339-356.

Rong, S. H. I., Yongfeng, J. I. A., & Chengzhi, W. A. N. G. (2009). Competitive and cooperative adsorption of arsenate and citrate on goethite. *Journal of Environmental Sciences*, 21(1), 106-112.

Shah, S., & Prabhune, A. (2007). Purification by silica gel chromatography using dialysis tubing and characterization of sophorolipids produced from *Candida bombicola* grown on glucose and arachidonic acid. *Biotechnology Letters*, *29*(2), 267-272.

Shalat, S. L., Walker, D. B. & Finnell, R. H. 1996. Role of arsenic as a reproductive toxin with particular attention to neural tube defects. *Journal of Toxicology and Environmental Health,* 48**,** 253-272.

Sandlos, J., & Keeling, A. (2012). Giant mine: Historical summary. *Report submitted to Mackenzie Valley Environmental Review Board public registry*.

Scherer, O. J. (1985). Phosphorus, Arsenic, Antimony, and Bismuth Multiply Bonded Systems with Low Coordination Number—Their Role as Complex Ligands. *Angewandte Chemie International Edition in English*, *24*(11), 924-943.

Schofield, R. K., & Taylor, A. W. (1955). The measurement of soil pH. *Soil Science Society of America, 19*, 164-167.

Schwertmann, U. (1991). Solubility and dissolution of iron oxides. *Plant and Soil*. Volume 130 (1), 1–25. DOI: https://doi.org/10.1007/BF00011851.

Sidhu, P. S., Gilkes, R. J., Cornell, R. M., & Posner, A. M. (1981). Dissolution of iron oxides and oxyhydroxides in hydrochloric and perchloric acids. *Clays Clay Minerals,* 29 (4), 269-276. DOI: 10.1346/CCMN.1981.0290404.

Silverstein, R. M., Webster, F. X., Kiemle, D. J. & Bryce, D. L. 2014. Spectrometric identification of organic compounds, John Wiley & Sons.

Singh, S., Patel, P., Jaiswal, S., Prabhune, A. A., Ramana, C. V., & Prasad, B. L. V. (2009). A direct method for the preparation of glycolipid–metal nanoparticle conjugates: sophorolipids as reducing and capping agents for the synthesis of water re-dispersible silver nanoparticles and their antibacterial activity. *New Journal of Chemistry,* 33(3), 646-652.

Slizovskiy, I. B., Kelsey, J. W., & Hatzinger, P. B. (2011). Surfactant-facilitated remediation of metal-contaminated soils: efficacy and toxicological consequences to earthworms. *Environmental Toxicology and Chemistry, 30*(1), 112-123.

Smedley, P. L., & Kinniburgh, D. G. (2001). Source and behavior of arsenic in natural waters. *United Nations synthesis report on arsenic in drinking water*. World Health

Organization, Geneva, Switzerland. http://www. who. int/water_sanitation_health/dwq/arsenicun1. pdf, 1-61.

Smedley, P. L., & Kinniburgh, D. G. (2002). A review of the source, behaviour and distribution of arsenic in natural waters. *Applied Geochemistry, 17*, 517-568.

Smedley, P., Edmunds, W. & Pelig-Ba, K. (1996). Mobility of arsenic in groundwater in the Obuasi gold-mining area of Ghana: some implications for human health. *Geological Society, London, Special Publications,* 113**,** 163-181.

Smith, K. S. (1999). Metal sorption on mineral surfaces: an overview with examples relating to mineral deposits. The environmental geochemistry of mineral deposits. *Reviews in Economic Geology,* 6, 161-182.

Smith, A. H., Lingas, E. O., & Rahman, M. (2000). Contamination of drinking-water by arsenic in Bangeladesh: a public health emergency. *Bulletin of the World Health Organization, 78*(9), 1093-1103.

Song, D., Li, Y., Liang, S., & Wang, J. (2013). Micelle behaviors of sophorolipid/rhamnolipid binary mixed biosurfactant systems. *Colloids and Surfaces A: Physicochemical and Engineering Aspects*, *436*, 201-206.

Somasundaran, P. (2006). Encyclopedia of surface and colloid science (Vol. 2). CRC Press.

Stumm, W., Morgan, J. J., & Drever, J. I. (1996). Aquatic chemistry. *Journal of Environmental Quality*, 25(5), 1162.

Takizawa, T., Nakayama, N., Haniu, H., Aoki, K., Okamoto, M., Nomura, H, Tanaka, M., Sobajima, A., Yoshida, K., Kamanaka, T. & Ajima, K. (2017). Titanium Fiber Plates for Bone Tissue Repair. *Advanced Materials*. DOI: https://doi.org/10.1002/adma.201703608

Tessier, A., Campbell, P. G., & Bisson, M. (1979). Sequential extraction procedure for the speciation of particulate trace metals. *Analytical Chemistry*, *51*(7), 844-851.

Theis, T. L. & Singer, P. C. 1974. Complexation of iron (II) by organic matter and its effect on iron (II) oxygenation. *Environmental Science & Technology,* 8**,** 569-573.

US Environmental Protection Agency (USEPA), 1986. Test Methods for Evaluating Solid Waste, Physical/Chemical Methods, EPA Publication SW-846, Method 9081, https://www.epa.gov/sites/production/files/2015-12/documents/9081.pdf (Retrived 2012)

Varade, D., Joshi, T., Aswal, V. K., Goyal, P. S., Hassan, P. A. & Bahadur, P. 2005b. Effect of salt on the micelles of cetyl pyridinium chloride. *Colloids and Surfaces A: Physicochemical and Engineering Aspects,* 259**,** 95-101.

Veizer, J., Hoefs, J., Lowe, D. R., & Thurston, P. C. (1989). Geochemistry of Precambrian carbonates: II. Archean greenstone belts and Archean sea water. *Geochimica et Cosmochimica Acta*, *53*(4), 859-871.

Wagman, D. D., Evans, W. H., Parker, V. B., Schumm, R. H., & Halow, I. (1982). *The NBS tables of chemical thermodynamic properties. Selected values for inorganic and C1 and C2 organic substances in SI units*. National Standard Reference Data System.

Wang, S. (2003). Biosurfactant enhanced remediation of heavy metal contaminated soil (Doctoral dissertation, Concordia University).

Wang, S., & Mulligan, C. N. (2009 a). Arsenic mobilization from mine tailings in the presence of a biosurfactant. *Applied Geochemistry, 24*(5), 928-935.

Wang, S., & Mulligan, C. N. (2009 b). Rhamnolipid biosurfactant-enhanced soil flushing for the removal of arsenic and heavy metals from mine tailings. *Process Biochemistry, 44*(3), 296-301.

Wayland, M. (2004). Mackenzie River Basin: State of the Aquatic Ecosystem Report*, 2003*. [Fort Smith, NWT]: Mackenzie River Basin Board.

Webera, A., Maya, A., Zeiner, T., & Góraka, A. (2012). Downstream processing of biosurfactants. *Chemical Engineering Trans,* 27:115–120.

Weisseborn, P. K., Warren, L. J., & Dunn, J. G. (1995). Selective flocculation of ultrafine iron ore. 1. Mechanism of adsorption of starch onto hematite. *Colloids and Surfaces A: Physicochemical and Engineering Aspects*, *99*(1), 11-27.

Wentworth, C. K. (1922). A scale of grade and class terms for clastic sediments. *The Journal of Geology*, *30*(5), 377-392.

Wu, X., Xu, L. Y., Zhang, X. X., Song, Y., Wang, X., & Jia, Y. F. (2012). Speciation transformation and behavior of arsenic in soils under anoxic conditions. *Huan jing ke xue= Huanjing kexue*, *33*(1), 273-279.

Wu, S. C., Cheung, K. C., Luo, Y. M. & Wong, M. H. 2006. Effects of inoculation of plant growth-promoting rhizobacteria on metal uptake by *Brassica juncea*. *Environmental Pollution,* 140**,** 124-135.

Yong, R. N., Galvez-Cloutier, R., & Phadungchewit, Y. (1993). Selective sequential extraction analysis of heavy-metal retention in soil. *Canadian Geotechnical Journal*, 30(5), 834-847.

Yong, R. N., Mulligan, C. N. & Fukue, M. 2014. Sustainable Practices in Geoenvironmental Engineering, Second Edition, CRC Press.

Yu, H. Y., Li, F. B., Liu, C. S., Huang, W., Liu, T. X., & Yu, W. M. (2016). Chapter Five-Iron Redox Cycling Coupled to Transformation and Immobilization of Heavy Metals: Implications for Paddy Rice Safety in the Red Soil of South China. *Advances in Agronomy*, *137*, 279-317.

Zhou, S., Xu, C., Wang, J., Gao, W., Akhverdiyeva, R., Shah, V., & Gross, R. (2004). Supramolecular assemblies of a naturally derived sophorolipid. *Langmuir*, *20*(19), 7926-7932.

APPENDICES

APPENDIX I

RESULT OF THE SPECIATION OF ARSENIC FROM MINE TAILING

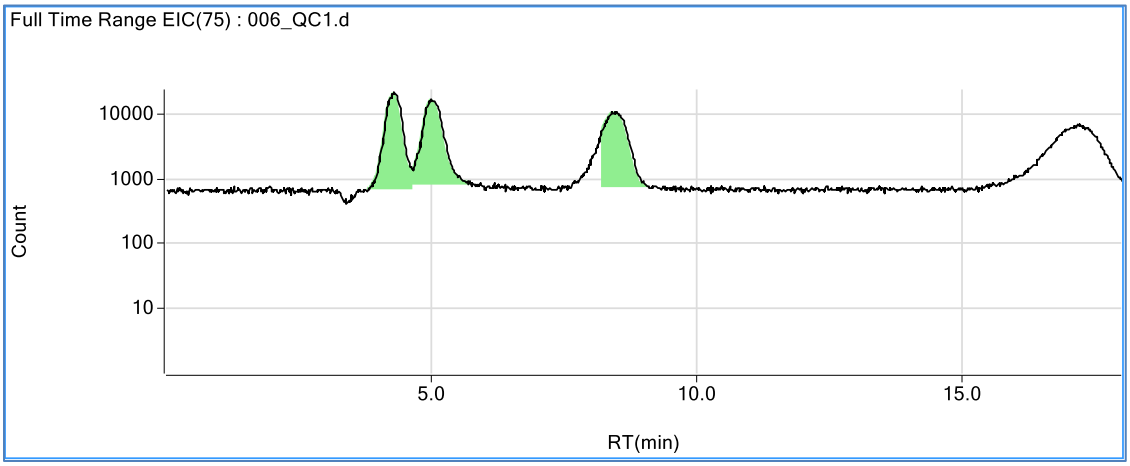

Chromatogram of the mine tailings extracted by 1% rhamnolipids at pH 11.

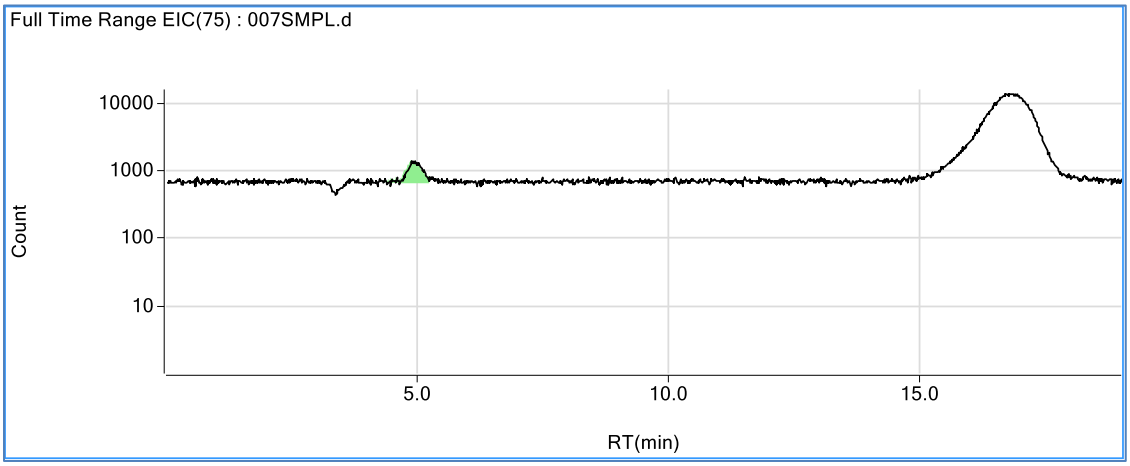

Chromatogram of the mine tailings extracted by 0.1% sophorolipids (no pH adjustment).

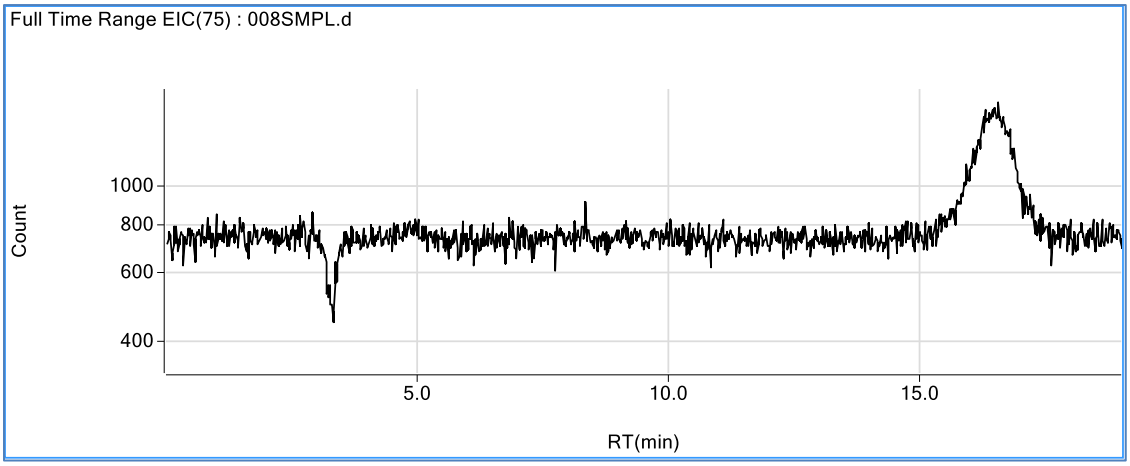

Chromatogram of the mine tailings extracted by 1% rhamnolipids (no pH adjustment).

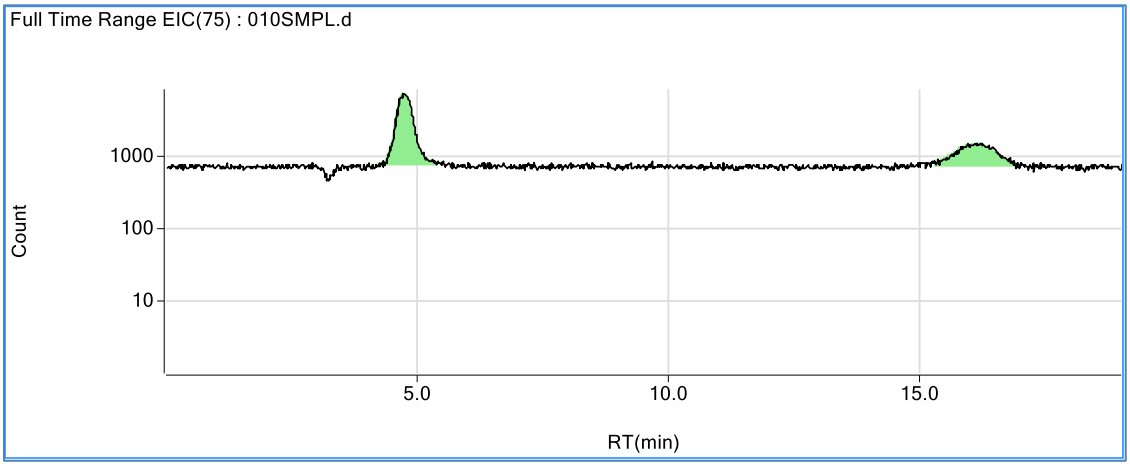

Chromatogram of the mine tailings extracted by 1% sophorolipids (no pH adjustment).

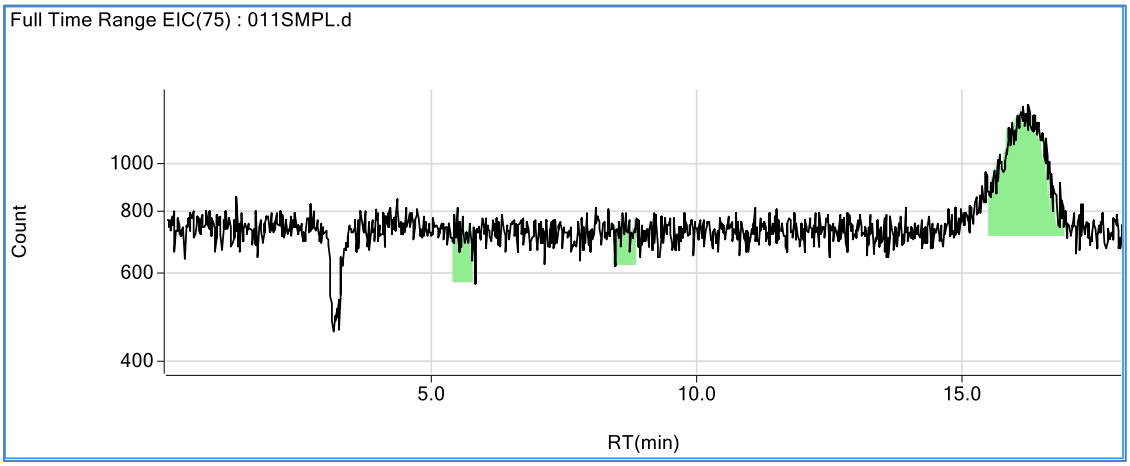

Chromatogram of the mine tailings extracted by distilled water at pH 11

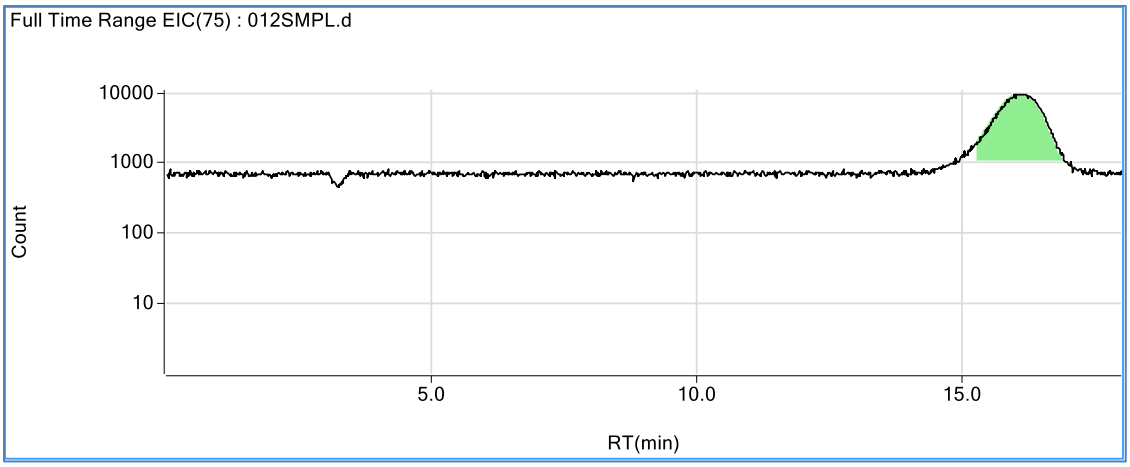

Chromatogram of the mine tailings extracted by distilled water (no pH adjustment).

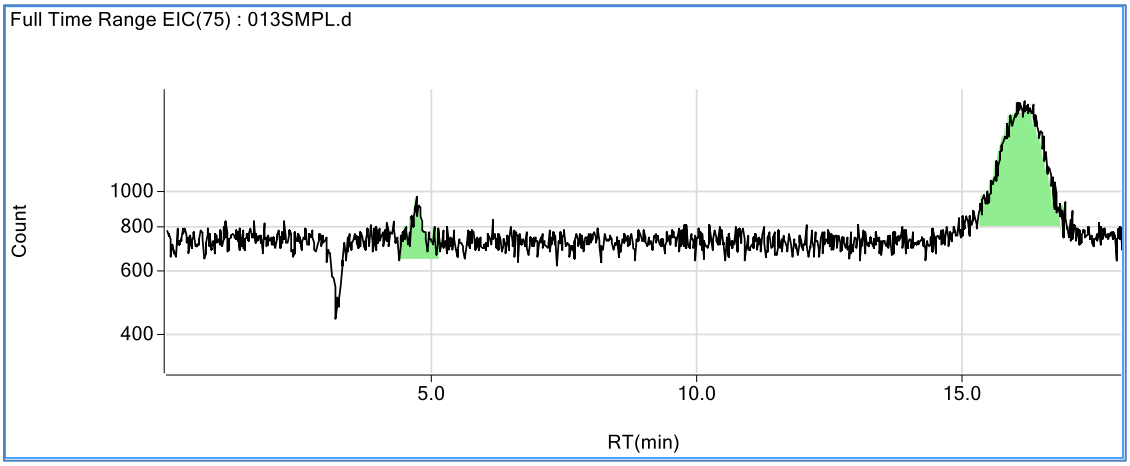

Chromatogram of the mine tailings extracted by 0.1% rhamnolipids (no pH adjustment).

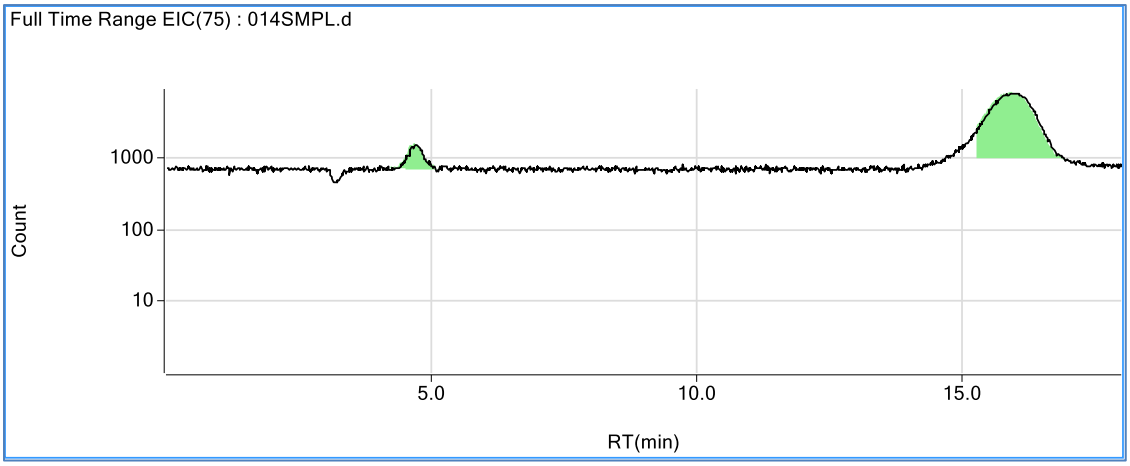

Chromatogram of the mine tailings extracted by, sophorolipids (no pH adjustment).

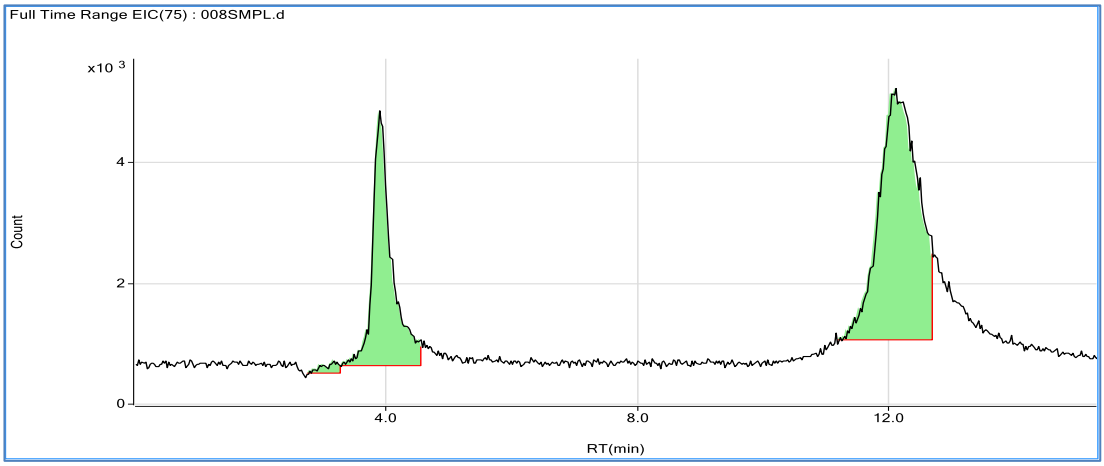

Chromatogram of the mine tailings extracted by 1% sophorolipid at pH 4 (1).

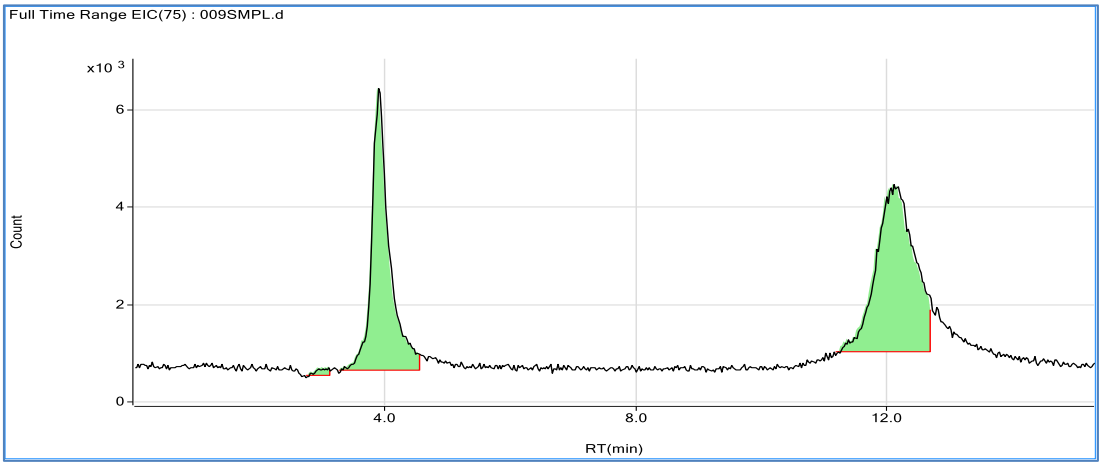

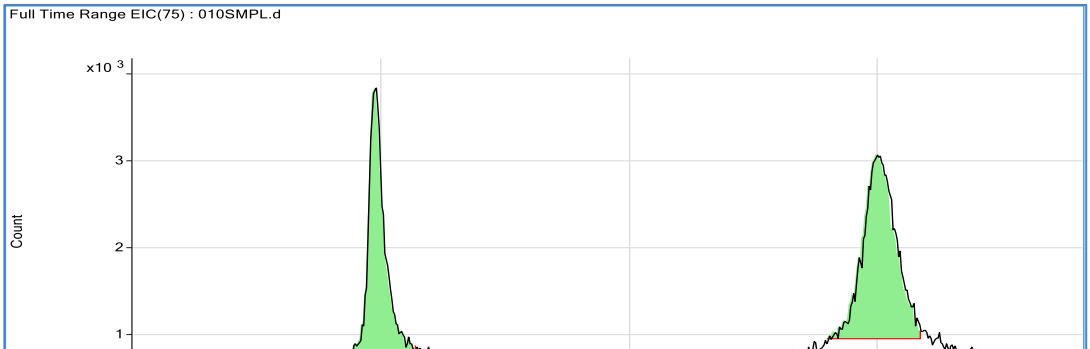

Chromatogram of the mine tailings extracted by 1% sophorolipid at pH 6 (1).

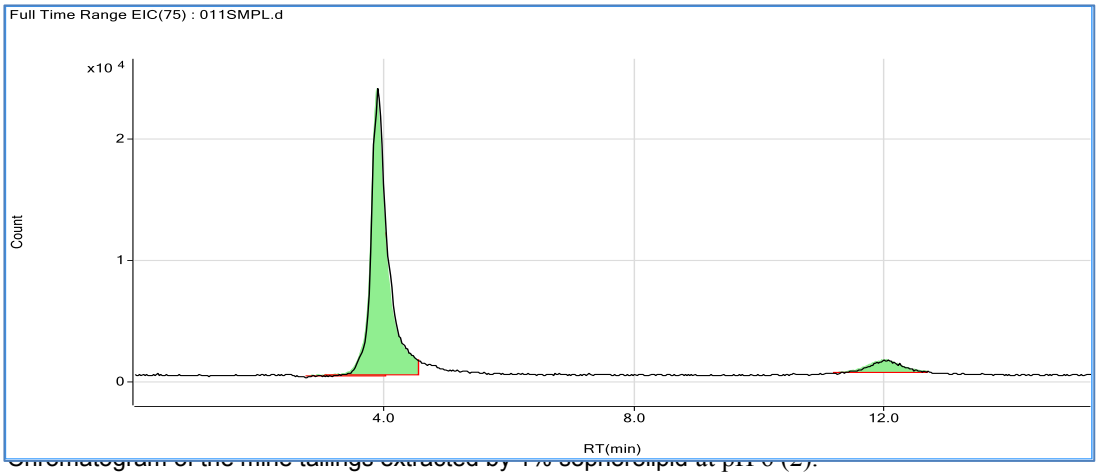

Chromatogram of the mine tailings extracted by 1% sophorolipid at pH 6 (2).

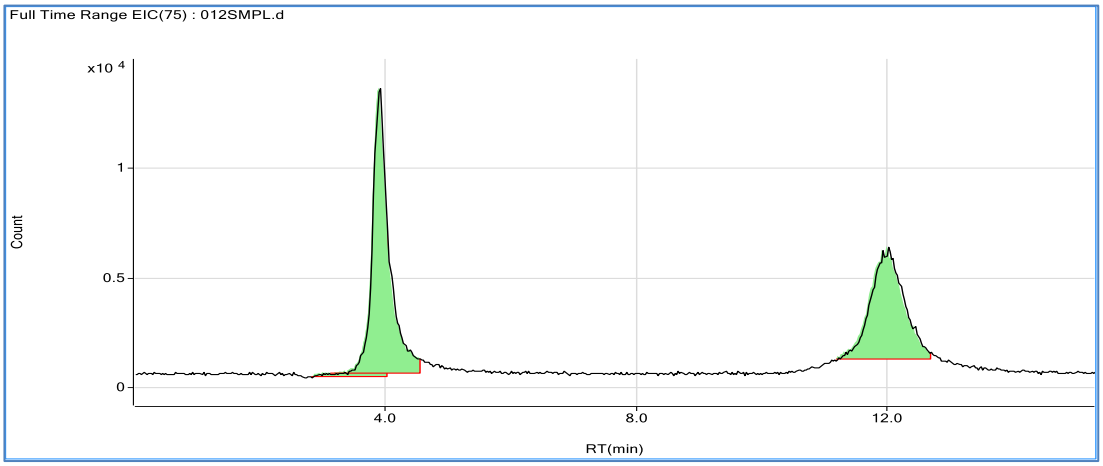

Chromatogram of the mine tailings extracted by 1% sophorolipid at pH 10 (1).

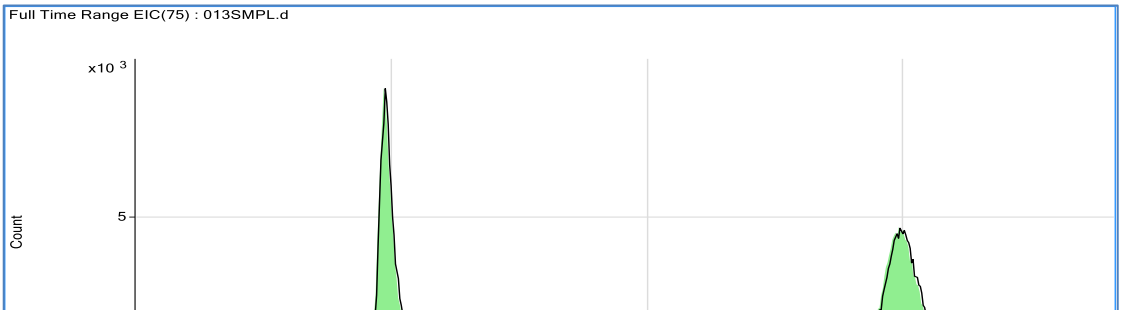

Chromatogram of the mine tailings extracted by 1% sophorolipid at pH 10 (2).

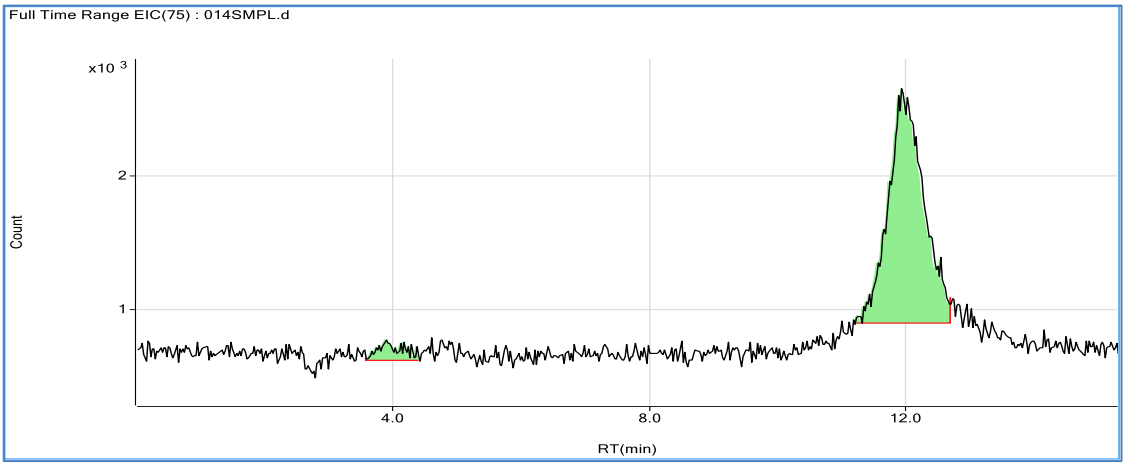

Chromatogram of the mine tailings extracted by deionized water at pH 6 (1).

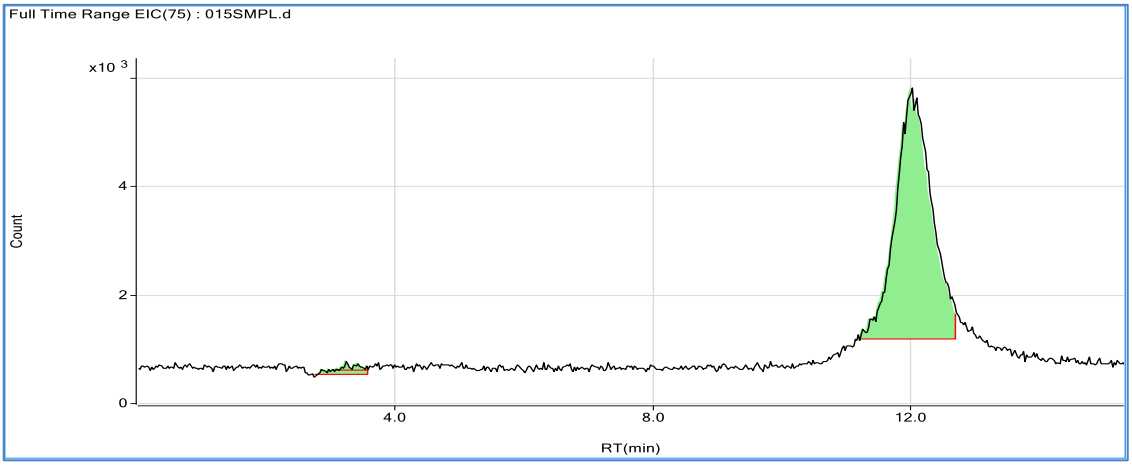

Chromatogram of the mine tailings extracted by deionized water at pH 6 (1).

APPENDIX II

SEM ANALYSIS

Project 1: Untreated mine tailing sample

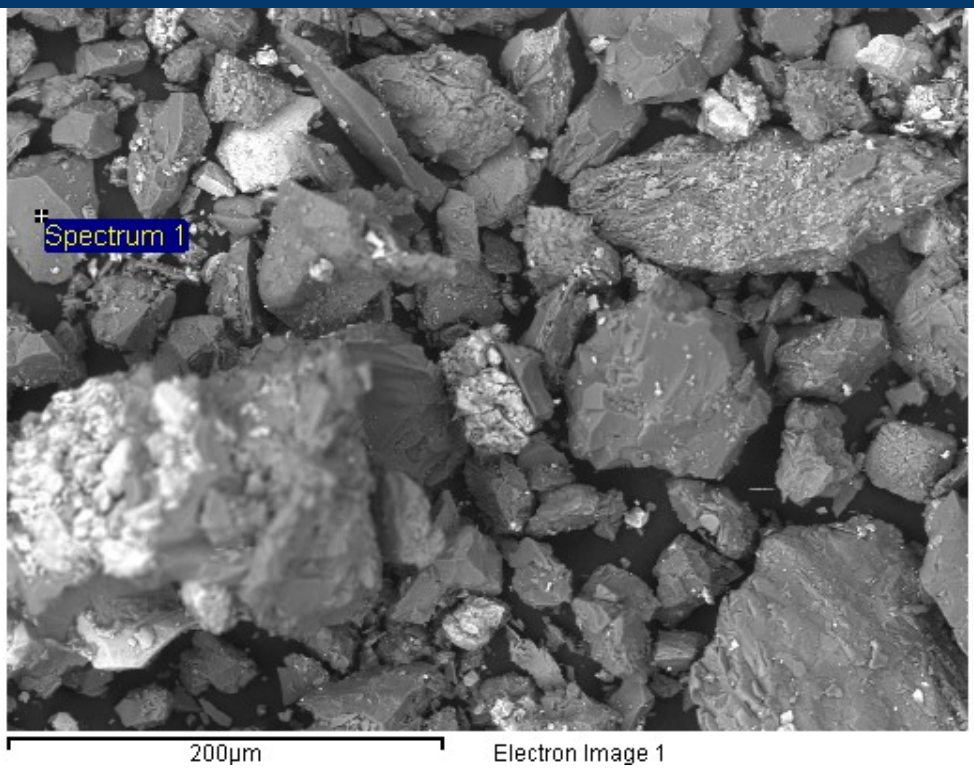

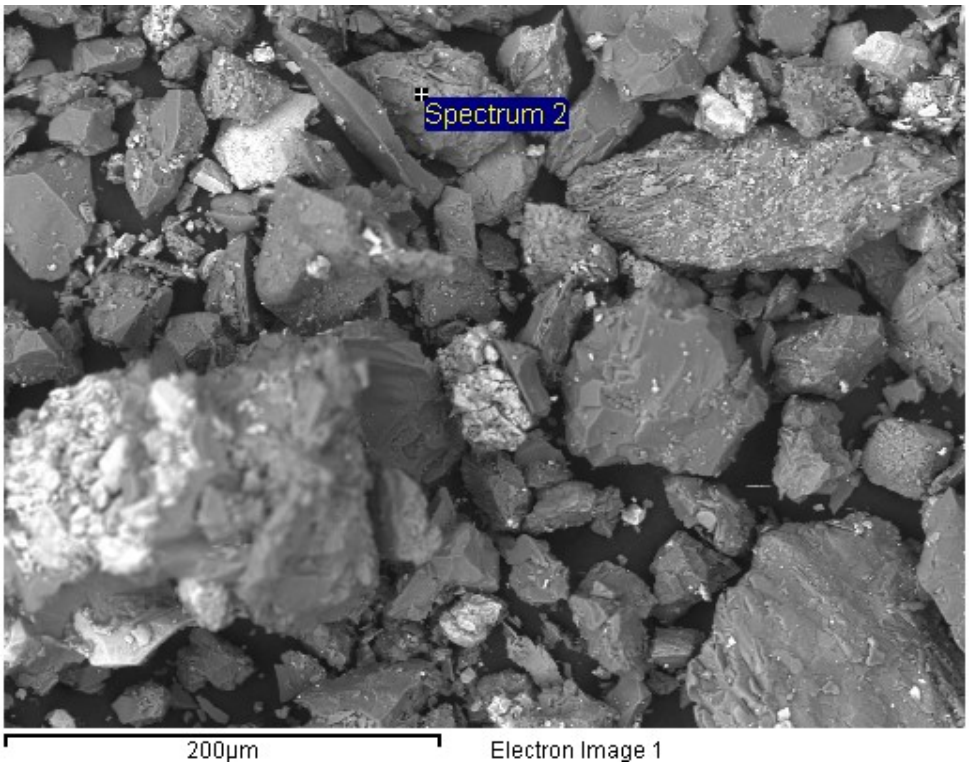

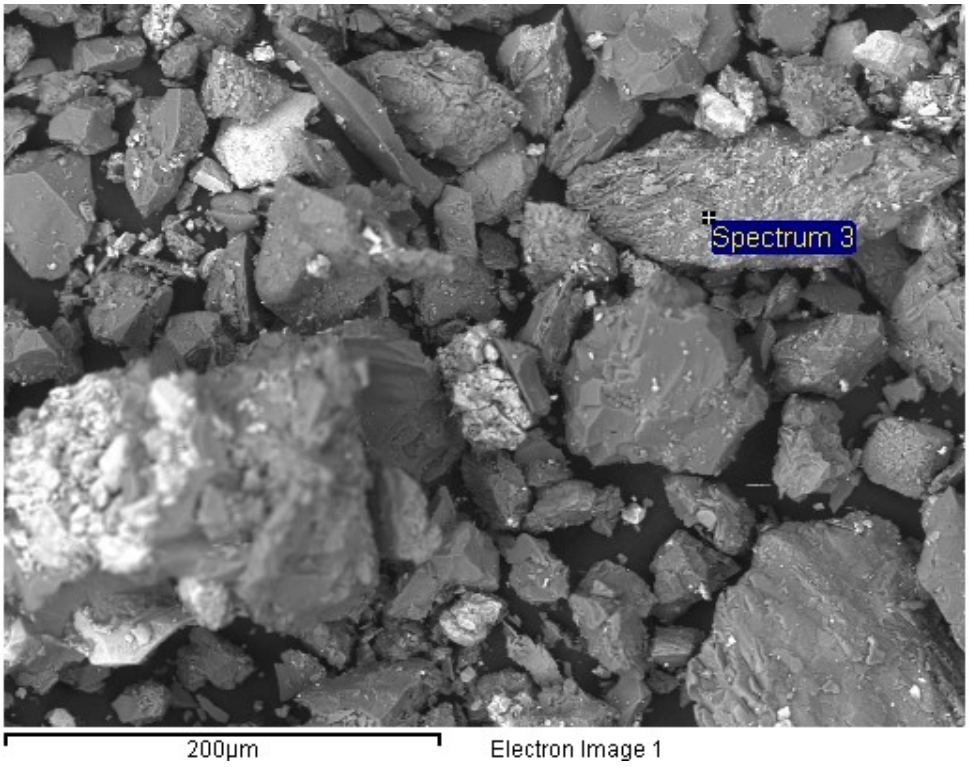
Spectrum 3
200µm
Electron Image 1

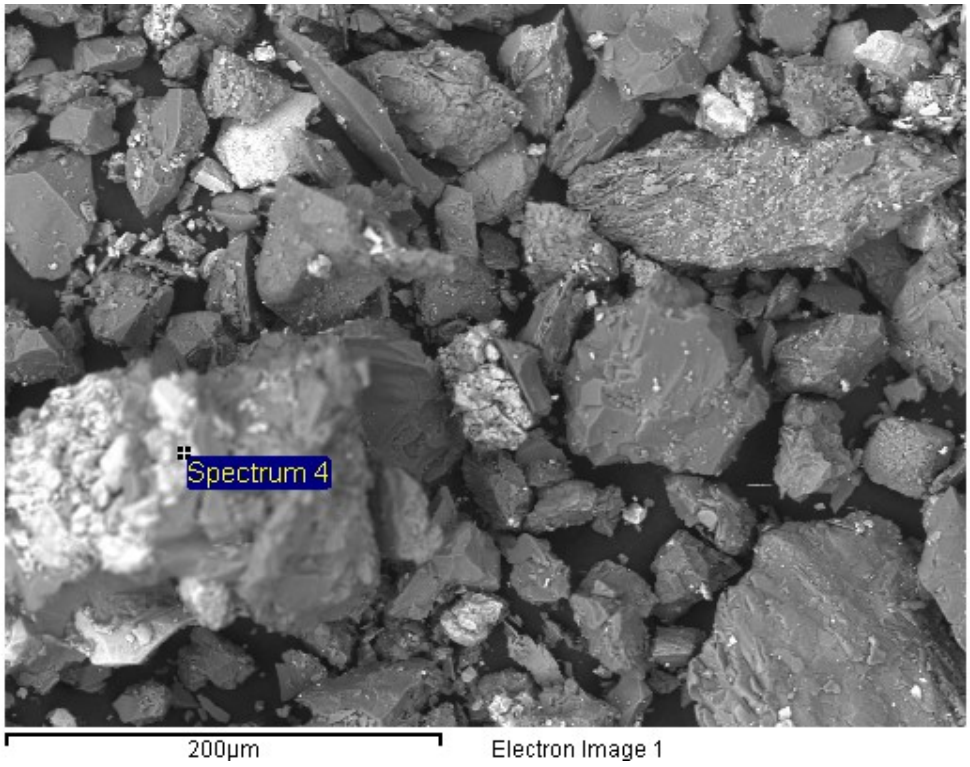
Spectrum 4
200µm
Electron Image 1

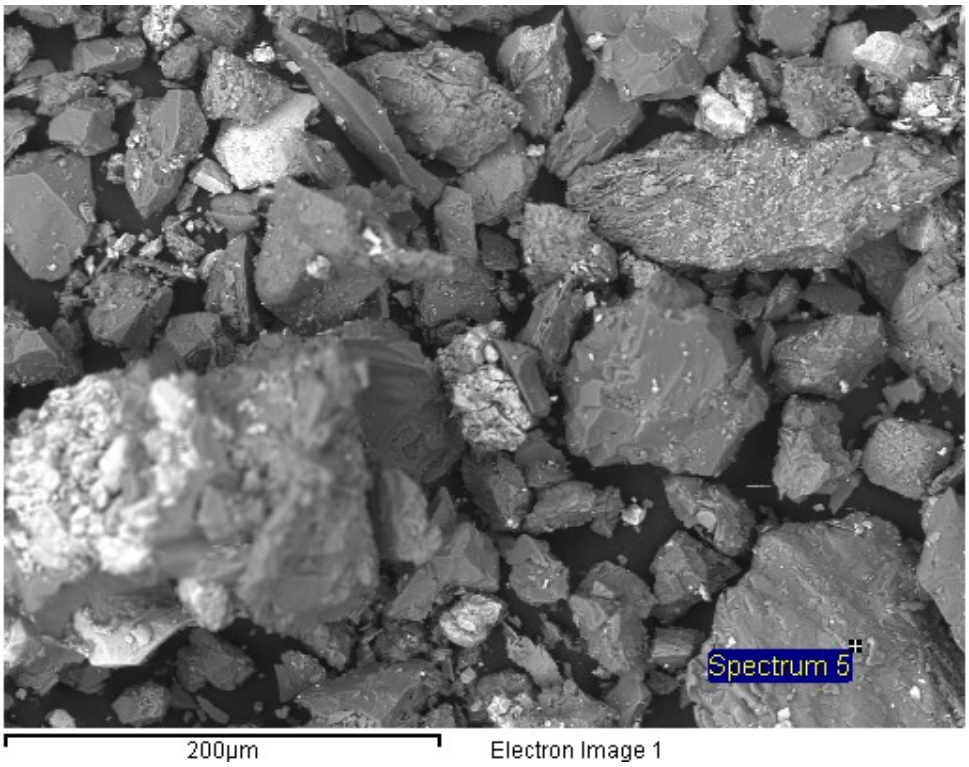
Spectrum 5
200µm
Electron Image 1

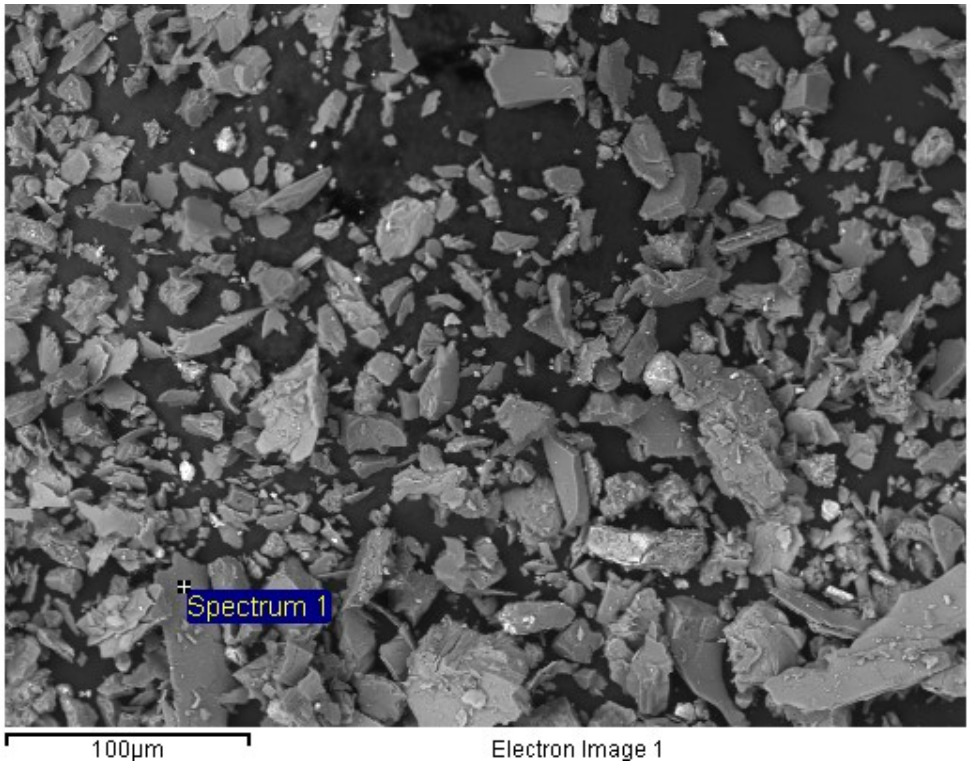
Spectrum 1
100µm
Electron Image 1

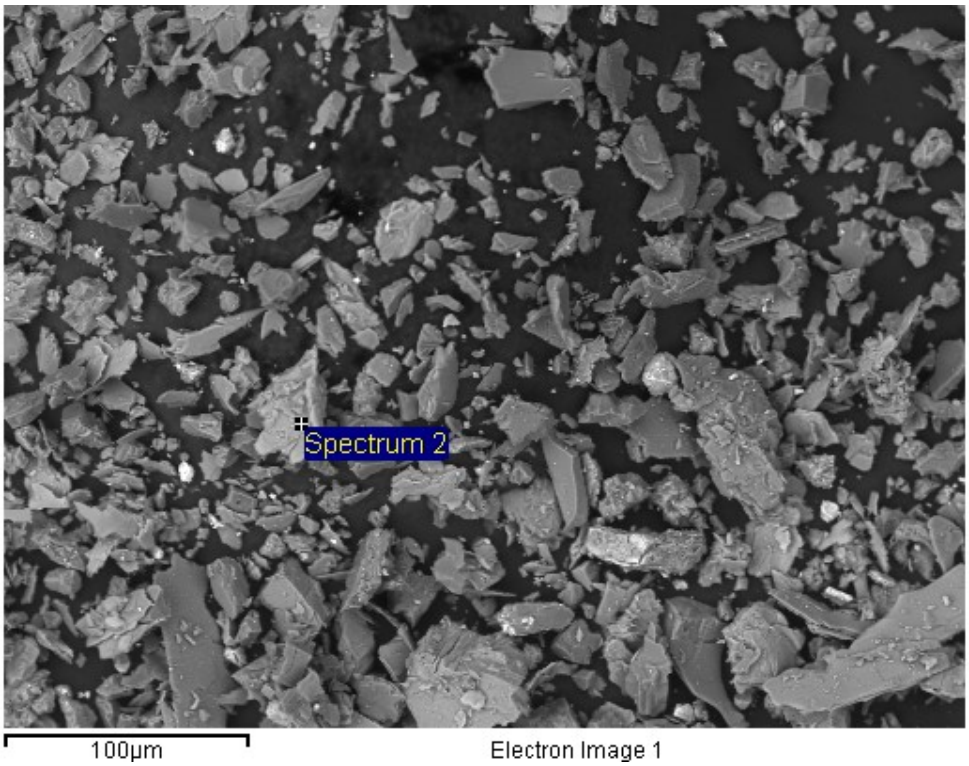
Spectrum 2
100µm
Electron Image 1

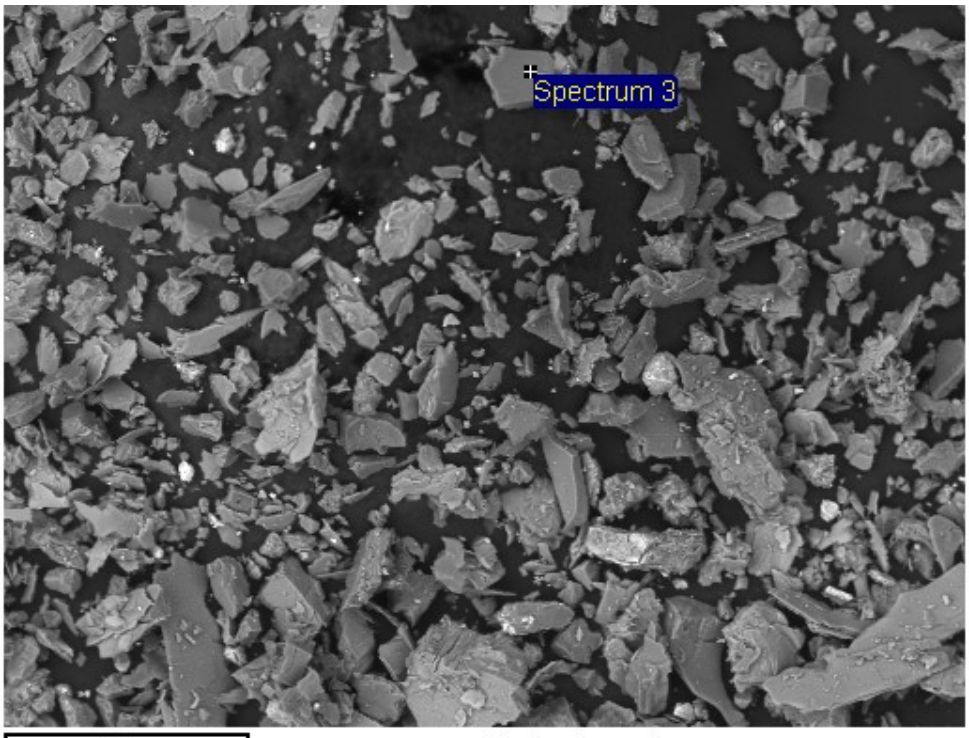
Spectrum 3
100µm
Electron Image 1

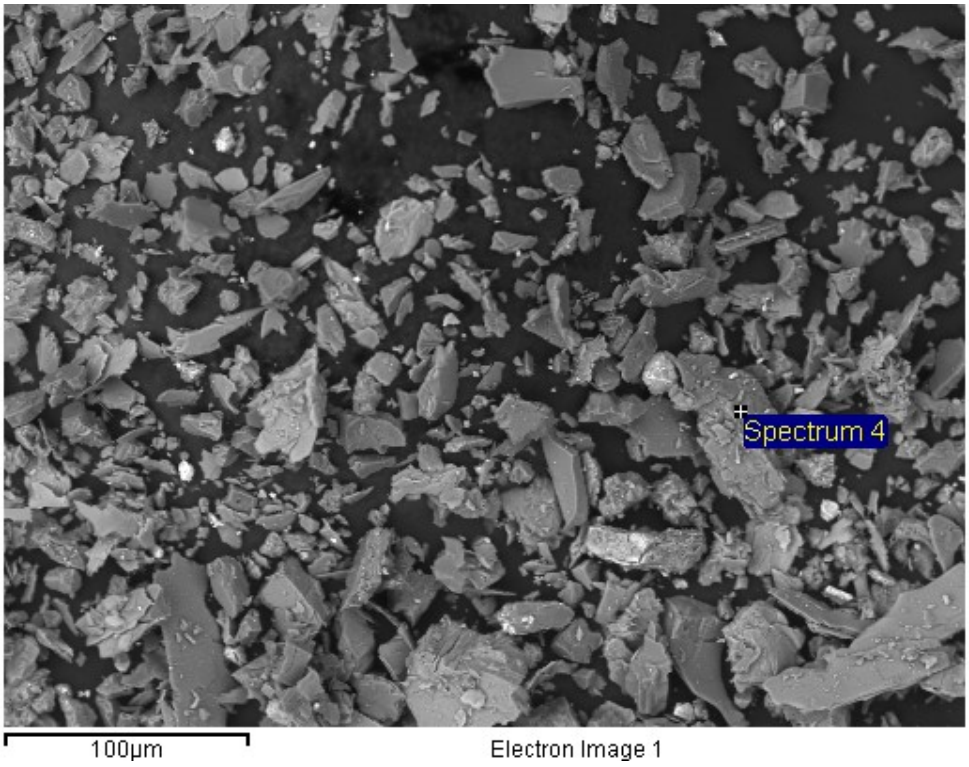
Spectrum 4
100µm
Electron Image 1

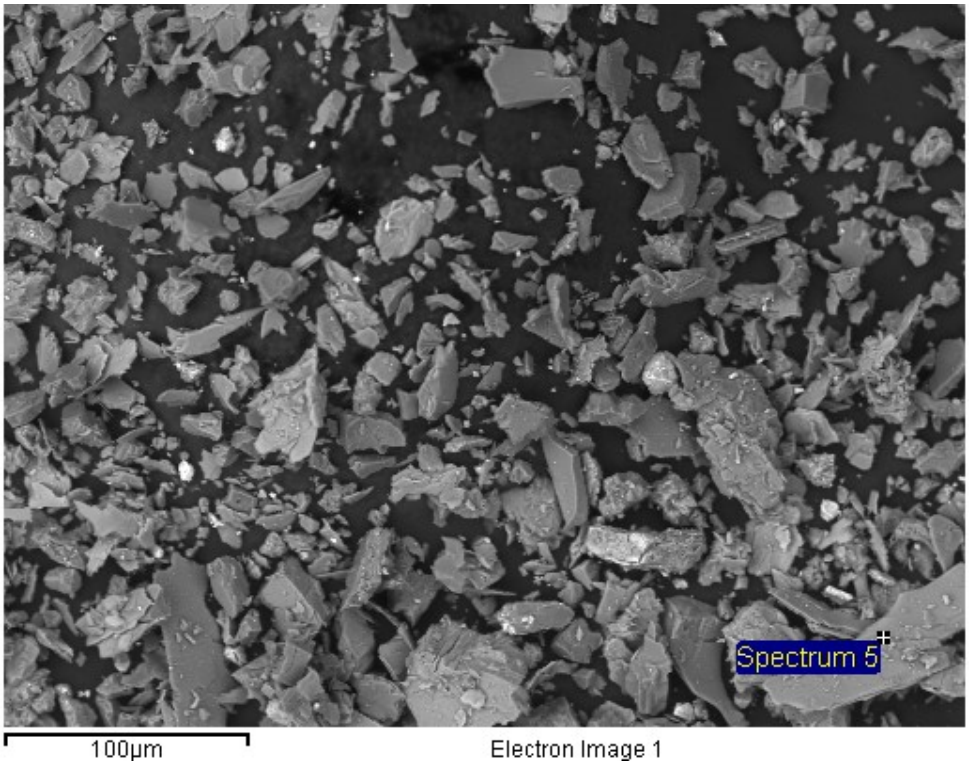
Spectrum 5
100µm
Electron Image 1

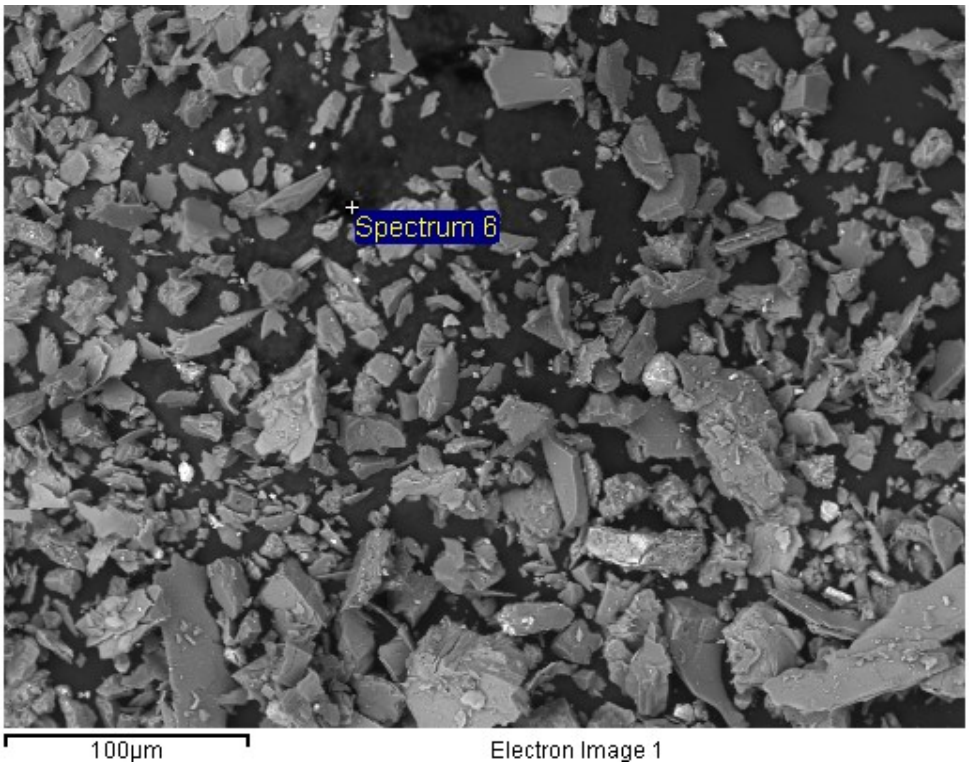
Spectrum 6
100µm
Electron Image 1

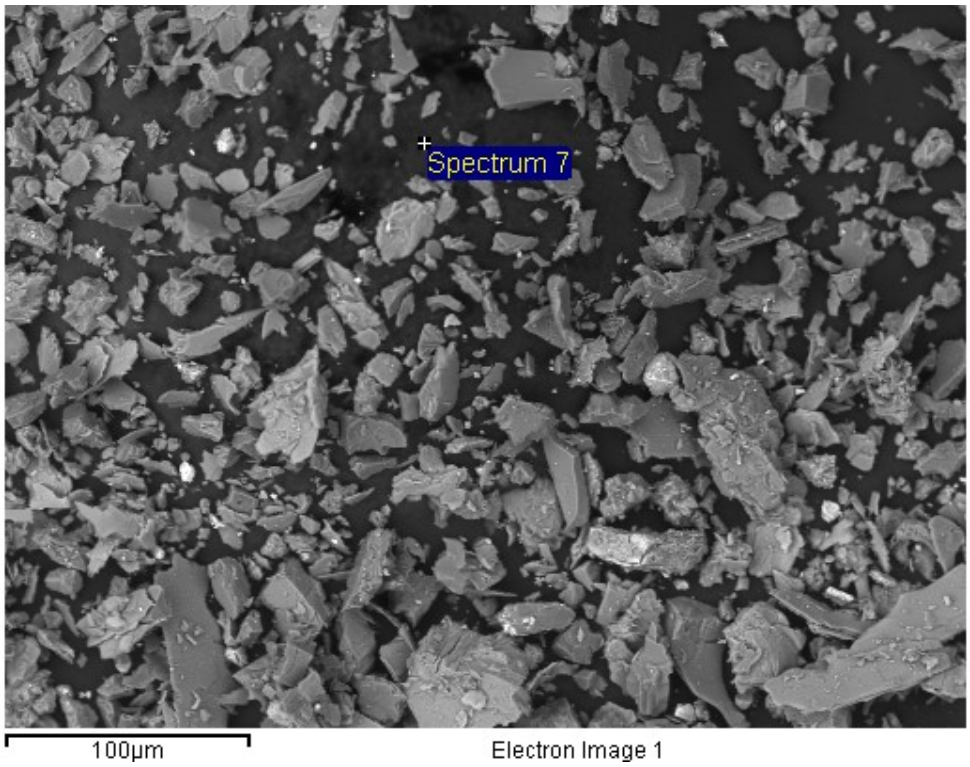
Spectrum 7
100µm
Electron Image 1

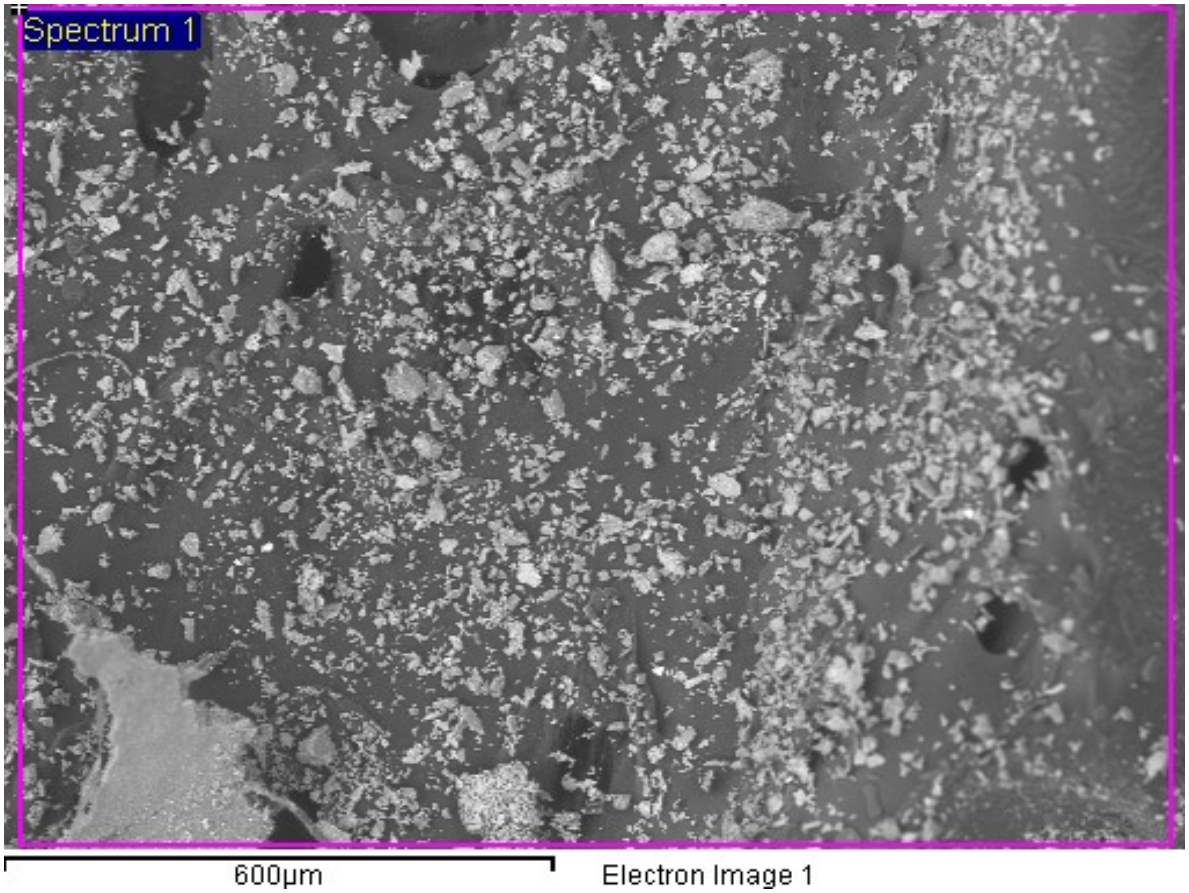

Processing option : All elements analysed (Normalised)

Spectrum	In stats.	Mg	Al	Si	K	Ca	Fe	As	Total
Spectrum 1	Yes	6.14	17.42	41.56	4.29	9.51	20.60	0.50	100.00
Mean		6.14	17.42	41.56	4.29	9.51	20.60	0.50	100.00
Std. deviation		0.00	0.00	0.00	0.00	0.00	0.00	0.00	
Max.		6.14	17.42	41.56	4.29	9.51	20.60	0.50	
Min.		6.14	17.42	41.56	4.29	9.51	20.60	0.50	

All results in weight%

SL 0.5%

8/6/2014 1:08:00 PM

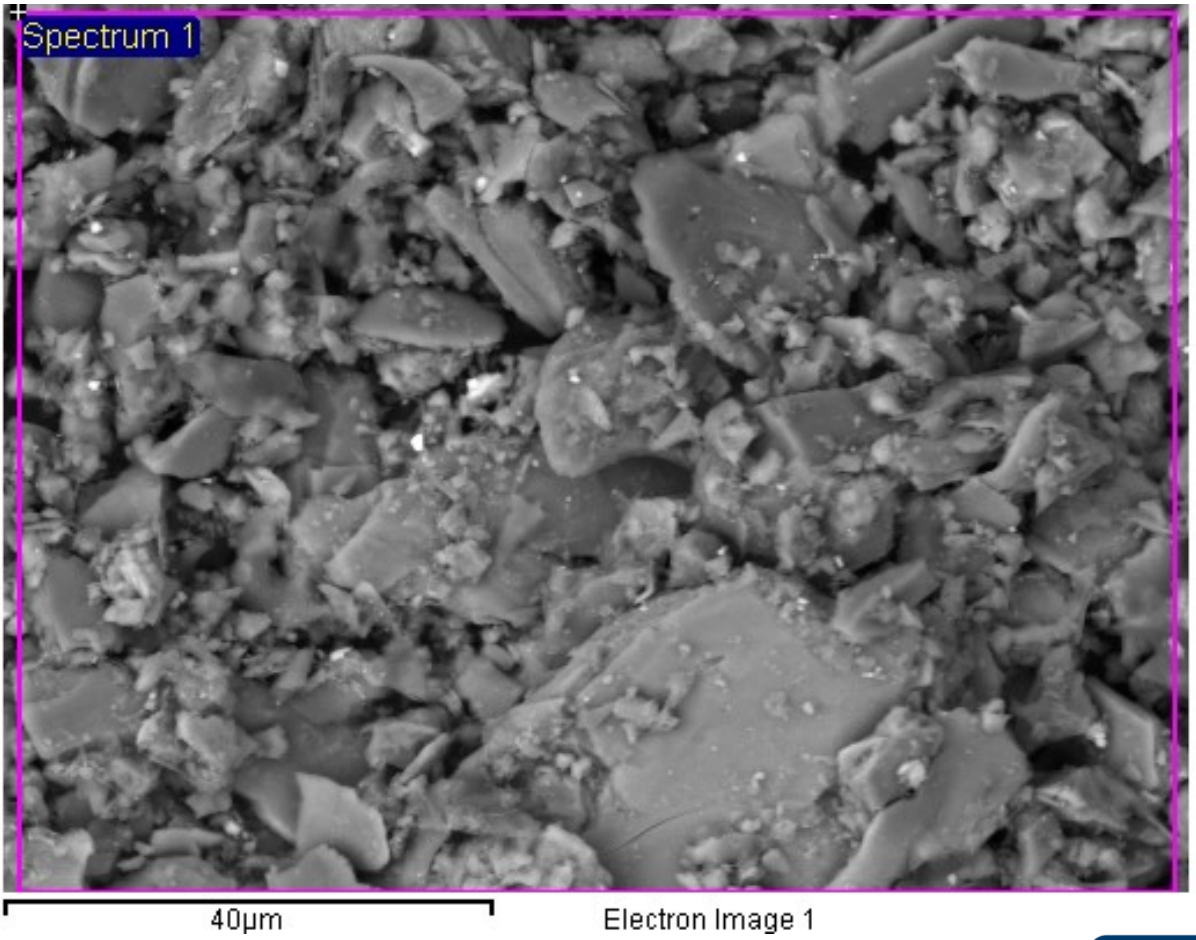

SL 0.5%

8/6/2014 1:10:16 PM

Spectrum processing :

Peak possibly omitted : 2.626 keV

Processing option : All elements analyzed (Normalised)

Number of iterations = 3

Standard :

Na Albite 1-Jun-1999 12:00 AM

Mg MgO 1-Jun-1999 12:00 AM

Al Al2O3 1-Jun-1999 12:00 AM

Si SiO2 1-Jun-1999 12:00 AM

K MAD-10 Feldspar 1-Jun-1999 12:00 AM

Ca Wollastonite 1-Jun-1999 12:00 AM

Ti Ti 1-Jun-1999 12:00 AM

Fe Fe 1-Jun-1999 12:00 AM

As InAs 1-Jun-1999 12:00 AM

Element	Weight%	Atomic%
Na K	1.05	1.46
Mg K	6.70	8.83
Al K	15.71	18.64
Si K	42.50	48.45
K K	4.47	3.66
Ca K	8.46	6.76
Ti K	1.31	0.87
Fe K	19.73	11.31
As L	0.07	0.03
Totals	100.00	

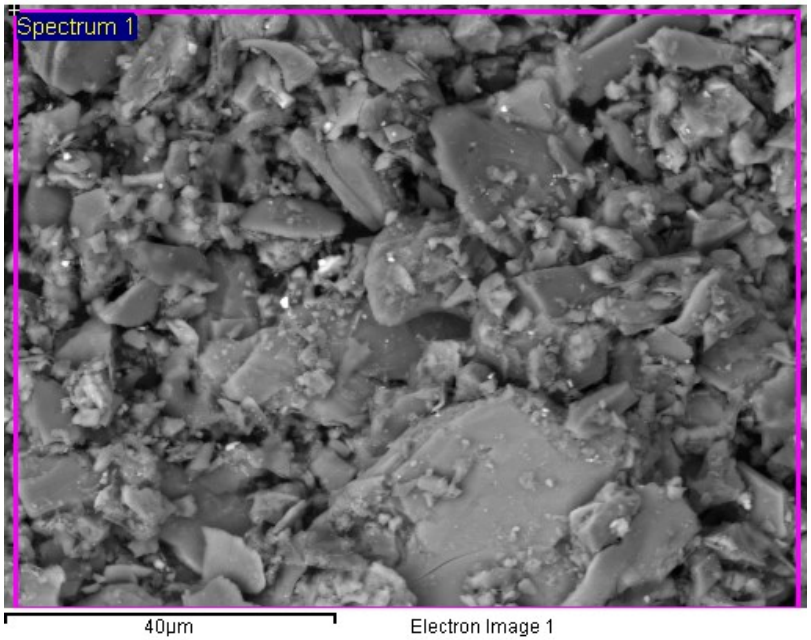

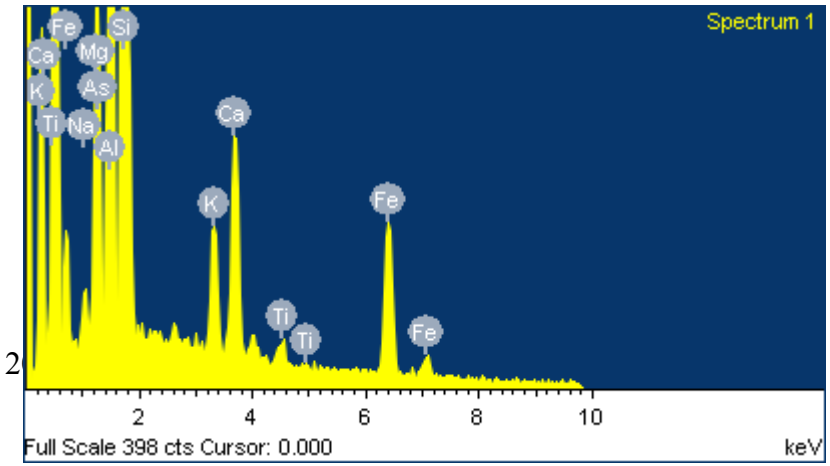

Comment:

SL 0.5%

8/6/2014 1:11:39 PM

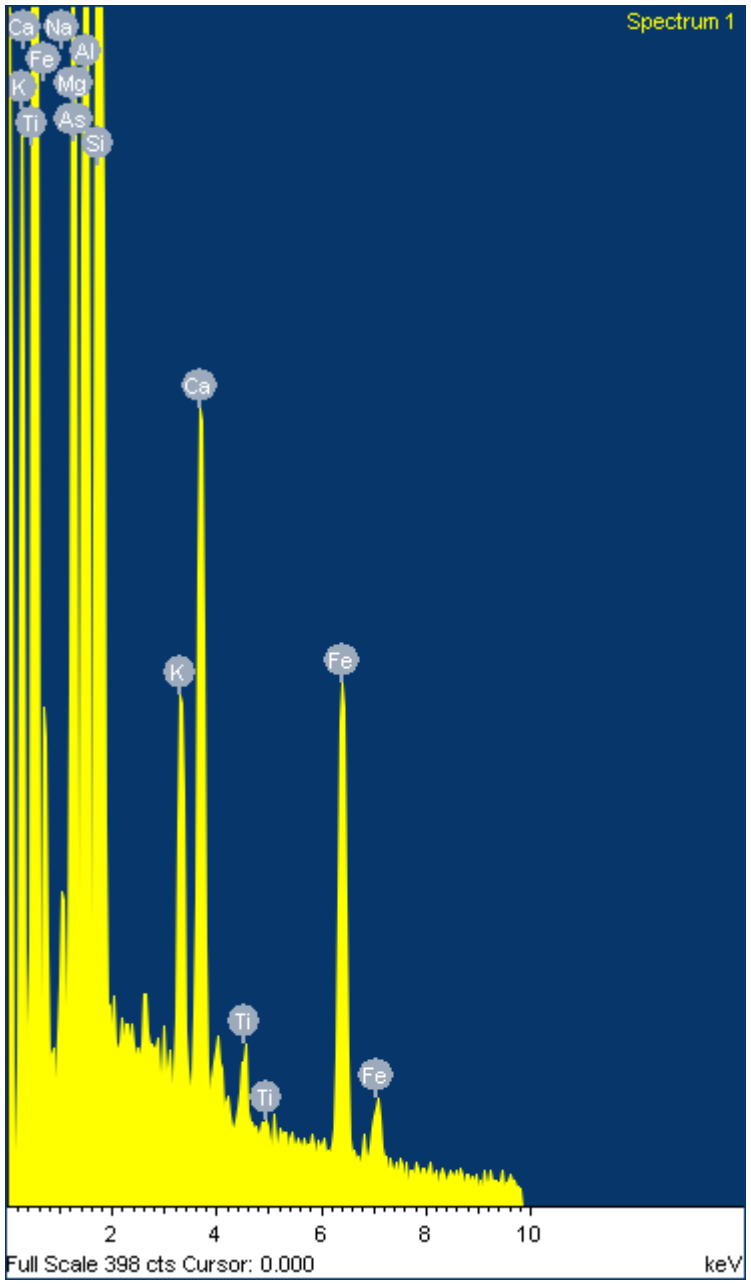

Quantitative results

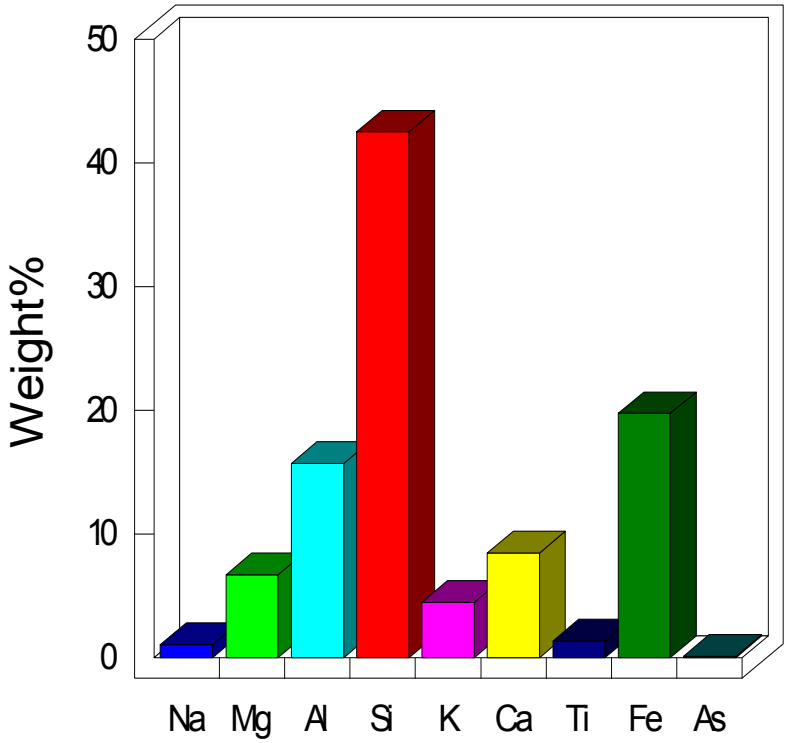

Comment:

INCA

SL 1%

8/6/2014 1:13:29 PM

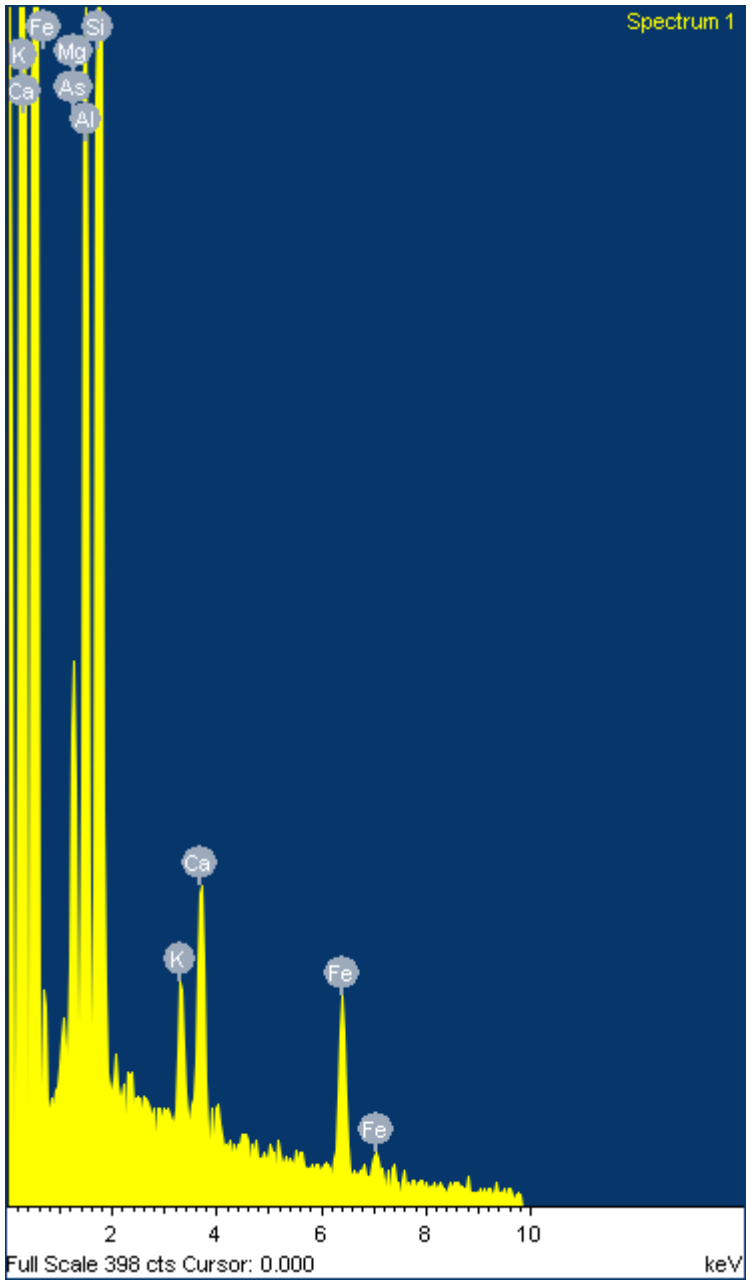

Quantitative results

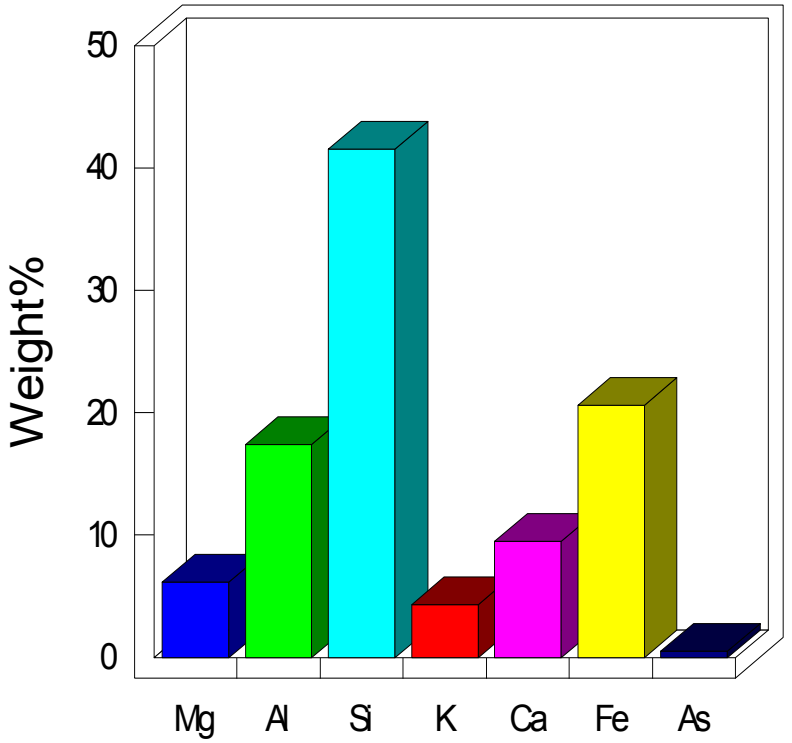

Comment:

DI WATER

8/6/2014 1:22:05 PM

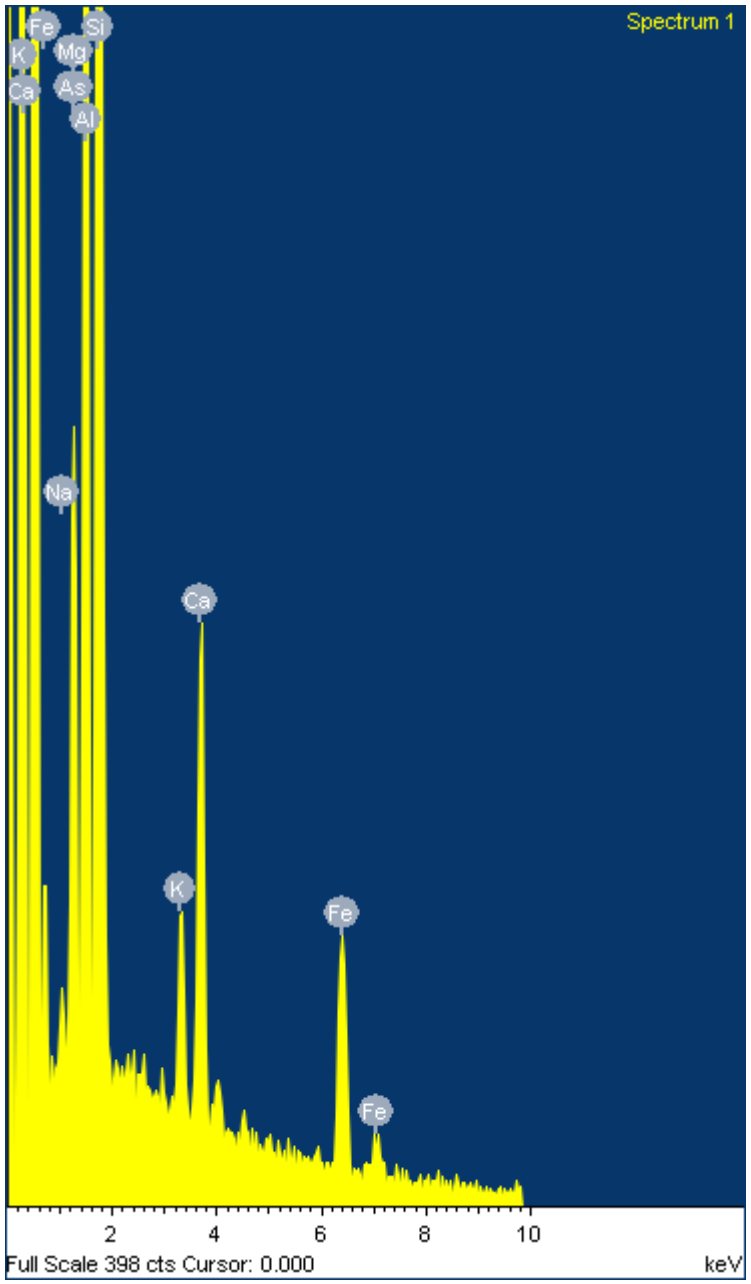

Quantitative results

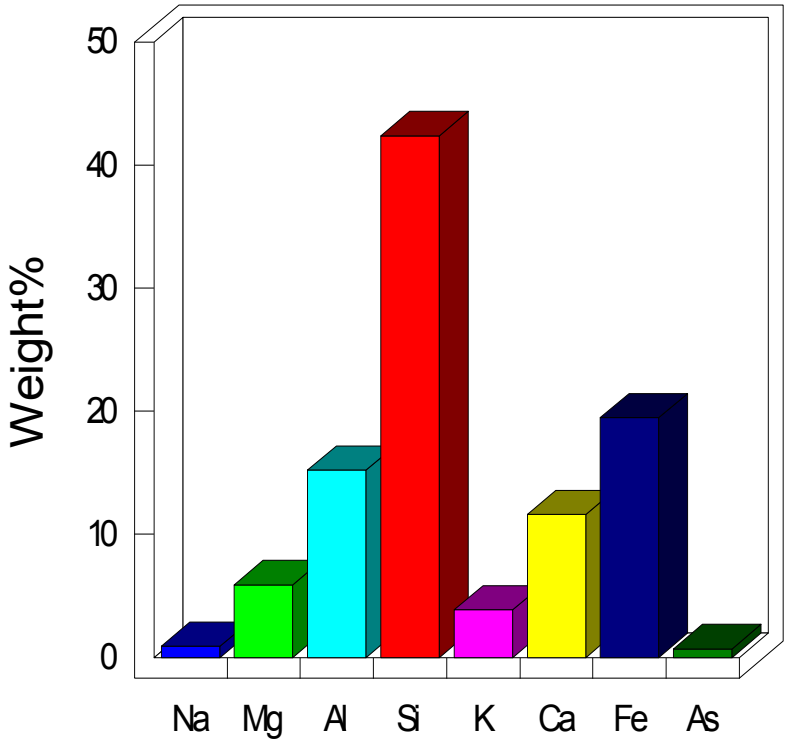

Comment:

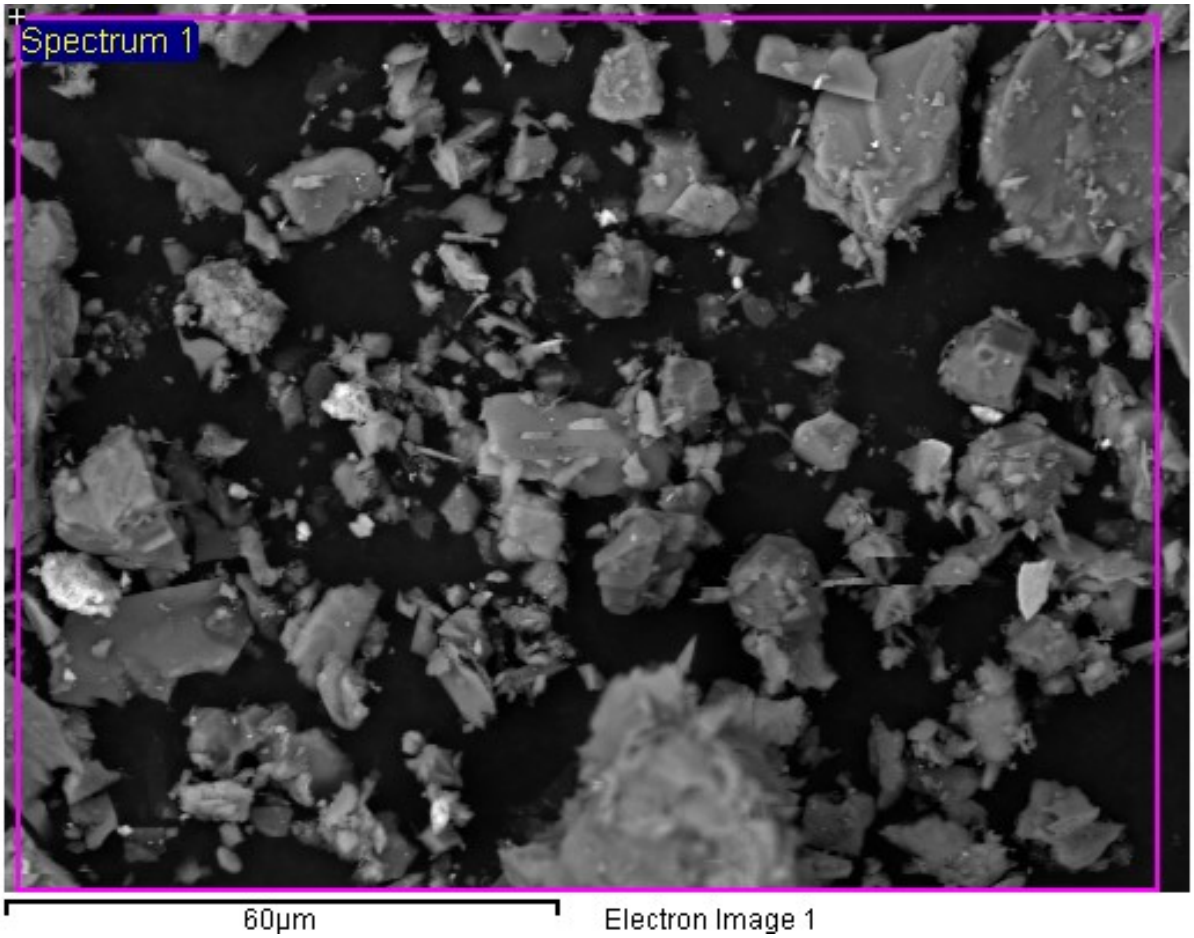

Processing option : All elements analysed (Normalised)

Spectrum	In stats.	Na	Mg	Al	Si	K	Ca	Fe	As	Total
Spectrum 1	Yes	0.89	5.90	15.22	42.37	3.85	11.60	19.48	0.69	100.00
Mean		0.89	5.90	15.22	42.37	3.85	11.60	19.48	0.69	100.00
Std. deviation		0.00	0.00	0.00	0.00	0.00	0.00	0.00	0.00	
Max.		0.89	5.90	15.22	42.37	3.85	11.60	19.48	0.69	
Min.		.89	.90	5.22	2.37	.85	1.60	9.48	.69	

All results in weight%

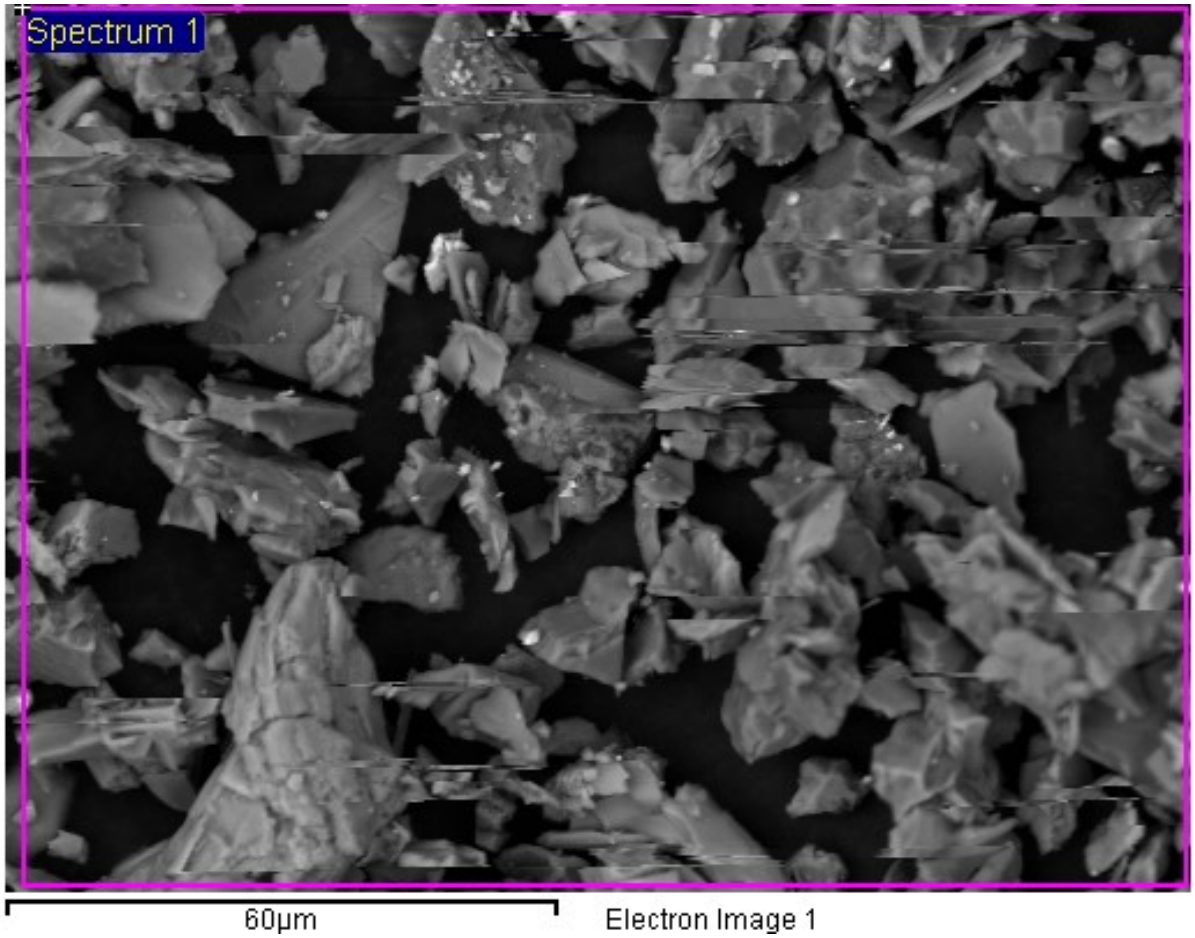

Spectrum processing :

No peaks omitted

Processing option : All elements analyzed (Normalised)

Number of iterations = 3

Standard :

Na Albite 1-Jun-1999 12:00 AM

Mg MgO 1-Jun-1999 12:00 AM

Al Al2O3 1-Jun-1999 12:00 AM

Si SiO2 1-Jun-1999 12:00 AM

K MAD-10 Feldspar 1-Jun-1999 12:00 AM

Ca Wollastonite 1-Jun-1999 12:00 AM

Ti Ti 1-Jun-1999 12:00 AM

Fe Fe 1-Jun-1999 12:00 AM

As InAs 1-Jun-1999 12:00 AM

Comment:

Element	Weight%	Atomic%
Na K	1.05	1.46
Mg K	4.60	6.05
Al K	13.20	15.66
Si K	48.11	54.80
K K	3.69	3.02
Ca K	9.14	7.30
Ti K	2.29	1.53
Fe K	17.35	9.94
As L	0.57	0.24
Totals	100.00	

H_2O_2 50µM

8/6/2014 1:30:10 PM

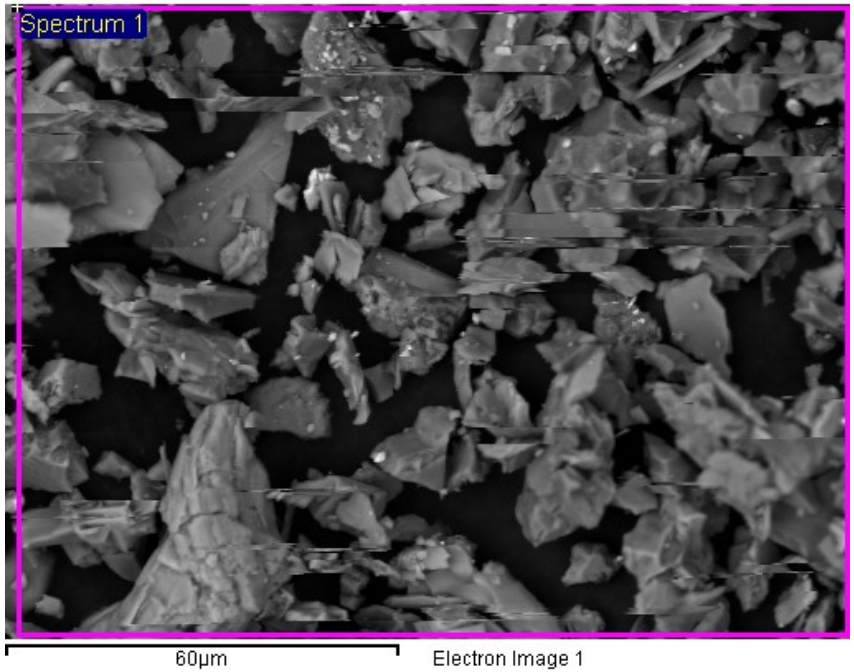

Quantitative results

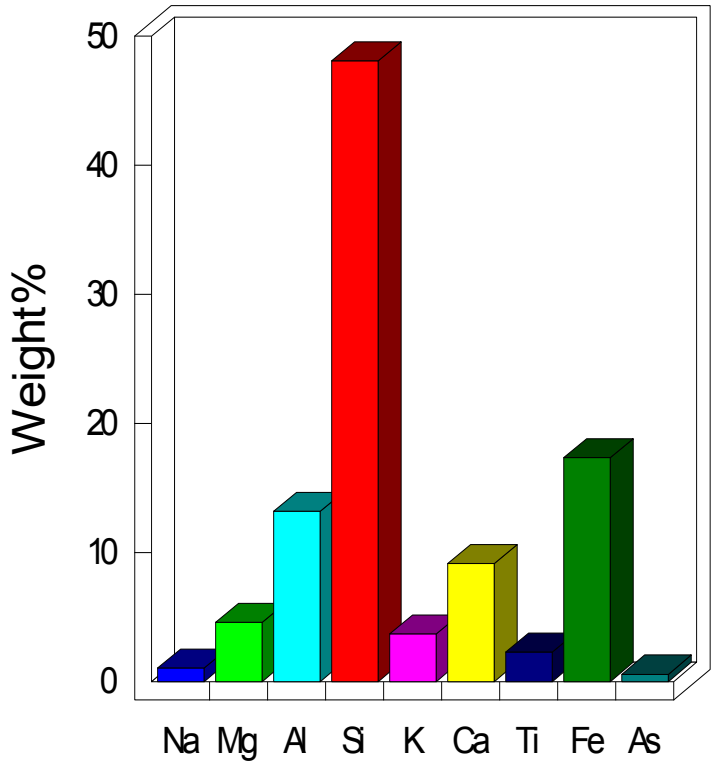

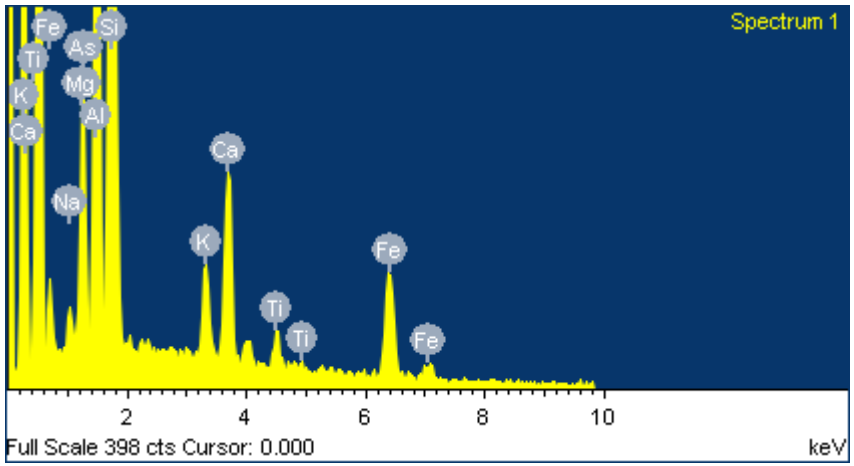

2

Comment:

inca

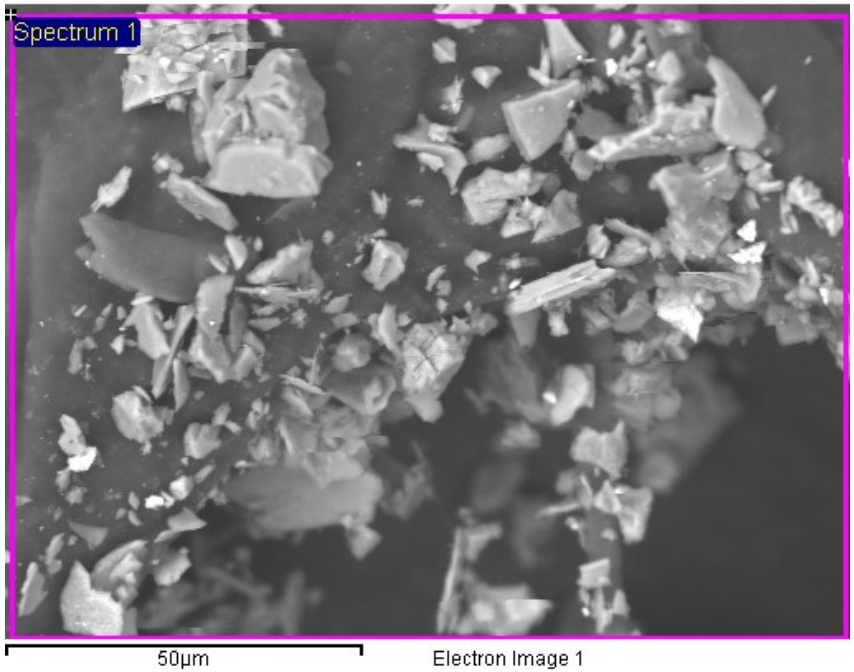

Quantitative results

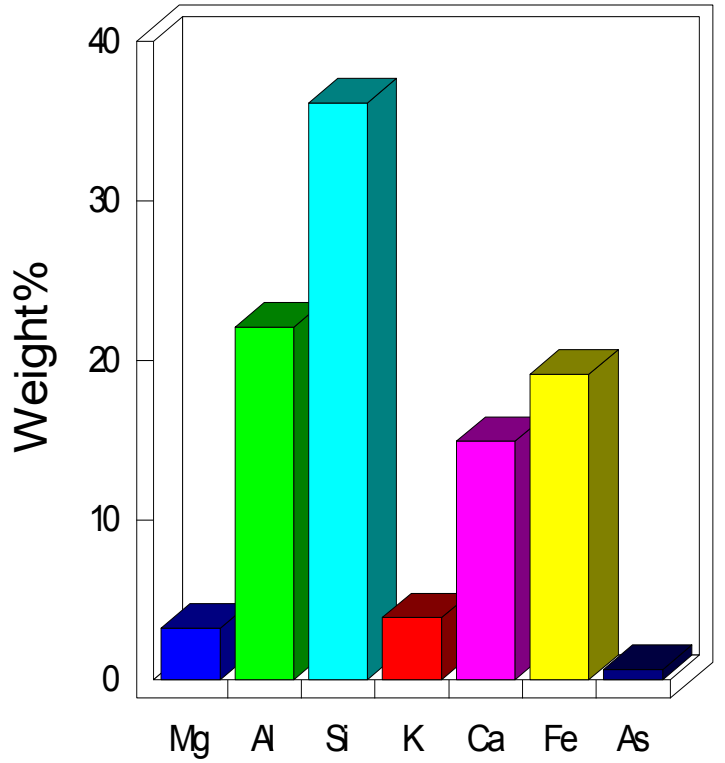

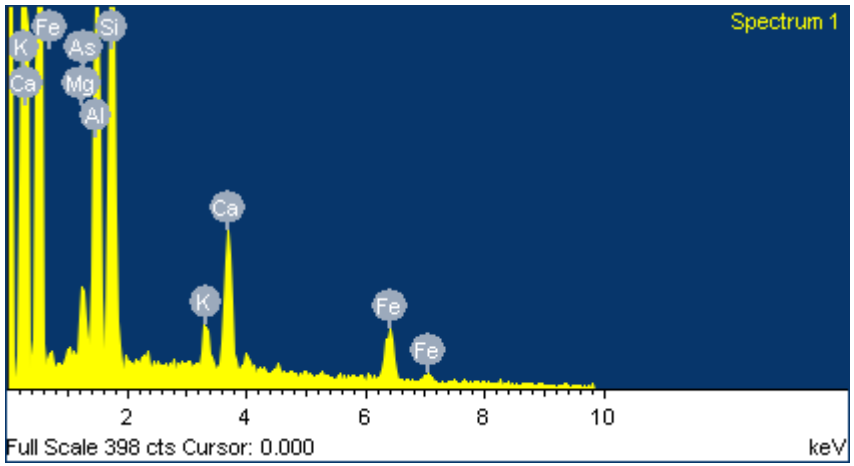

2

Comment:

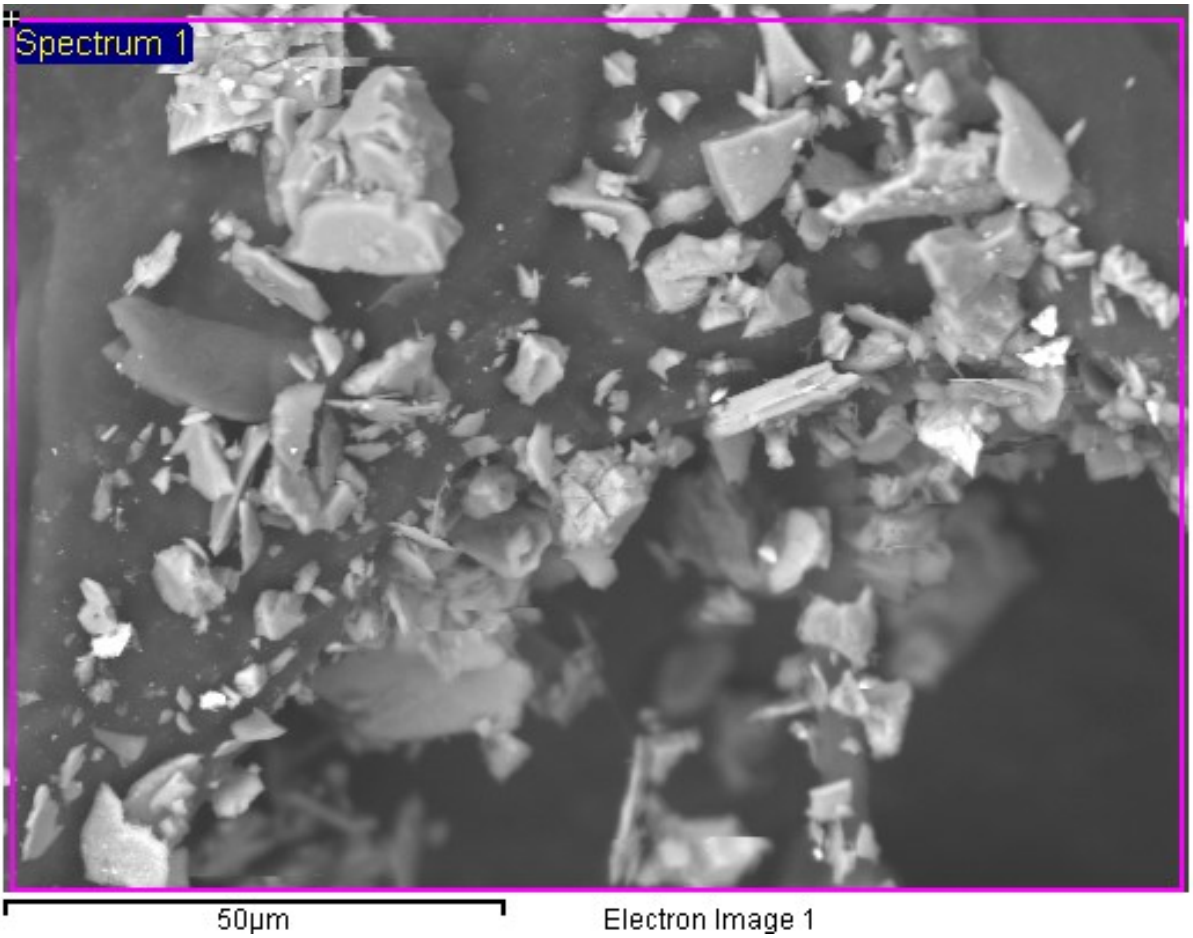

Processing option: All elements analysed (Normalised)

Spectrum	In stats.	Mg	Al	Si	K	Ca	Fe	As	Total
Spectrum 1	Yes	3.22	22.08	36.12	3.89	14.93	19.13	0.64	100.00
Mean		3.22	22.08	36.12	3.89	14.93	19.13	0.64	100.00
Std. deviation		0.00	0.00	0.00	0.00	0.00	0.00	0.00	
Max.		3.22	22.08	36.12	3.89	14.93	19.13	0.64	
Min.		3.22	22.08	36.12	3.89	14.93	19.13	0.64	

All results in weight%

APPENDIX III

RESULT DSL ANALYSIS OF SOPHOROLIPIDS

Malvern Instruments File name: 2016-07-25 25 Jul 2016 7:01:59 PM

Record	Type	Sample Name	Measurement Date and Time	T	Z-Ave	PdI	Intensity Mean	Volume Mean	Number Mean	Pk 1 Mean Int	Pk 2 Mean Int
				°C	d.nm		d.nm	d.nm	d.nm	d.nm	d.nm
1	Size	sl 2 1	July-25-16 5:15:24 PM	22.0	9.958	0.061	10.68	8.860	7.630	10.68	0.000
2	Size	sl 2 2	July-25-16 5:19:01 PM	21.9	10.16	0.062	10.97	8.756	7.394	10.97	0.000
3	Size	sl mine 2 1	July-25-16 5:27:05 PM	21.9	15.86	0.397	81.28	10.47	8.539	14.09	328.9
4	Size	sl 2 unfiltered 1	July-25-16 5:30:28 PM	22.0	494.8	0.920	914.0	11.87	8.043	1794	10.19
5	Size	sl 2 unfiltered 2	July-25-16 5:32:22 PM	22.0	484.9	0.910	852.7	11.66	7.773	10.65	1831
6	Size	sl 2 unfiltered 3	July-25-16 5:34:16 PM	22.0	701.9	1.000	1022	23.10	8.417	10.97	1876
7	Size	sl fe 2 1	July-25-16 5:37:29 PM	22.1	10.13	0.044	10.79	8.956	7.712	10.79	0.000
8	Size	sl fe 2 2	July-25-16 5:39:23 PM	22.1	10.20	0.052	10.91	8.947	7.645	10.91	0.000
9	Size	sl 4 unfiltered 1	July-25-16 5:42:25 PM	21.9	1101	1.000	1483	24.85	6.987	1789	7.814
10	Size	sl 4 unfiltered 2	July-25-16 5:44:19 PM	21.9	2042	1.000	720.0	8.668	7.124	962.7	8.226
11	Size	sl mine 4 1	July-25-16 5:47:03 PM	22.1	7.034	0.172	146.0	6.191	4.826	7.415	4114
12	Size	sl mine 4 2	July-25-16 5:48:57 PM	22.0	6.764	0.159	8.065	3.150	1.633	8.268	1.910
13	Size	sl 4 1	July-25-16 5:52:41 PM	21.9	8.230	0.038	8.679	7.420	6.507	8.679	0.000
14	Size	sl 4 2	July-25-16 5:54:35 PM	22.0	8.094	0.077	8.789	7.031	5.933	8.789	0.000
15	Size	sl 4 3	July-25-16 5:56:28 PM	22.0	8.010	0.120	8.902	7.209	6.170	8.902	0.000
16	Size	sl 6 1	July-25-16 5:59:02 PM	22.0	5.710	0.182	7.005	2.618	1.448	7.228	1.751
17	Size	sl 6 2	July-25-16 6:00:55 PM	22.0	6.060	0.194	134.8	5.618	4.607	6.349	4466
18	Size	sl 6 3	July-25-16 6:02:50 PM	22.0	5.945	0.182	150.3	5.455	4.490	6.152	4365
19	Size	sl 12 1	July-25-16 6:06:05 PM	22.0	8.101	0.436	28.31	4.428	3.605	6.034	70.49
20	Size	sl 12 2	July-25-16 6:07:59 PM	22.0	8.044	0.470	27.14	4.664	4.024	5.574	60.32
21	Size	sl 12 3	July-25-16 6:09:54 PM	22.0	8.023	0.459	28.02	1.323	0.9925	6.785	73.20
22	Size	sl mine 12 1	July-25-16 6:12:35 PM	22.0	31.88	0.399	1464	43.50	9.246	11.46	4192
23	Size	sl mine 12 2	July-25-16 6:14:28 PM	22.0	42.89	0.235	493.6	19.87	8.307	11.97	5104
24	Size	sl mine 12 3	July-25-16 6:16:21 PM	22.0	32.40	0.225	274.0	12.54	4.139	13.98	470.5
25	Size	sl mine 8 1	July-25-16 6:20:09 PM	22.0	139.4	0.523	576.7	7.815	2.289	194.7	5.917
26	Size	sl mine 8 2	July-25-16 6:22:03 PM	22.0	115.1	0.655	755.3	21.86	5.393	101.6	274.1
27	Size	sl mine 8 3	July-25-16 6:23:57 PM	22.0	66.62	0.809	538.9	13.93	5.810	131.9	6.511
28	Size	sl mine 12b 1	July-25-16 6:27:37 PM	22.0	1169	0.303	1265	2274	1049	1202	5485
29	Size	sl mine 12b 2	July-25-16 6:29:31 PM	22.0	1054	0.428	1195	3963	706.3	864.7	5336
30	Size	sl mine 12b 3	July-25-16 6:31:25 PM	22.0	1199	0.436	1076	3695	752.9	839.8	5471
31	Size	sl mine 12c 1	July-25-16 6:34:07 PM	22.0	150.7	0.244	197.3	72.75	29.76	203.3	36.51
32	Size	sl mine 12c 2	July-25-16 6:36:01 PM	22.0	153.2	0.212	194.4	115.6	42.26	194.4	0.000
33	Size	sl mine 12c 3	July-25-16 6:37:55 PM	22.0	149.1	0.213	191.5	162.8	112.8	191.5	0.000
34	Size	sl mine 10 1	July-25-16 6:40:26 PM	22.0	199.8	0.179	239.6	226.5	140.2	239.6	0.000
35	Size	sl mine 10 2	July-25-16 6:42:19 PM	22.0	198.3	0.180	241.1	225.5	132.3	241.1	0.000
36	Size	sl mine 10 3	July-25-16 6:44:13 PM	22.0	198.1	0.215	226.6	210.3	137.6	226.6	0.000

Malvern Instruments File name: 2016-07-25 25 Jul 2016 7:01:59 PM

Pk 3 Mean Int	Pk 1 Area Int	Pk 2 Area Int	Peak 3 Area Intensity	Aggregation Index	Scattering Angle
d.nm	Percent	Percent	Percent		°
0.000	100.0	0.0	0.0		90.0
0.000	100.0	0.0	0.0		90.0
0.000	78.7	21.3	0.0		90.0
0.000	50.7	49.3	0.0		90.0
0.000	53.7	46.3	0.0		90.0
5560	57.0	37.4	5.7		90.0
0.000	100.0	0.0	0.0		90.0
0.000	100.0	0.0	0.0		90.0
313.1	64.3	20.0	10.3		90.0
0.000	74.6	25.4	0.0		90.0
0.000	96.6	3.4	0.0		90.0
0.000	96.5	3.5	0.0		90.0
0.000	100.0	0.0	0.0		90.0
0.000	100.0	0.0	0.0		90.0
0.000	100.0	0.0	0.0		90.0
0.000	95.2	4.8	0.0		90.0
0.000	97.1	2.9	0.0		90.0
0.000	96.7	3.3	0.0		90.0
0.000	65.4	34.6	0.0		90.0
0.000	60.6	39.4	0.0		90.0
1.111	61.7	32.5	5.8		90.0
98.98	63.0	34.7	2.3		90.0
800.8	81.2	8.4	5.6		90.0
5368	83.0	10.7	3.9		90.0
5177	77.3	9.4	8.1		90.0
5.882	58.5	16.5	12.6		90.0
3599	73.1	14.6	12.3		90.0
0.000	98.5	1.5	0.0		90.0
0.000	92.6	7.4	0.0		90.0
0.000	94.9	5.1	0.0		90.0
0.000	96.0	4.0	0.0		90.0
0.000	100.0	0.0	0.0		90.0
0.000	100.0	0.0	0.0		90.0
0.000	100.0	0.0	0.0		90.0
0.000	100.0	0.0	0.0		90.0
0.000	100.0	0.0	0.0		90.0

Malvern Instruments File name: 2016-07-25 25 Jul 2016 7:01:59 PM

Record	Type	Sample Name	Measurement Date and Time	T	Z-Ave	PdI	Intensity Mean	Volume Mean	Number Mean	Pk 1 Mean Int	Pk 2 Mean Int
				°C	d.nm		d.nm	d.nm	d.nm	d.nm	d.nm
37	Size	sl 5percent 1	July-25-16 6:47:34 PM	22.0	28.23	0.405	684.4	34.35	11.44	15.81	1225
38	Size	sl 5percent 2	July-25-16 6:49:27 PM	22.0	26.09	0.428	648.1	33.58	10.65	16.12	931.9
39	Size	sl 5percent 3	July-25-16 6:51:21 PM	22.0	29.44	0.420	625.6	38.20	11.19	16.06	815.6

Size Distribution Report by Number

v2.2

Malvern

Sample Details

Sample Name: sl 12 2

SOP Name: mansettings.nano

General Notes:

File Name:	2016-07-25.dts	**Dispersant Name:**	Water
Record Number:	20	**Dispersant RI:**	1.330
Material RI:	1.59	**Viscosity (cP):**	0.9540
Material Absorbtion:	0.010	**Measurement Date and Time:**	July-25-16 6:07:59 PM

System

Temperature (°C):	22.0	**Duration Used (s):**	50
Count Rate (kcps):	22.9	**Measurement Position (mm):**	3.00
Cell Description:	Disposable low volume cu...	**Attenuator:**	11

Results

			Size (d.nm):	% Number:	St Dev (d.n...
Z-Average (d.nm):	8.044	**Peak 1:**	4.024	100.0	0.9272
PdI:	0.470	**Peak 2:**	0.000	0.0	0.000
Intercept:	0.881	**Peak 3:**	0.000	0.0	0.000

Result quality : Refer to quality report

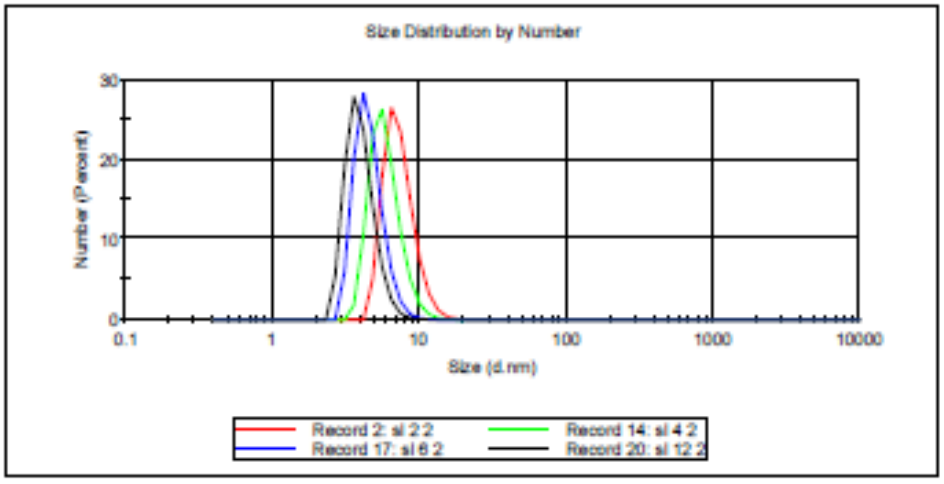

Size Distribution Report by Number

v2.2

Malvern

Sample Details

Sample Name: sl mine 12c 3
SOP Name: mansettings.nano
General Notes:

File Name:	2016-07-25.dts	**Dispersant Name:**	Water
Record Number:	33	**Dispersant RI:**	1.330
Material RI:	1.59	**Viscosity (cP):**	0.9540
Material Absorbtion:	0.010	**Measurement Date and Time:**	July-25-16 6:37:55 PM

System

Temperature (°C):	22.0	**Duration Used (s):**	50
Count Rate (kcps):	328.4	**Measurement Position (mm):**	3.00
Cell Description:	Disposable low volume cu...	**Attenuator:**	11

Results

			Size (d.nm):	% Number:	St Dev (d.n...
Z-Average (d.nm):	149.1	**Peak 1:**	112.8	100.0	37.46
PdI:	0.213	**Peak 2:**	0.000	0.0	0.000
Intercept:	0.893	**Peak 3:**	0.000	0.0	0.000

Result quality : Good

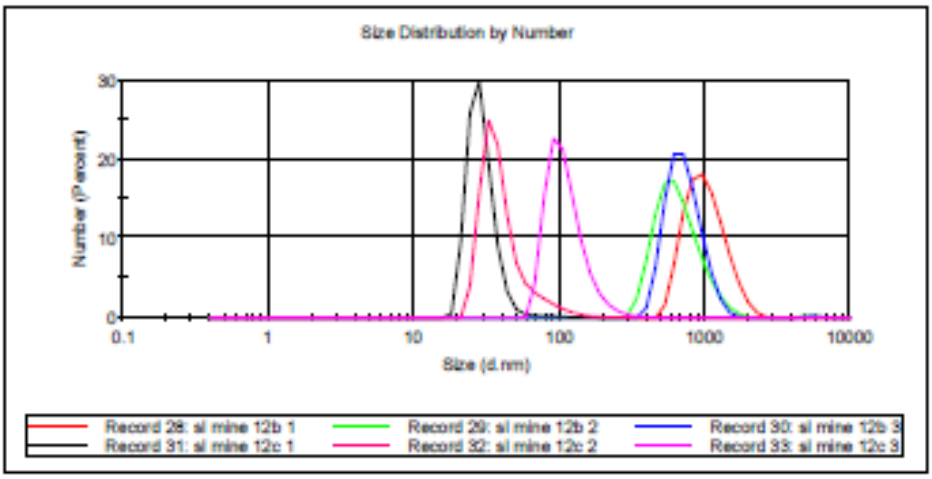

Size Statistics Report by Number

v2.0

Malvern

Sample Details

Sample Name: si mine 2 1

File Name: 2016-07-25.dts

SOP Name: mansettings.nano

Measurement Date and Time: July-25-16 5:27:05 PM

Z-Average (nm):	15.856	**Derived Count Rate (kcps):**	58.0102806091...
Standard Deviation:	0	**Standard Deviation:**	0
%Std Deviation:	0	**%Std Deviation:**	0
Variance:	0	**Variance:**	0

Size d.nm	Mean Number Percent	Std Dev Number Percent	Size d.nm	Mean Number Percent	Std Dev Number Percent	Size d.nm	Mean Number Percent	Std Dev Number Percent	Size d.nm	Mean Number P
0.4000	0.0		5.615	5.7		78.82	0.0		1106	
0.4632	0.0		6.503	18.9		91.26	0.0		1281	
0.5365	0.0		7.531	28.4		105.7	0.0		1484	
0.6213	0.0		8.721	22.3		122.4	0.0		1718	
0.7195	0.0		10.10	14.1		141.8	0.0		1990	
0.8332	0.0		11.70	7.3		164.2	0.0		2305	
0.9649	0.0		13.54	3.3		190.1	0.0		2669	
1.117	0.0		15.69	1.3		220.2	0.0		3091	
1.294	0.0		18.17	0.5		255.0	0.0		3580	
1.499	0.0		21.04	0.1		295.3	0.0		4145	
1.736	0.0		24.38	0.0		342.0	0.0		4801	
2.010	0.0		28.21	0.0		396.1	0.0		5560	
2.328	0.0		32.67	0.0		458.7	0.0		6439	
2.696	0.0		37.84	0.0		531.2	0.0		7458	
3.122	0.0		43.82	0.0		615.1	0.0		8635	
3.615	0.0		50.75	0.0		712.4	0.0		1.000e4	
4.187	0.0		58.77	0.0		825.0	0.0			
4.849	0.0		68.06	0.0		955.4	0.0			

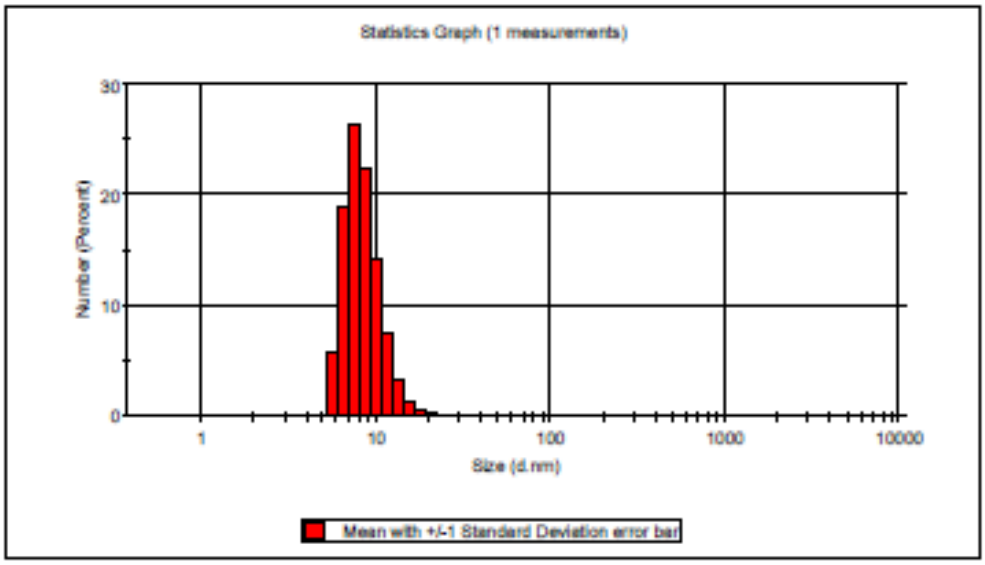

Size Statistics Report by Number

v2.0

Malvern

Sample Details

Sample Name: sl mine 4 1

File Name: 2016-07-25.dts

SOP Name: mansettings.nano

Measurement Date and Time: July-25-16 5:47:03 PM

Z-Average (nm):	7.033726	**Derived Count Rate (kcps):**	36.2854652404...
Standard Deviation:	0	**Standard Deviation:**	0
%Std Deviation:	0	**%Std Deviation:**	0
Variance:	0	**Variance:**	0

Size d.nm	Mean Number Percent	Std Dev Number Percent
0.4000	0.0	
0.4632	0.0	
0.5365	0.0	
0.6213	0.0	
0.7195	0.0	
0.8332	0.0	
0.9649	0.0	
1.117	0.0	
1.294	0.0	
1.499	0.0	
1.736	0.0	
2.010	0.0	
2.328	0.0	
2.696	0.0	
3.122	4.4	
3.615	16.5	
4.187	26.0	
4.849	24.0	

Size d.nm	Mean Number Percent	Std Dev Number Percent
5.615	15.6	
6.503	8.1	
7.531	3.5	
8.721	1.3	
10.10	0.4	
11.70	0.1	
13.54	0.0	
15.69	0.0	
18.17	0.0	
21.04	0.0	
24.36	0.0	
28.21	0.0	
32.67	0.0	
37.84	0.0	
43.82	0.0	
50.75	0.0	
58.77	0.0	
68.06	0.0	

Size d.nm	Mean Number Percent	Std Dev Number Percent
78.82	0.0	
91.26	0.0	
105.7	0.0	
122.4	0.0	
141.8	0.0	
164.2	0.0	
190.1	0.0	
220.2	0.0	
255.0	0.0	
295.3	0.0	
342.0	0.0	
396.1	0.0	
458.7	0.0	
531.2	0.0	
615.1	0.0	
712.4	0.0	
825.0	0.0	
955.4	0.0	

Size d.nm	Me Number
1106	
1281	
1484	
1718	
1990	
2305	
2669	
3091	
3580	
4145	
4801	
5560	
6439	
7458	
8635	
1.000e4	

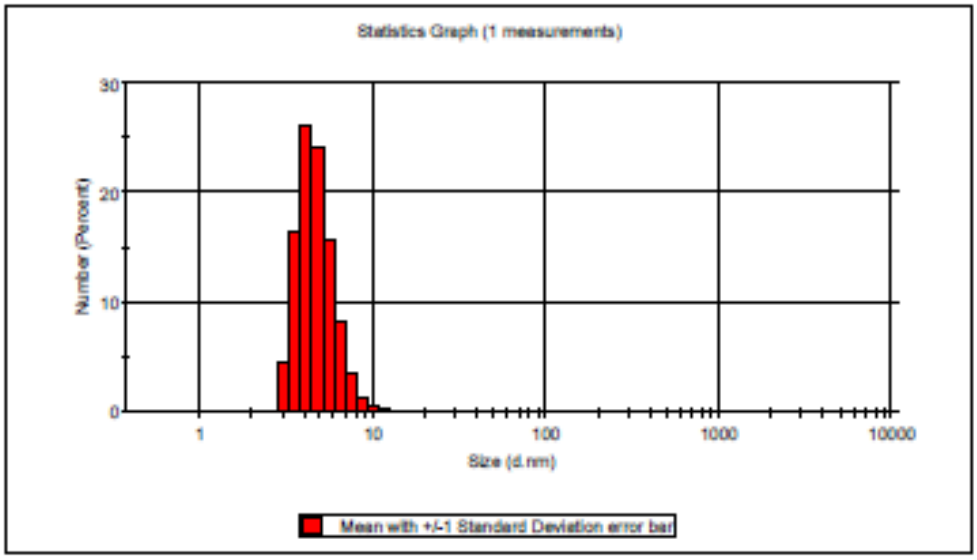

Size Statistics Report by Number

v2.0

Malvern

Sample Details

Sample Name: sl mine 8 1

File Name: 2016-07-25.dts

SOP Name: mansettings.nano

Measurement Date and Time: July-25-16 5:20:09 PM

Z-Average (nm):	139.4355	**Derived Count Rate (kcps):**	58.6562690734...
Standard Deviation:	0	**Standard Deviation:**	0
%Std Deviation:	0	**%Std Deviation:**	0
Variance:	0	**Variance:**	0

Size d.nm	Mean Number Percent	Std Dev Number Percent	Size d.nm	Mean Number Percent	Std Dev Number Percent	Size d.nm	Mean Number Percent	Std Dev Number Percent	Size d.nm	Mean Number P
0.4000	0.0		5.815	0.5		76.83	0.0		1106	
0.4632	0.0		6.503	0.3		91.28	0.0		1281	
0.5365	0.0		7.531	0.1		105.7	0.0		1484	
0.6213	0.0		8.721	0.0		122.4	0.0		1718	
0.7195	0.0		10.10	0.0		141.8	0.0		1990	
0.8332	0.0		11.70	0.0		164.2	0.0		2305	
0.9649	0.0		13.54	0.0		190.1	0.0		2669	
1.117	0.0		15.69	0.0		220.2	0.0		3091	
1.294	0.0		18.17	0.0		255.0	0.0		3580	
1.499	4.0		21.04	0.0		295.3	0.0		4145	
1.736	18.8		24.36	0.0		342.0	0.0		4801	
2.010	31.4		28.21	0.0		396.1	0.0		5560	
2.328	24.3		32.67	0.0		458.7	0.0		6439	
2.696	10.5		37.84	0.0		531.3	0.0		7456	
3.122	4.4		43.82	0.0		615.1	0.0		8635	
3.615	2.7		50.75	0.0		712.4	0.0		1.000e4	
4.187	1.9		58.77	0.0		825.0	0.0			
4.849	1.1		68.06	0.0		955.4	0.0			

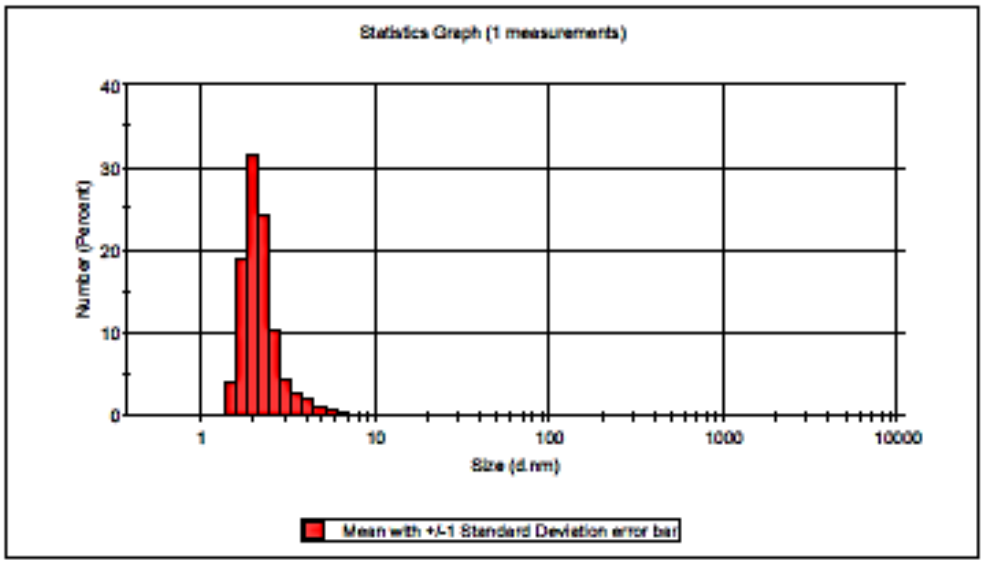

Size Statistics Report by Number

v2.0

Malvern

Sample Details

Sample Name: sl mine 10 1

File Name: 2016-07-25.dts

SOP Name: mansettings.nano

Measurement Date and Time: July-25-16 6:40:26 PM

Z-Average (nm):	199.7749	**Derived Count Rate (kcps):**	938.541437797...
Standard Deviation:	0	**Standard Deviation:**	0
%Std Deviation:	0	**%Std Deviation:**	0
Variance:	0	**Variance:**	0

Size d.nm	Mean Number Percent	Std Dev Number Percent	Size d.nm	Mean Number Percent	Std Dev Number Percent	Size d.nm	Mean Number Percent	Std Dev Number Percent	Size d.nm	Mea Number P
0.4000	0.0		5.615	0.0		78.82	3.1		1106	
0.4632	0.0		6.503	0.0		91.28	12.0		1281	
0.5365	0.0		7.531	0.0		105.7	20.1		1484	
0.6213	0.0		8.721	0.0		122.4	20.9		1718	
0.7195	0.0		10.10	0.0		141.8	16.4		1990	
0.8332	0.0		11.70	0.0		164.2	11.0		2305	
0.9649	0.0		13.54	0.0		190.1	6.6		2669	
1.117	0.0		15.69	0.0		220.2	4.1		3091	
1.294	0.0		18.17	0.0		255.0	2.5		3580	
1.499	0.0		21.04	0.0		295.3	1.5		4145	
1.736	0.0		24.38	0.0		342.0	0.8		4801	
2.010	0.0		28.21	0.0		396.1	0.4		5560	
2.328	0.0		32.67	0.0		458.7	0.2		6439	
2.696	0.0		37.84	0.0		531.2	0.1		7458	
3.122	0.0		43.82	0.0		615.1	0.0		8635	
3.615	0.0		50.75	0.0		712.4	0.0		1.000e4	
4.187	0.0		58.77	0.0		825.0	0.0			
4.849	0.0		68.06	0.0		955.4	0.0			

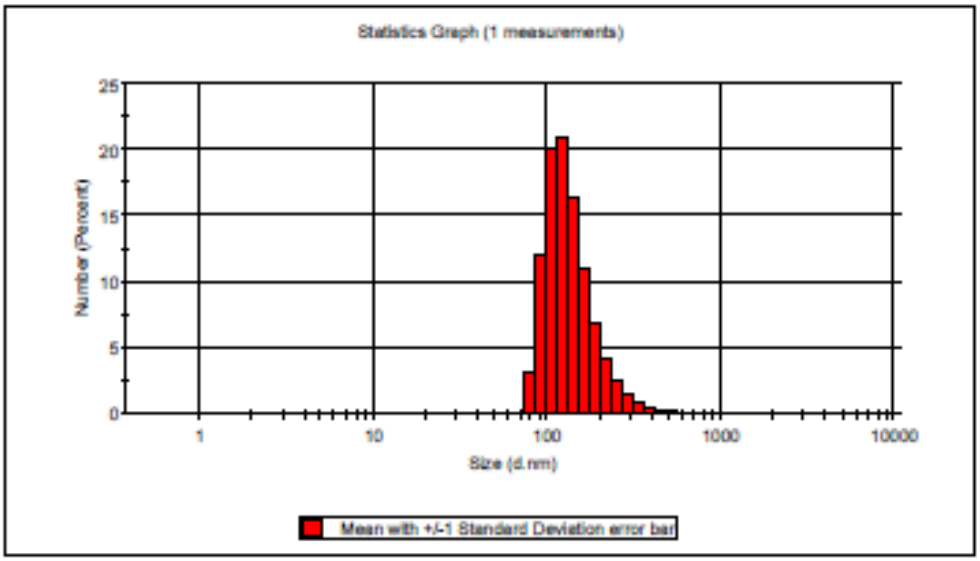

Size Statistics Report by Number

v2.0

Malvern

Sample Details

Sample Name: sl mine 12 1

File Name: 2016-07-25.dts

SOP Name: mansettings.nano

Measurement Date and Time: July-25-16 6:12:35 PM

Z-Average (nm):	31.87863	**Derived Count Rate (kcps):**	59.5475273132...
Standard Deviation:	0	**Standard Deviation:**	0
%Std Deviation:	0	**%Std Deviation:**	0
Variance:	0	**Variance:**	0

Size d.nm	Mean Number Percent	Std Dev Number Percent	Size d.nm	Mean Number Percent	Std Dev Number Percent	Size d.nm	Mean Number Percent	Std Dev Number Percent	Size d.nm	Mean Number Percent
0.4000	0.0		5.815	0.0		76.82	0.0		1106	
0.4632	0.0		6.503	7.0		91.28	0.0		1281	
0.5366	0.0		7.531	22.6		105.7	0.0		1484	
0.6213	0.0		8.721	30.5		122.4	0.0		1718	
0.7195	0.0		10.10	22.6		141.8	0.0		1990	
0.8332	0.0		11.70	11.5		164.2	0.0		2305	
0.9649	0.0		13.54	4.2		190.1	0.0		2669	
1.117	0.0		15.69	1.1		220.2	0.0		3091	
1.294	0.0		18.17	0.2		255.0	0.0		3580	
1.499	0.0		21.04	0.0		295.3	0.0		4145	
1.736	0.0		24.36	0.0		342.0	0.0		4801	
2.010	0.0		28.21	0.0		396.1	0.0		5560	
2.328	0.0		32.67	0.0		458.7	0.0		6439	
2.696	0.0		37.84	0.0		531.2	0.0		7456	
3.122	0.0		43.82	0.0		615.1	0.0		8635	
3.615	0.0		50.75	0.0		712.4	0.0		1.000e4	
4.187	0.0		58.77	0.0		825.0	0.0			
4.849	0.0		68.06	0.0		955.4	0.0			

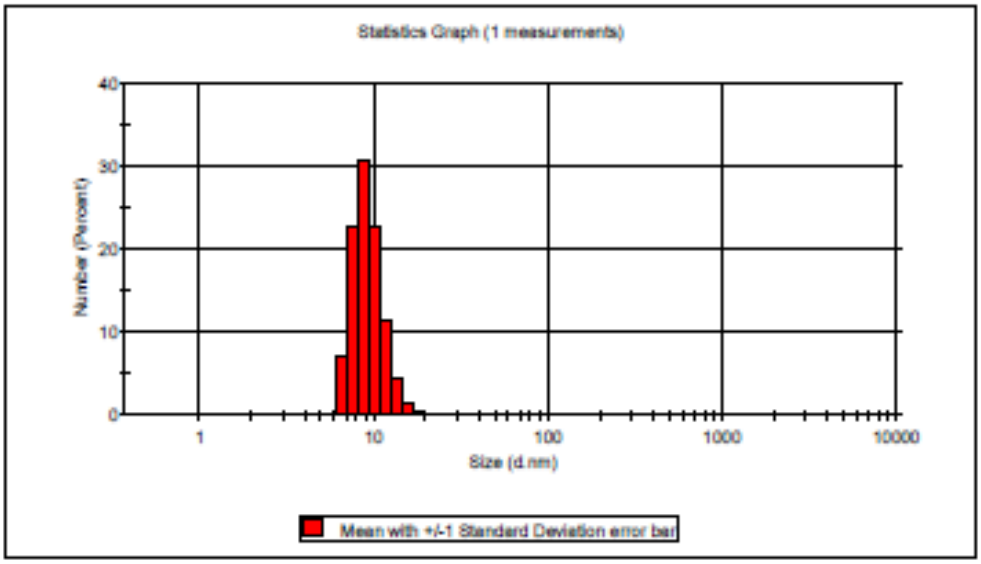

Size Statistics Report by Number

v2.0

Malvern

Sample Details

Sample Name: si fe 2 1
File Name: 2016-07-25.dts
SOP Name: mansettings.nano
Measurement Date and Time: July-25-16 5:37:29 PM

Z-Average (nm):	10.13409	**Derived Count Rate (kcps):**	123.422622680...
Standard Deviation:	0	**Standard Deviation:**	0
%Std Deviation:	0	**%Std Deviation:**	0
Variance:	0	**Variance:**	0

Size d.nm	Mean Number Percent	Std Dev Number Percent
0.4000	0.0	
0.4602	0.0	
0.5365	0.0	
0.6213	0.0	
0.7195	0.0	
0.8332	0.0	
0.9649	0.0	
1.117	0.0	
1.294	0.0	
1.499	0.0	
1.736	0.0	
2.010	0.0	
2.328	0.0	
2.696	0.0	
3.122	0.0	
3.615	0.0	
4.187	0.0	
4.849	2.7	

Size d.nm	Mean Number Percent	Std Dev Number Percent
5.615	12.8	
6.503	24.8	
7.531	26.2	
8.721	18.1	
10.10	9.5	
11.70	4.0	
13.54	1.4	
15.69	0.4	
18.17	0.1	
21.04	0.0	
24.36	0.0	
28.21	0.0	
32.67	0.0	
37.84	0.0	
43.82	0.0	
50.75	0.0	
58.77	0.0	
68.06	0.0	

Size d.nm	Mean Number Percent	Std Dev Number Percent
78.82	0.0	
91.28	0.0	
105.7	0.0	
122.4	0.0	
141.8	0.0	
164.2	0.0	
190.1	0.0	
220.2	0.0	
255.0	0.0	
295.3	0.0	
342.0	0.0	
396.1	0.0	
458.7	0.0	
531.2	0.0	
615.1	0.0	
712.4	0.0	
825.0	0.0	
955.4	0.0	

Size d.nm	Mean Number P
1106	
1281	
1484	
1718	
1990	
2305	
2669	
3091	
3580	
4145	
4801	
5560	
6439	
7456	
8635	
1.000e4	

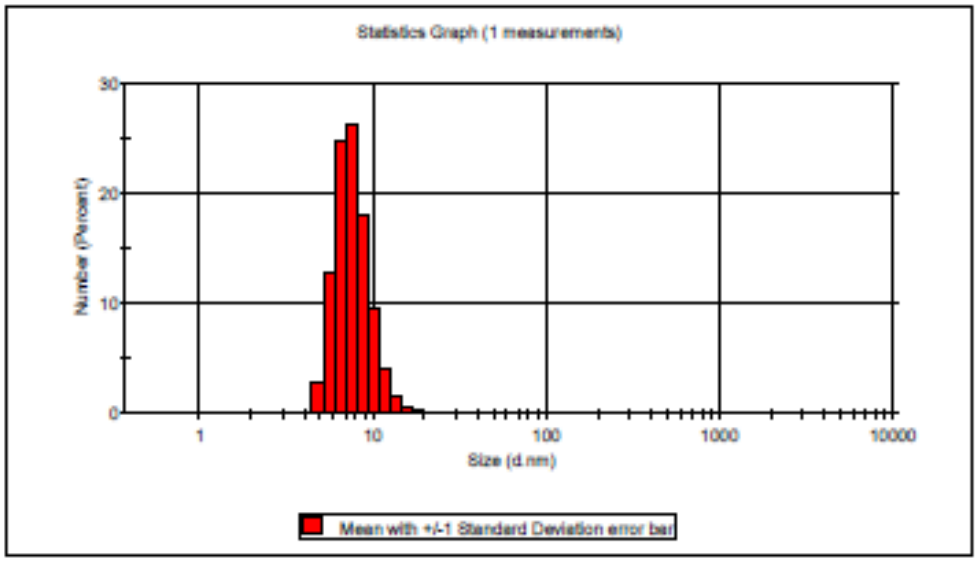

Size Distribution Report by Number

v2.2

Malvern

Sample Details

Sample Name: sl 5percent 1

SOP Name: mansettings.nano

General Notes:

File Name:	2016-07-25.dts	**Dispersant Name:**	Water
Record Number:	37	**Dispersant RI:**	1.330
Material RI:	1.59	**Viscosity (cP):**	0.9540
Material Absorption:	0.010	**Measurement Date and Time:**	July-25-16 6:47:34 PM

System

Temperature (°C):	22.0	**Duration Used (s):**	50
Count Rate (kcps):	229.1	**Measurement Position (mm):**	3.00
Cell Description:	Disposable low volume cu...	**Attenuator:**	10

Results

			Size (d.nm):	% Number:	St Dev (d.n...
Z-Average (d.nm):	28.23	**Peak 1:**	11.44	100.0	2.669
PdI:	0.405	**Peak 2:**	0.000	0.0	0.000
Intercept:	0.889	**Peak 3:**	0.000	0.0	0.000

Result quality : Refer to quality report

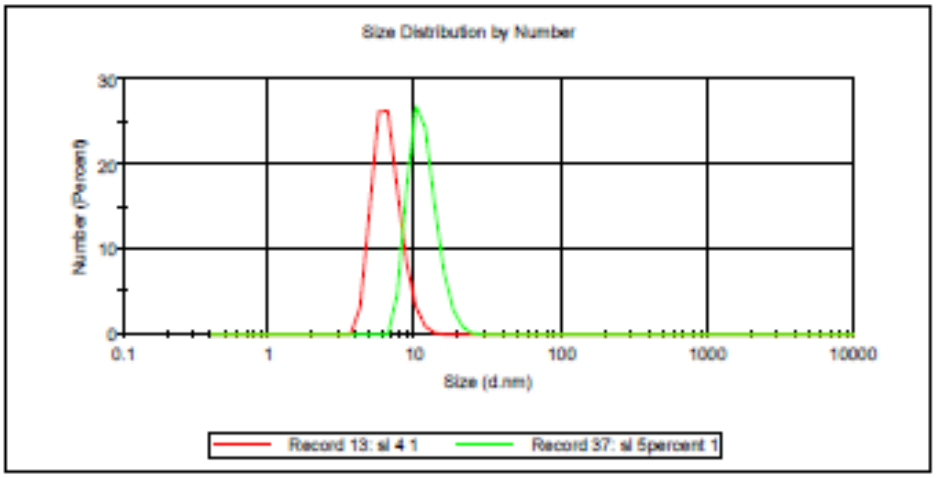

Size Statistics Report by Number

v2.0

Malvern Instruments Ltd - © Copyright 2008

Malvern

Sample Details

Sample Name: si 5percent 1

File Name: 2016-07-25.dts

SOP Name: mansettings.nano

Measurement Date and Time: July-25-16 6:47:34 PM

Z-Average (nm):	28.23398	**Derived Count Rate (kcps):**	815.181399531...
Standard Deviation:	0	**Standard Deviation:**	0
%Std Deviation:	0	**%Std Deviation:**	0
Variance:	0	**Variance:**	0

Size d.nm	Mean Number Percent	Std Dev Number Percent	Size d.nm	Mean Number Percent	Std Dev Number Percent	Size d.nm	Mean Number Percent	Std Dev Number Percent	Size d.nm	Mean Number P
0.4000	0.0		5.815	0.0		76.82	0.0		1109	
0.4632	0.0		6.503	0.0		91.28	0.0		1281	
0.5365	0.0		7.531	4.7		105.7	0.0		1484	
0.6213	0.0		8.721	17.3		122.4	0.0		1718	
0.7195	0.0		10.10	26.9		141.8	0.0		1990	
0.8333	0.0		11.70	24.3		164.2	0.0		2305	
0.9649	0.0		13.54	15.3		190.1	0.0		2669	
1.117	0.0		15.69	7.4		220.2	0.0		3091	
1.294	0.0		18.17	2.9		255.0	0.0		3580	
1.499	0.0		21.04	0.9		295.3	0.0		4145	
1.736	0.0		24.36	0.2		342.0	0.0		4801	
2.010	0.0		28.21	0.0		396.1	0.0		5560	
2.328	0.0		32.67	0.0		458.7	0.0		6439	
2.696	0.0		37.84	0.0		531.2	0.0		7456	
3.122	0.0		43.82	0.0		615.1	0.0		8635	
3.615	0.0		50.75	0.0		712.4	0.0		1.000e4	
4.187	0.0		58.77	0.0		825.0	0.0			
4.849	0.0		68.06	0.0		955.4	0.0			

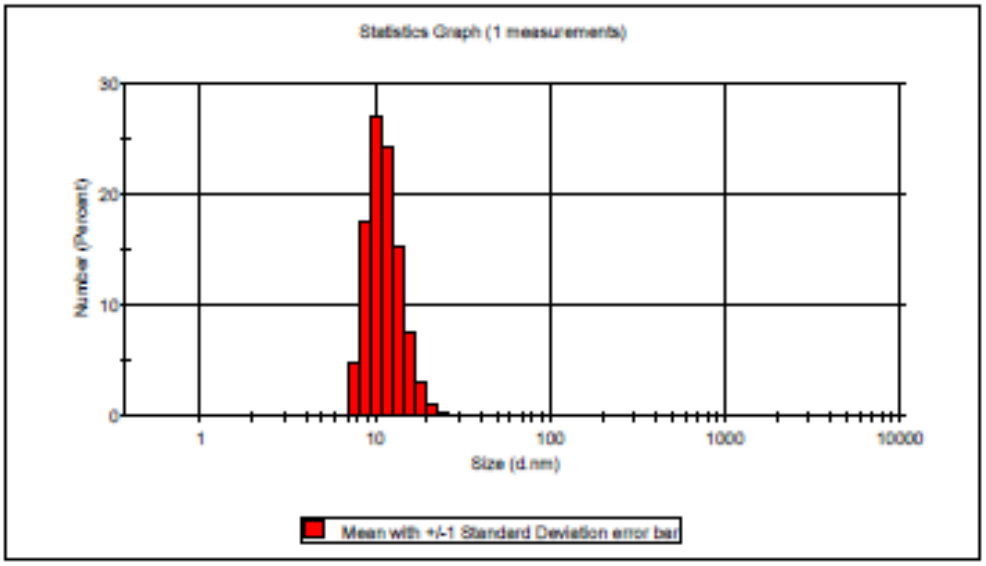

Size Distribution Report by Number

v2.2

Malvern

Sample Details

Sample Name: real sl 4 % 3
SOP Name: mansettings.nano
General Notes:

File Name:	sl 2%.dts	**Dispersant Name:**	Water
Record Number:	10	**Dispersant RI:**	1.330
Material RI:	1.59	**Viscosity (cP):**	1.0031
Material Absorption:	0.010	**Measurement Date and Time:**	December-19-16 12:01:09 PM

System

Temperature (°C):	20.0	**Duration Used (s):**	120
Count Rate (kcps):	102.9	**Measurement Position (mm):**	3.00
Cell Description:	Disposable low volume cu...	**Attenuator:**	9

Results

			Size (d.nm):	% Number:	St Dev (d.n...
Z-Average (d.nm):	78.30	**Peak 1:**	13.37	100.0	3.324
PdI:	0.722	**Peak 2:**	0.000	0.0	0.000
Intercept:	0.887	**Peak 3:**	0.000	0.0	0.000

Result quality : Refer to quality report

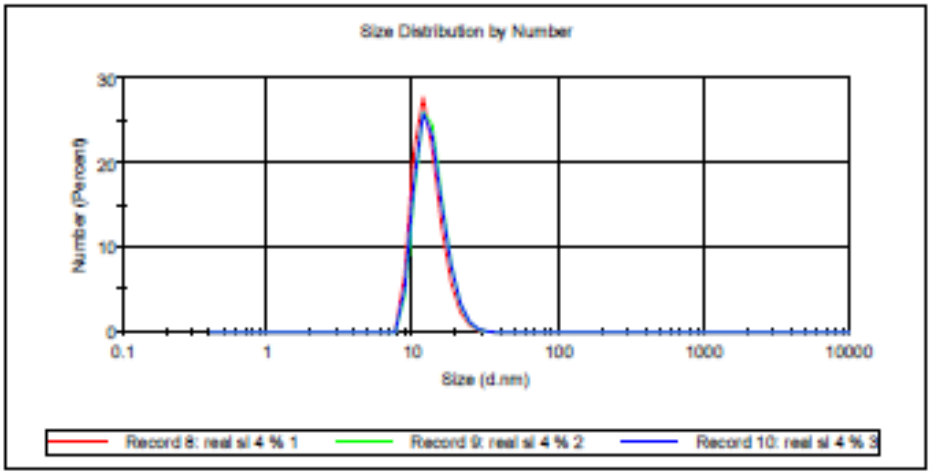

Size Distribution Report by Number

v2.2

Malvern

Sample Details

Sample Name: sl 4% 3
SOP Name: mansettings.nano
General Notes:

File Name:	sl 2%.dts	**Dispersant Name:**	Water
Record Number:	7	**Dispersant RI:**	1.330
Material RI:	1.59	**Viscosity (cP):**	1.0031
Material Absorption:	0.010	**Measurement Date and Time:**	December-19-16 11:43:57 AM

System

Temperature (°C):	20.0	**Duration Used (s):**	120
Count Rate (kcps):	368.3	**Measurement Position (mm):**	3.00
Cell Description:	Disposable low volume cu...	**Attenuator:**	10

Results

			Size (d.nm):	% Number:	St Dev (d.n...
Z-Average (d.nm):	296.9	**Peak 1:**	11.98	100.0	2.807
PdI:	1.000	**Peak 2:**	0.000	0.0	0.000
Intercept:	0.828	**Peak 3:**	0.000	0.0	0.000

Result quality : Refer to quality report

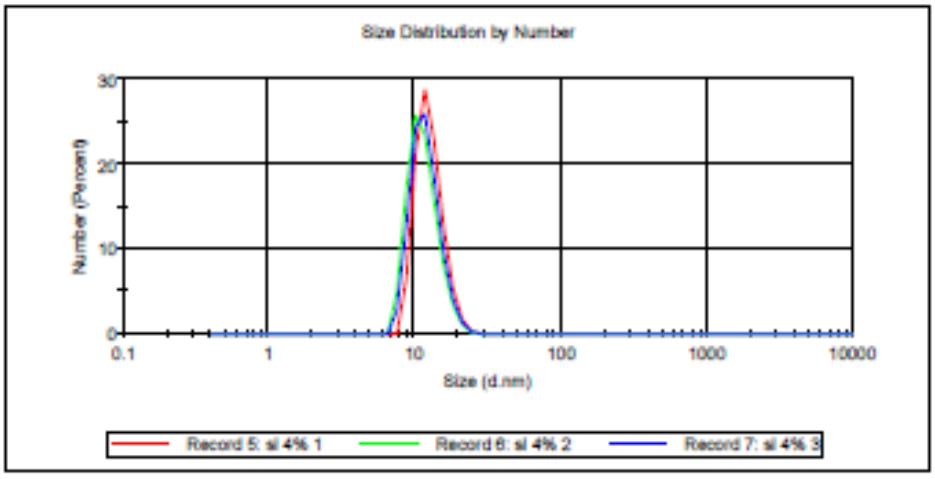

Size Distribution Report by Number

v2.2

Malvern

Sample Details

Sample Name: jar 6- 20mg/L 3

SOP Name: mansettings.nano

General Notes:

File Name:	2016-12-19.dts	**Dispersant Name:**	Water
Record Number:	4	**Dispersant RI:**	1.330
Material RI:	1.59	**Viscosity (cP):**	1.0031
Material Absorbtion:	0.010	**Measurement Date and Time:**	December-19-16 11:10:47 AM

System

Temperature (°C):	20.0	**Duration Used (s):**	120
Count Rate (kcps):	239.5	**Measurement Position (mm):**	3.00
Cell Description:	Disposable low volume cu...	**Attenuator:**	10

Results

			Size (d.nm):	% Number:	St Dev (d.n...
Z-Average (d.nm):	318.9	**Peak 1:**	10.27	100.0	2.468
PdI:	1.000	**Peak 2:**	0.000	0.0	0.000
Intercept:	0.838	**Peak 3:**	0.000	0.0	0.000

Result quality : Refer to quality report